Engineering Library

APR 9 4 193

U. S. DEPARTMENT OF COMMERCE

BUREAU OF STANDARDS JOURNAL OF RESEARCH

Vol. 10 JANUARY, 1933 No. 1

CONTENTS

RP. No.	TITLE AND AUTHOR	Page
512.	White-metal bearing alloys: Mechanical properties at different temperatures and service tests. Harry K. Herschman and John L. Basil	1
513.	The cause and elimination of night effects in radio range-beacon reception. H. Diamond	7
514.	The heat capacity, heat of sublimation, and heat of solution of phosphorus pentoxide. Mikkel Frandsen	35
515.	The interference method of measuring thermal expansion. George E. Merritt	59
516.	Effect of lathe cutting conditions on the hardness of carbon and alloy steels. T. G. Digges	77
517.	Measurements of ultra-violet solar radiation in various localities. W. W. Coblentz, R. Stair, and J. M. Hogue	79
518.	Effect of service temperature conditions on the electromotive force of unsaturated portable standard cells. J. H. Park	89
519.	The Thomas recording gas calorimeter. R. S. Jessup	99
520.	Compressive strength of steel columns incased in brick walls. Albert L. Harris, A. H. Stang, and J. W. McBurney	123
521.	Further description and analysis of the first spectrum of xenon. C. J. Humphreys and W. F. Meggers	139

BUREAU OF STANDARDS JOURNAL OF RESEARCH

CONTENTS OF RECENT NUMBERS

July, 1932 (Vol. 9, No. 1)

RP453. The use of α-benzoinoxime in the determination of molybdenum. H. B. Knowles. Price 5 cents.
RP454. Effect of zinc coatings on the endurance properties of steel. W. H. Swanger and R. D. France. Price 5 cents.
RP455. Power input and dissipation in the positive column of a cæsium discharge. F. L. Mohler. Price 5 cents.
RP456. Thermal expansion of some silicates of elements in Group II of the periodic system. R. F. Geller and Herbert Insley. Price 5 cents.
RP457. An automatic reverberation meter for the measurement of sound absorption. W. F. Snyder. Price 5 cents.
RP458. Note on the probable presence of 2, 2-dimethylpentane in a mid-continent petroleum. Johannes H. Bruun and Mildred M. Hicks-Bruun. Price 5 cents.
RP459. Notes on the orifice meter: The expansion factor for gases. Edgar Buckingham. Price 5 cents.
RP460. Theory of voltage dividers and their use with cathode ray oscillographs. Melville M. Peters, George F. Blackburn, and Paul T. Hannen. Price 10 cents.

August, 1932 (Vol. 9, No. 2)

RP461. A vacuum tube amplifier for feeble pulses. L. F. Curtiss. Price 5 cents.
RP462. Infra-red spectra of helium. William F. Meggers and G. H. Dieke. Price 5 cents.
RP463. Tests of cellular sheet-steel flooring. J. M. Frankland and H. L. Whittemore. Price 10 cents.
RP464. The influence of temperature on the evolution of hydrogen sulphide from vulcanized rubber. A. D. Cummings. Price 5 cents.
RP465. Some of the factors which affect the measurement of sound absorption. V. L. Chrisler and Catherine E. Miller. Price 5 cents.
RP466. The reciprocal spherical aberration of an optical system including higher orders. Harold F. Bennett. Price 5 cents.
RP467. An attachment for turning approximately spherical surfaces of small curvature on a lathe. I. C. Gardner. Price 5 cents.
RP468. Wave lengths and Zeeman effects in lanthanum spectra. William F. Meggers. Price 5 cents.
RP469. Note on the freezing point of "iso-octane" 2, 2, 4-trimethylpentane Johannes H. Bruun and Mildred M. Hicks-Bruun. Price 5 cents.
RP470. A twin-bomb method for the accurate determination of pressure-volume-temperature data and a simple method for the accurate measurement of high pressure. Edward W. Washburn. Price 5 cents.

September, 1932 (Vol. 9, No. 3)

RP471. A new determination of the atomic weight of osmium. Raleigh Gilchrist. Price 5 cents.
RP472. "Moisture expansion" of ceramic whiteware. R. F. Geller and A. S. Creamer. Price 5 cents.
RP473. Infra-red arc spectra photographed with xenocyanine. W. F. Meggers and C. C. Kiess. Price 5 cents.
RP474. Tensile properties of cast nickel-chromium-iron alloys and of some alloy steels at elevated temperatures. William Kahlbaum and Louis Jordan. Price 5 cents.
RP475. The comparison of high voltage X-ray generators. Lauriston S. Taylor and K. L. Tucker. Price 5 cents.
RP476. The structure of the chromic acid plating bath: The theory of chromium deposition. Charles Kasper. Price 5 cents.
RP477. Physical properties and weathering characteristics of slate. D. W. Kessler and W. H. Sligh. Price 10 cents.
RP478. Radiation from cæsium and other metals bombarded by slow electrons. C. Boeckner. Price 5 cents.
RP479. A simplified precision formula for the inductance of a helix with corrections for the lead-in wires. Chester Snow. Price 5 cents.
RP480. Register studies in offset lithography. C. G. Weber and R. M. Cobb. Price 5 cents.
RP481. Creep at elevated temperatures in chromium-vanadium steels containing tungsten or molybdenum. William Kahlbaum and Louis Jordan. Price 5 cents.

Research papers, where price is given, are already available, and others will be available in the near future as separates for purchase from the Superintendent of Documents, United States Government Printing Office, Washington, D. C.

U. S. DEPARTMENT OF COMMERCE
ROY D. CHAPIN, Secretary
BUREAU OF STANDARDS
LYMAN J. BRIGGS, Acting Director

BUREAU OF STANDARDS JOURNAL OF RESEARCH

January, 1933
Vol. 10, No. 1

UNITED STATES
GOVERNMENT PRINTING OFFICE
WASHINGTON : 1933

For sale by the Superintendent of Documents, Washington, D. C. - - Price 25 cents; $2.50 per year on subscription

For a partial list of previous research papers appearing in BUREAU OF STANDARDS JOURNAL OF RESEARCH see pages 2 and 3 of the cover

WHITE-METAL BEARING ALLOYS: MECHANICAL PROPERTIES AT DIFFERENT TEMPERATURES AND SERVICE TESTS

By Harry K. Herschman and John L. Basil

ABSTRACT

A study was made of the wear resistance and other mechanical properties of 11 white-metal bearing alloys. These included 2 tin-base and 8 lead-base alloys and 1 cadmium-zinc alloy. Each of the properties, with the exception of wear resistance was determined at several temperatures, ranging from 20° to 200° C. (68° to 390° F.). Resistance to wear was determined only at 20° C. No one of the alloys tested was found to excel in all of the mechanical properties studied. Thus, the tin-base alloys showed higher resistance to wear and in most cases had higher Izod impact values, at each temperature of test, than the lead-base alloys, but in most cases, showed lower resistance to pounding than the lead-base and cadmium-zinc alloys. The hardness numbers and compressive properties of the tin-base alloys were found to be lower than those for the alkaline-metal hardened lead alloys and a cadmium-zinc alloy. The mechanical properties of the lead-antimony-tin alloys were, in most cases, higher as the tin content was increased.

Crank-shaft bearings of four compositions were prepared for service tests in United States Army class B trucks. These compositions consisted of two tin-base and two lead-base alloys. The results of these tests indicated that the tin-base alloys were superior in their wear resistance to the lead-base alloys. These results were consistent with those obtained on wear in the laboratory tests.

The usual white-metal bearing alloys require in their composition tin or antimony or both. These elements are so-called "strategic" metals and the potential military demand for them is considerable. These facts were responsible for the sponsoring by the War Department of recent studies at the Bureau of Standards aimed toward the reduction or possible elimination of the amounts of tin and antimony needed for bearing metals.

One phase of this work was a study of white-metal bearing alloys with particular reference to the wear resistance and such other mechanical properties as appeared to be of chief significance in the service of such alloys in bearings. The compositions of the alloys studied appear in Table 1. A more complete discussion of the details and results of this investigation was presented in a paper [1] before the June, 1932, meeting of the American Society for Testing Materials. Some additional work has since been completed. This included (1) a metallographic study of the alloys tested and (2) the determination of the mechanical properties of hardened lead B (Table 1).

[1] H. K. Herschman and J. L. Basil, Mechanical Properties of White Metal Bearing Alloys at Different Temperatures, Proc. A. S. T. M., vol. 32, pt. 2, p. 536, 1932.

TABLE 1.—*Results of chemical analyses of white-metal bearing alloys*

Alloy designation	Lead	Tin	Antimony	Copper	Cadmium	Zinc	Other constituents, per cent
	Per cent	*Per cent*	*Per cent*	*Per cent*	*Per cent*	*Per cent*	
No. 1		90.9	4.6	4.5			
No. 3		83.8	8.1	8.1			
No. 6	62.3	20.8	15.5	1.4			
No. 7	78.8	8.4	12.8				
No. 8	79.7	5.0	15.3				
No. 10	87.0	1.2	11.8				
No. 11	88.1		11.9				
Hardened lead F [1]	96.93	.18		.1			Hg 0.33, Ba 1.70, Ca 0.70.
Hardened lead B [2]	98.0						Na 0.65, K 0.3, Ca 0.75, Li 0.4.
Cadmium-zinc [3]					82.0	18	
A [4]	80.6	3.8	13.5	1.0	.2		Ni 0.2, As 0.6.

[1] Analysis by the National Lead Co.
[2] Nominal composition as given by the Maywood Chemical Co.
[3] Nominal composition.
[4] Analysis made by J. A. Scherrer, Bureau of Standards.

Each of the properties of the white-metal bearing alloys, with the exception of wear resistance, was determined at several temperatures ranging from 20° to 200° C. (68° to 390° F.), since it is in reality the properties at the higher temperatures that play the major part in determining the success or failure of a bearing metal under service conditions. The properties studied at these various temperatures included resistance to impact (Izod test) and to pounding (repeated impact), the strength in compression and Brinell hardness. Resistance to wear was determined only at 20° C. In addition to the laboratory tests, which included those items above described, service tests were run on a series of crank-shaft bearings, prepared of four compositions, and installed in United States Army class B trucks. The compositions of these alloys are listed in Table 2.

TABLE 2.—*Chemical composition of white-metal bearing alloys used in service tests*

Designation	Tin	Lead	Copper	Antimony	Barium	Calcium
	Per cent	*Per cent*	*Per cent*	*Per cent*	*Per cent*	*Per cent*
A [1]	90.48	0.58	4.26	4.69		
B [2]	90.0		10.0			
C [1]	3.27	82.52	.15	14.05		
D [2]		97.5			1.75	0.75

[1] Analysis by the Bohn Aluminum & Bronze Co. [2] Compositions are nominal values.

The wear test specimens were prepared by casting the white-metal alloy on the periphery of a bronze ring and were then finish machined. Resistance to wear was determined on the "universal Amsler wear testing machine" modified to permit testing under low loads and in the presence of kerosene.

The pounding, single-blow impact, and compression test specimens were chill cast, one-eighth inch oversize to allow for finish machining. The hardness specimens were chill-cast disks. The apparatus used in the pounding tests consisted essentially of a 2-pound hammer dropped through a distance of 2 inches on the specimen. The single-blow impact tests were made on an Izod impact machine of 120 foot-pound capacity. Brinell hardness numbers were determined with a

Rockwell hardness testing machine equipped with a 10-mm ball under a 60-kg load. A Riehle 10,000-pound capacity tension-compression machine was employed for the compression tests. A special strain gage was designed for measuring the deformation of specimens under compression at elevated temperatures. Each apparatus described,

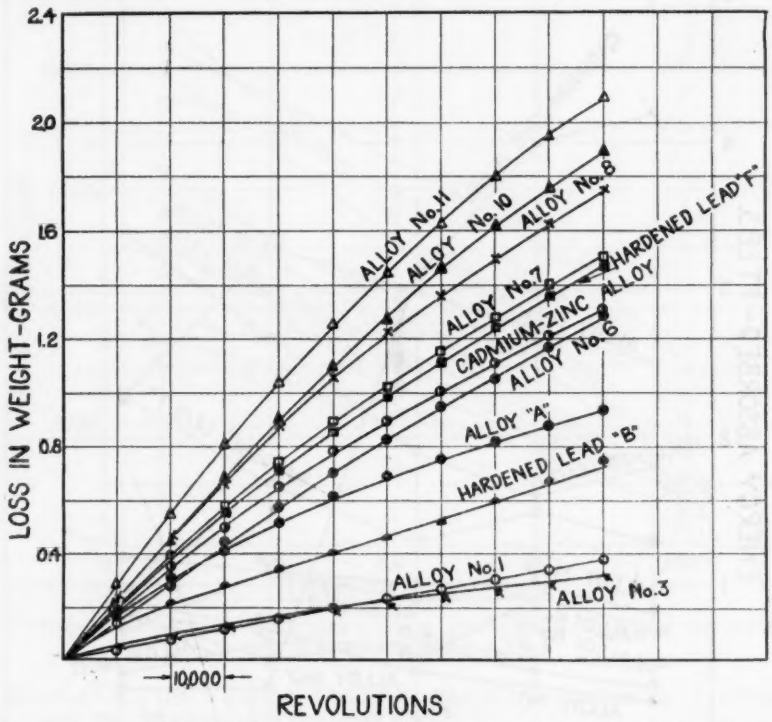

FIGURE 1.—*Relation between wear and revolutions for white-metal bearing alloys tested on Amsler wear testing machine*

All alloys were tested against S. A. E. No. 1045 steel heat treated to give a Brinell hardness number of 240.

with the exception of the Amsler wear machine, was equipped with a heating element to provide for the elevated temperature tests.

No one of the alloys considered was found to excel in all of the mechanical properties studied. Thus the tin-base alloys showed higher resistance to wear (fig. 1) and in most cases had higher Izod impact values (fig. 2) at each temperature of test than did the lead-base alloys. In most cases, however, the tin-base alloys showed lower

resistance to pounding than the lead-base and cadmium-zinc alloys. The hardness number and the compressive properties (fig. 3) of the tin-base alloys were found to be lower than those of the cadmium-zinc alloys and of the hardened-lead alloys F and B. The mechanical

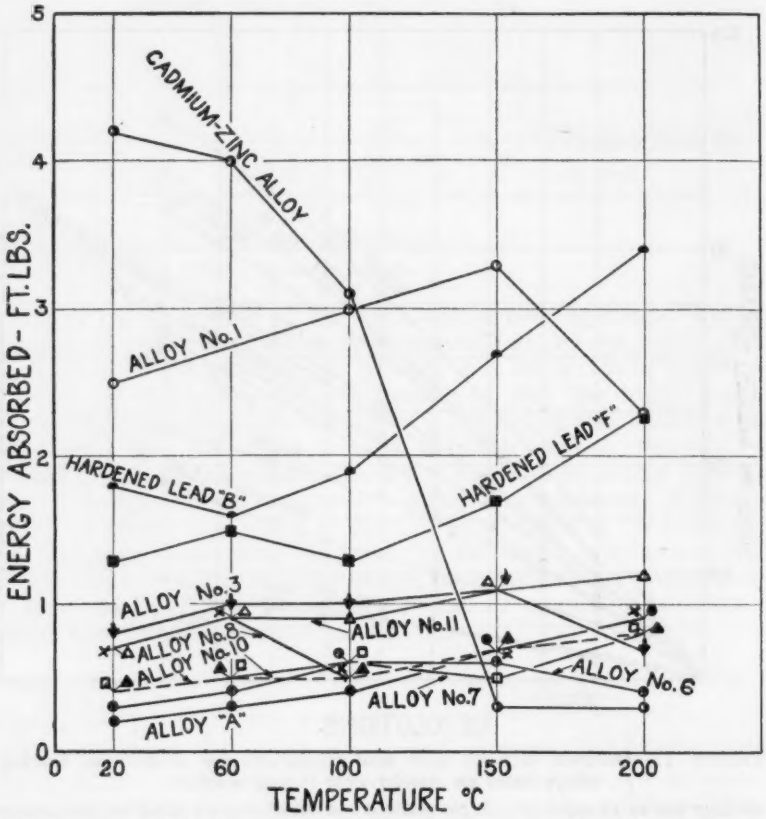

FIGURE 2.—*Effect of temperature upon the impact resistance (Izod test) of white-metal bearing alloys*

properties of the lead-antimony-tin alloys, in most cases, were higher as the tin content was increased.

The results obtained in the service tests showed that the tin-base alloys were superior in their wear resistance to both the hardened lead F and the lead-antimony-tin alloy containing about 3 per cent tin. These results were consistent with the laboratory results on wear.

Acknowledgments are due to the following companies who cooperated in various phases of the work described: The Bunting Brass & Bronze Co., the National Lead Co., the Bohn Aluminum & Bronze Co., and the Maywood Chemical Co.

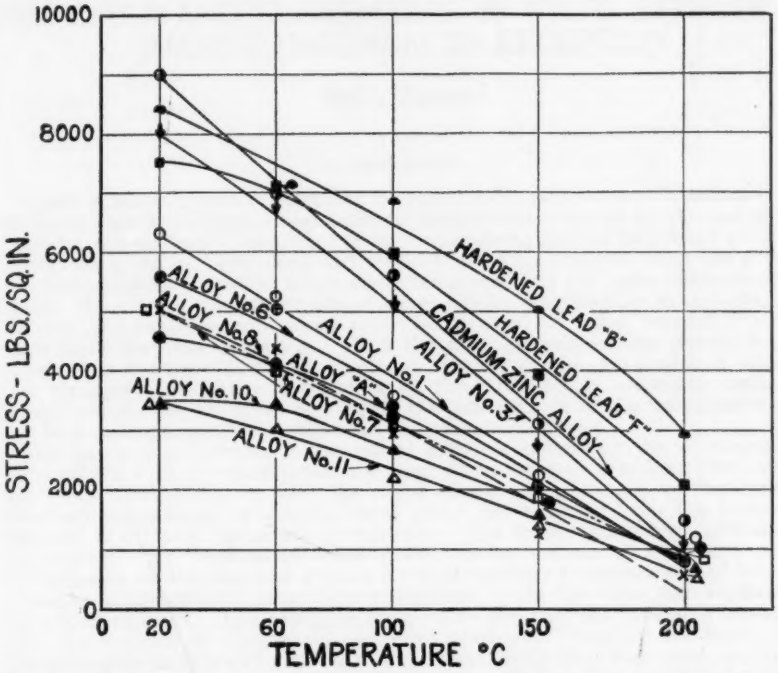

FIGURE 3.—*Relation of compression stress, producing 0.3 per cent deformation, to temperature of test*

WASHINGTON, October 8, 1932.

THE CAUSE AND ELIMINATION OF NIGHT EFFECTS IN RADIO RANGE-BEACON RECEPTION

By H. Diamond

ABSTRACT

A new antenna system is described for use at radio range-beacon stations which eliminates the troublesome night effects hitherto experienced in the use of the range-beacon system. Considerable data, comprising ground and flight measurements, are given on both aural and visual type range beacons using the present loop transmitting antennas, which show the severity of the night effects encountered. Because of the magnitude of these effects, particularly in mountainous country, the range-beacon course often becomes of no value beyond about 30 miles from the beacon station. With the new antenna system developed, referred to as the transmission-line antenna system, the beacon course is satisfactory throughout its entire distance range, the night effects becoming negligible. Experimental data are given comparing the performance of the transmission-line and loop antenna systems under nearly identical conditions.

The paper also includes a theoretical analysis explaining the occurrence of night effects with the range-beacon system when using loop transmitting antennas. The analysis shows that the night effects are produced by horizontally polarized components in the sky wave which are radiated from the horizontal elements of the loop transmitting antennas. The transmission-line antenna system employs four vertical antennas placed on the corners of a square; two of the antennas on the diagonal corners working together to replace one of the loop antennas of the present range-beacon stations, while the other two replace the other loop antenna. The principle upon which the antenna system is based has been the subject of considerable experimentation in England for some time. The arrangement employed differs in important particulars from ones previously used, and is the result of trial of a number of expedients. The significant element of the system consists of the use of transmission lines for confining the radiation to the four vertical antennas.

CONTENTS

	Page
I. Introduction	8
1. Nature of night effects	8
2. Factors influencing magnitude of night effects	9
II. Data on night effects for range beacons using loop transmitting antennas	9
1. Ground and flight observations on aural and visual type range beacons	9
2. Variable nature of night effects	12
3. Automatic recording of night effects	16
III. Theory of night effects	17
IV. Experimental work on special transmitting antennas	19
1. Early work	19
2. Special test	20
3. Experimental work on early arrangements	21
4. Night observations on Marconi-Adcock antenna	22
V. Transmission-line antenna system	23
1. Electrical-circuit arrangement	24
2. Experimental installations	25
3. Elimination of night effects with transmission-line antenna system	26
4. Polarization of wave at receiving point	29
5. Electrical performance of TL-antenna system	29
6. Obstruction lighting of TL-antenna system	33
VI. Acknowledgment	34

I. INTRODUCTION

During the past year, the research division of the Aeronautics Branch, Department of Commerce, located at the Bureau of Standards, has carried on an extensive research program on the problem of night effects; that is, the course variations occurring in the use of the radio range-beacon system at night. The characteristics and cause of the night effects have been determined, and a new transmitting antenna system has been developed for the range-beacon stations which eliminates these troublesome effects. For reasons which will become apparent from the description of the new antenna system, it has been named the transmission-line antenna system (abbreviated TL-antenna). This paper presents a theoretical analysis of the phenomena underlying the occurrence of night effects with the range-beacon system and gives full details of the new transmitting antenna, including the experimental work leading up to its development. In addition, the results are given of a large number of measurements on range-beacon stations using the present loop-antenna system and on two experimental installations using the new transmission-line antenna system. The data include measurements at night at varying distance from the respective beacon stations, both on the ground and in the air, and give comparative results under nearly identical conditions for the conventional loop antenna system and for the new TL-antenna system.

1. NATURE OF NIGHT EFFECTS

Night effects are inherent in practically every system of radio direction determination which makes use of the directional properties of the loop antenna, and have been the subject of considerable study and experimental work for some time, notably in England. Night effects in connection with the use of the radio range-beacon system in the United States were first observed by Pratt,[1] in 1927, in night flights on the aural type beacon at Bellefonte, Pa. With the radio range beacon these effects take the form of rapid and irregular variation of the indicated beacon courses, so that an airplane following the true course will receive, in varying amounts, off-course indications to the right, off-course indications to the left, and on-course indications. When the fluctuations of the indicated course are less than about $\pm 10°$, it is feasible for the pilot to follow the true course by averaging a large number of successive course indications, but only with a fair degree of accuracy. When the course variations exceed 10° by an appreciable amount, it is not possible for the pilot to follow the true course, even by the averaging process. Such large night effects are common in mountainous country, beginning at distances from 20 to 50 miles from the range-beacon station. Beyond about 30 miles the beacon course becomes of no value. These facts, definitely established by the research work of the past year to be characteristic of range beacons employing the present loop antenna system, indicated clearly that the range beacons would be of little use at night in mountainous terrain, where they are most needed, unless means could be developed to elminate these errors.

[1] H. Pratt, Apparent Night Variations With Crossed-coil Radio Beacons, Proc. I. R. E., vol. 16, pp. 652-657, May, 1928.

2. FACTORS INFLUENCING MAGNITUDE OF NIGHT EFFECTS

It has been found that the magnitude of the night effects is greatest during winter nights, next during summer nights, next during winter days (particularly within a few hours of sunrise and sunset), and, finally, is least during summer days. Because of the negligible occurrence of course variations obtained during the daytime, the term "night effects" has been applied to this phenomenon. Other factors, in addition to time and season of the year, have considerable influence upon the magnitude of the night effects. Some of these are: Nature of the terrain over which the range-beacon wave is transmitted, location of the transmitting and receiving points, distance of the receiving location from the transmitting station, and form of the receiving antenna. A qualitative measure of the degree of influence of these factors will appear from the data given in this paper. In general, the night effects are most pronounced over mountainous terrain, and the magnitude of the course variations increases with distance of the receiving point from the transmitting station. The influence of time of day, season of year, nature of the terrain, and distance from the transmitting station is about the same as in radio direction finding, thus bearing out conclusions by Smith-Rose [2] on the reversibility of night effects in directional reception and transmission.

It is interesting to note that the type of signal used for the course indications has no bearing upon the magnitude of the night effects. A series of ground measurements made on the Washington and Bellefonte aural beacons and the College Park and Bellefonte visual beacons, at distances from the respective beacon stations ranging from 35 to 100 miles, showed the magnitude of course variations with the two types of beacons to be the same. Full corroboration of these results was later obtained in a large number of night test flights on the range beacons located on the Midcontinent Airway between Albuquerque, N. Mex., and Los Angeles, Calif. The range beacons were tested under identical conditions, first using aural and then visual operation, and the average night effects obtained were the same with both. In addition, a special test was carried out to examine the phenomena underlying the night effects. This test showed that the night effects were due entirely to the type of transmitting antenna employed, and were therefore the same for the two types of beacons, since they employ the same antenna systems.

Typical data which lead to the conclusions outlined in the foregoing discussion on the properties and behavior of night effects are given in the next section.

II. DATA ON NIGHT EFFECTS FOR RANGE BEACONS USING LOOP TRANSMITTING ANTENNAS

1. GROUND AND FLIGHT OBSERVATIONS ON AURAL AND VISUAL TYPE RADIO RANGE BEACONS

The data given in Figure 1 (*a*) to (*d*), inclusive, represent typical night effects obtained during ground observations on the Washington (D. C.) aural and the College Park (Md.) visual radio range beacons.

[2] R. L. Smith-Rose, Radio direction Finding by Transmission and Reception, Proc. I. R. E., vol. 17, pp. 425–478, March, 1929.

Figure 1 (*a*) and (*b*) are for the aural beacon and Figure 1 (*c*) and (*d*) for the visual beacon. The beacons were operating on 272 and 290 kc, respectively. The receiving point was, respectively, at 60 and 95 miles from the beacon stations, being chosen so that at least one mountain range lay between the receiving and transmitting points. A large number of observations of this type were taken on

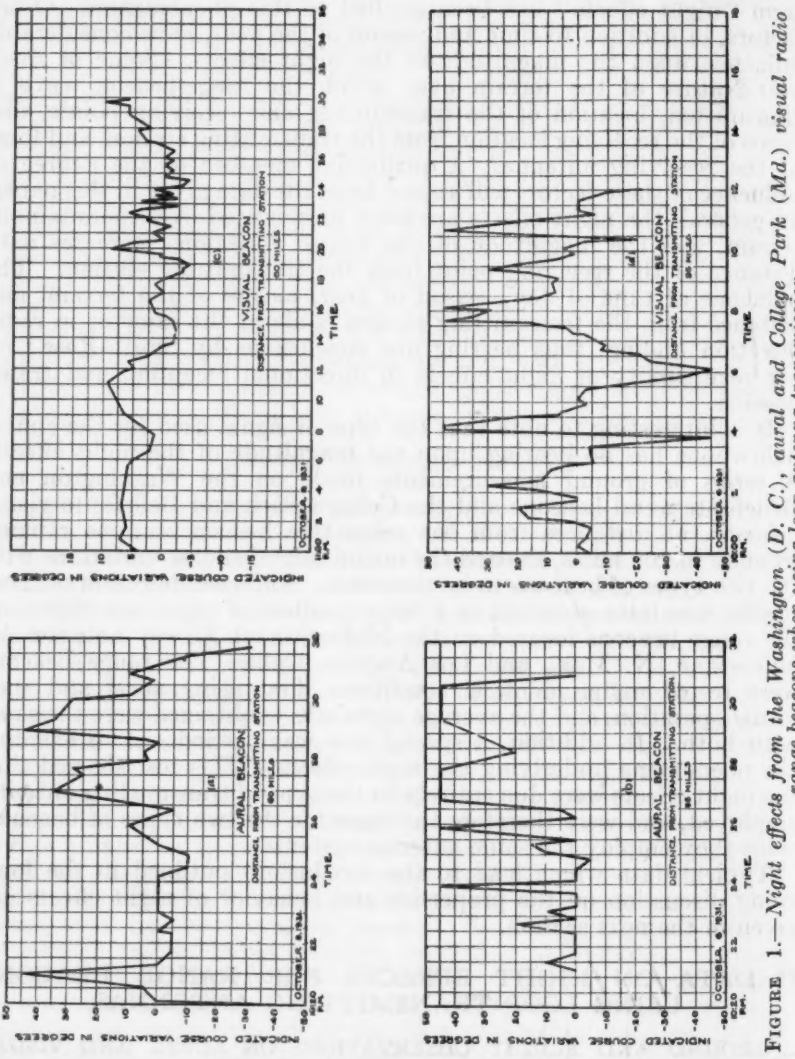

FIGURE 1.—*Night effects from the Washington (D. C.), aural and College Park (Md.) visual radio range beacons when using loop antenna transmission*

the two beacon stations mentioned and also on the aural and visual type beacons at Bellefonte, Pa. (284 and 326 kc respectively), to secure information on the magnitude of the night effects to be expected with the two types of beacons at varying distances from the stations. Measurements were made at distances ranging from 30 to 100 miles. These measurements showed that the night effects for the two types of beacons, although apt to be quite different over a

short interval, became very nearly equal when averaged over a longer period of time. Also the magnitude of the night effects increased with increasing distance from the transmitting stations.

Additional data for night effects from both types of beacons over mountainous terrain are given in Figure 2. The measurements were taken at St. Thomas, Pa., chosen because of its location in the Allegheny Mountains and because the courses from the four stations could be made to intersect at that point without interrupting service from the aural beacons. St. Thomas is about 70 miles south of Bellefonte and 80 miles northwest of Washington.

A study of Figures 1 and 2 shows that the average night effects are very nearly of the same magnitude for either aural or visual type beacons. As will be shown later in this paper this is in strict accordance with the theoretical considerations of the problem. Corroboration of this conclusion was had from the results of night flight tests on the

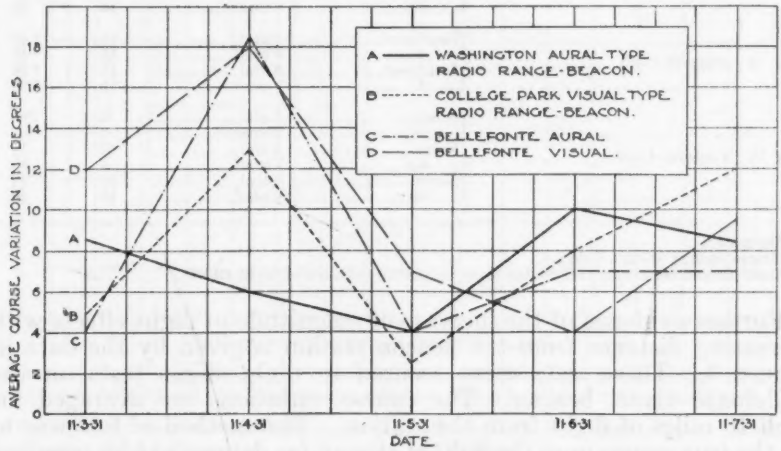

FIGURE 2.—*Summary of data on the Washington aural beacon, the College Park visual beacon, and the Bellefonte aural and visual beacons taken at St. Thomas, Pa., 70 miles south of Bellefonte and 80 miles northwest of Washington*

Courses from all the beacons intersected at this point.

radio range beacons between Albuquerque, N. Mex., and Fontana, Calif., on the Midcontinent Airway. The tests on each of these range beacons comprised four complete night flights, two of which were with aural and two with visual operation. The procedure was to follow the west course of each beacon away from the station using aural operation, return using visual operation, follow the east course away from the station using visual operation and return again to the station using aural operation. In this way the behavior of the night effects with each type of operation under nearly identical conditions could be determined. The essential results obtained are given in Table 1. Referring to Table 1, the distance of no night effects was considered to be that in which the variation of the indicated beacon course was less than $\pm 3°$. The limit of useful distance range of the course was determined on the basis of two criteria; first, that the course variations exceeded $\pm 12°$, and secondly that off-course excursions of 6 to 8 miles produced no apparent change in the average course indication.

TABLE 1.—*Representative results of night flights on Midcontinent Airway radio range beacons showing night effects as a function of type of beacon operation (aural or visual) and of distance from the beacon station*

Date	Range-beacon station	Course	Type of operation	Distance of no night effects	Limit of useful distance range
				Miles	*Miles*
1932 Mar. 28	Albuquerque, N. Mex.	West	Aural	25	40–45
		do	Visual	25	40
		East	Aural	20	40
		do	Visual	20	40
Apr. 4	Winslow, Ariz.	West	Aural	30	[1] 70
		do	Visual	30	[1] 70
		East	Aural	30	70
		do	Visual	30	70
Apr. 13	Kingman, Ariz.	West	Aural	15–20	35–40
		do	Visual	15–20	35–40
		East	Aural	10	35
		do	Visual	10	35
May 3	Daggett, Calif.	Southwest	Aural	15	[2] 40
		do	Visual	15	[2] 40
		Southeast	Aural	15	[1] 70
		do	Visual	15	[1] 70
May 15	Fontana, Calif.	West	Aural	6	([3])
		do	Visual	6	([3])
		East	Aural	6	15
		do	Visual	6	15
		North	Aural	10	20
		do	Visual	10	20

[1] Estimated.
[2] Course ends at Mount Baldy.
[3] Multiple and bent course effects too severe to permit estimate of night effects.

Further evidence of the increase of magnitude of night effects with increasing distance from the beacon station is given by the data in Figure 3. These data were secured in night flight tests on the Bellefonte visual beacon. The course variations are averaged for each 10 miles of flight from the station. The method of test was to fly the true course over the lighted airway (as determined by previous flight tests during the daytime) and to record departures of the course indications from an "on-course" reading. Readings were taken only for each change in course indication. The number of readings for a given 10-mile period therefore serves as a measure of the frequency of occurrence of the night effects.

2. VARIABLE NATURE OF NIGHT EFFECTS

Besides showing the relation between magnitude of night effects and distance from the station Figure 3 also indicates the difference in the magnitude of night effects obtained on different nights. Table 2 gives a summary of measurements on the College Park visual beacon over a period of about a month. Most of the measurements were made at Front Royal, Va., located 65 miles due west of College Park beyond the first ridge of the Blue Ridge mountains. The

time of each test was from about 8 p. m. to midnight except where otherwise stated in Table 2. During six of the tests simultaneous measurements were made (on a 90° course of the College Park beacon) at Richmond, Va., about 105 miles south of College Park over flat terrain. The third column of Table 2 gives the average of all the course variations observed during a given night's test. The number of readings taken during each test is given in the fourth column. The fifth column gives the percentage of these readings

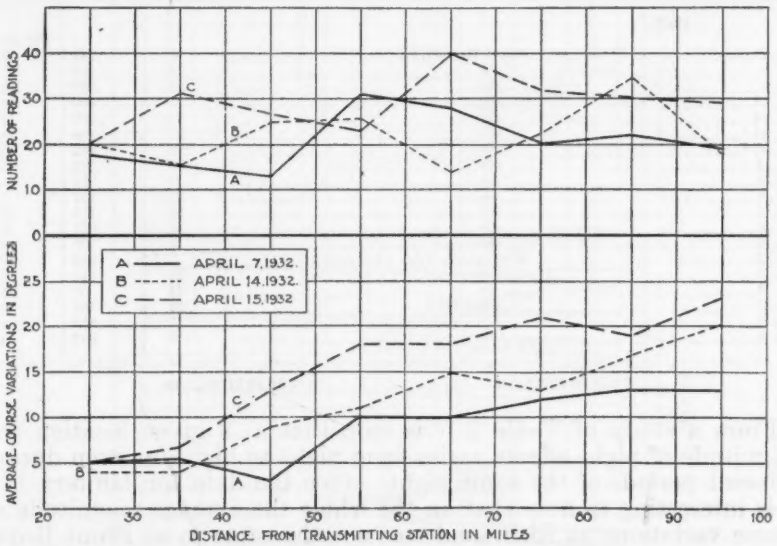
NUMBER OF READINGS
AVERAGE COURSE VARIATIONS IN DEGREES
A —— APRIL 7,1932.
B ------ APRIL 14,1932.
C — — APRIL 15,1932
DISTANCE FROM TRANSMITTING STATION IN MILES

FIGURE 3.—*Summary of night observations in an airplane on the night effects from the Bellefonte visual radio range beacon using loop transmitting antennas*

These graphs show the average course variations as a function of distance from the beacon station.

for which the course variations were ±45°. The third, fourth, and fifth columns combine to give a fair picture of the severity and frequency of occurrence of the course variations. The 45° readings represent the maximum course variations observed; being the maximum off-course indication which can be read with either the aural or visual type beacon. With the radio range-beacon system, a swing off-course greater than 45° by a given amount gives the same course indications as a swing less than 45° by the same amount. Thus, for example, a 60° swing is of necessity recorded and plotted as a 30° swing.

TABLE 2.—*Summary of measurements taken at Front Royal and Richmond, Va., on College Park visual radio range beacon*

Front Royal is 65 miles due west of College Park beyond the first range of the Blue Ridge Mountains, while Richmond is 105 miles south of College Park over flat terrain.

Date	Receiving location	Average course variations (in degrees)	Total readings	45° readings
1932				*Per cent*
Jan. 2	Front Royal, Va.	14	243	8.6
Jan. 7	do	26	225	27.5
Jan. 8	do	20	350	20.3
Jan. 13	do	21	420	16.0
Jan. 14	do	24	290	15.0
Jan. 15 [1]	do	18	198	19.2
Jan. 15 [2]	do	29	262	44.3
Feb. 2	do	10	383	2.9
Feb. 3	do	8	301	.3
Feb. 4	do	10.5	191	2.6
Feb. 5	do	14	415	10.3
Feb. 6	do	14	351	10.8
Feb. 9	do	7	286	0
Feb. 2	Richmond, Va.	3.7	216	0
Feb. 3	do	25	312	23.0
Feb. 4	do	23	66	16.7
Feb. 5	do	12	167	11.4
Feb. 6	do	11	416	6.5
Feb. 9	do	8	311	1.6

[1] 8.38 to 9.52 p. m. [2] 10.10 to 11.25 p. m.

From a study of Table 2 it is seen that at a given location the magnitude of night effects varies from night to night, or even during different periods of the same night. (See the data for January 15.) It is interesting to note that on the whole the average magnitude of course variations at Richmond was not the same as at Front Royal on corresponding nights.

A summary of similar data for the Bellefonte visual beacon, using loop antennas, is given in the third and fourth columns of Table 5. The receiving point was at Sunbury, Pa., about 50 miles east of Bellefonte and separated from Bellefonte by several mountain ranges. The variability of the magnitude of the night effects from night to night is again evident. In interpreting the data given in the tables, particularly with regard to the numerical average of the course variations for a given run, it should be remembered that course variations greater than 45° by a given amount are recorded as variations less than 45° by the same amount. In this way the value of the average given for nights having large night effects is smaller than the true average. A special test was made to determine the extent of course variations exceeding 45°. The data obtained is plotted in Figure 4, and was secured by orienting the beacon space pattern so that the receiving point was 45° to one side of a true course. On-course indications then corresponded to 45° variations and off-course indications (to the other side of the course) corresponded to variations greater than 45°. Obviously, 90° variations were the maximum that could be secured with this test. As will be seen from Figure 4, a number of such variations were observed.

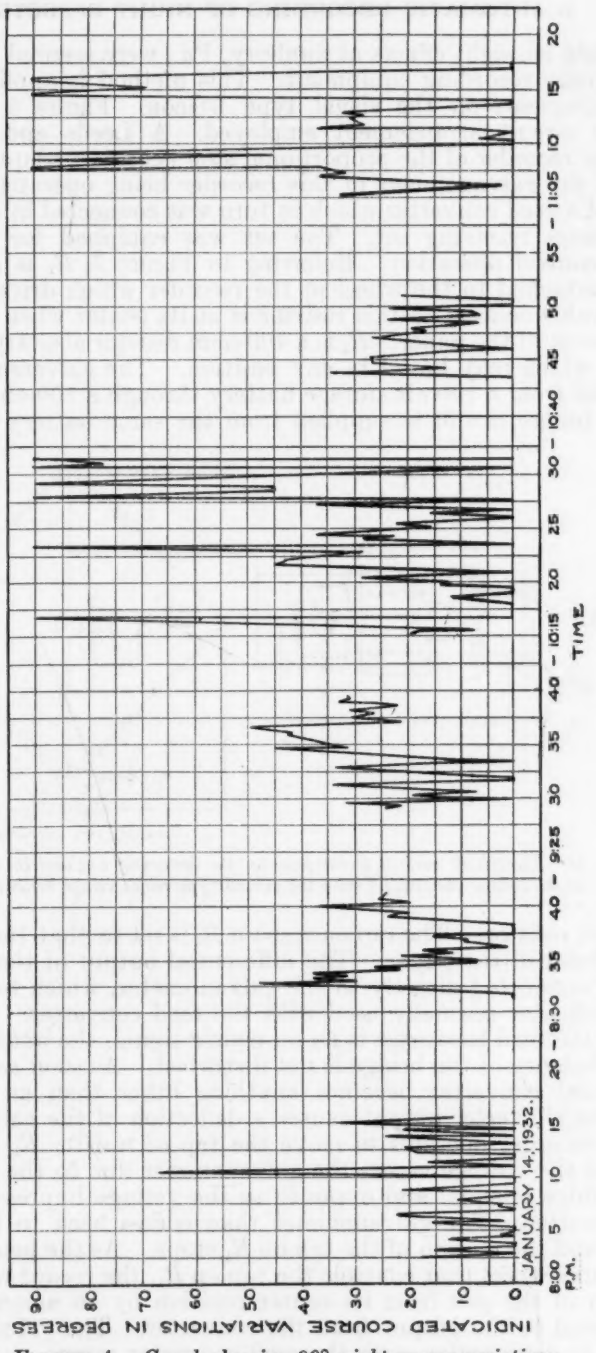

FIGURE 4.—*Graph showing 90° night course variations*

Observations taken on College Park visual radio range beacon at receiving point 65 miles west of College Park

3. AUTOMATIC RECORDING OF NIGHT EFFECTS

The data on night effects at Sunbury, Pa., were secured by the use of automatic recording equipment. This method is applicable only to measurements on the visual type beacon. Figure 5 shows the electrical circuit arrangement employed. A Leeds and Northrup frequency recorder of the proportional step type was adapted for this purpose, the galvanometer of this recorder being operated from the output of a reed converter which in turn was connected in the output of a beacon receiving set. The set was equipped for automatic volume control operation. Referring to Figure 5, R_1 is a 200-ohm resistor attached to the wheel in the recorder which drives the pen. The movable contact to this resistor is at its center when the pen is at the center of the paper. R_2 is a 400-ohm resistor also with a sliding contact, which may be set in any position. The galvanometer field is supplied from a 10-volt storage battery through a 100-ohm resistor, and the bridge circuit is supplied from the same battery through a

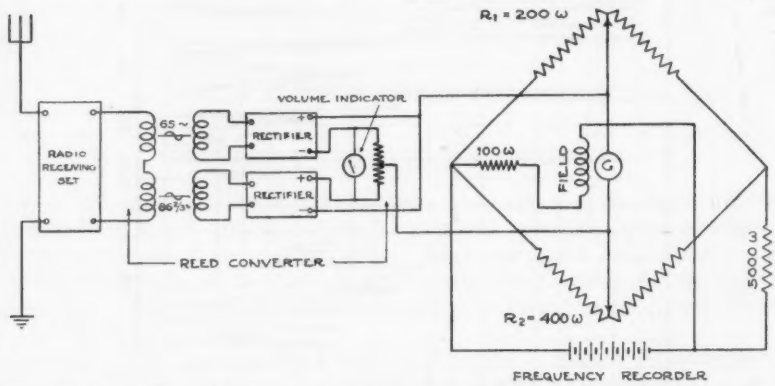

FIGURE 5.—*Electrical circuit arrangement for securing automatic records of night course variations with the visual type radio range beacon*

5,000-ohm resistor. The tap on resistor R_2 is set so that the pen runs at the center of the paper. The differential output of the reed converter is connected directly to the galvanometer, which replaces the course indicator normally used with the reed converter. When the input to the reed converter is an on-course signal, the output is zero, and the balance of the bridge is not disturbed. As soon as the input to the reed converter becomes anything other than an on-course signal, the converter output causes a deflection of the galvanometer and the recorder operates to move the tap of resistor R_1 to a point such that the voltage across the galvanometer due to the unbalance of the bridge is equal and opposite to the voltage impressed by the reed converter. The galvanometer than comes back to its normal position and the motion of the tap on R_1 stops. As the pen is carried by the same wheel that controls the tap on R_1, the record will show a deflection of the pen from its center position by an amount that is proportional to the output from the converter. The volume indicator used in conjunction with the reed converter serves as a check of the degree of automatic volume control attained with the receiving

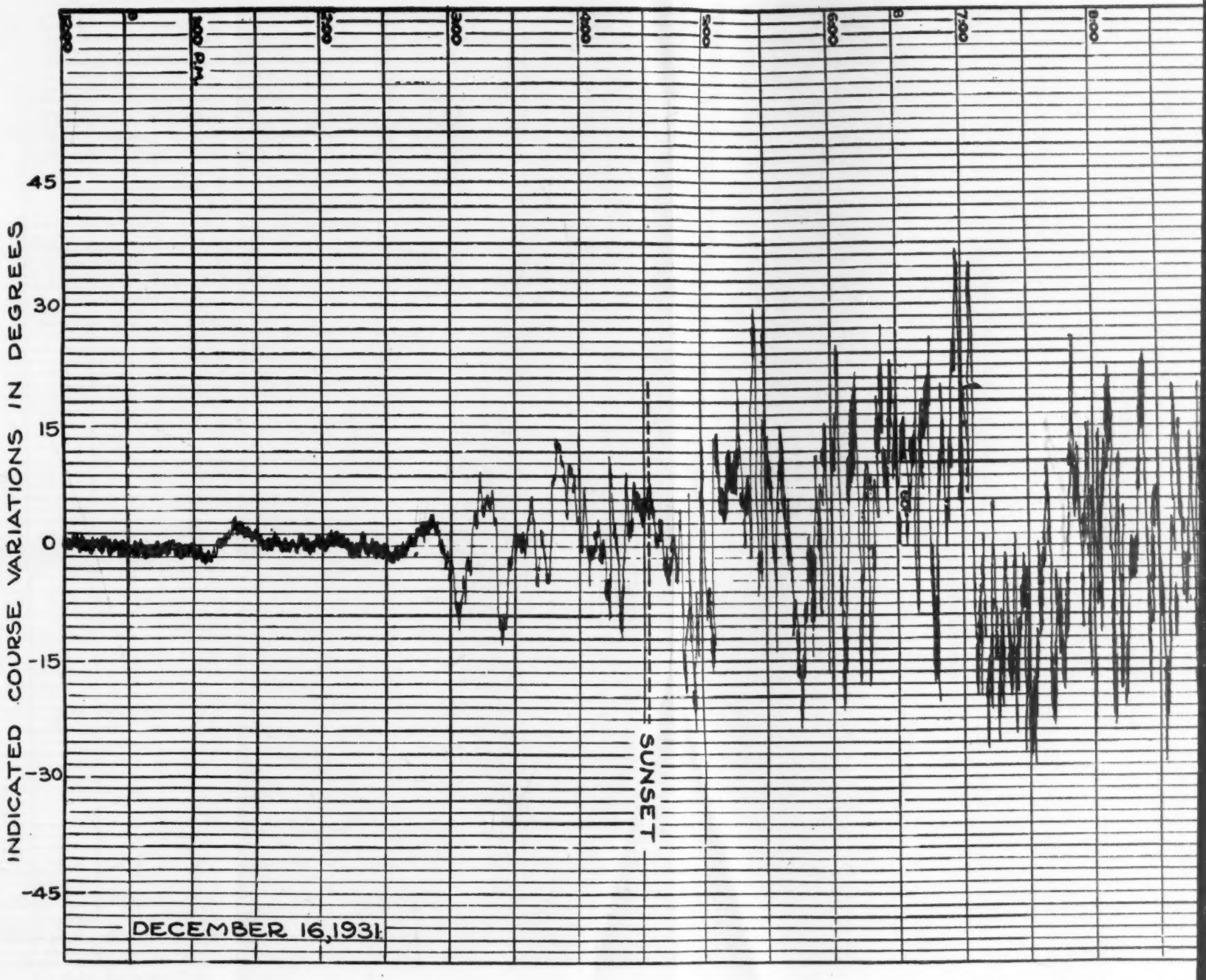

148938—33. (Face p. 17.)

FIGURE 6.—*Automatic records of t*

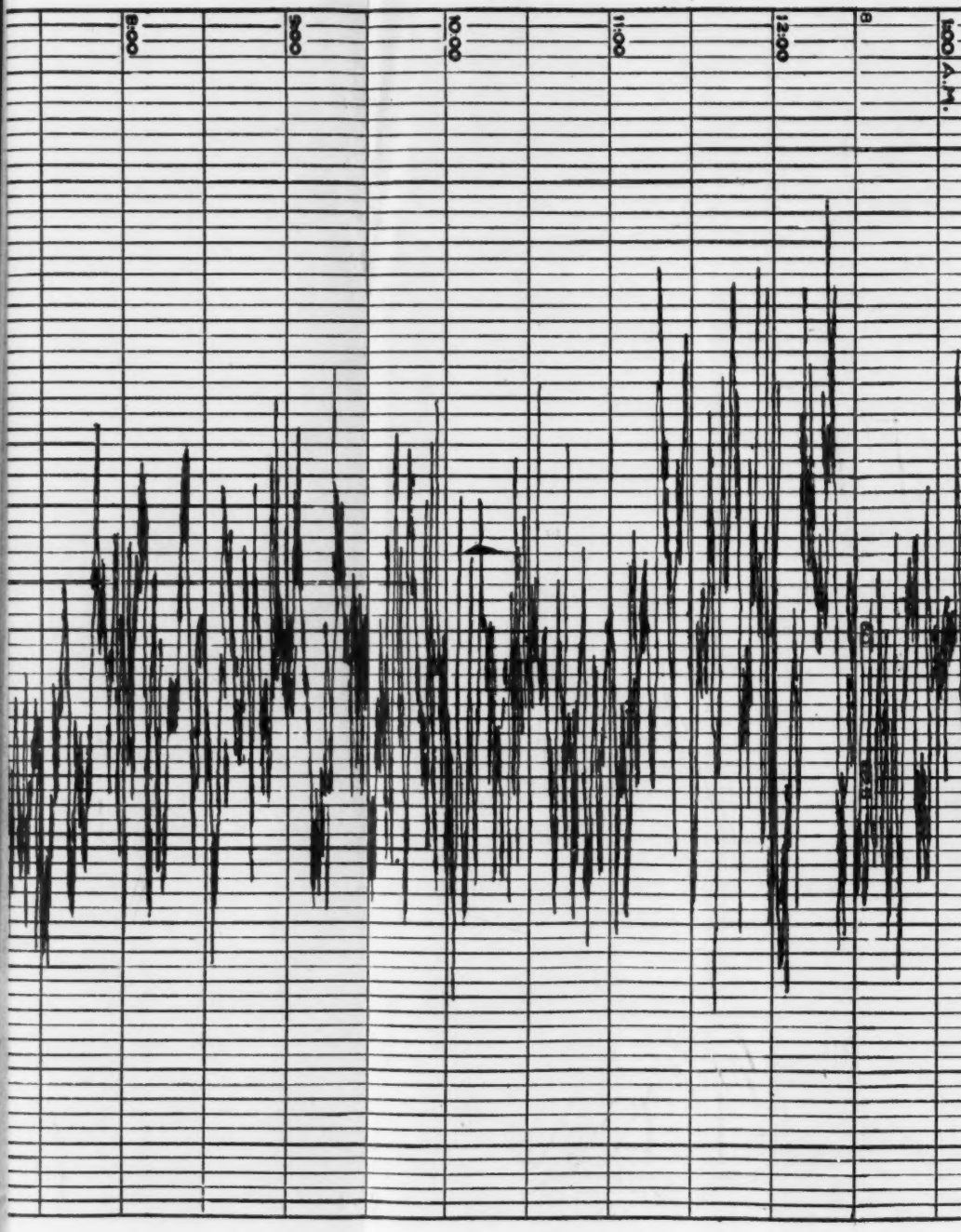

6.—*Automatic records of the indicated beacon course corresponding to a 24-hour run on the Daggett (Cali*

Receiving station at Kingman, Ariz., approximately 175 miles from

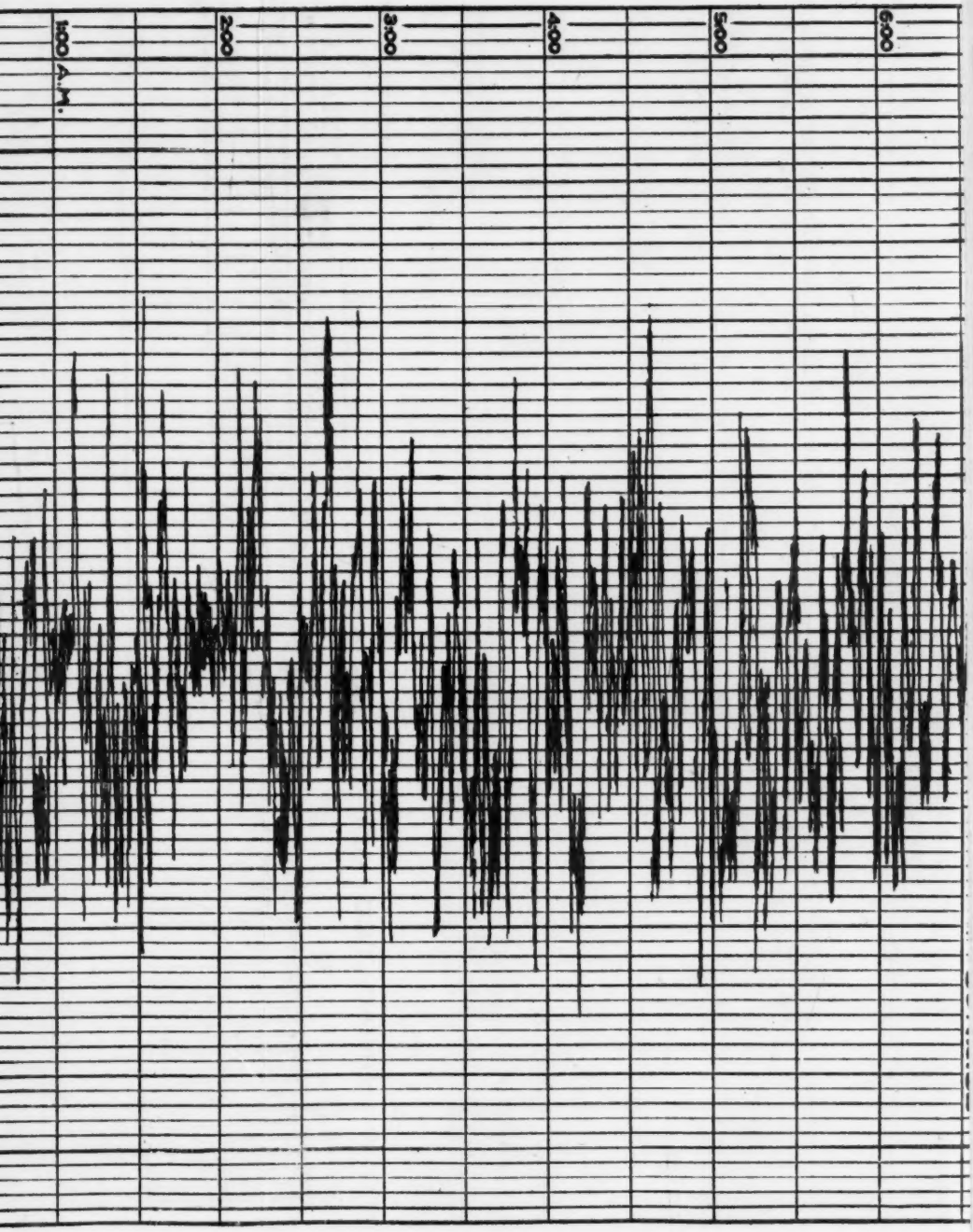

gett (Calif.) visual type radio range beacon using loop antenna transmission

miles from Daggett.

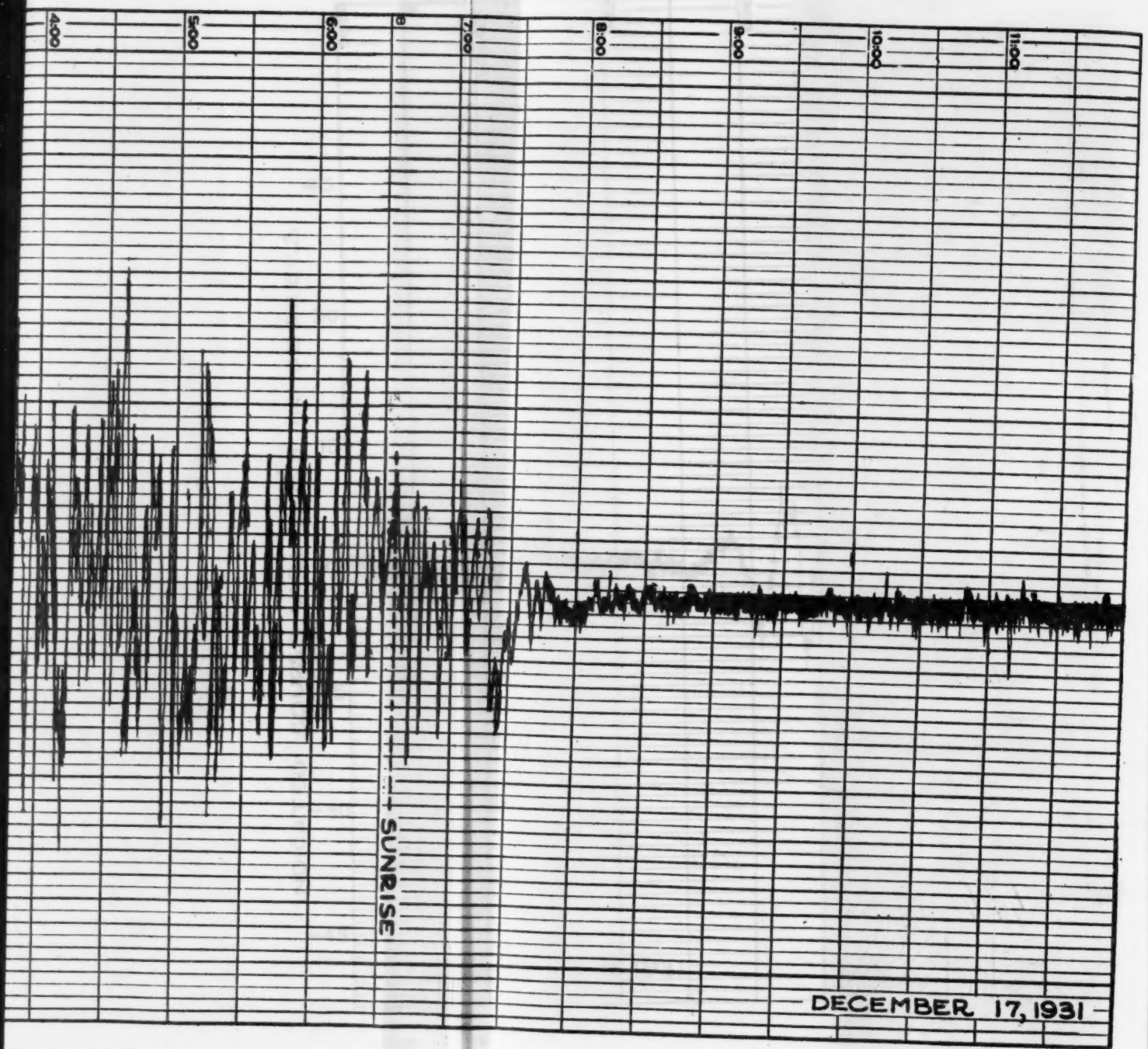

tenna transmission

set, so that the record may be corrected for changes in volume if found necessary.

A typical record obtained with this arrangement is shown in Figure 6. The record represents a continuous 24-hour run on the Daggett (Calif.) range beacon taken on December 16 to 17, inclusive, 1931. The receiving station was at Kingman, Ariz., about 175 miles from Daggett. This record is of interest in that it shows the magnitude of the course variations as a function of time of day (during the late fall season). Note that the night effects begin about two hours before sunset and occur throughout the night until about one hour after sunrise.

III. THEORY OF NIGHT EFFECTS

The theory underlying the production of night effects with the radio range beacon system using loop transmitting antennas will now be briefly outlined. The three component electric fields radiated from a loop transmitting antenna are:[3]

(*a*) Vertically polarized electric field

$$E_1 = E_0 \cos\alpha\cos\beta \tag{1}$$

(*b*) Horizontally polarized electric field, in plane of propagation of radio wave

$$E_2 = E_0 \cos\alpha\sin\beta \tag{2}$$

(*c*) Horizontally polarized electric field, perpendicular to plane of propagation

$$E_3 = E_0 \sin\alpha\sin\beta \tag{3}$$

In these equations α is the angle between the plane of propagation and the plane including the loop antenna, while β is the angle of elevation. The plane of propagation is the vertical plane containing the transmitting and receiving points. As will be shown, it is the horizontally polarized electric field component (E_3) perpendicular to the plane of propagation, which is responsible for the production of night effects. It is important to note that this component is produced entirely by radiation from the horizontal wires of the transmitting loop antenna.

Consider now the electric field received at a distant receiving point having substantially zero angle of elevation with respect to the transmitter. In the daytime, the first component only is received. This is the ground wave. The voltage induced in a vertical receiving antenna by the ground wave is given by

$$E_A' = K_0 E_0 \cos\alpha\cos\omega_0 t \tag{4}$$

where K_0 is a factor incorporating the efficiency of the receiving antenna and attenuation of the ground wave and $\omega_0 = 2\pi \times$ frequency. At night, in addition to the ground wave, an indirect wave reflected from the Kennelly-Heaviside layer is received. This wave contains all three component electric fields. It is well known, however, that the state of polarization of the electric field in the indirect wave received may be different from that for the field transmitted by the

[3] W. H. Murphy, Space Characteristics of Antennas, J. Frank. Inst., vol. 201, p. 424, 1926.

loop antenna, rotation of the plane of polarization taking place during reflection from the ionized layer. Let us now consider the voltage induced in a vertical receiving antenna by the indirect wave. We will assume that the rotation of plane of polarization occurs about the line indicating direction of propagation of the wave as an axis. Voltage is then induced in the vertical receiving antenna not only by the portion of the first electric field component still remaining vertically polarized but also by the portions of the second and third components which have become vertically polarized due to the rotation of the plane of polarization. The induced voltage becomes:

$$\begin{aligned} E_A'' = {} & E_0(1+\rho_v)\{K_1\cos\beta + K_2\sin\beta\}\cos\alpha\cos(\omega_0 t+\varphi) \\ & + E_0(1+\rho_v)\{K_3\sin\beta\}\sin\alpha\cos(\omega_0 t+\varphi) \end{aligned} \tag{5}$$

where

ρ_v = coefficient of reflection at the ground for vertically polarized waves arriving at an angle of incidence $(90°-\beta)$.

K_1, K_2, and K_3 are factors by which the original electric field components must be multiplied to obtain the portions remaining in or rotated into the vertical plane. These factors also include the effect of attenuation.

ϕ = time phase angle between indirect and ground waves.

The total induced voltage in the vertical receiving antenna produced by the ground and indirect waves is therefore

$$\begin{aligned} E_A = {} & K_0 E_0\cos\alpha\cos\omega_0 t \\ & + E_0(1+\rho_v)\{K_1\cos\beta + K_2\sin\beta\}\cos\alpha\cos(\omega_0 t+\varphi) \\ & + E_0(1+\rho_v)\{K_3\sin\beta\}\sin\alpha\cos(\omega_0 t+)\varphi \end{aligned} \tag{6}$$

Similarly, the voltage induced in a vertical receiving antenna by a second loop transmitting antenna crossed at right angles to the first is given by equation (7).

$$\begin{aligned} E_B = {} & K_0 E_0\sin\alpha\cos\omega_0 t \\ & + E_0(1+\rho_v)\{K_1\cos\beta + K_2\sin\beta\}\sin\alpha\cos(\omega_0 t+\varphi) \\ & - E_0(1+\rho_v)\{K_3\sin\beta\}\cos\alpha\cos(\omega_0 t+\varphi) \end{aligned} \tag{7}$$

Equations (6) and (7) represent the two voltages induced in a vertical antenna by the wave radiated from a radio range-beacon station. A beacon course is produced when the two induced voltages are equal. During the daytime (since only the ground wave is received) this occurs when $|\cos\alpha| = |\sin\alpha|$ or at $\alpha = 45°$, 135°, 225°, and 315°. At night, courses occur when the right-hand sides of equations (6) and (7) are equal. Assuming values of

$$\begin{aligned} &\beta = 60° \qquad K_0 = 1 \qquad E_0 = 1 \\ &1+\rho_v = 1.9 \qquad K_1 = K_2 = K_3 = 0.5 \\ &\varphi = \pi \end{aligned}$$

we obtain

$$E_A = -0.3\cos\alpha - 0.82\sin\alpha \tag{8}$$

$$E_B = -0.3\sin\alpha + 0.82\cos\alpha \tag{9}$$

Solving for $|E_A| = |E_B|$ gives

$$\alpha = 25°,\ 115°,\ 205°,\ \text{and}\ 295° \tag{10}$$

The effect of the indirect wave is thus to cause a virtual rotation of the beacon space pattern. The rotational effect is obviously produced by the third terms of the right-hand sides of equations (6) and (7). These correspond to the electric field components which were originally horizontally polarized perpendicular to the plane of propagation when transmitted from the loop antenna, but which have been rotated in part into the vertical plane through rotation of the plane of polarization of the total electric field. The degree of rotation of the beacon space pattern will obviously depend upon the magnitudes of these components in relation to the other components represented in equations (6) and (7), and will vary irregularly as this relation changes. Such change occurs whenever the indirect wave changes in magnitude, phase, or state of polarization, all of which depend upon the refractive properties of the ionized layer.

It is to be noted that the above conception of a rotating or swinging beacon space pattern is not strictly correct, since it requires that the conditions governing the reflection of the sky wave at the ionized layer be the same in all directions about the range-beacon station. However, the analysis outlined gives a fair conception of what occurs in so far as a given receiving point is concerned.

IV. EXPERIMENTAL WORK ON SPECIAL TRANSMITTING ANTENNAS

Since it is apparent from the above analysis that the night effects are produced by the horizontally polarized electric field components radiated from the horizontal members of the transmitting loop antennas, the indicated cure is to eliminate or neutralize such radiation.

1. EARLY WORK

The influence of the horizontal elements of a loop antenna upon the production of night effects was determined a number of years ago in application to direction finding systems using loop antennas for reception. An antenna having the same directional properties as the loop antenna but free from the effects of the horizontal elements was described in a British patent [4] issued to R. E. Ellis in 1919. The principle involved has also been variously attributed to F. Adcock and T. L. Eckersley.[5] Adcock was apparently the first to make experiments based on the principle. The application of the same principle to directional transmitting antennas appeared in a British patent [6] issued to J. Robinson, H. L. Crowther, and W. H. Derriman in 1923. Considerable study and experimental work on the development of this type of antenna system for direction finding purposes [7] and for use with the rotating beacon transmitter [8] have been carried on by Smith-Rose and Barfield since 1926. The antenna system described in this paper is based on the same fundamental principle. However, the arrangement employed differs in important particulars from ones previously used and is the result of actual trial of a number

[4] British patent 130490.
[5] T. L. Eckersley, The Effect of the Heaviside Layer on the Apparent Direction of Electromagnetic Waves, Radio Review, vol. 2, pp. 60 and 231, 1921.
[6] British patent 198522.
[7] R. L. Smith-Rose and R. H. Barfield, The Cause and Elimination of Night Errors in Radio Direction-Finding, J. I. E. E., vol 64, pp. 831–838, 1926. R. H. Barfield, Recent Developments in Direction Finding Apparatus, J. I. E. E., vol. 68, pp. 1052–1069, 1930.
[8] R. L. Smith-Rose, A Theoretical Discussion of Various Possible Aerial Arrangements for Rotating Beacon Transmitters, J. I. E. E., vol. 66, pp. 270–274, 1928.

of expedients. Several of the older arrangements were tried and found unsuitable.

2. SPECIAL TEST

Before beginning a detailed account of the experimental work leading up to the development of the new antenna system, it is of interest to describe a special test from which representative results are shown in Figure 7. This test was devised to determine whether other factors in addition to the rotational effect described in Section III contributed to the production of night effects, particularly with the visual type beacon. It was considered necessary to prove that the influence of selective audio fading, phase distortion, and other similar phenomena was negligible before proceeding with the problem of eliminating the radiation from the horizontal elements of the loop transmitting antennas. The test consisted of observing the apparent

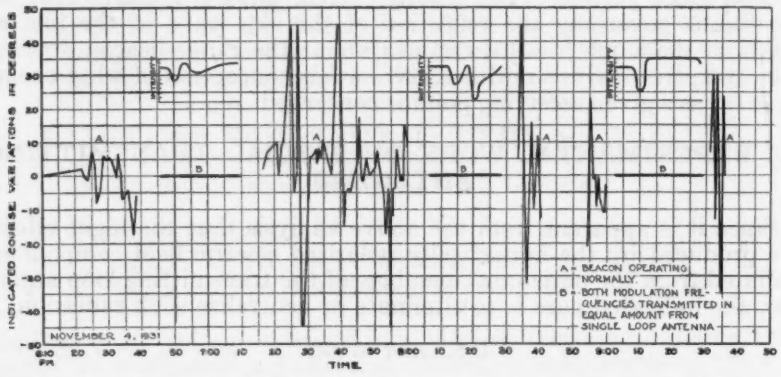
INDICATED COURSE VARIATIONS IN DEGREES
NOVEMBER 4, 1931
TIME
A - BEACON OPERATING NORMALLY
B - BOTH MODULATION FREQUENCIES TRANSMITTED IN EQUAL AMOUNT FROM SINGLE LOOP ANTENNA

FIGURE 7.—*Special test showing negligible influence upon the production of night effects of all factors other than the rotational effect described in Section III*

Observations taken on College Park visual radio range beacon at receiving point 80 miles northwest of College Park

beacon course produced at a distant receiving point when only one loop antenna was being used for transmission, the loop antenna current being modulated in equal amounts at the two beacon modulation frequencies. For this condition an on-course reading should be obtained at the receiving point at all times (night or day), unless selective audio fading or some other similar factor entered into the picture. Rotation of the figure-of-eight transmission characteristic could result only in equal changes in the intensity of the two audio-frequency signals received, the two signals remaining equal to each other throughout. The results obtained indicated definitely that the rotational phenomenon was the only factor of importance in the production of night effects. The recording of night effects (with the beacon operating normally) immediately before and after this special test insured that the test was being carried on under conditions conducive to the production of night effects. The presence of fading of the received signal intensity during this test (see fig. 7) corroborated this conclusion.

3. EXPERIMENTAL WORK ON EARLY ARRANGEMENTS

The two principal older arrangements which were considered for possible use with the radio range beacon are shown in Figure 8 (*a*) and (*b*). In each case only one-half of the complete antenna system required for a range-beacon installation is shown, and thus corresponds to one loop antenna of the present range-beacon installations. Figure 8 (*a*) represents the original antenna of Adcock except that loading coils are inserted in each vertical antenna circuit to resonate it to the radio-frequency of the transmitter. It will be observed that the two vertical antennas are so coupled to the transmitter that the current in one antenna is in opposite direction to the current in the other

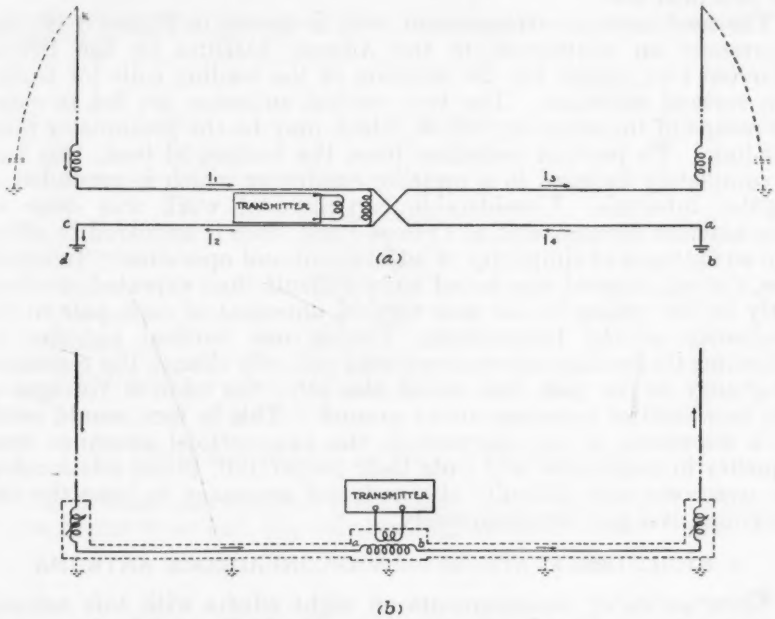

FIGURE 8.—*Early transmitting antenna arrangements tried at College Park, Md., but found unsuitable*

(*a*) Adcock arrangement; (*b*) Marconi adaptation of Adcock antenna

antenna. This corresponds exactly to the conditions in the vertical wires of the loop antenna. The electric field components radiated from this antenna are given by equations (11) and (12) and correspond to the components E_1 and E_2 for the loop antenna. (See equations (1) and (2).)

$$E_1 = E_o \cos \alpha \cos^3 \beta \tag{11}$$
$$E_2 = E_o \cos \alpha \sin \beta \cos^2 \beta \tag{12}$$

The horizontal component E_3 is not transmitted with much intensity, since the currents in the horizontal wires nearly cancel each other, as may be seen by reference to Figure 8 (*a*). Consequently, the presence of the indirect wave at the receiving point no longer produces rotation of the transmission characteristic. It is interesting to note

that not only is the component field which produces night effects eliminated with this antenna arrangement, but the other component fields are reduced in the indirect wave (as compared with loop antenna transmission) in the ratio $\cos^2 \beta$. One of the cosine factors results from the directivity in the vertical plane of a single vertical antenna and the second cosine factor from the differential action of the two vertical antennas acting together. An antenna of the type shown in Figure 8 (*a*) was constructed at College Park, Md., but was not used extensively because of difficulties of adjustment. In order that $I_1 = I_2$, and $I_3 = I_4$, it was necessary to insert balancing impedances in the ground leads *ab* and *cd*. The procedure required for determination of the correct values for these impedances was considered too difficult for practical use.

The next antenna arrangement tried is shown in Figure 8 (*b*) and represents an adaptation of the Adcock antenna by the British Marconi Co., except for the addition of the loading coils for tuning the vertical antennas. The two vertical antennas are fed in series by means of the coupling coil *ab*, which may be the goniometer rotor winding. To prevent radiation from the horizontal lead, this lead is completely inclosed in a metallic conductor which is grounded at regular intervals. Considerable experimental work was done on this antenna arrangement at College Park, since it appeared to afford the advantages of simplicity of adjustment and operation. In actual use, the adjustment was found more difficult than expected, particularly in the tuning of the two vertical antennas of each pair to the frequency of the transmitter. Tuning one vertical antenna by adjusting its loading inductance would not only change the resonance frequency of the pair, but would also alter the relative voltages of the two vertical antennas above ground. This in turn would result in a departure of the currents in the two vertical antennas from equality in magnitude and from their proper 180° phase relationship. To overcome this difficulty it was found necessary to tune the two antennas of a pair simultaneously.

4. NIGHT OBSERVATIONS ON MARCONI-ADCOCK ANTENNA

Three series of measurements on night effects with this antenna system were made. In the first tests, the horizontal lead was supported on short posts 3 feet high. The shielding arrangement comprised 4 wires placed along a cylinder 1 foot in diameter, with the horizontal lead along the axis of the cylinder. The shielding wires were connected together at each 10-foot interval and were grounded at the two ends and at the center to the station ground wire system. To secure an idea of the reduction in night effects obtained, the measurements made included periodic observations on the College Park service beacon which uses loop transmitting antennas. A summary of the comparative night effects observed is given under Test I of Table 3. In the second series of tests, the horizontal feeder was inclosed in a lead sheath laid along the ground and connected at its two ends and center to the station ground wire system. The results obtained, in comparison with loop antenna transmission, are given under Test II of Table 3. In the third series of measurements, the station ground wire system was extensively improved. The normal station ground system consisted of two concentric circles, 75 and 150 feet in diameter, interconnected by eight radial spokes which

joined directly underneath the central beacon tower. Three additional circles, 40, 120, and 180 feet in diameter and eight additional spokes were added. Also, ground rods were provided at 10-foot intervals along each lead sheath, the lead sheath being connected to these ground rods as well as to the improved ground system. The results obtained are tabulated under Test III in Table 3. In consequence of the lack of improvement in freedom from night effects, it was concluded that a totally different arrangement, other than shielding, would be required for eliminating radiation from the horizontal elements of the transmitting antenna.

TABLE 3.—*Summary of night effects observed on Marconi-Adcock antenna system in comparison with the conventional loop antenna transmission*

The transmitting stations were located at College Park, Md., and the receiving point at Front Royal, Va., 65 miles due west of College Park.

Test	Date	Type of antenna	Average course variations (in degrees)	Total number of readings	45° readings
	1932				*Per cent*
I	January 2	Marconi-Adcock	6.5	238	0
		Loop antenna	14.0	243	8.6
II	January 7	Marconi-Adcock	11.0	218	.5
		Loop antenna	26.0	225	27.5
	January 8	Marconi-Adcock	7.0	205	0
		Loop antenna	20.0	350	20.3
III	January 13	Marconi-Adcock	14.0	407	10.0
		Loop antenna	21.0	420	16.0
	January 14	Marconi-Adcock	13.3	384	5.0
		Loop antenna	24.0	290	14.5
	January 15	Marconi-Adcock	13.2	359	10.0
		Loop antenna	24.0	460	33.5

V. TRANSMISSION-LINE ANTENNA SYSTEM

The antenna arrangement finally adopted is illustrated in Figure 9. As in Figure 8 (*a*) and (*b*), only one-half of the complete transmitting

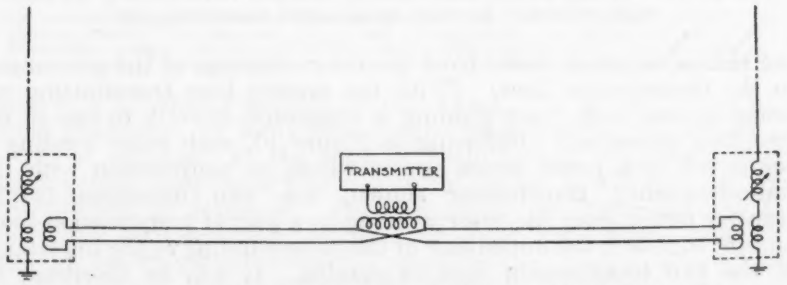

FIGURE 9.—*Transmission-line antenna developed at College Park, Md.*

antenna system is shown. The significant element of the system is the particular means employed to confine the radiation to the vertical antennas. A 2-wire parallel-conductor transmission line is used to feed power from the goniometer to each vertical antenna, these transmission lines being of such a nature as not to radiate. The efficient means for eliminating horizontal radiation thus provided makes it feasible to reduce the residual errors to much smaller values than was

possible with any of the early arrangements. The use of transmission lines also affords efficient transfer of power from the goniometer to the vertical antennas.

1. ELECTRICAL CIRCUIT ARRANGEMENT

Each transmission line is coupled to its vertical antenna by means of an impedance-matching transformer. The secondary winding of this transformer is tapped to permit accurate matching of its input impedance to the surge impedance of the transmission line. In this way reflection from the load end and consequent radiation from the line are minimized. The manner of connection of the input ends of the transmission lines to the range-beacon transmitting set is indicated in Figure 10. The transmitting set and goniometer are unaltered. The change lies in the addition of means for transferring

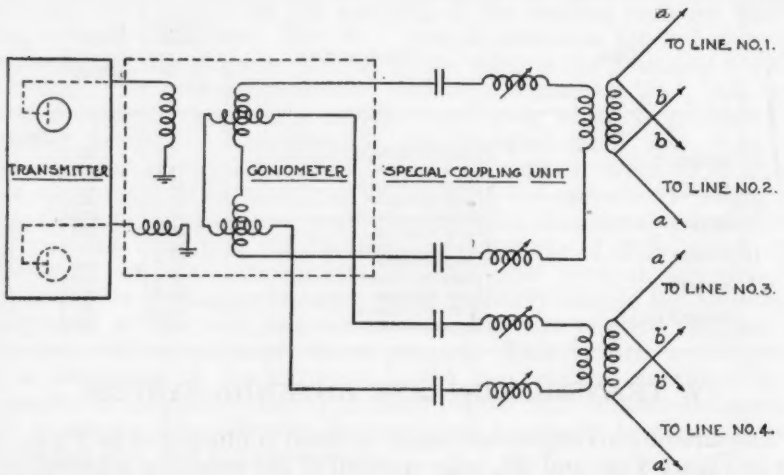

FIGURE 10.—*Circuit arrangement showing electrical connections of the transmission lines to the radio range-beacon transmitting set*

the radio-frequency power from the rotor windings of the goniometer to the transmission lines. (With the present loop transmitting antenna system each rotor winding is connected directly to one of the two loop antennas.) Referring to Figure 10, each rotor winding is connected in a tuned series circuit which, in conjunction with the radio-frequency transformer shown, has two functions: (*a*) To transfer power from the rotor winding to a pair of transmission lines, and (*b*) to match the impedance of the rotor winding to the impedance of the two transmission lines in parallel. It will be observed, by reference to the letters *a*, *b*, etc., on the leads to the transmission lines that, for each pair of lines, the connections of one transmission line to the radio-frequency transformer are reversed with respect to the connections for the other transmission line. This insures that the currents in the vertical antennas of a pair flow in opposite directions.

2. EXPERIMENTAL INSTALLATIONS

Two experimental installations of the transmission-line antenna system were made and thoroughly tested, one at College Park, Md., where it was developed, and the second at Bellefonte, Pa. The latter installation afforded an opportunity to test the operation of the system in mountainous terrain. A perspective view of the installation at Bellefonte is given in Figure 11. The four vertical antennas shown are spaced at the corners of a square, the pair (*1*, *2*) working together in place of one loop antenna of the present range-beacon antenna system and the pair (*3*, *4*) in place of the second loop antenna. Special attention is paid to increasing the effective capacitance of each vertical antenna to ground, thereby securing as great an antenna current as possible. To this end, each vertical antenna consists of six vertical wires arranged as elements of a cylinder 4 feet in diameter. The vertical antennas are approximately 75 feet high, the two antennas of a pair being spaced 400 feet apart. To insure a fixed low ground resistance, an individual ground wire system (not shown in fig. 11) is provided at the base of each vertical antenna. Each ground system consists of two concentric circles, one 75 feet and the other 150 feet in diameter. The two circles are interconnected by eight radial spokes which join directly under the vertical antenna. With this set-up, approximately 4 amperes was obtained at the base of each antenna, the radiated field intensity being approximately 75 per cent of that obtained with the conventional loop antenna. To secure greater field intensity and also a more permanent antenna structure, installations of this antenna system on the airways will employ insulated steel towers, 125 feet high and spaced 500 feet apart.

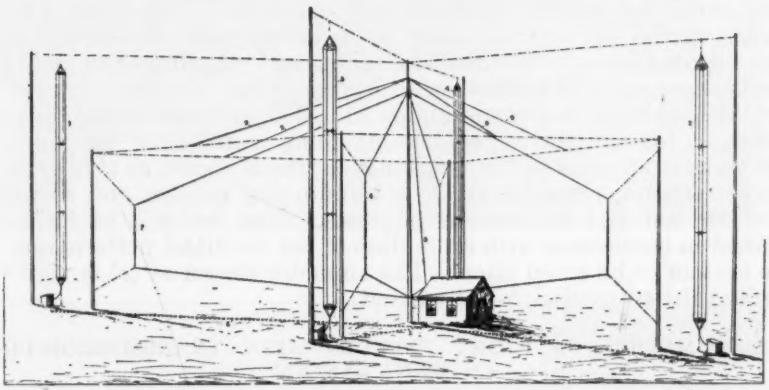

FIGURE 11.—*Perspective view showing the experimental transmission-line antenna installation at Bellefonte, Pa., and also the old loop antenna system, together with its central course-bending antenna*

This installation provided means for measurements of night effects alternately from the two antenna systems. The numerals *1*, *2*, *3*, and *4* designate the four vertical elements of the TL-antenna system; *5*, the transmission lines feeding these antennas; *6* and *7*, the loop antennas; *8*, the down lead of the course-bending antenna; and *9*, the flat-top elements for this antenna.

The tuning boxes which house the antenna loading coils and the transmission line coupling transformer are located each near the base of one vertical antenna and are provided with complete shielding to preclude the possibility of stray radiation. The transmission lines

consist of ordinary 2-conductor 600-volt cable with a lead sheath, and are buried about 18 inches below the ground surface. The lead sheath provides mechanical protection. Special care must be taken that the lead sheath (particularly that portion near the antenna end) is not electrically connected to the ground wire system, except by way of its continuous connection with the earth; otherwise ground return currents concentrate along the lead sheath thereby reintroducing some night effects.

In addition to the transmission-line antenna system, Figure 11 shows the old loop antenna system, together with the central course-bending antenna which were employed at the Bellefonte visual range beacon station. This installation was left intact to facilitate comparison of the night effects produced by the loop and transmission-line antenna systems. Means were provided for rapid switching of the goniometer output circuits to either antenna arrangement.

Figure 12 shows in greater detail the arrangement employed for supporting the vertical antennas and also (at the left of the photograph) the means for suspending the loop antennas at their far ends. The shielded house containing the tuning and coupling equipment for the vertical antenna is also shown in Figure 12. An interior view of the shielded house is given in Figure 13. The antenna tuning coils are shown at (*a*) and the impedance matching transformer for coupling the vertical antenna to the transmission line is shown at (*b*); (*c*) and (*d*) correspond, respectively, to a terminating resistor and a switch used for test and adjustment purposes. This use will be fully explained in connection with an outline of the electrical performance of the system to be given later. The ammeter shown at (*e*) is used for reading the transmission-line current.

3. ELIMINATION OF NIGHT EFFECTS WITH TRANSMISSION-LINE ANTENNA SYSTEM

An idea of the effectiveness of the transmission-line antenna system in eliminating night course variations may be had by reference to Figures 14 and 15, which represent data secured on the Bellefonte range beacon. Figure 14 (*a*) corresponds to a 24-hour record at Sunbury, Pa., 50 miles east of Bellefonte, loop antenna transmission being employed at Bellefonte. Figure 14 (*b*) is a similar record for the transmission-line antenna system. While these runs were taken on successive nights, they may be used for a direct comparison of performance of the two antenna systems, since other observations (on the Bellefonte aural beacon) showed that the night effects were of about the same magnitude and duration on both nights. Figure 15 shows the results of measurements taken in a night flight on the two antenna systems, and is typical of the results obtained in a large number of similar flight tests. Figure 15 (*a*) is for the outgoing trip during which loop antennas were used at the beacon station, while Figure 15 (*b*) is for the return trip during which TL-antenna transmission was employed. The airplane followed as closely as possible the route marked out by the beacon course during a day flight. The variations shown for the first 18 miles are departures of the airplane from the straight course, not night effects. A comparison of the results with the two antenna systems shows that, while the beacon course became of no further value beyond 45 miles from the station when using loop antenna transmission, it was perfectly satisfactory

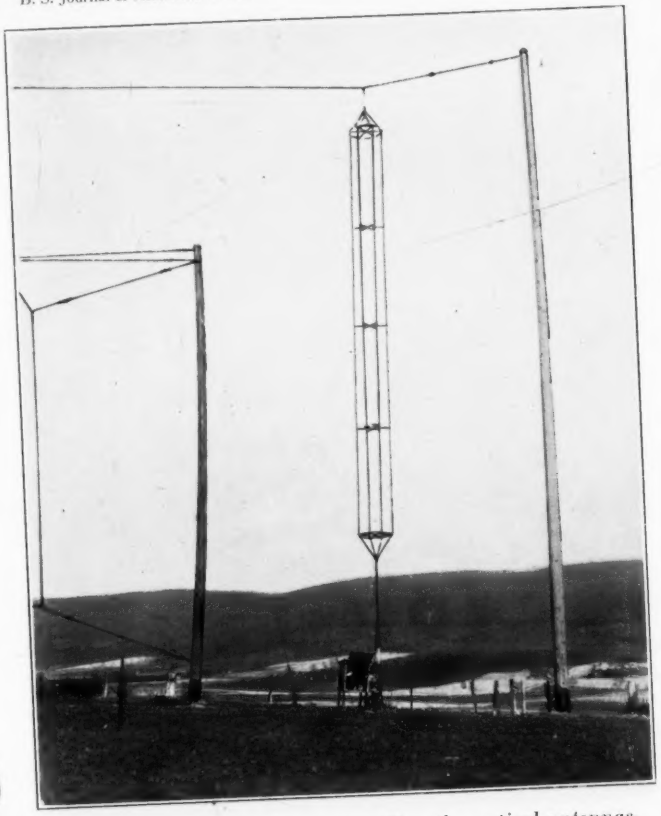

FIGURE 12.—*Manner of suspending the vertical antennas*

One end of loop antenna suspension is also shown (at the left).

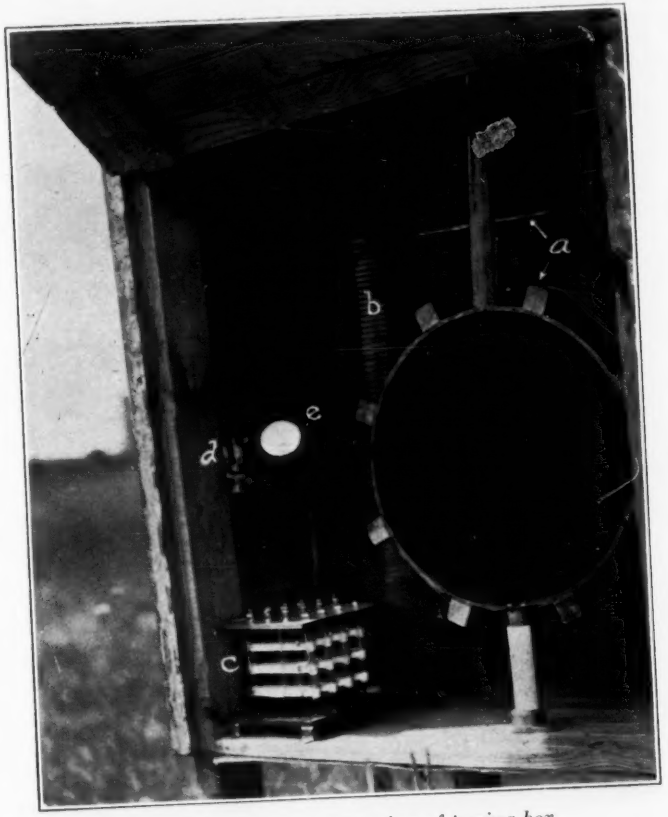

FIGURE 13.—*Interior view of tuning box*

a, Antenna loading coils; *b*, antenna coupling transformer; *c*, terminating resistor for use in testing and adjusting for proper transmission-line termination; *d*, switch; *e*, ammeter for reading line current. The use of *c*, *d*, and *e* will be explained in connection with Figure 18.

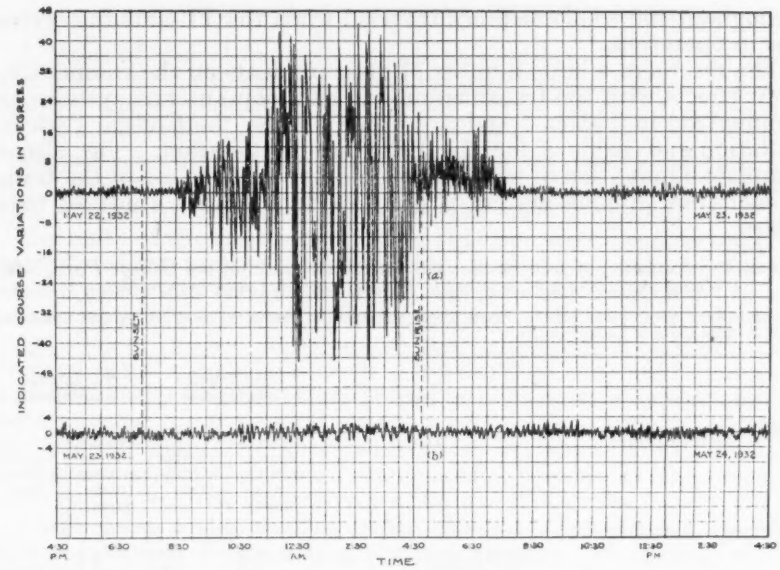

FIGURE 14.—*Twenty-four hour records showing comparative course variations with loop and transmission-line antenna systems at Bellefonte visual radio range beacon station*

(*a*) Loop antenna transmission; (*b*) TL-antenna transmission.

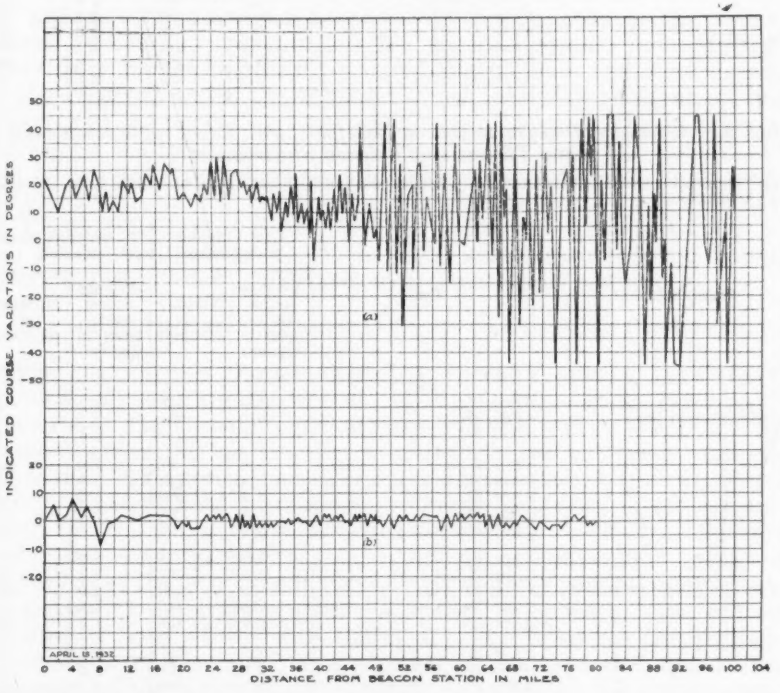

FIGURE 15.—*Night observations in an airplane on comparative night effects with loop and transmission-line antenna systems at Bellefonte visual radio range beacon station*

(*a*) Loop antenna transmission; (*b*) TL-antenna transmission.

throughout the whole distance traveled when the TL-antenna system was in operation.

The results of a large number of measurements on the comparative night effects with the transmission-line and loop-antenna systems are summarized in Tables 4 and 5. Table 4 is for the College Park installation and Table 5 for the Bellefonte installation. The almost complete elimination of night effects obtained by the use of the transmission-line antenna system is quite evident from a study of these tables.

TABLE 4.—*Summary of comparative measurements made on the College Park, Md., visual radio range beacon with TL and loop antenna transmission*

The receiving points were located at Front Royal, Va. (65 miles west of College Park), and at Richmond, Va. (105 miles south of College Park).

Receiving point	Date	Loop antenna transmission		TL-antenna transmission	
		Average course variations (in degrees)	Number of readings	Average course variations (in degrees)	Number of readings
Front Royal, Va.	Feb. 2, 1932	10.0	383	2.4	192
	Feb. 3, 1932	8.0	301	2.1	141
	Feb. 4, 1932	10.5	191	2.0	70
	Feb. 5, 1932	14.0	415	1.7	285
	Feb. 6, 1932	14.0	351	1.5	247
	Feb. 9, 1932	7.0	286	1.9	196
Richmond, Va.	Feb. 2, 1932	3.7	216	2.4	134
	Feb. 3, 1932	25.0	312	2.3	262
	Feb. 4, 1932	23.0	66	2.5	387
	Feb. 5, 1932	12.0	167	1.7	314
	Feb. 6, 1932	11.0	416	.8	286
	Feb. 9, 1932	8.0	311	2.3	191

TABLE 5.—*Summary of measurements on Bellefonte, Pa., visual radio range beacon using TL and loop antenna transmission*

Receiving points at McConnelsburgh, Pa. (70 miles south of Bellefonte), and at Sunbury, Pa. (50 miles east of Bellefonte).

Receiving point	Date	Loop antenna transmission		TL-antenna transmission	
		Average course variations (in degrees)	Number of readings	Average course variations (in degrees)	Number of readings
	1932				
McConnelsburgh, Pa.	Feb. 24	13.0	188	2.1	126
	Feb. 25	26.0	231	2.4	150
	Feb. 27			2.1	340
Sunbury, Pa.	Apr. 1	9.0	97	1.0	388
	Apr. 11	8.8	113	1.5	80
	Apr. 12	5.1	219	1.2	148
	Apr. 14	4.5	84	1.6	124
	Apr. 15	9.0	96	1.6	159
	Apr. 18	7.0	175	1.3	258
	Apr. 19	15.5	167	1.1	168
	Apr. 20	8.5	265	1.0	297
	Apr. 21	7.5	146	1.2	115
	Apr. 22	2.5	151	1.2	114
	Apr. 23	3.0	141	1.1	109
	Apr. 24	4.0	159	1.2	129
	May 13	13.1	85	1.5	104
	May 14	7.4	93	.6	138
	May 15	9.1	264	.8	219
Average		9.0		1.4	

4. POLARIZATION OF WAVE AT RECEIVING POINT

A series of special tests were made at Sunbury, Pa., on the transmissions from the Bellefonte set-up, to determine the state of polarization of the received wave at Sunbury. In addition to the receiving set, reed converter and automatic recorder for taking records of the indicated beacon course, a second receiving set, reed converter, and two automatic recorders were provided for taking the polarization data. The two recorders were connected each to the output of one of the units of the reed converter, so that one recorder measured the intensity of the received 65-cycle signal and the second recorder the intensity of the received 86⅔-cycle signal. The receiving set was connected to a loop receiving antenna, the plane of which was oriented perpendicular to the direction of the range-beacon station. The received signal was therefore zero in the daytime. At night, however, the horizontally polarized electric field present in the downcoming sky wave affected the horizontal elements of the loop receiving antenna. The recorders thus took separate records of the instantaneous intensity of the horizontally polarized components present in the received wave and modulated respectively at 65 and 86⅔-cycles.

A discussion of the records taken with this arrangement, together with a complete theoretical analysis explaining the results, will be given in a forthcoming paper in this Journal. It is of interest to summarize here briefly some of the results obtained. When loop antenna transmission was employed, the records showed that night variations in the indicated beacon course were invariably accompanied by horizontally polarized electric field components in the received wave. When the transmission-line antenna system was employed, practically no horizontally polarized components could be detected in the received wave, the received signal intensity being at all times lower than the prevailing noise and "static" level. This is in accordance with the theoretical analysis given in Sections III and IV, since the horizontally polarized electric field component (E_3), most readily detected with the receiving set-up employed, is completely eliminated in TL-antenna transmission, and the other two components (E_1 and E_2) in the indirect wave, which might affect the receiving antenna after changes in their polarization, are materially reduced.

5. ELECTRICAL PERFORMANCE OF TL-ANTENNA SYSTEM

The use of the transmission-line antenna system involves the problem of accurate control of the time phase angle between the currents in the two vertical antennas of each pair. When the time phase angle is 180°, a true figure-of-eight space pattern is obtained; when it is 180° minus the space phase angle between the two vertical antennas, a cardioid is obtained. For phase angles intermediate to those two values, a space pattern intermediate to the true figure-of-eight and cardioid results. This affords a convenient means for alignment of the four beacon courses with airway routes converging on an airport at arbitrary angles. Altering the space pattern radiated by one or both of the directional antennas changes the points of intersection of the two patterns and, in consequence, the angular direction of the four equisignal zones or courses. The requirement for a central open-type course bending antenna, such as is employed with the loop antenna system, is thus obviated.

The use of this method of altering the angular direction of the beacon courses in order to align them with airway routes at arbitrary angles is clearly shown in Figure 16. The space pattern for one directional antenna is successively shown as *A*, *B*, and *C*, corresponding to a time phase angle between the currents in the two vertical antennas equal to 180°, 165°, and 150°, respectively. The angular alignment of the four beacon courses produced by the intersection of this pattern with the space pattern *D* for the second directional antenna (indicated by *1*, *2*, *3*, *4*; *1′*, *2′*, *3′*, *4′*, and *1″*, *2″*,

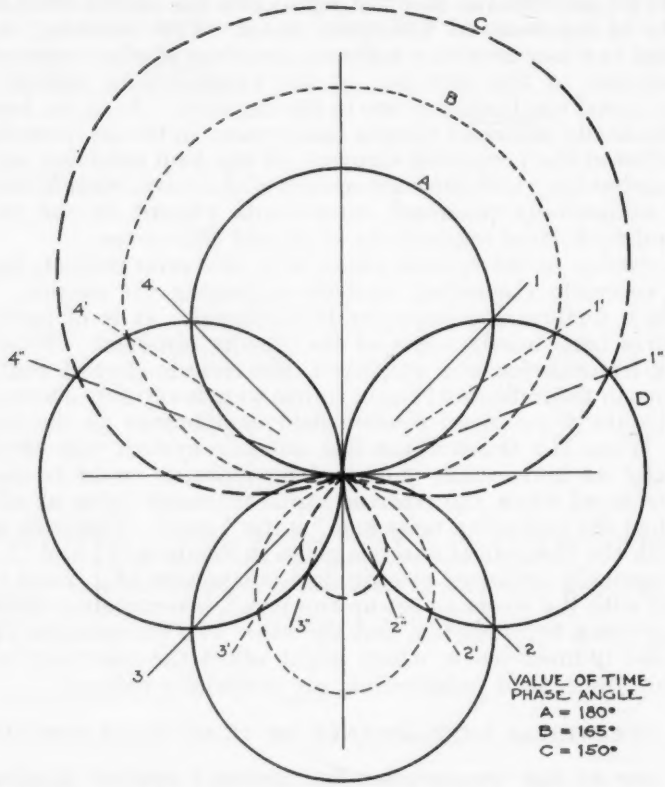

FIGURE 16.—*Polar pattern illustrating effect of changing the time phase angle between the currents in the two vertical antennas of a pair upon the angular direction of the four beacon courses*

3″, *4″*) is seen to be different for each of the three conditions assumed. The means available for altering the time phase angle between the currents in the two vertical antennas of a pair are quite simple, consisting either of slightly detuning one antenna or inserting a condenser or inductor in series with the input of one or both of the transmission lines. In Figure 17 is shown a polar diagram for the Bellefonte installation which was altered in the manner just described so that courses *A* and *B* coincided with the airway routes to New York and Cleveland, respectively. These routes intersect at Bellefonte at an angle of 166°.

The property of the new antenna system which permits alteration of its radiated space pattern, while thus seen to be of technical and economic advantage, also imposes a special operational requirement on the system. Obviously, the phase angle between the currents in the two vertical antennas of a pair must be kept constant within rather close limits, or the angular direction of the beacon courses will vary from time to time. This requires special design of the vertical antennas, the antenna tuning and coupling units, the transmission lines and the means for transferring power from the goniometer to the transmission lines. The use of tightly coupled impedance-matching transformers at both ends of each transmission line obviates any difficulty from variable phase relationship in any of the equipment excepting the antennas. In the latter, an unbalanced change in tuning for any reason, such as the effect of nearby poles, faulty insulators, etc., during wet weather, will result in a change in

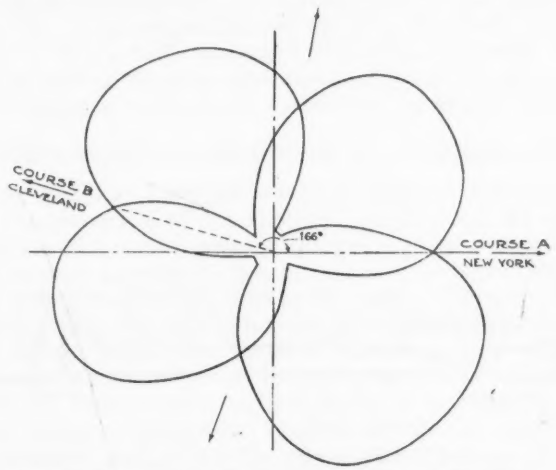

FIGURE 17.—*Polar diagram for Bellefonte TL-antenna installation showing alignment of the east and west courses with the airway routes to New York and Cleveland*

phase angle between the two antenna currents. Care in installation of the antenna system is required to prevent unbalanced detuning. In the experimental installation at Bellefonte the maximum effect of such detuning over a period of several months was found to be about 5°. The use of insulated steel towers as the vertical antennas, with the consequent absence of wooden poles and suspension wires, is expected to improve the electrical performance of the system in this respect. Complete elimination of this problem of operation is looked for as a result of experimental work now in progress on an arrangement for securing automatic compensation for any change in phase angle. This method utilizes the transmission lines themselves for securing the desired interlocking of phase.

Of interest is the method adopted for tuning the two vertical antennas of a pair, securing the proper phase angle between their currents, and at the same time insuring proper termination for the

transmission lines so that they will not radiate. Referring to Figure 18, a switch S is provided at the load end of each transmission line so that the line may be terminated either by the primary of the antenna transformer T or by a resistor R equal to the surge impedance of the line. During the adjustment of each vertical antenna, the transmission line to the second antenna of the pair is terminated by the resistor R. The switch S is thrown so that the antenna transformer T is excited, and the loading coil L_1 and the fine tuning coil L_2 adjusted for maximum antenna current I_A. The line current I_L'' at the receiving end of the line is then recorded and compared with the reading corresponding to resistance termination. These two readings are generally not the same at the beginning of an adjustment. The tap on the secondary winding of transformer T is then changed in small steps, the antenna being retuned to maximum current for each step, and the line current I_L'' recorded. The adjustment is

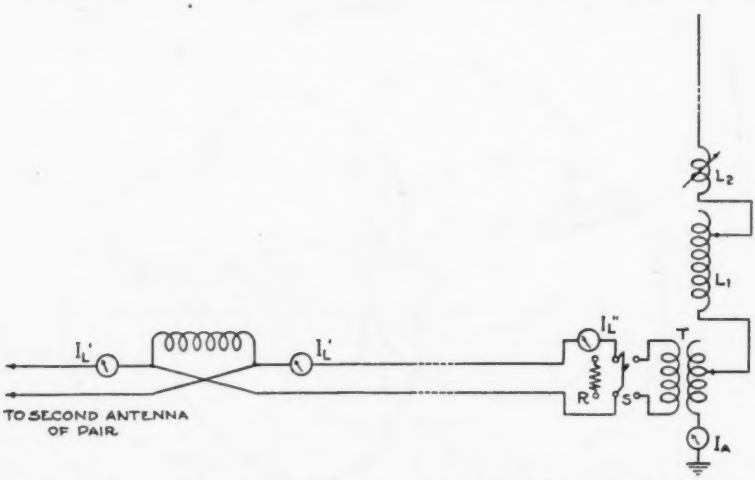

FIGURE 18.—*Circuit arrangement illustrating method of adjusting the TL-antenna system for proper tuning, phase angle and transmission-line termination*

chosen for which I_L'' reads the same whether the transmission line feeds into the transformer T or the resistor R. This is, however, still not the proper condition of adjustment; it corresponds to an input transformer inpedance equal in magnitude but not in phase to the surge impedance of the line. Reflection along the line still occurs as may be seen from the fact that the input current to the transmission line, I_L', is not the same for resistance and transformer termination. The next step is to detune the antenna slightly by adding inductance in L_1 or L_2 until I_L' reads the same whether the transmission line is terminated by the resistor or by the antenna transformer. The apparent input impedance of the antenna transformer is now a pure resistance equal to the characteristic line resistance. The same series of adjustments is repeated for the second antenna of the pair, the transmission line to the first antenna being now terminated by the resistor provided. After this adjustment is completed, the two antennas may be excited together without disturbing the adjustment of either.

It is next necessary to determine the phase angle between the currents in the two antennas and to adjust it to the desired value. This is accomplished by removing the voltage from the pair of antennas not under test and inserting a milliammeter in one of these antennas. To insure that this antenna remains in tune, the voltage is removed from the input end of the transmission line feeding it and a resistor connected across this end equal to the characteristic line resistance. This antenna being equidistant from the pair of antennas under test, the current induced in it from the pair depends upon the time phase angle between the currents in the two antennas of the pair. For 180° phase angle, the induced current is zero; the greater the departure from 180°, the greater the induced current. The milliammeter reading this current may be calibrated directly in phase angle. If desired, this reading may be made within the beacon house rather than at the antenna by measuring the voltage across the resistor terminating the transmission line coupled to this antenna. This method of measuring the phase angle may be combined with the arrangement for controlling the phase angle (which consists of inserting a condenser or inductor in series with the input end of one or both of the transmission lines feeding the two antennas under test) to give rapid means for periodic phase checking and correction for slight variations.

6. OBSTRUCTION LIGHTING OF TL-ANTENNA SYSTEM

One of the incidental problems which came up during this development was the provision of obstruction lights for the TL-antenna system. Because of the high poles employed and because of the location of the beacon near an airport, it was necessary to install an obstruction light at the top of each of the four outer poles. The problem involved was to run the lighting wires up these poles without at the same time absorbing power from the vertical antennas only 20 feet away. Besides absorption of power and consequent loss in efficiency, it was feared that the induction of radio-frequency currents in the lighting wires would serve to detune the vertical antennas, perhaps in uneven amounts, thereby disturbing the phase relationships of the system; and also to produce radiation from the horizontal wires of the lighting circuits thereby affecting adversely the degree of elimination of night effects. The problem was solved by inserting radio-frequency choke coils in the lighting wires at the base of each pole and providing by-pass condensers on the power side of the choke coils. The arrangement proved quite satisfactory, the presence of the lighting cable having no effect upon the tuning of the system or upon its operation in eliminating night effects.

In the case of obstruction lighting of the insulated steel towers intended for use on the airways, the problem is very similar. The tower itself may constitute one of the lighting wires, while the other wire is kept at the same radio-frequency potential as the tower by means of radio-frequency by-pass condensers. The choke coil and condenser arrangement described above is then also suitable for use with the insulated tower system.

VI. ACKNOWLEDGMENT

The author desires to acknowledge the parts played in this development by his coworkers in the Bureau of Standards and others. Appreciation is extended to G. H. Wintermute and H. M. Horsman for research in the operation of the experimental transmitting set-ups and for many measurements in the field, to G. L. Davies for the data secured on the Midcontinent Airway and for assistance in the theoretical analysis of the results obtained, to W. S. Hinman for field set-ups and tests, to F. G. Kear for the design of the transmission-line coupling units, and to W. E. Jackson (airways division) for suggestions and discussions of results. Special acknowledgment is due to Col. H. H. Blee, director of aeronautic development, Aeronautics Branch, for his inspirational direction of this project, to Dr. J. H. Dellinger, chief of the radio section, Bureau of Standards, for many helpful suggestions during the progress of the work, and to Capt. F. C. Hingsburg, chief engineer of the airways division, for cooperation in the provision of test facilities and equipment.

WASHINGTON, October 4, 1932.

THE HEAT CAPACITY, HEAT OF SUBLIMATION, AND HEAT OF SOLUTION OF PHOSPHORUS PENTOXIDE

By Mikkel Frandsen

ABSTRACT

The heat capacity of the vapor of P_2O_5 at atmospheric pressure and at temperatures between the sublimation point and 1,100° C. was determined by subliming the P_2O_5 through a silica tube heated in a tubular electric furnace with a nearly constant temperature along the main part of the axis, collecting the vapor in a Dewar flask charged with water, measuring calorimetrically the sum of the heat content of the vapor and the heat of solution, and deducting the latter. The method was tested by similar experiments with superheated steam, and the results were found to be in good agreement with accepted results for this substance. For P_2O_5 vapor, $C_{p\ (1\ atm.)}=36.8\pm1.0$, $cal._{15}\ mole^{-1}\ °C.^{-1}$ over the range 360° to 1,100° C.

The heat capacity of the usual metastable crystalline form of phosphorus pentoxide between room temperature and the sublimation point was determined by the calorimetric method of mixtures applied to samples sealed in silica tubes. Result, $C_p=(22.17+0.07804t-8.45\times10^{-5}t^2)\pm1.6$ per cent, $cal._{15}\ mole^{-1}\ °C.^{-1}$, between 25° and 350° C.

The heat of sublimation was calculated as the difference in heat content of the vapor and the solid, respectively, at the sublimation point, and found to be $L=8.8\pm1.3$ $kg\text{-}cal._{15}\ mole^{-1}$ at 358° C.

The heat of solution of metastable crystalline phosphorus pentoxide at 25° C. was measured by breaking sealed glass tubes, containing this material, under water in a calorimeter. When metaphosphoric acid is formed, $Q=42.0\pm2.1$ $kg\text{-}cal._{15}\ mole^{-1}$, and when orthophosphoric acid is formed $Q=54.4\pm2.1$ $kg\text{-}cal._{15}\ mole^{-1}$. The heat of transformation of meta— into orthophosphoric acid was computed to be 6.2 ± 1.9 $kg\text{-}cal._{15}\ mole^{-1}$.

The sublimation point was estimated, from various vapor pressure measurements performed by other investigators, to be 358° ± 7° C.

CONTENTS

		Page
I.	Introduction	35
II.	Purification of material	36
III.	Heat capacity of phosphorus pentoxide vapor	36
	1. Apparatus and procedure	36
	2. Supplementary determinations	40
	3. Test of the method with steam	41
	(*a*) Procedure	41
	(*b*) Data and discussion	42
	4. Results for phosphorus pentoxide	45
IV.	Heat capacity of crystalline phosphorus pentoxide	50
	1. Experimental equipment and procedure	50
	2. Data, heat content, and heat capacity	52
V.	Heat of sublimation of crystalline phosphorus pentoxide	54
VI.	Heat of solution of crystalline phosphorus pentoxide	55
VII.	Acknowledgments	58

I. INTRODUCTION

The information which may be obtained from the literature in regard to the thermal properties of phosphorus pentoxide is incomplete and very uncertain. This may probably be ascribed partly to

the difficulties experienced in working with this substance at elevated temperatures and partly to the failure of early investigators to obtain the substance in a pure state. Phosphorus pentoxide is extremely hygroscopic, and the phosphoric acid, formed by absorption of moisture, will, at high temperatures, attack nearly all materials from which a suitable apparatus may be constructed. Glass and silica, when heated in contact with an appreciable amount of moist phosphorus pentoxide, invariably break on cooling, apparently on account of differences in shrinkage.

The present paper presents the results of determinations of the heat capacity of metastable crystalline phosphorus pentoxide between room temperature and the sublimation point, the heat of sublimation of this substance, and the heat capacity of the vapor between the sublimation point and 1,100° C. These quantities have never been measured before. The heat of solution of metastable crystalline phosphorus pentoxide in water has been redetermined, and an average value for the sublimation point has been derived from vapor pressure measurements performed by other investigators.

The investigation was undertaken at the request of the Fixed Nitrogen Research Laboratory of the Department of Agriculture in order to supply thermal data needed in a thermodynamic investigation of the industrial processes involved in the manufacture of fertilizer from phosphate rock.

II. PURIFICATION OF MATERIAL

The phosphorus pentoxide used in this investigation was prepared from one of the best grades of the commercial product by sublimation in a current of oxygen in a 2-inch iron tube at about 800° C., according to the method of Finch and Fraser.[1] The iron tube was heated electrically instead of by gas. In this process lower oxides of phosphorus are oxidized completely, as shown by the fact that a solution of the purified product does not reduce solutions of silver nitrate [2] or mercuric chloride.[3]

After sublimation the oxidized product absorbs some moisture from the atmosphere, but by resublimation in the absence of atmospheric moisture and at pressures not exceeding 1 atmosphere, it yields pure crystalline phosphorus pentoxide.

III. HEAT CAPACITY OF PHOSPHORUS PENTOXIDE VAPOR

1. APPARATUS AND PROCEDURE

The method by which the heat capacity of phosphorus pentoxide vapor was determined consisted in subliming phosphorus pentoxide through a silica tube placed in an electric furnace in which the vapor was heated to the desired temperature. Emerging in jet form through a narrow opening the heated vapor was collected in a calorimeter, consisting of a Dewar flask containing a known amount of water, and there dissolved. The heat capacity of the calorimeter, the rise in temperature, and the heat of solution were then used in calculating

[1] Finch, G. I., and Fraser, R. P., J. Chem. Soc., vol. 129, pp. 117–119, 1926.
[2] Finch, G. I., and Peto, R. H. K., J. Chem. Soc., vol. 121, p. 692, 1922.
[3] Whitaker, H., J. Chem. Soc., vol. 127, p. 2219, 1925.

the heat content of the vapor at the temperature at which it emerged from the furnace.

The apparatus used is shown in Figure 1. A Pyrex flask, *F*, contained the purified phosphorus pentoxide mixed with a little phosphoric acid, which had been formed by the action of absorbed moisture. Through a ground joint, *A*, the glass flask was connected to an apparatus made from vitreous silica, which is able to withstand the action of phosphorus pentoxide at high temperatures. Moisture was expelled from the silica apparatus, before the ground joint connection was made, by passing a current of dry air through it while the walls were heated. The subsequent entrance of moisture through the ground joint was prevented by surrounding this with a seal of molten tin covered with a layer of carbon black. A small electric furnace, *E*, maintained a temperature of about 500° C. around the ground joint, whereby the tin was kept molten and condensation of phosphorus pentoxide in this part of the apparatus was prevented. The lower end of the furnace was plugged with asbestos to prevent draft around the heated connection. Pure phosphorus pentoxide was first sublimed from *F* into the silica bulb, *C*, where it condensed in the usual metastable, crystalline form. Care was taken not to heat the flask *F* too strongly in order to avoid volatilization of metaphosphoric acid from the mixture. Even after sublimation it was necessary to keep the flask *F* heated, for two reasons: First, the flask invariably broke on cooling, owing to different rates of contraction of the glass and the residue; second, the phosphorus pentoxide subsequently sublimed out of *C* was thereby prevented from returning to the flask *F*.

The silica tube, *B*, has at the center a well in which a platinum-platinumrhodium (10 per cent Rh) thermocouple was placed. From the lower end of the well four amply spaced projections extend close to the walls of the tube; they served to protect the well from being broken off by its own weight when the apparatus was in a horizontal position. The end of the silica tube, *B*, is drawn out into a narrow spout, 3 mm in diameter at the orifice, and is connected by another ground joint to the silica tube, *M*, and to a drying tube that served to guard the inside of the apparatus against atmospheric moisture.

The main furnace, *G*, contained two mutually independent heating coils, by means of which a nearly uniform temperature could be maintained throughout the main part of the furnace, anywhere in the interval from room temperature to 1,100° C. This is illustrated in Figure 2, which shows the temperatures that were maintained along the axis of the furnace in five sets of determinations made both on phosphorus pentoxide and on water. Temperatures below the thermocouple well were measured with thermocouples inserted through the bottom of the furnace. In each case the external resistances were adjusted until the temperature at the bottom of the well was equal to that at a distance of 40.6 cm from the top of the furnace. The temperature at these two points will hereafter be designated as the furnace temperature. By reproducing the temperatures at those two points the temperatures prevailing in various other parts of the furnace during any run could be reproduced automatically as often as desired. Figure 2 represents conditions in the furnace before the vapor passed into it. The dotted portion added to the middle curve helps to show the effect of the auxiliary heater, as it represents temperatures observed in the lower half of the furnace when the auxiliary heater remained turned off.

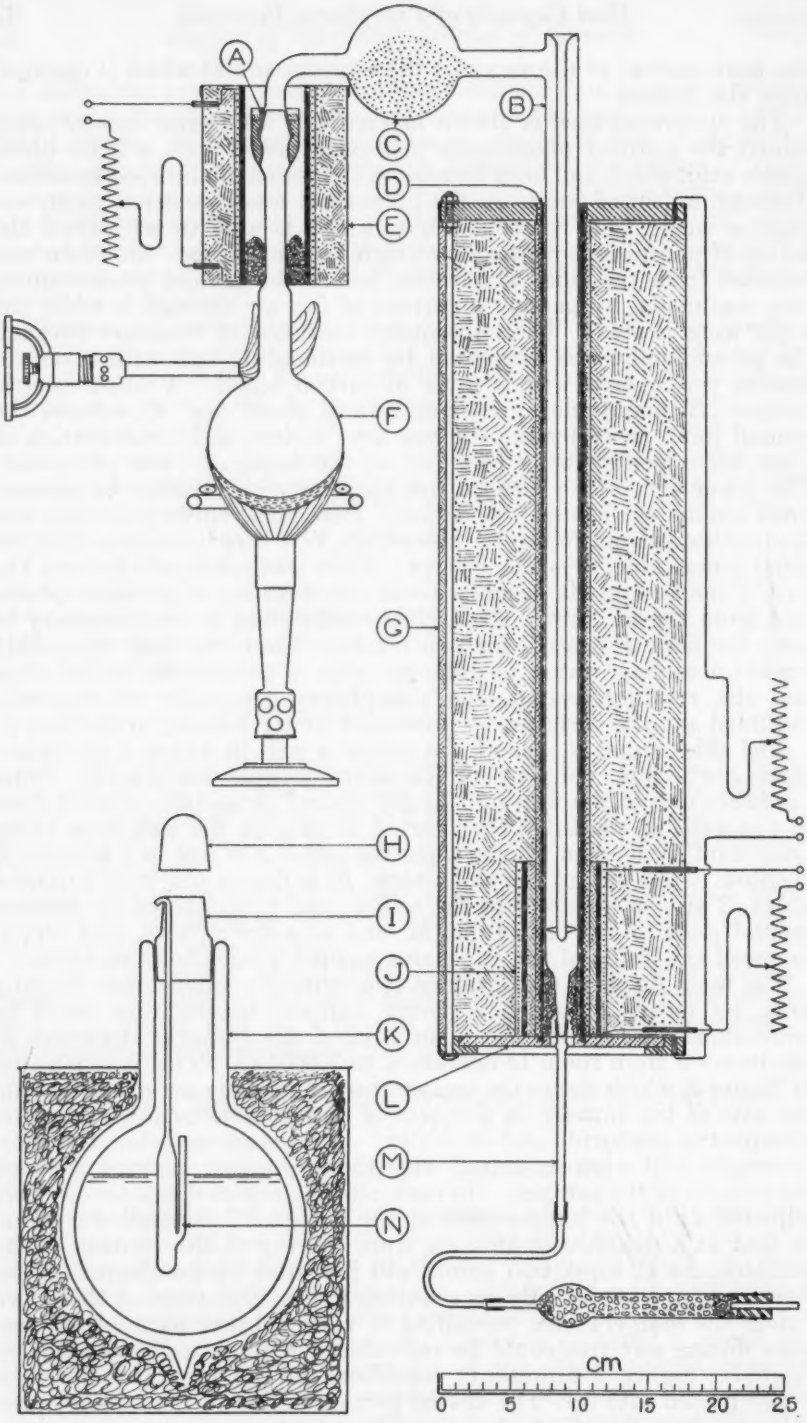

FIGURE 1.—*Apparatus for determining the heat content of vapor of phosphorus pentoxide*

The 2-liter Dewar flask, *K*, shown in Figure 1, served as a calorimeter and was charged with 1,500 g of distilled water in preparation for a run. It could be closed with a cap, *H*, and a collar, *I*, both of which were made from Pyrex laboratory glass and ground to fit. The piece, *N*, suspended from a small notch in the collar, served during a run as an outlet for air and as a trap for water vapor and phosphorus pentoxide; it was placed in position after the fore period, just before the heated vapor was passed into the calorimeter, and was pushed over the edge of the collar into the flask just after, so that the cap might be put on and the flask shaken. The neck and top parts of the flask were covered with a couple of large cloths. The calorimeter was stirred by shaking, and a Beckmann thermometer was used for measuring the temperature rise. The calorimeter was kept in a room with

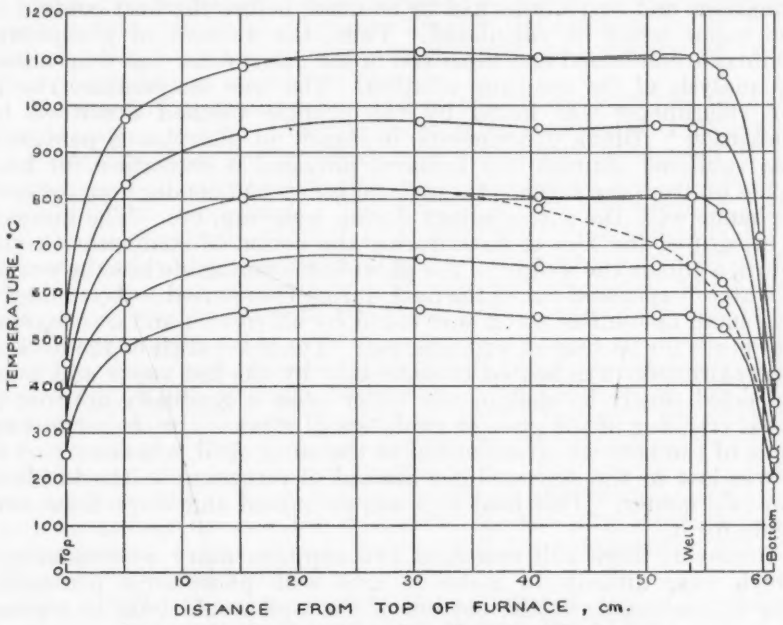

FIGURE 2.—*Temperatures along the axis of the furnace*

practically constant temperature, except during the short period in which hot vapor was charged into it.

In preparing for a run the furnace, *G*, was brought to the desired temperature, the calorimetric fore period was recorded and the Dewar flask with its contents was weighed. The tube, *M*, was then removed, and phosphorus pentoxide was sublimed through the furnace by heating the bulb, *C*, with one or two gas burners. The upper part of the silica tube, *B*, must also be heated to prevent condensation in it, and when a high temperature was desired the vapor could be preheated considerably in that part of the tube before entering the furnace. In two to three minutes the issuing vapor had heated the constricted outlet sufficiently, and the calorimeter, with the cap removed, the air-outlet piece, *N*, in position, and the water in a swirling motion, was brought under the spout and the collar, *I*, pressed against the alundum plate, *L*. At the higher temperatures most of the vapor

reached the water and dissolved; at lower temperatures it condensed, to a considerable extent, in the neck of the Dewar flask. The calorimeter was held under the spout for a measured length of time, usually 90 seconds, during which period 4 to 16 g of phosphorus pentoxide was partly condensed and partly dissolved in it. The calorimeter was then removed from the furnace and shaken, after replacement of the cap, until the phosphorus pentoxide was completely dissolved and the neck cooled off to the temperature of the solution; this usually required about 10 minutes. Subsequently, the Dewar flask with contents was weighed, and the after period recorded.

2. SUPPLEMENTARY DETERMINATIONS

In connection with each experiment various supplementary determinations and corrections had to be made before the heat content of the vapor could be calculated. Thus, the amount of phosphorus pentoxide condensed and dissolved in the calorimeter was determined by analysis of the resulting solution. The true temperature rise in the calorimeter was found by the graphic method described by Dickinson.[4] Blank experiments, in which no phosphorus pentoxide was sublimed through the furnace, provided a correction for heat taken up from the furnace through radiation and conduction, for heat exchange with the surroundings during weighing, etc. The increase in weight of the Dewar flask during the period of condensation and solution equals the weight of the phosphorus pentoxide less the weight of water evaporated out of the flask during that period. Accordingly, this small amount of water was found by difference, and a correction was made for its heat of vaporization. The inner shell of the neck of the calorimeter was heated considerably by the hot vapor and must be cooled slowly by shaking the water upon it gradually in order to avoid cracking of the glass or evolution of steam. In the meantime, some of the heat was transmitted to the outer shell, whence a part of it was lost to the surroundings instead of returning to the inside of the calorimeter. This heat loss was estimated and corrections were made for it.

However, there still remained two supplementary determinations which were difficult to make in runs with phosphorus pentoxide. The thermocouple at the bottom of the well would tend to register the temperature of the walls instead of that of the vapor; moreover, the vapor suffered a certain drop in temperature, dependent upon the rate of flow, in passing from the level of the thermocouple to the orifice of the spout. Measurements of the temperature of the vapor at the orifice of the spout were therefore desirable. Again, the radiation from the furnace to the calorimeter was greater in the main experiments than in the blank experiments, because in the former the spout had been heated by the first, uncollected vapors. It follows that the temperature of the spout before and during a run ought to be measured in order that a correction for the increase in radiation during a run might be made. These determinations were made in runs with steam, and from the results corresponding data were calculated for phosphorus pentoxide, which in direct measurements is apt to attack the thermocouple and which in general is more difficult and more expensive to work with than steam.

[4] Dickinson, H. C., B. S. Bull., vol. 11, p. 231, 1915.

3. TEST OF THE METHOD WITH STEAM

As the heat capacity of steam at high temperatures is relatively well known, experiments on steam make it possible to estimate the accuracy with which determinations with this apparatus can be made. A series of experiments and appertaining supplementary determinations were accordingly made on water vapor. The main series of experiments with steam consisted of two or three runs at each of five different temperatures in the range from 500° to 1,100° C.

(a) PROCEDURE

In the steam experiments the calorimeter was held under the spout for the same length of time as in the phosphorus pentoxide runs, and the rate of vaporization was so chosen that the amount of heat transferred to the calorimeter became roughly the same as in the phosphorus pentoxide runs, usually corresponding to a temperature rise of from 3° to 5° C. in the calorimeter.

The amount of steam condensed in the calorimeter was found as the increase in weight of the Dewar flask with contents. In contrast to phosphorus pentoxide, which was completely condensed in the calorimeter, an appreciable amount of steam left the Dewar flask again without condensing. The weight of this uncondensed steam and the temperature at which it left the Dewar flask had to be ascertained in order that a correction might be made for the amount of heat thus escaping the calorimeter. To this end supplementary experiments were performed with the same rate of vaporization as in the main experiments. The rate of vaporization from the flask, F, was found by determining its loss in weight in about half an hour, during which period the amount condensed in the calorimeter was determined twice in the same manner as during the main experiments. The weight of steam escaping condensation during the experimental period was then easily found by difference. Fortunately, it was not necessary to know the exit temperature of the uncondensed steam very accurately because the amount of the escaping steam was relatively small. From several observations its temperature was estimated to be about 110° C.

The superheated vapor entered the calorimeter, not at the furnace temperature, but at the temperature which it had at the orifice of the spout. This temperature was measured with three platinum-platinumrhodium (10 per cent Rh) thermocouples the wire diameters of which were 0.644, 0.405, and 0.202 mm, respectively. These thermocouples were successively placed at the center of the orifice with at least 50 mm of the wires adjoining the weld set in vertical position in order to have them surrounded and heated by the issuing jet of vapor. With each couple, measurements were made before and during vaporization. The correct temperatures were subsequently obtained by plotting the observed temperatures against the cross-sectional area of the wires, and extrapolating back to the axis at which this area becomes zero.

The temperatures at the level of the well bottom were found to be identical inside and around the well, both before and during vaporization. These temperatures were not changed by the passage of vapor through the silica tube; at least, they remained constant during the usual preheating period of 3 minutes and the subsequent calorimetric

period of 90 seconds. It took from 2 to 3 minutes for the vapor to heat the spout, during which period the temperatures at the upper end of the spout and at the orifice increased and became constant. In the steady state thus established the temperature of the vapor at the upper end of the spout was equal to, or only about one degree lower than, the furnace temperature. From this it may be seen that the vapor actually was heated to the furnace temperature; that is, to the temperature at the bottom of the well, which was a little lower than the temperature in the middle of the furnace, as may be seen from Figure 2. In the steady state the temperature of the vapor at the orifice was appreciably lower than the furnace temperature; for example, it was found to be 3° and 36° C. below the furnace temperature at 550° and 1,100° C., respectively, at the usual rate of vaporization.

The temperature of the spout itself was also measured, both before and after the preheating period, in order that a correction might be made for the increased radiation from the heated spout, which escaped measurement in the blank experiments.

(b) DATA AND DISCUSSION

The main series of experiments with steam consisted in 12 runs, details of which are given in Table 1. The furnace temperatures employed in these experiments were in each case close to one of the five temperatures, 550°, 650°, 800°, 950°, and 1,100° C., which also were approximated in the experiments with phosphorus pentoxide. The difference between the furnace temperature and the temperature of the vapor at the orifice is the drop in temperature which the vapor suffered in passing from the bottom of the well to the orifice of the spout. The rate of vaporization was close to 3.8 g of water per minute in all experiments. In runs 4 and 5 the experimental period was 2.0 minutes; in all the other runs it was 1.5 minutes. The experimental period multiplied by the rate of vaporization equals the sum of condensed and uncondensed vapor. The heat loss from the outer shell of the neck of the calorimeter is independent of the furnace temperature. This is due to the fact that in experiments with steam the temperature of the inner shell did not exceed the boiling point of water, on account of reevaporation from the moist inner surface.

TABLE 1.—*Determinations of the heat content of superheated steam*

Run No.	Furnace temperature	Temperature of vapor at orifice	Rate of vaporization	Weight of condensate	Weight of uncondensed vapor	Heat transferred to calorimeter	Correction from blank experiments	Final calorimeter temperature
	°C.	°C.	g Min^{-1}	g (vac.)	g (vac.)	cal.$_{15}$	cal.$_{15}$	°C.
1	546	543	4.115	5.407	0.766	4,829	255	23.86
2	548	545	4.138	5.441	.766	4,940	313	24.37
3	549	546	4.081	5.356	.766	4,915	347	24.94
4	649	644	3.566	6.572	.561	6,174	326	25.60
5	650	645	3.698	6.836	.561	6,398	371	24.70
6	803	795	3.599	5.045	.353	5,111	290	25.98
7	804	796	3.622	5.080	.353	5,191	303	25.63
8	952	934	3.687	5.166	.364	5,927	409	25.61
9	953	935	3.273	4.680	.230	5,083	180	28.77
10	947	929	3.876	5.389	.425	6,193	391	25.83
11	1,105	1,069	4.378	5.674	.893	6,948	332	29.51
12	1,096	1,060	3.503	4.578	.676	5,807	400	28.22

TABLE 1.—*Determinations of the heat content of superheated steam*—Continued

Run No.	Increase of radiation from spout	Heat lost from neck	Correcting to 25° C. (add)	Heat transferred by uncondensed vapor	Total heat content $H_t - H_{25}$	Sensible heat (obs.) $H_t - H_{100}$	Sensible heat (calc.) $H_t - H_{100}$	$\frac{\text{Obs.} - \text{Calc.}}{\text{Obs.}} \times 100$
	cal.$_{15}$	*cal.*$_{15}$	*cal.*$_{15}$	*cal.*$_{15}$	*cal.*$_{15}$ *mole*$^{-1}$	*cal.*$_{15}$ *mole*$^{-1}$	*cal.*$_{15}$ *mole*$^{-1}$	*Per cent*
1	3	50	−6	158	14, 850	3, 781	3, 850	−1. 88
2	3	50	−3	161	14, 933	3, 864	3, 869	−. 13
3	3	50	0	163	14, 973	3, 904	3, 878	. 67
4	7	62	4	145	15, 795	4, 726	4, 775	−1. 04
5	7	62	−2	140	15, 656	4, 587	4, 784	−4. 30
6	10	50	5	114	16, 967	5, 898	6, 187	−4. 90
7	10	50	3	116	17, 078	6, 009	6, 196	−3. 11
8	18	50	3	155	18, 827	7, 758	7, 523	3. 03
9	18	50	18	96	18, 695	7, 626	7, 533	1. 22
10	18	50	4	183	18, 905	7, 836	7, 474	4. 62
11	25	50	26	429	19, 807	8, 738	8, 849	−1. 27
12	25	50	15	336	20, 112	9, 043	8, 760	3. 13

The following notation may be used in calculating the heat content of the vapor at the orifice temperature:

H_t = molal heat content of steam at t° C.
H_{25} = molal heat content of water at 25° C.
Q = amount of heat transferred to the calorimeter.
b = correction obtained by blank experiments.
Δr = increase in radiation from the preheated spout.
Δn = heat lost from the neck of the Dewar flask.
t_f = final calorimeter temperature.
f = correction for deviation of t_f from 25° C.
c = weight of condensed vapor in grams.
u = weight of uncondensed vapor in grams.

We must have

$$H_t - H_{25} = \left[Q - b - \Delta r + \Delta n + f + \frac{u}{18.016} (H_{110} - H_{25}) \right] \cdot \frac{18.016}{u + c} \quad (1)$$

and

$$f = (t_f - 25) \cdot c \quad (2)$$

According to the determinations by Osborne, Stimson, and Fiock[5] $H_{100} - H_{25} = 2{,}675.99 - 104.71$, international joules per gram or

$$H_{100} - H_{25} = 11{,}069 \text{ cal.}_{15} \text{ mole}^{-1} \quad (3)$$

Assuming the heat capacity of steam between 100° and 110° C. to be 2.012 international joules per gram per °C.[6], we find

$$H_{110} - H_{100} = 86.61 \text{ cal.}_{15} \text{ mole}^{-1} \quad (4)$$

Addition of equations (3) and (4) gives

$$H_{110} - H_{25} = 11{,}156 \text{ cal.}_{15} \text{ mole}^{-1} \quad (5)$$

[5] Osborne, N. S., Stimson, H. F., and Fiock, E. F., B. S. Jour. Research, vol. 5 (RP209), p. 479, 1930.
[6] International Critical Tables, vol. 5, p. 82, 1929.

From equations (1), (2), and (5) we then obtain

$$H_t - H_{25} = \left[Q - b - \Delta r + \Delta n + (t_f - 25) \cdot c + \frac{u}{18.016} \times 11{,}156 \right] \frac{18.016}{u + c} \quad (6)$$

The heat content of the vapor at the orifice temperature is calculated by substituting in equation (6) the experimentally determined data in Table 1.

The amount of heat, a, transferred to the calorimeter by the uncondensed vapor is

$$a = (H_t - H_{110}) \times \frac{u}{18.016} \quad (7)$$

which with equation (5) gives

$$a = [(H_t - H_{25}) - 11{,}156] \cdot \frac{u}{18.016} \quad (8)$$

Values of a, calculated from this equation, are included in Table 1. It will be noticed that they are small compared to the total amount of heat transferred to the calorimeter. A large relative error in a is not of much importance, therefore, for the accuracy of the final results.

The latent heat of vaporization constitutes a large part of the total heat content of the vapor. The sensible heat of the superheated steam, defined as $H_t - H_{100}$, is obtained separately, as may be seen from equation (3), by subtracting 11,069 $cal._{15}$ $mole^{-1}$ from the total heat content, $H_t - H_{25}$. Average values for the sensible heat, obtained by other methods, may be calculated directly by means of the formula [7] for the mean specific heat of superheated steam between 100° C. and t°C., and at a pressure of 1 atmosphere,

$$c_{100,t} = 0.4574 + 0.0000462t \quad (9)$$

In the range between 270° and 1,400° C. this formula is based upon the trustworthy experimental results of Holborn and Henning,[8] obtained by measuring the amount of heat given up to a calorimeter by a stream of superheated steam, not permitted to condense in the calorimeter. Observed and calculated values of the sensible heat, or, in other words, experimental values obtained in this investigation and values calculated from equation (9), are included in Table 1, together with the deviation between them in per cent. The agreement is quite satisfactory; in fact, the average numerical deviation is only 2.44 per cent.

The agreement between observed and calculated values of the sensible heat is further illustrated in Figure 3, in which the experimentally determined values given in Table 1 are shown together with a curve obtained by means of equation (9); that is to say, a curve based upon the experimental work of Holborn and Henning. It is concluded that although the method described is not to be considered as an improvement in regard to determinations of the heat content of superheated steam, it certainly can be applied to phosphorus

[7] Holborn, L., Scheel, K., and Henning, F., Wärmetabellen der physikalisch-technischen Reichsanstalt (Vieweg and Sohn, Braunschweig), p. 58, 1919.
[8] Holborn, L., and Henning, F., Ann. Physik, vol. 18, p. 739, 1905; vol. 23, p. 809, 1907.

pentoxide vapor with the expectation of obtaining results accurate within a few per cent.

4. RESULTS FOR PHOSPHORUS PENTOXIDE

Data obtained in 13 experiments performed on phosphorus pentoxide vapor are summarized in Table 2. The furnace temperatures were measured directly, as in the experiments with steam. As the vapor pressures of the amorphous and the vitreous modifications of

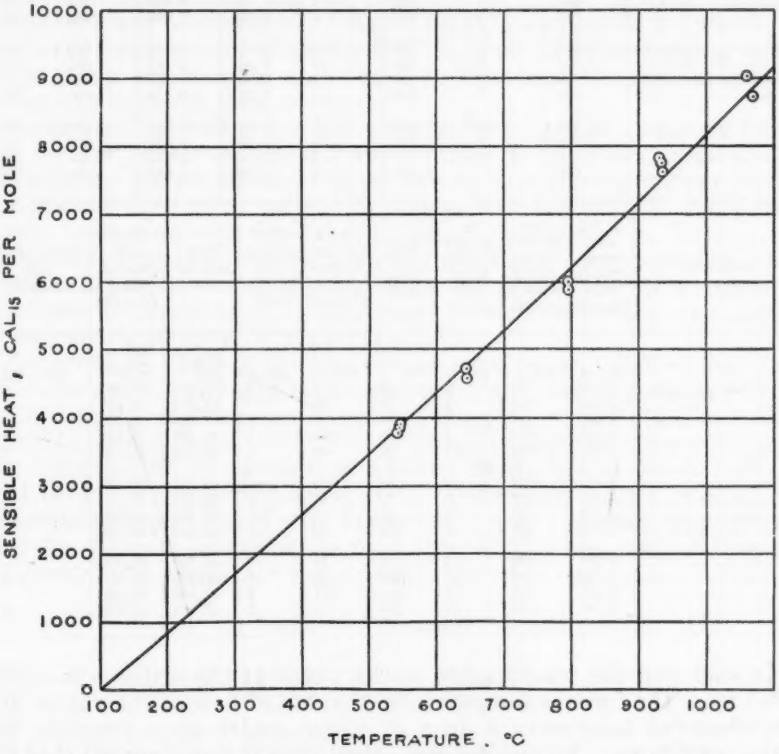

FIGURE 3.—*The sensible heat of steam at atmospheric pressure as a function of the temperature*

The curve is based upon data obtained by Holborn and Henning. ⊙, indicates results found with apparatus shown in Figure 1.

phosphorus pentoxide are less than one atmosphere at temperatures below 600° C., condensation of the vapor into one of these modifications might be expected to take place below that temperature. However, no indication of such a condensation was observed; in fact, the vapor came through the furnace in the two first runs, with a furnace temperature of 549° C., as well as in all the other runs, overcoming the external pressure of one atmosphere; and afterwards no traces of solid phosphorus pentoxide were found in the silica tube. This indicates that the transformation requires higher pressures, such as are easily obtained in closed systems.

TABLE 2.—*Determinations of the heat content of phosphorus pentoxide vapor*

Run No.	Furnace temperature	Well-orifice drop	Temperature of vapor at orifice	Experimental period	Weight of phosphorus pentoxide	Equivalent rate of steam	Evaporated water	Final calorimeter temperature
	°C.	°C.	°C.	Min.	g(vac.)	g min.$^{-1}$	g	°C.
1	549	4	545	1.5	6.848	2.357	0.015	23.19
2	549	4	545	1.5	6.728	2.317	.040	23.08
3	655	5	650	2.0	11.011	2,790	.040	25.29
4	655	5	650	2.0	17.407	4.408	.206	26.69
5	812	8	804	1.5	9.105	2.996	.065	26.45
6	805	11	794	1.5	4.161	1.369	.033	24.35
7	801	9	792	1.5	7.203	2.372	.050	25.45
8	949	26	923	1.5	2.360	.758	.026	21.88
9	950	20	930	1.5	8.771	2.818	.080	24.50
10	958	22	936	1.5	9.594	3.079	.088	24.70
11	1,098	36	1,062	1.5	13.889	4.358	.100	26.63
12	1,098	37	1,061	1.5	12.159	3.813	.489	25.97
13	1,095	37	1,058	1.5	12.159	3.813	.036	25.81

Run No.	Total heat measured in calorimeter	Correction from blank experiments	Increase of radiation from spout	Heat lost from neck	Heat lost by evaporation of water	Correcting to 25° C. (add)	Heat of solution	Heat content of vapor $H_t - H_{25}$	Obs.−Calc. / obs. ×100
	cal.$_{15}$	cal.$_{15}$	cal.$_{15}$	cal.$_{15}$	cal.$_{15}$	cal.$_{15}$	cal.$_{15}$ mole^{-1}	cal.$_{15}$ mole^{-1}	Per cent
1	3,710	254	3	76	9	−2	45,950	27,400	2.26
2	3,590	254	3	74	25	−2	45,910	26,490	−1.09
3	6,052	357	7	103	25	0	47,020	28,000	−9.47
4	9,358	256	7	103	182	5	48,220	28,350	−8.11
5	5,631	326	10	91	40	2	46,560	38,130	4.77
6	2,677	344	10	42	20	−1	45,110	36,300	.96
7	4,496	296	10	72	31	1	46,060	38,600	7.07
8	1,998	538	18	29	16	−1	44,460	44,990	9.55
9	5,766	506	18	109	49	−1	46,490	40,950	.00
10	6,261	494	18	119	54	−1	46,700	40,970	−.49
11	9,222	508	25	206	61	4	47,630	44,000	−4.11
12	8,015	520	25	206	301	2	47,280	45,930	.35
13	8,045	528	25	206	22	2	47,280	42,930	−6.36

In each run the temperature of the vapor at the orifice was calculated from the furnace temperature, the rate of flow of the vapor, and the observed temperature drop of steam under approximately the same conditions. In making this calculation it was assumed that the temperature drop of the phosphorus pentoxide vapor between the thermocouple well and the orifice was the same as that of steam at the same temperature, and flowing at an equivalent rate, defined by the relation

$$r_1 c_1 = r_2 c_2 \qquad (10)$$

where r is the rate of flow, c is specific heat, and the subscripts 1 and 2 refer to phosphorus pentoxide and steam, respectively. The rate r_1, of a stream of phosphorus pentoxide is found by dividing the amount, w, condensed during the experiment by the experimental period, p. Values of w and p are given in Table 2. Values of c_2 are obtained from the literature;[9] and c_1 is constant and equal to 0.26 cal.$_{15}$ per g, as will be shown later. Equivalent rates of steam, calculated from equation (10), are included in Table 2. The temperature drop of the steam at the rate r_2, was calculated from the observed

[9] See footnote 7, p. 44.

temperature drop at the same furnace temperature and at a rate of flow r_s by means of the equation

$$d_2 = d_s \cdot \left(\frac{r_s}{r_2}\right)^{0.2} \tag{11}$$

where d represents temperature drop, and the subscripts refer to the two rates of flow.

Equation (11) is an approximate relation derived, after making certain simplifying assumptions, from an equation given by Walker, Lewis, and McAdams [10] for the heat lost by a fluid flowing through a tube of lower temperature. Equation (11) was tested for steam at a furnace temperature of about 600° C., and at rates ranging from 1.3 to 6.0 g per minute, and found to represent the measurements within the limits of their accuracy.

Corresponding values for the temperature drop of steam and the rate of flow, observed at different furnace temperatures, are given in Table 3. Substitution of these values, and the equivalent rates, in equation (11) gives values for the well-orifice drop in the phosphorus pentoxide experiments. In some runs, however, there is an additional correction, owing to the use of a preheating period shorter than the usual three minutes required to bring the spout to a constant maximum temperature. In such runs a small correction was added to the calculated drop in temperature.

For example, in run 6 the furnace temperature was 805° C. and the equivalent rate 1.369 g of steam per minute; Table 3 gives $d_s = 8$°C. and $r_s = 3.61$ g of steam per minute at 806° C.; substitution in equation (11) then gives $d_2 = 9.7$° C. In this run the heating period was only 2.5 minutes, on account of which a correction of about 1.5° C. must be added, according to separate experiments with steam. The well-orifice drop in run 6 was, therefore, 11° C. Subtraction of this from the furnace temperature gives 794° C. for the temperature of the phosphorus pentoxide vapor at the orifice of the spout.

TABLE 3.—*Supplementary experiments with steam*

Furnace temperature	Rate of vaporization	Well-orifice drop
° C.	$g\ min^{-1}$	° C.
549	4.31	3
655	3.63	5
806	3.61	8
952	3.61	17.5
1,097	3.83	36

The amount of phosphorus pentoxide collected in the calorimeter was determined by gravimetric analysis, according to the method of Hoffman and Lundell.[11] Because a small amount of water evaporated from the calorimeter, the increase in weight of the calorimeter during the experimental period of a run was always a little less than the analytically determined weight of phosphorus pentoxide. The weight of evaporated water was easily determined by difference, and a correction

[10] Walker, H., Lewis, W. K., and McAdams, W. H., Principles of Chemical Engineering (McGraw-Hill Book Co., New York, N. Y.), pp. 135, 149, 1927.
[11] Hoffman, J. I., and Lundell, G. E. F., B. S. Jour. Research, vol. 5 (RP200), p. 279, 1930.

was made for its heat of vaporization. The amount of heat lost from the neck of the Dewar flask was greater in runs 3 and 4 than in runs 1 and 2 on account of a longer experimental period, and less around 800° C. than at 550° and 650° C. on account of less condensation in the neck of the Dewar flask. Above 800° C. it increases with the temperature of the vapor.

The heat content of the vapor at the orifice temperature is calculated from the equation

$$H_t - H_{25} = \left[Q - b - \Delta r + \Delta n + (t_f - 25) \cdot w \cdot s_{25} + \frac{e}{18.016} \times 11{,}069 \right] \frac{M}{w} - Q_{(soln.)} \tag{12}$$

in which the significance of Q, b, Δr, Δn, and t_f is the same as in the experiments with steam; H_{25} is the molal heat content of the crystalline phosphorus pentoxide at 25° C.; w designates the weight of phosphorus pentoxide collected in the calorimeter; e, the weight of water evaporated between the calorimetric fore and after periods; and M, the molecular weight, 142.04, of phosphorus pentoxide. The specific heat, s_{25}, of crystalline phosphorus pentoxide at 25° C. and the heat of solution, Q (soln.), of the same substance are obtained from equation (20) and Figure 8, respectively, both of which are given later.

In Figure 4 the experimentally determined values for the heat content of the vapor, calculated by means of equation (12), are shown plotted against the temperature. It is seen that the results are best represented by a straight line. From the molecular weight determinations of Tilden and Barnett [12] it is known that the molecular formula of phosphorus pentoxide vapor at bright red heat is more nearly P_4O_{10} than P_2O_5. The simpler formula and the name phosphorus pentoxide are employed merely for convenience. The equation for the straight line, calculated from the data in Table 2 by the method of least squares, is found to be

$$H_t - H_{25} = 6{,}720 + 36.81t \tag{13}$$

The deviations of the observed values from the curve average 4.20 per cent, as against 2.44 per cent in Table 1. The increase in error may probably be ascribed to irregularities in the heat of solution of phosphorus pentoxide, which, as shown later, depends upon the relative amounts of meta- and orthophosphoric acids formed in the solution.

The "error," m_o, of the straight line, computed as

$$m_o = 2\sqrt{\frac{m^2}{n(n-1)}} \tag{14}$$

where n is the total number of observations, and m represents deviations of the observed values from the straight line, is 1,170 calories per mole. Barring constant errors, this means that the probability that values for the heat content calculated from equation (13) differ from the true values of this quantity by more than 1,170 calories per mole, is only 4.55 per cent. However, the "error" of the

[12] Tilden, W. A., and Barnett, R. E., J. Chem. Soc., vol. 69, p. 154, 1896.

heat of solution of crystalline phosphorus pentoxide, namely, ± 560 calories per mole, is transferred to the preceding determinations of the heat content of the vapor. Hence the total "error" of the straight line is

$$\pm\sqrt{1{,}170^2+560^2}=\pm 1{,}300 \text{ cal.}_{15} \text{ mole}^{-1}$$

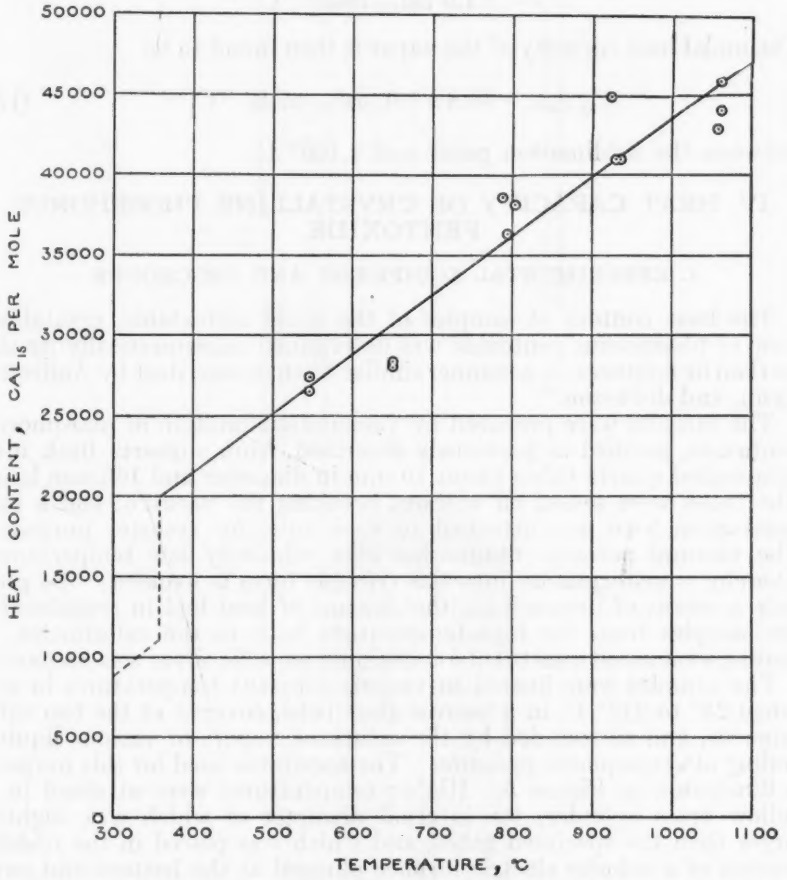

FIGURE 4.—*The heat content of phosphorus pentoxide vapor at atmospheric pressure as a function of the temperature*

The complete equation for the heat content of the vapor is then

$$H_t - H_{25} = (6{,}720 + 36.81t) \pm 1{,}300, \text{ cal.}_{15} \text{ mole}^{-1} \qquad (15)$$

The molal heat capacity, $C_{p,\,1\text{ atm.}}$, of the vapor equals the slope of the line in Figure 4, which is constant and equal to 36.81 calories per mole per degree. The error of the slope, δ, is not affected by the error of the heat of solution, but is determined solely by the accidental errors of the heat content determinations. Attributing two-thirds of the "error" calculated from these to the second term of the right

side of equation (13), we have

$$\delta \times t = \pm \tfrac{2}{3} \times 1{,}170 \text{ cal.}_{15} \text{ mole}^{-1} \tag{16}$$

Substituting 800° C. for t as the approximate average of the experimental temperatures, we find

$$\delta = \pm 1.0 \text{ cal.}_{15} \text{ mole}^{-1\circ}\text{C.}^{-1}$$

The molal heat capacity of the vapor is then found to be

$$C_{p,\,1\text{ atm.}} = 36.8 \pm 1.0, \text{ cal.}_{15} \text{ mole}^{-1\circ}\text{C.}^{-1} \tag{17}$$

between the sublimation point and 1,100° C.

IV. HEAT CAPACITY OF CRYSTALLINE PHOSPHORUS PENTOXIDE

1. EXPERIMENTAL EQUIPMENT AND PROCEDURE

The heat content of samples of the usual metastable, crystalline form of phosphorus pentoxide was determined calorimetrically by the method of mixtures, in a manner similar to that described by Andrews, Lynn, and Johnston.[13]

The samples were prepared by vacuum sublimation of phosphorus pentoxide, purified as previously described, from a quartz flask into thin-walled quartz tubes about 10 mm in diameter and 165 mm long. The tubes were sealed off without breaking the vacuum, and a fine constantan wire was attached to each tube for transfer purposes. The vacuum permits sublimation at a relatively low temperature, whereby transformation into the vitreous form is avoided. To provide a means of determining the amount of heat lost in transferring the samples from the high-temperature bath to the calorimeter, a similar, evacuated quartz tube containing metallic silver was prepared.

The samples were heated to various constant temperatures in the range 25° to 212° C. in a narrow glass tube, covered at the top with asbestos, and surrounded by the saturated vapors of various liquids boiling at atmospheric pressure. The apparatus used for this purpose is illustrated in Figure 5. Higher temperatures were attained in a hollow brass cylinder, the internal diameter of which was slightly larger than the specimen tubes, and which was placed in the middle portion of a tubular electric furnace plugged at the bottom and covered at the top with asbestos. At the end of the heating period the brass body was lifted to the top of the furnace by means of a wire attached to it, and the sample immediately transferred to the calorimeter. In order to make sure that the samples each time would reach the temperature of the heating bath, they were always left in it for at least three hours. By separate determinations it was found that after this length of time none of the samples would take up a measurable amount of heat. Similarly, it was found that an after period of about one hour was necessary and sufficient to insure complete temperature equalization in the calorimeter.

The calorimeter consisted of a silvered Dewar tube, 5.1 by 25.4 cm, surrounded by appropriate insulating material, and containing about

[13] Andrews, D. H., Lynn, G., and Johnston, J., J. Am. Chem. Soc., vol. 48, p. 1274, 1926.

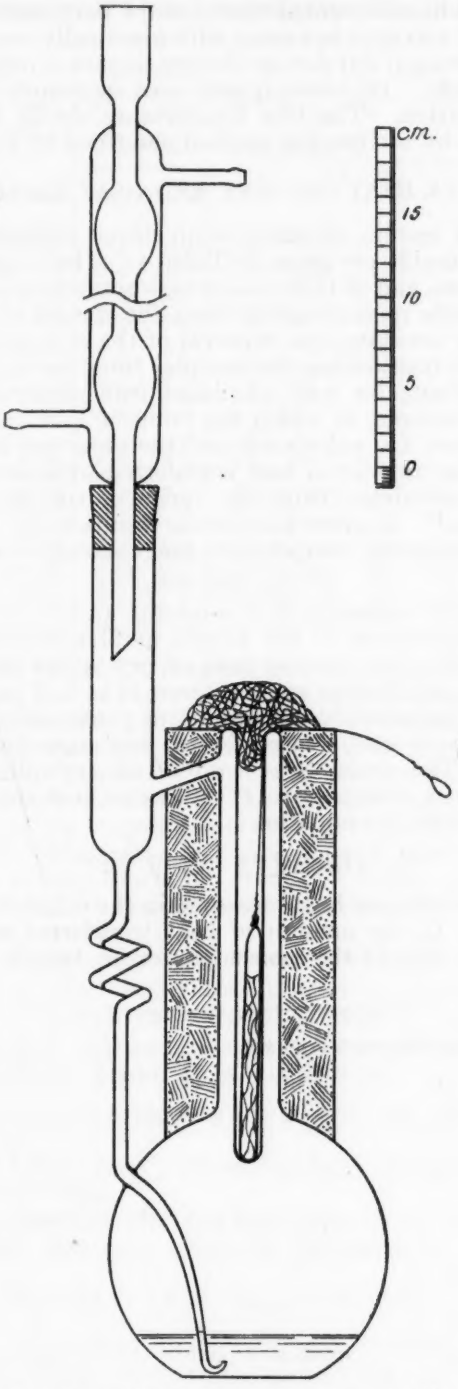

FIGURE 5.—*Constant temperature vapor bath*

300 g of water, a hand-operated stirrer, and a Beckmann thermometer. The calorimeter was kept in a room with practically constant temperature and only brought out during the few moments required for transferring the sample. Its heat capacity was accurately determined by electrical calibration. The true temperature rise in the calorimeter was determined by the graphic method described by Dickinson.[14]

2. DATA, HEAT CONTENT, AND HEAT CAPACITY

Experimental results obtained with three different samples of phosphorus pentoxide are given in Table 4. The weights in vacuum of the three tubes, and of their contents, were determined subsequent to the calorimetric measurements from the weight of the specimens before and after breaking and removal of the contents, respectively. The heat lost in transferring the samples from the high-temperature bath to the calorimeter was calculated from determinations made with the silver sample, in which the transfer loss was found as the difference between the calculated and the observed heat content of the sample. The amount of heat transferred with the silica containing-tubes was calculated from the range of cooling and the heat capacity of silica.[15] In order to refer the results to 25° C. as the lower end of the experimental temperature range, a correction

$$f=(t_f-25)\cdot w\cdot s_{25}$$

was added to the measured heat content; as before, t_f is the final calorimeter temperature, w the weight of phosphorus pentoxide in the sample, and s_{25} the specific heat of crystalline phosphorus pentoxide at 25° C., which later will be shown to be 0.17 calorie per gram. Above 250° C. vaporization of phosphorus pentoxide within the tube becomes appreciable and a correction, i, was made for this as shown in the table. The molal heat content of crystalline phosphorus pentoxide, H_t, at a temperature, t° C., less its heat content at 25° C., was calculated from the equation

$$H_t-H_{25}=[Q+q-Q_s+f-i]\times\frac{M}{w} \tag{18}$$

where Q is the amount of heat measured in the calorimeter, q the heat lost in transfer, Q_s the amount of heat transferred with the silica-containing tube, and M the molecular weight, 142.04, of phosphorus pentoxide.

[14] See footnote 4, p. 40.
[15] International Critical Tables, vol. 5, p. 105, 1929.

TABLE 4.—*Determinations of the heat content of crystalline phosphorus pentoxide*

Run No.	Bath temperature	Weight of phosphorus pentoxide	Weight of silica	Final calorimeter temperature	Heat transferred to calorimeter	Heat lost in transfer	Heat transferred with silica	Correcting to 25° C. (add)	Correction for vaporization	Heat content of phosphorus pentoxide	Obs.−Calc. / Obs. ×100
	° C.	g (vac.)	g (vac.)	° C.	cal.$_{15}$	cal.$_{15}$	cal.$_{15}$	cal.$_{15}$	cal.$_{15}$	cal.$_{15}$ mole^{-1}	Per cent
1	34.90	12.7209	7.0476	23.56	38.59	0.2	14.45	−3.11		237	−0.8
2	76.57	12.7209	7.0476	22.67	189.62	1.4	70.55	−5.04		1,289	−4.2
3	131.2	12.7209	7.0476	23.15	423.2	3.0	146.7	−4.00		3,076	4.0
4	183.3	12.7209	7.0476	24.03	630.8	6.0	225.0	−2.10		4,575	−1.0
5	238.0	12.7209	7.0476	24.63	889.4	9.4	312.7	−.80		6,536	.1
6	36.0	8.8274	6.8536	24.25	32.7	.1	14.11	−1.26		280	.7
7	64.4	8.8274	6.8536	25.48	112.1	.5	48.8	.72		1,038	3.5
8	99.9	8.8274	6.8536	25.60	220.4	1.0	95.9	.90		2,034	1.5
9	131.4	8.8274	6.8536	25.52	321.0	1.7	139.9	.78		2,954	0
10	164.5	8.8274	6.8536	25.64	434.0	3.2	188.7	.96		4,015	.1
11	183.6	8.8274	6.8536	26.42	500.8	3.8	216.9	2.13		4,663	.8
12	210.2	8.8274	6.8536	26.93	595.4	5.0	257.3	2.90		5,568	.4
13	76.57	3.2269	10.1655	22.84	131.1	1.4	101.45	−1.19		1,314	−1.8
14	131.2	3.2269	10.1655	23.89	277.7	3.3	210.2	−.61		3,089	4.5
15	183.3	3.2269	10.1655	24.98	416.2	6.4	322.5	−.01		4,406	−5.0
16	239.0	3.2269	10.1655	24.09	590.4	10.4	453.8	−.50		6,449	−1.8
17	288.0	3.2269	10.1655	24.69	758.5	15.7	570.9	−.17	0.29	8,928	6.3
18	288.0	3.2269	10.1655	25.04	752.4	15.7	570.0	.02	.29	8,708	3.9
19	335.0	3.2269	10.1655	24.23	886.6	22.2	690.1	−.42	1.49	9,543	−6.6
20	335.0	3.2269	10.1655	24.53	888.0	22.2	689.8	−.26	1.49	9,623	−5.7

Figure 6 shows the molal heat content in Table 4 plotted against the temperature, and a curve representing the graphic average of the experimental results. It is seen that the results obtained with the three different samples generally are in good agreement, in spite of the fact that the respective weights of phosphorus pentoxide and the relative amounts of silica in the samples were quite different. The deviations of the experimental results from the curve indicate the precision of the results, and are given in the last column of Table 4. The average deviation from the curve is 2.63 per cent, whereas the "error" of the curve itself is computed to be 1.57 per cent by means of equation (14).

The curve in Figure 6 is closely represented by the equation

$$H_t - H_{25} = (-578.2 + 22.17t + 0.03902t^2 - 2.817 \times 10^{-5} \times t^3) \pm 1.57 \text{ per cent, cal.}_{15} \text{ mole}^{-1} \quad (19)$$

By differentiation of this equation the heat capacity of metastable, crystalline phosphorus pentoxide is found to be

$$C_p = \frac{dHt}{dt} = 22.17 + 0.07804t - 8.451 \times 10^{-5}t^2, \text{ cal.}_{15} \text{ mole}^{-1}\ ^\circ C.^{-1} \quad (20)$$

The "error" of values for C_p calculated from this expression is estimated to be 1.6 per cent.

According to equation (20) the heat capacity of crystalline phosphorus pentoxide increases with the temperature. We find, for example

$$C_{25} = 24.07 \pm 0.38, \text{ cal.}_{15} \text{ mole}^{-1}\ ^\circ C.^{-1}$$

and

$$C_{300} = 38.08 \pm 0.60, \text{ cal.}_{15} \text{ mole}^{-1}\ ^\circ C.^{-1}$$

The specific heat at 25° C. is

$$c_{25} = 0.1694 \pm 0.0027, \text{ cal.}_{15}\ g^{-1}\ {}^{\circ}C.^{-1}$$

It must be remembered that equations (19) and (20) have only been shown to apply in the range from 25° to about 350° C.

V. HEAT OF SUBLIMATION OF CRYSTALLINE PHOSPHORUS PENTOXIDE

The sublimation point of metastable, crystalline phosphorus pentoxide, is found from plots of various vapor pressure determinations against the temperature, as the temperature at which the vapor pressure is equal to one atmosphere. The determinations by Hoeflake and Scheffer[16] give 359.0° C. as the sublimation point. Three

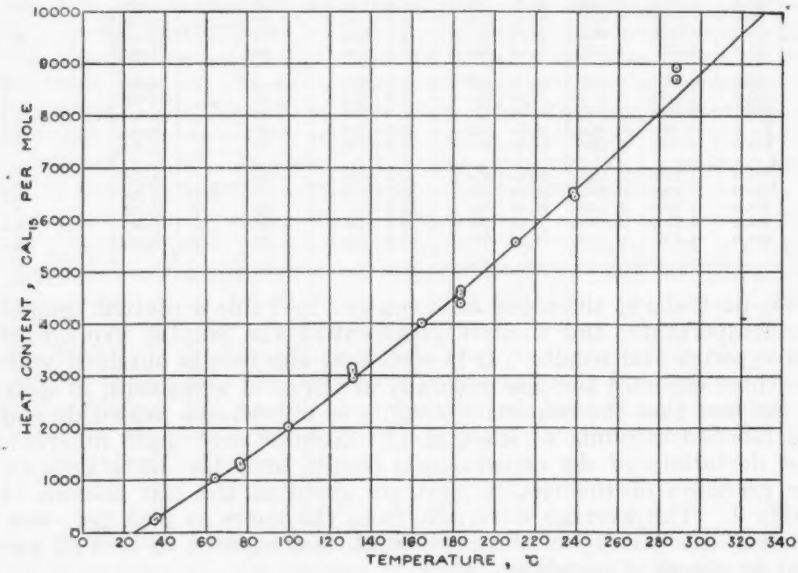

FIGURE 6.—*The heat content of the ordinary crystalline form of phosphorus pentoxide as a function of the temperature*

sets of determinations by Smits and Deinum [17] lead to the values 356.6°, 362.0°, and 370.5° C., respectively; the average of these three temperatures is 363.0° C. Two sets of determinations by Smits and Rutgers [18] give 354.9° and 346.1° C., respectively, or an average value of 350.5° C. The mean of these three average values, finally, gives 358 ± 7° C. as the sublimation point. At this temperature the heat content of the vapor is

$$H_{358}^{(vap.)} - H_{25}^{(cryst.)} = 19{,}900 \pm 1{,}300, \text{ cal.}_{15}\ \text{mole}^{-1}$$

according to equation (15); and the heat content of the solid is

$$H_{358}^{(cryst.)} - H_{25}^{(cryst.)} = 11{,}070 \pm 170, \text{ cal.}_{15}\ \text{mole}^{-1}$$

[16] Hoeflake, J. M., and Scheffer, M. F., Rec. trav. chim., vol. 45, p. 191, 1926.
[17] Smits, A., Z. physik. Chem., Abt. A, vol. 149, p. 337, 1930.
[18] Smits, A., and Rutgers, A. J., J. Chem. Soc., vol. 125, p. 2573, 1924.

according to equation (19). The heat of sublimation, found as the difference between the heat content of the vapor and of the solid, respectively, is then

$$L_{(subl.)} = 8{,}800 \pm 1{,}300, \text{ cal.}_{15} \text{ mole}^{-1} \quad (21)$$

In Figure 4 the heat of sublimation is represented graphically by the sudden increase in heat content of phosphorus pentoxide at the sublimation point.

VI. HEAT OF SOLUTION OF CRYSTALLINE PHOSPHORUS PENTOXIDE

Several samples of crystalline phosphorus pentoxide were prepared by subliming purified phosphorus pentoxide from a half-liter glass flask into a glass tube with several constrictions, sealed to the flask at one end and connected to a P_2O_5 drying tube, open to the atmosphere, at the other. The sublimation was carried out at atmospheric pressure, under which conditions formation of the vitreous modification of phosphorus pentoxide in the sublimed product does not occur. After sublimation the glass tube was sealed off at the constrictions, and the samples were weighed.

The heat of solution was determined in a large silvered Dewar flask containing about 1,500 g of distilled water at room temperature, and a Beckmann thermometer. As usual the heat capacity of the calorimeter was determined by electrical calibration. The sample tube was placed in the water and allowed to remain until complete temperature equalization had taken place, when it was broken under the water with a long, specially made screw clamp of the same temperature as the water. To avoid transfer of heat from the hands of the operator through the screw clamp to the water, the screw clamp was covered at the upper end with rubber and at the lower end with vaseline. The weight of the glass from the broken sample was carefully determined after the calorimetric experiment, and the weight of phosphorus pentoxide was then found by difference.

The results of five determinations are given in Table 5. It is noticed that the weights of phosphorus pentoxide, and therefore also the concentrations of the resulting solutions, cover the same range as those in Table 2. Furthermore, the final calorimeter temperatures are nearly identical in the two tables. The heat of solution may, therefore, be expected to be practically the same in these two series of experiments. To the heat capacity of the calorimeter must be added that of the sample and containing tube. A deduction is made for the small amount of mechanical energy added to the system by breaking the sample-containing tube. A series of preliminary experiments showed that in the concentration range considered here the heat of solution decreases with decreasing concentration in spite of the heat of dilution of phosphoric acid. In order to find out whether this is caused by a variation in the relative amounts of meta-and orthophosphoric acids formed, the solution in each experiment given in Table 5 was titrated immediately after the calorimetric measurements, first with methyl orange indicator, to which the first hydrogen ion of both acids is acid, and second with phenolphthalein, to which the second hydrogen ion of orthophosphoric acid is acid,[19] and from

[19] Prideaux, E. B. R., Chem. News, vol. 99, p. 161, 1909.

the results was calculated the mole fraction of metaphosphoric acid in the mixture of meta-and orthophosphoric acids. The plot in

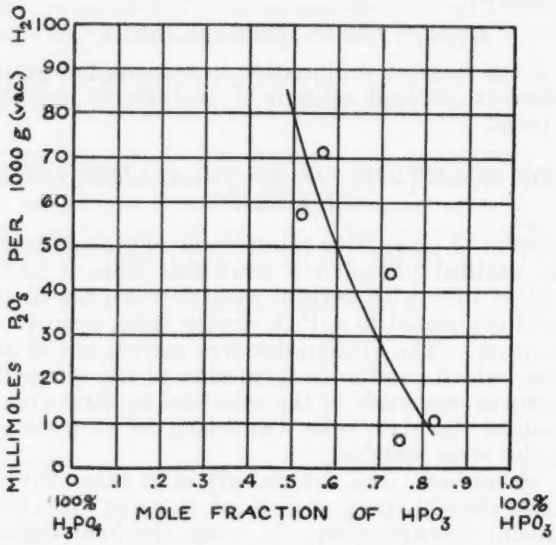

FIGURE 7.—*Variation, with the concentration, of the relative amounts of meta-and orthophosphoric acid, formed by solution of crystalline phosphorus pentoxide in water at 25° C.*

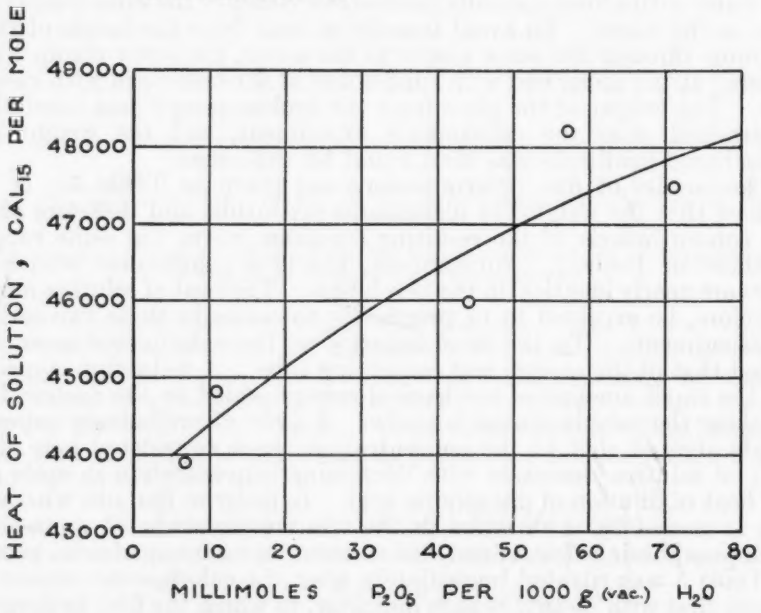

FIGURE 8.—*Heat of solution of the ordinary crystalline form of phosphorus pentoxide as a function of the concentration*

Figure 7 shows that the relative amount of metaphosphoric acid decreases with increasing concentration. As heat is evolved by the

transformation of meta-into orthophosphoric acid, the observed increase in the heat of solution with increasing concentration is thereby explained. Figure 8 shows the heat of solution plotted against the concentration. The "error" of the curve, calculated from the deviations of the experimental results by means of equation (14), is found to be ± 560 calories.

TABLE 5.—*Determinations of the heat of solution of phosphorus pentoxide*

Run No.	Weight of phosphorus pentoxide	Millimoles P_2O_5 per 1,000 g (vac.) H_2O	Final calorimeter temperature	Heat evolved in calorimeter	Mole fraction of HPO_3	Heat of solution	Obs.-Calc. / Obs. ×100
	g (vac.)		*° C.*	*cal.* $_{15}$		*cal.* $_{15}$ *mole*$^{-1}$	*Per cent*
1	1.4351	6.74	26.4	443.5	0.748	43,890	−0.55
2	2.3318	10.94	26.4	735.8	.823	44,820	.80
3	9.3891	43.98	27.5	3,040.2	.722	45,990	−1.41
4	12.2138	57.10	28.2	4,145.8	.519	48,210	1.89
5	15.1624	71.18	29.0	5,068.1	.567	47,480	−0.80

The heat of transformation of meta- into orthophosphoric acid may now be calculated. Figure 7 shows that at a concentration of 11.5 millimoles of P_2O_5 per 1,000 g of H_2O, the mole fractions of HPO_3 and H_3PO_4 are 0.8 and 0.2, respectively. At this concentration the reaction attending the solution of one mole of phosphorus pentoxide is, therefore

$$P_2O_{5(cryst.)} + 1.4\ H_2O(l) + aq = 1.6\ HPO_{3(aq)} + 0.4\ H_3PO_{4(aq)} + (44{,}500 \pm 800)\ \text{cal.}_{15} \quad (22)$$

where the heat of solution has been obtained from Figure 8, and the "error" of both curves is included.

Similarly at 79.5 millimoles of P_2O_5 per 1,000 g H_2O the mole fractions of HPO_3 and H_3PO_4 are 0.5 each. The solution reaction is then

$$P_2O_{5(cryst.)} + 2\ H_2O(l) + aq = HPO_{3(aq)} + H_3PO_{4(aq)} + (48{,}200 \pm 800)\ \text{cal.}_{15} \quad (23)$$

In the concentration range considered here the heat of dilution of phosphoric acid [20] is negligibly small. Subtracting equation (22) from equation (23), and dividing both sides by 0.6, we find

$$HPO_{3(aq)} + H_2O(l) = H_3PO_{4(aq)} + (6{,}200 \pm 1{,}900)\ \text{cal.}_{15} \quad (24)$$

According to measurements by Giran [21] the amount of heat evolved in the last reaction is 3,150 calories. However, in dissolving pure metaphosphoric acid he made no correction for its partial conversion into orthophosphoric acid. Assuming that he obtained a conversion similar to that shown in Figure 7, his result becomes about 5,500 calories instead.

[20] International Critical Tables, vol. 5, p. 180, 1929.
[21] Giran, H., Ann. chim. phys., vol. 30, p. 203, 1903.

From equations (23) and (24) one obtains by addition and subtraction, respectively

$$P_2O_{5(cryst.)} + 3\ H_2O(l) + aq = 2\ H_3PO_{4(aq)} + (54{,}400 \pm 2{,}100)\ \text{cal.}_{15} \quad (25)$$

and

$$P_2O_{5(cryst.)} + H_2O(l) + aq = 2\ HPO_{3(aq)} + (42{,}000 \pm 2{,}100)\ \text{cal.}_{15} \quad (26)$$

Hence it is seen that the heat of solution of phosphorus pentoxide in water at 25° C. may vary between 54,400 and 42,000 calories per mole of phosphorus pentoxide, according to the relative amounts of ortho- and meta-phosphoric acids formed in the solution. The values obtained by Giran [22] and Thomsen [23] are 40,790 and 35,600 calories per mole, respectively. It is thought that the samples of phosphorus pentoxide used by these investigators gave low results on account of possible contamination with lower oxides of phosphorus and meta-phosphoric acid.

VII. ACKNOWLEDGMENTS

The author is indebted to Dr. E. W. Washburn, under whose direction this work was done; to Dr. J. I. Hoffman, for analyzing the solutions of phosphorus pentoxide; and to Dr. F. D. Rossini, for assisting in the electrical calibration of the various calorimeters used in this investigation.

WASHINGTON, August 11, 1932.

[22] See footnote 21, p. 57.
[23] Thomsen, J., Thermochemistry (Longmans, Green & Co., New York), 1908.

RP515

THE INTERFERENCE METHOD OF MEASURING THERMAL EXPANSION

By George E. Merritt

ABSTRACT

This paper is in response to numerous inquiries for details of the method developed at this bureau and described in Scientific Papers Nos. 393 and 485, and several articles in outside publications. It is intended as a manual for the use of those who wish to measure thermal expansions by the interferometric method. As such, a more complete description of the apparatus and methods developed can be included than would be in order in a paper dealing primarily with the results of a particular set of measurements. The apparatus, method of making specimens, forms for taking data, and computation of data, each is the subject of a careful exposition. An appendix contains tables and special calculations.

CONTENTS

		Page
I.	Introduction	59
II.	Construction and adjustment of apparatus	61
	1. The furnace	61
	2. Temperature measuring apparatus	61
	3. The illuminating viewing apparatus	64
III.	Preparation and adjustment of the specimen	66
	1. Types of sample	66
	2. Methods of preparation	66
	3. Adjustment	67
	4. Introducing the specimen into the furnace	68
IV.	Observations to be made before starting the run	68
	1. Recording thick edge of interferometer	68
	2. Aperture of iris diaphragm	69
	3. Initial position of fringes	69
	4. Balance of storage cell against standard cell	69
	5. Zero setting of galvanometer	69
	6. Sensitivity of galvanometer	69
	7. Initial temperature of cold junction and furnace	69
V.	The run	69
	1. Adjustment of the heating current	70
	2. Watching the fringes	70
	3. Preparing to read the temperature	70
VI.	Records	70
VII.	Computing and plotting	71
VIII.	Appendix	73
	1. Computations relating to oxidizable specimens	76

I. INTRODUCTION

This paper is in response to numerous requests for details of the interferometric methods, apparatus and procedure developed at this bureau and described briefly in Scientific Papers Nos. 393 and 485 and in several outside publications. It includes later developments in apparatus and technique and full information regarding procedure.

The apparatus described lends itself equally well to the determination to a high degree of accuracy of the linear expansion under equilibrium conditions, or to the determination of the continuous changes in length taking place in a material while being heated or cooled at a predetermined rate which may or may not be uniform. The results obtained by the two procedures are not always the same and it is necessary for the experimenter to consider carefully which procedure is the one which will yield the information he desires.

Since materials differ greatly in the rate with which they reach equilibrium, an investigator attempting to obtain measurements under equilibrium conditions should give careful consideration to this rate at the temperatures involved. For certain kinds of work it is the practice to hold the specimen for a sufficient length of time at each temperature where measurements are to be taken. Cases have occurred in this laboratory where equilibrium conditions were not reached even after several hours.

In the case of a material where the expansion follows the increase in temperature in a regular way an approximate value for the expansion under equilibrium conditions may be obtained by heating continuously at a slow rate and neglecting the readings taken before the heating rate becomes established. In this case it must be assumed that the lag will be constant and that only "true" thermal expansion is taking place. Strictly speaking the only true thermal expansion is where an increase in size of a material results from an increase in effective size of the constituent molecules without any change in their relative arrangement. There are, however, certain effects of change of thermal energy occurring in different substances at different temperature ranges which result in a more or less sudden and drastic rearrangement of the molecules. These appear in the thermal expansion curve as irregularities of slope sometimes amounting to an actual reversal. Such rearrangement of the molecules into different configurations may be very rapid, such as the almost instantaneous conversion of alpha into beta quartz, or very slow, such as the annealing of glass. In either case a study of their nature can be made with this apparatus by heating at a definite rate with frequent readings on the temperature and change in length. This continuous or mobile procedure is not to be considered merely a convenient method of obtaining an approximation to the same value better obtained by means of the equilibrium procedure, but may be thought of as a means of obtaining an entirely different type of information. An insufficiently rapid change of temperature often masks the information sought, hence for a complete analysis several rates should be used and the results compared.

The point to be emphasized here is that neither the "equilibrium" nor the "mobile" procedure should be used indiscriminately, but that each problem should be analyzed and a decision reached as to the type of information desired so that the more appropriate procedure may be selected.

Because of the small size of specimen and the ease and rapidity of reading, the interferometric apparatus described in this paper is particularly advantageous when the mobile procedure is selected. The small size of the specimen and simplicity of temperature control are features which recommend its use in cases where the specimen is to be held at a constant temperature until reaching equilibrium.

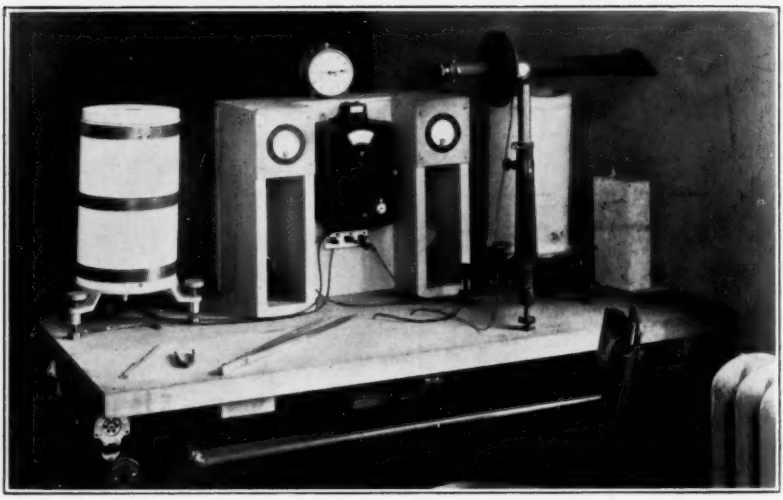

FIGURE 1.—*Assembled apparatus for thermal expansion measurements by the interference method*

UNIV. OF MICH.

II. CONSTRUCTION AND ADJUSTMENT OF APPARATUS

The apparatus consists of three main parts—a furnace for heating the specimen, a device for measuring the temperature, and a means for measuring the change in length. Figure 1 shows the set up.

1. THE FURNACE

A very satisfactory furnace of the tubular type, wound with 17 to 18 feet of chromel ribbon of 1-ohm resistance to the foot is illustrated in Figure 2. The ends of the ribbon are anchored to iron collars and either hard soldered to copper leads or carried out to the outside of the furnace and clamped to binding posts. Care must be taken that the insulation in a vertical direction is as nearly symmetrical as possible. If this is not done, there will be a temperature gradient between the thermocouple and the specimen which will give trouble.[1] The space between the heating tube and the outside of the furnace is filled with silocel or some other similar insulating material capable of standing high temperatures.

This furnace is heated by a 110-volt line current of from 1 to 5 amperes which should be controlled by means of rheostats. For nonmagnetic specimens either direct or alternating current is satisfactory. A convenient, though not necessary accessory, is a tapered wire rheostat which will take more current without overheating as the resistance is taken out. Furnaces of this type may be purchased on the market.

A small porcelain bucket is provided by means of which the specimen may be introduced into and removed from the furnace. The thermocouple is inserted through the bottom of the furnace and projects through a hole in the bottom of this bucket, so that the junction is almost, but not quite, in contact with the lower surface of B, Figure 2.

2. TEMPERATURE MEASURING APPARATUS

For temperature measurements a potentiometer set-up as shown in Figure 3 may be used. The electromotive force developed by the difference in temperature between the hot and cold junctions of the thermocouple is balanced across a galvanometer against the electromotive force of a 2-volt storage battery by means of resistances introduced by the dials of the potentiometer, the storage battery having been previously balanced against a standard cell by means of external rheostats. While the galvanometer sensitivity must drop very low to affect the accuracy of the reading, a rather close watch of the sensitiv-

[1] In order to control the temperature gradient in the furnace, it is desirable to check the temperature indicated by the thermocouple against the temperature existing at the same time in the location occupied by the specimen. A method for approximating this is by utilizing the well-known melting points of several of the more fusible metals.

In order to do this, it is only necessary to prepare a specimen consisting of one element of the desired metal and two elements of some more refractory metal, the expansion of which is not too different from that of the fusible metal. The specimen should be of small cross section in order not to delay the melt.

It is not necessary to count the fringes, but only to watch them carefully as the expected melting point approaches and to see that the heating schedule is the same as that to be used when making regular runs. The melting point is indicated by a rapid change in width of the fringes, culminating in their entire disappearance.

Since many substances have a bad effect on the surfaces of fused quartz, it is desirable to confine these tests to a few metals which have been found to have little effect on the surfaces and the melting points of which are well known, such as:

	°C.
Tin	231.9
Zinc	419.4
Aluminum	658.9
Silver	961

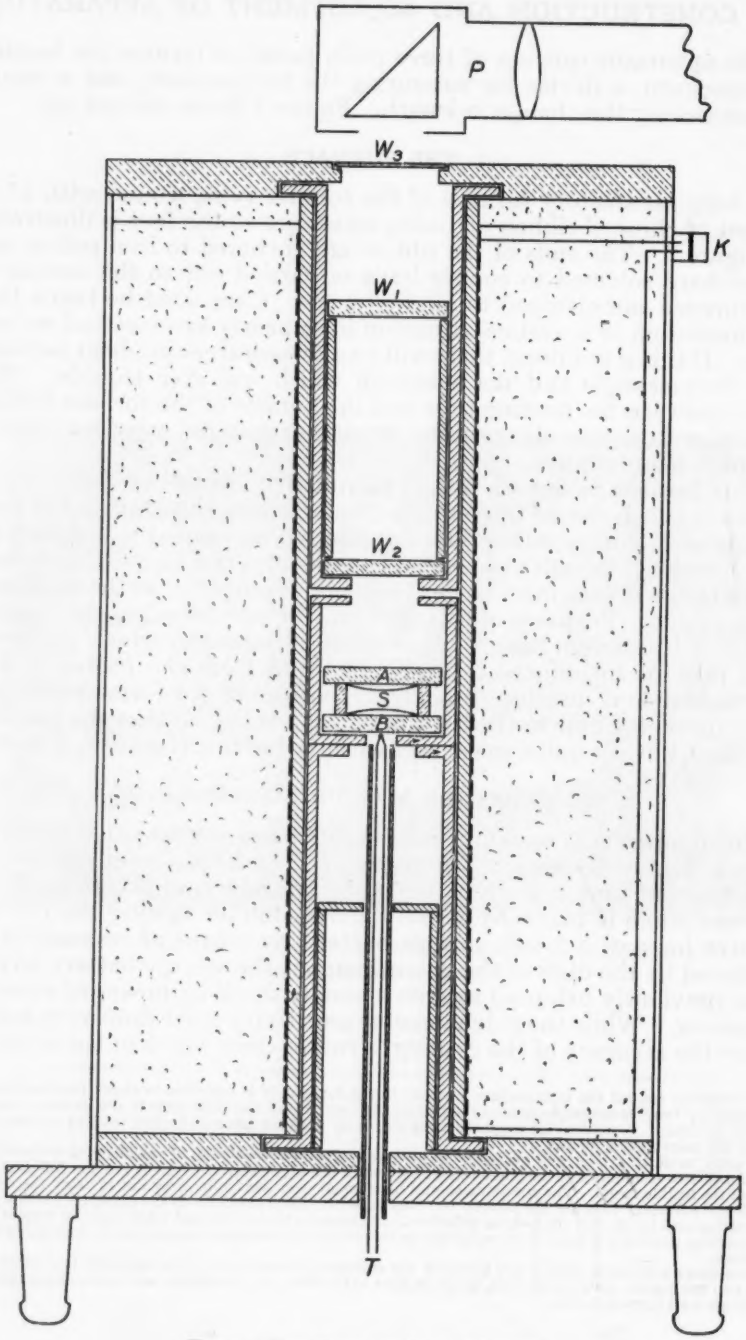

FIGURE 2.—*Cross section of furnace*

ity is desirable, because any change may be an indication of poor connections or other trouble.

A platinum, platinum-rhodium thermocouple is recommended. A table which gives the standard calibration for this kind of couple is shown on page 73. For use from room temperature to 1,000° C., a chromel-alumel couple may be used, and for temperatures below 300° C. a copper constantan thermocouple may be employed. The last two thermocouples are more sensitive than the Pt-PtRh couple.

The cold junction may consist of a pair of mercury filled glass tubes into which the two wires of the thermocouple and the wires to the potentiometer are inserted. The temperature of this junction must be well controlled and this is easily done by immersing both tubes in a vacuum bottle which may be filled with water or a mixture of

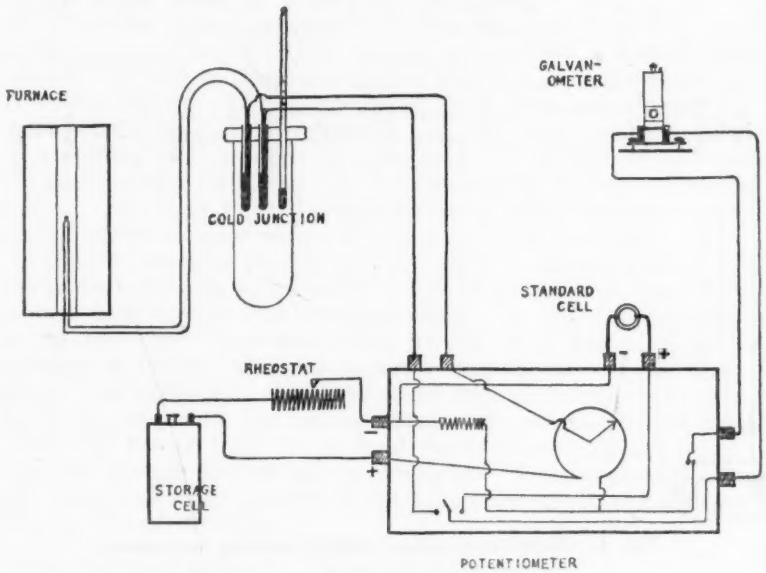

FIGURE 3.—*Potentiometer arrangement*

water and ground ice. The temperature of the cold junction may be read by means of a thermometer.

The galvanometer may be of the quartz suspension, moving concave mirror type, the radius of curvature of the mirror being about 50 cm. The image of a lamp filament is focused on a ground glass placed in such a position that it is convenient for the operator to read, zero being indicated by a black index mark on the ground glass. Lighter reference marks, used to determine the sensitivity, can be advantageously added without confusing the observer. The ground glass should be so arranged that it can be displaced to compensate for small drifts in the zero without readjusting the galvanometer.

A very convenient direct-reading potentiometer indicator may be obtained in which the galvanometer and standard cell are integral parts of the instrument, and a room temperature compensator eliminates the need for a specially controlled cold junction.

3. THE ILLUMINATING VIEWING APPARATUS

Figure 4 is a diagram of the essential optical parts of the viewing apparatus. Light from a source, H, which may be the capillary of a helium tube, or a real image of the same, is made parallel by the lens, L, and after reflection from the prism, R, falls on the interferometer plates, A and B. Here the light partially reflected from the lower surface of A and that from the upper surface of B is returned. That reflected from the upper surface of A is thrown to one side by virtue of the angle of 20′ between the two surfaces of A; and that from the lower surface of B is diffused, or reflected to one side in the same manner as that from the top of A. The reflected beams, from A lower and B upper, return nearly on their incident path and are brought to focus in two real images, both of which must fall on the opening in the

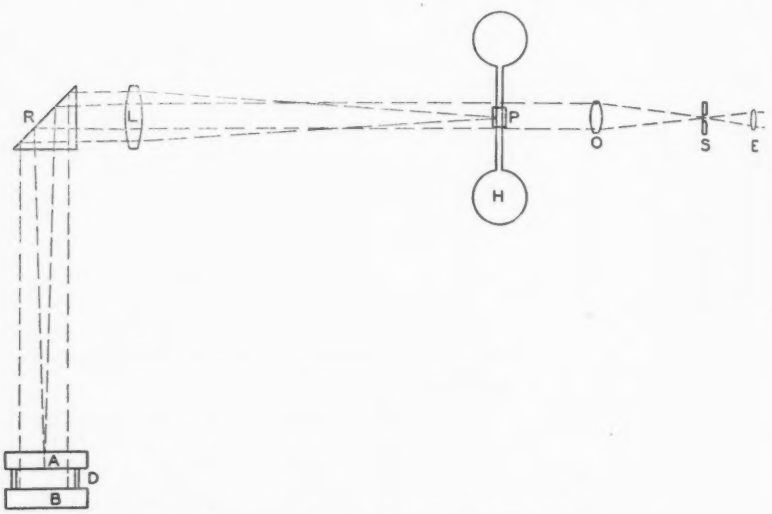

FIG. 4.—*Diagram of optical parts of viewing instrument*

diaphragm at P. When the central rays of these images are parallel, the telescope OSE focused for infinity will focus the fringes in the same plane as the image of the plates. This brings the reference mark on the lower surface of A into focus without parallax between it and the fringes.[2] If two trains of waves from one point in a source having traveled different paths fall upon a point in the retina of the eye, the resultant amplitude of vibration determines the brightness. If they are "in step" maximum brightness results. If, however, the "troughs" of one arrive with the "crests" of the other, destructive interference takes place resulting in relative darkness. If the two trains travel different distances, so that the difference in path is some whole number of wave lengths, then the waves will reach the eye in phase. If the difference in path is equal to some whole number of wave lengths plus one-half wave length, the waves in the two trains will be in

[1] See footnote 2 on p. 65.

opposite phase, so that destructive interference will take place.[2] In order that these conditions may be satisfied, the source H and the plate A must both be at the focal distance of the lens L from L. A small amount of deviation from these conditions may be compensated for by changing the focus of the telescope.

The lens L should be slightly canted so that light reflected from its surfaces will be thrown out of the field, and the prism R should, for the same reason, be slightly rotated about an axis normal to the plane of its hypotenuse.

The following procedure is recommended:

O, the objective of the telescope, should be brought close enough to P to take in a large part of the two interfering beams from A and B. The telescope should be previously focused on a distant object; and the cross wires, S, placed at the principal focus of O. Then, with H at the principal focus of L, the distance from L to A via R can be correctly adjusted by raising or lowering a well illuminated object in the path of the beam until it is in focus when viewed through the whole system The larger plate, B, is then substituted for this object; the eyepiece, E, removed and the light reflected from the upper surface of B brought into the field. If A, the smaller plate, is then laid directly on B and the eyepiece replaced, a set of fringes will be seen. Likewise, any reference marks or other features on the surfaces of either of these plates will be seen to be in focus.

In order to energize the helium tube a high voltage current is needed. This is conveniently supplied by a 110 to 12,000 volt transformer of the kind used for the smaller neon signs. In order to prevent overheating the tube, thus shortening its life, it is well to introduce a resistance of 100 to 150 ohms in series with the primary of the transformer. As a criterion, the bulbs at the ends of the helium tube should not, in operation, be too hot to touch. Furthermore, the capillary (which gets hotter than the ends of the tube) should not be allowed to get hot enough to give off sodium light. A conveniently arranged switch will enable one to turn off the light when not in use, thus lengthening the life of the tube.

---

[1] Extract from Theory of Optics, A. Schuster, Ch. IV, p. 76.

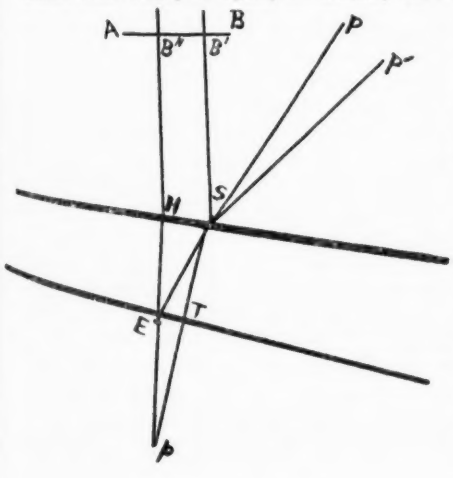

The simplest case of a film of variable thickness would be presented by a transparent wedge (fig. 45).

A plane wave AB falling on the wedge, we may select one ray $B'S$ reflected at S toward P, and another, $B''H$, such that after refraction at H and reflexion at E, it meets the upper surface at the same point S. Owing to the inclination of the two surfaces, the refracted ray SP' is not now coincident with SP, though the inclination is small, if the angle of the wedge is small. The difference in optical length between the two rays is $2\mu\epsilon \cos\gamma$ or taking account of the change of phase at reflexion, $2\mu\epsilon \cos\gamma + \frac{\lambda}{2}$. In this expression ϵ denotes the length of the perpendicular from S to the lower surface of the plate (which may be taken as the thickness of the plate at S) and γ is the angle of incidence on the lower surface. The inspection of the figure explains how the expression is derived. Neglecting all rays which have suffered more than one internal reflexion, an eye placed so as to receive both rays SP and SP' and focused on S, will observe a maximum or minimum of light, according as $2\mu\epsilon \cos\gamma$ is an odd or even multiple of half the wave length.

The interferometer plates A and B are of clear transparent fused quartz and should not contain large bubbles or other imperfections. The surfaces of each plate should be flat to one-fifth of a fringe or better throughout the central parts and inclined to each other at an angle of about 20′ for the reasons already explained. It is well to choose A about 27 mm in diameter and B, slightly larger (30 mm). Both A and B should be 4 or 5 mm thick.

III. PREPARATION AND ADJUSTMENT OF THE SPECIMEN

The specimen consists of three elements which are placed between the two interferometer plates A and B in contact with the lower surface of A and the upper surface of B.

1. TYPES OF SAMPLE

The specimen is usually arranged as a tripod, the feet of which may be either projecting parts of the same piece of material, or consist of three separate fragments. Metallic specimens or those already of tubular form (such as glass tubing) are often constructed as rings. Three scallops are, however, taken out of the upper and lower ends of this ring so that the specimen consists effectively of three perpendicular rods of the material joined by three bridgelike arches which do not touch either the top or the bottom plate. (See fig. 4.)

Massive materials which are easily cut and ground are usually made into rough pyramids, tetrahedrons, or cones. The bases of these should be concave or grooved so that each piece rests solidly on three feet. The point of contact with the upper plate should be well within the base limited by these contact points. Three such elements, each sitting solidly on its own feet, constitute a single specimen in which the expansion obtained from a reference mark in the center of the upper plate is an average of the expansions of all three.[3]

2. METHODS OF PREPARATION

Some of the softer terra cottas and clays can be roughed into shape with a file or even scraped with a knife; harder ones must be ground on a carborundum wheel, while glass and the harder ceramic materials can be best formed on a revolving cast-iron lap charged with carborundum powder in water. For shaping many of the small specimens it is very convenient to use a dentists' grinding motor with flexible shaft and a variety of steel and carborundum cutters. After bringing the three elements within a few hundredths of a millimeter of the same height in one of these ways, they are usually finished on a dry carborundum knife stone of rather fine grain. The most advantageous length for the specimen is between 5 and 10 mm.

A particular problem is presented in the preparation of glaze samples. In this case a sample of the glazed body should be broken up and a piece bearing an uncracked flake of glaze 3 or 4 mm long and perhaps half as wide, selected. The body is then ground away and the sample inspected with a microscope to insure the removal of all traces of undissolved body material. A binocular microscope is preferable for this purpose. This flake, which may be as thin as 0.2 mm and will probably not be thicker than 0.6 mm is measured

[3] J. Wash. Acad. Sci. vol. 9, No. 10, May 19, 1919.

by means of a micrometer and ground so that it is of the same thickness along one edge ond very nearly plane parallel. It is then placed on a sheet of dark cardboard and very carefully broken with a needle or fine pointed knife into a number of small pieces. Three of these pieces are selected and placed on the lower plate as is done with the larger specimens, but in this case if the fringes are not of the right width, it is better to substitute another piece from the number available than to grind one down. Usually no measurements are made with the micrometer after the flake of glaze is broken into small pieces. The less area these pieces have, the better, as there will be less likelihood of included air films, etc. The only requirement is that they have wide enough bases compared with their heights, to be stable.

3. ADJUSTMENT

When the three elements of a specimen (whether separate pieces or parts of a ring) are the same length as nearly as can be read on a micrometer caliper,[4] they are ready for a trial between the plates. First, the lower plate should be placed in the focus of the viewing apparatus and the reflection from its upper surface found. This is distinguished by being clear and free from shadows of striæ and other imperfections in the interior of the plate. A still better criterion is the following:

If, when the reflection of a surface is found, the upper plate is laid directly on the lower, fringes should be seen at once if the reflection in question is that of the upper surface of B. If they do not appear, or are faint and hazy, remove the upper plate and eyepiece of the observing system, and adjust the leveling screws until the reflection of the other surface of B comes into the field. Then replace the eyepiece and upper plate, when sharp black fringes should appear at once.

When the reflection of the top surface has been located and the eyepiece is in place, the three elements of the specimen are placed on B at the corners of an equilateral triangle. The elements should be moved slightly with the fingers in order to feel any grit which may have eluded the previous cleaning. If any is found, the elements should be removed and cleaned before proceeding. The plate, A, is then held slightly above the specimen and turned about a vertical axis into a position such that the refractive effect of the upper plate will not throw the light reflected from the lower plate out of the field. When this position is found, the plate is set gently on top of the specimen. If the micrometer has been used carefully, fringes should be seen at once. If they are not visible, take a glass rod drawn to a point about as fine as an ordinary pencil and press with this carefully on the top plate near the reference mark. If this does not bring fringes into view, inspect the elements carefully to see that none of them has been laid on its side. This is by no means an uncommon occurrence, especially with specimens approximately tetrahedral in shape. If all are found erect, they should be remeasured. It is well to see if any one of them is, perhaps, a whole hundredth or tenth of a millimeter longer than another.

[4] The usual metric micrometer has divisions representing hundredths of a millimeter; an English instrument should have the smallest division 1/1000 inch. An effort should be made in either case to estimate tenths of the smallest division.

When the fringes have been found, press with the glass rod until sure that the plates are resting in a position of stable equilibrium. If the fringes are too wide or too narrow, the elements must be adjusted in length. When a slight pressure is exerted on the upper plate near the reference mark, the fringes move toward the thick side of the space between the plates, that is, toward the longest of the three elements. This indicates which one is to be shortened. It should be remembered that the method by which the elements are now being compared is far more sensitive than the micrometer, hence only a relatively slight change needs to be made.

4. INTRODUCING THE SPECIMEN INTO THE FURNACE

Having the fringes of the desired width, about 2 mm between centers, the plates and specimen, which now constitute an interferometer, may be picked up with a pair of cork-tipped tweezers and placed in the bucket. This bucket should now be lowered carefully into the furnace either by means of a long bail of thin platinum wire permanently attached, or by a pair of internally expanding forceps with small pins made to fit the holes near the upper edge of the bucket. If wire is used, it should be flexible enough to bend easily out of the way. If forceps are used, the lid of the bucket, a porcelain disk with a 2-cm hole in the center, must be put in after the bucket is set in place.

After the specimen has been let down into the furnace and the viewing apparatus adjusted, the glass rod should again be pressed against the center of plate A in order to make certain that nothing has shaken loose during the transfer, and that the interferometer in its container is resting solidly in the furnace. At this time it should be noted which side of the interfererometer is the thicker. The viewing apparatus is then swung to one side, the tube or thimble containing the fused quartz windows W_1 and W_2 put in, the cover with the glass window W_3 placed on top, and the viewing apparatus returned and adjusted.[5]

IV. OBSERVATIONS TO BE MADE BEFORE STARTING THE RUN

1. RECORDING THICK EDGE OF INTERFEROMETER

When making the last test with the glass rod, it is advisable, as already stated, just before closing the furnace, to place the rod near the center of the upper plate and exert a slight downward pressure in order to see that the plate is seated solidly. This pressure produces a slight compression which shifts the fringes slightly toward the thick side of the wedge-shaped space between the two plates. This direction should be noted. The fringes will move in the opposite direction when the specimen expands. It is well to draw a small diagram of the field showing the position of the fringes and the elements of the specimen, indicating which is the thick side of the interferometer.

[5] A convenient arrangement for adjusting specimens and transferring them to the furnace without the necessity for readjusting the viewing apparatus is to have a stand set alongside of the furnace at a height such that specimens on it will be the same distance from the table as they will be when in the furnace. If this stand, or the furnace, or both can be leveled, it is possible to arrange things so that the viewing apparatus may be swung from one position to the other and will need very little or no change to be equally in adjustment for both positions.

2. APERTURE OF IRIS DIAPHRAGM

The most advantageous aperture for the iris diaphragm in the observing system should be determined and the diaphragm set there before starting. This precaution is necessary because a change in the size of aperture shifts the observed position of the fringes, which, during the run, would introduce an error of two-tenths or three-tenths of a fringe. For runs which are to be carried to higher temperatures, the aperture should be small in order to minimize the effect of scattered light from the incandescant furnace. If, during the run, the fringes become faint, the condition can probably be remedied by releveling the viewing instrument rather than by changing the aperture of the diaphragm.

3. INITIAL POSITION OF FRINGES

The position of the reference mark with respect to the nearest fringes should be noted and recorded. If the viewing apparatus has a movable cross wire in the eyepiece, it may be desirable to measure this fraction with some accuracy, as its value is important in the case of the smaller specimens or those of low expansion where the total expansion causes but few fringes to pass. In the case of most specimens, however, where the fringes cross the reference mark in relatively rapid succession, the first fringe to cross may be taken as zero and the temperature at the time of transit used as the "room temperature."

4. BALANCE OF STORAGE CELL AGAINST STANDARD CELL

The storage battery should then be balanced against the standard cell.

5. ZERO SETTING OF GALVANOMETER

The zero setting of the galvanometer can usually be accomplished by moving the ground glass until the zero mark falls under the image of the lamp filament.

6. SENSITIVITY OF GALVANOMETER

After the preceding adjustment the key of the potentiometer should be closed and the galvanometer deflection brought to zero by moving the dials. Then, as a check on the sensitivity, one of the dials should be turned one step and the resulting deflection noted and compared with previous readings.

7. INITIAL TEMPERATURE OF COLD JUNCTION AND FURNACE

The temperature of the cold junction should now be read and the difference, if any, between it and the furnace recorded. Even when using the direct-reading potentiometer indicator which has the room temperature compensator, it is desirable to read and record the room temperature outside the furnace as well as the temperature indicated by the thermocouple.

V. THE RUN

Everything necessary for recording the results should be obtained before turning on the heating current.

1. ADJUSTMENT OF THE HEATING CURRENT

Only experience with the individual furnace will reveal how much current is needed at a given temperature to produce a given heating rate. Complete and accurate records of the heating current, times, and resulting temperatures for a few runs will supply all the data needed for successful regulation. The heating schedule used in calibrating the furnace should be adhered to as closely as possible. Immediately after each observation of temperature, the rate should be calculated and the requisite changes in the heating current made. A schedule of increments may be prepared for a particular furnace, but this should be checked and revised from time to time, since the characteristics of a furnace change as the heating ribbon deteriorates with repeated use.

With specimens of low thermal diffusivity or with thick specimens of materials of any kind, there will be a slower inflow of heat into the specimen, so that the temperature indicated by the thermocouple may exceed the average temperature of the specimen by an amount too great to neglect in cases where it is desirable to measure the expansion under equilibrium conditions with a high degree of accuracy. This is particularly true at the lower temperatures, say from room temperature up 100° or 200°. In order to bring the specimen into equilibrium conditions with the least expenditure of time, it is well to make all specimens as small as is practicable without sacrificing stability or sufficient height. Data for the amount of current necessary for holding the temperature of the furnace constant should also be collected.

2. WATCHING THE FRINGES

It is important that the attention of the observer be constantly on his work, as each passing fringe must be counted. There is no other way of telling after a lapse of time whether the fringe on the reference mark is the first or the fifth to come into this position since the last observation. To be sure, when the heating rate is constant and the form of the expansion curve of the material is known, less continuity of attention is permissible because it is practically certain that the fringes will follow each other at regular intervals; but unusual care should be exercised wherever there is any uncertainty regarding the substance or in the neighborhood of expected changes.

3. PREPARING TO READ THE TEMPERATURE

The potentiometer should be set before an expected temperature reading. The galvanometer is then kept on zero by movements of the dials and at the same time the fringe is watched as it approaches the reference mark. When the fringe is exactly on the mark, the setting of the galvanometer is verified by a quick glance and the dials allowed to remain in that position until read.

VI. RECORDS

Where the temperature is not to be read for every fringe, the time of transit of each fringe should be recorded on a separate sheet of paper.

A convenient record form is shown below:

Substance, glass.

Date. Dec. 1, 1922.
Serial No. S 107.
Run No. 1.
Source. Glass section No. 43

Length of Specimen L_0=0.7640 cm. Value of $\frac{\lambda}{2L_0}$ 0.3845.

Temperature of cold junction $\frac{22°\text{ C.}}{\text{mv } 125}$. Room temperature 23° C.

I	II	III	IV	V	VI	VII	VIII
Transit time	Fringes N	$N\frac{\lambda}{2L_0}$	Air correction	ΔL in	Potentiometer readings	Corrected for cold junction	Temperature
		μ/cm	μ/cm	μ/cm	*microvolts*	*microvolts*	°C.
12.56	0	0	0	0	6	131	23
1.55	10	3.85	.37	4.22	303	428	70
1.28	20	7.69	.62	8.31	605	730	112

In the first column is written the time of transit of the fringe recorded in the second. In the sixth column is the reading of the potentiometer at that time. In the seventh, this reading is corrected for the temperature of the cold junction.[6] The eighth column is derived from the seventh by means of Table 1 of the appendix. These columns are all filled in during the run. The number of the coming fringe is recorded as soon as it is fully decided it is the next one to be used. As soon as it is centered on the reference mark, the time is read and recorded. Then the potentiometer is read and recorded, the correction added and the temperature found by reference to the calibration table for the thermocouple.

These operations consume time, so care must be exercised that no fringe be allowed to pass unobserved while the attention is distracted. If their movement is very rapid, it may be best to record only the time, number of fringe, and microvolts until the region of rapid expansion has been passed.

VII. COMPUTING AND PLOTTING

The third, fourth, and fifth columns are calculated after completing the run. The values of the third column are obtained by multiplying the number of fringes shown in the second column by a previously calculated factor $\frac{\lambda}{2L_0}$ the equation:

$$\Delta L = N\frac{\lambda}{2L_0} + \text{air correction}$$

where N is the number of fringes, λ is the wave length (in microns) of the light used, and $N\frac{\lambda}{2}$ is the apparent amount in microns that the

[6] This is done by adding the number of microvolts equivalent to the temperature of the cold junction to the reading of the dials. If melting ice made from pure water is kept around the cold junction, this correction reduces to zero.

specimen has expanded. When this quantity is divided by the original length of the specimen, L_0, in centimeters, we have ΔL, the expansion of a centimeter of the material in microns.[7] To facilitate the calculations, the factor $\frac{\frac{\lambda}{2}}{L_0}$ is calculated separately. $\frac{\lambda}{2}$ for the yellow helium line is 0.29378μ. at 15° C. and 760 mm. The expression $N\frac{\frac{\lambda}{2}}{L_0}$ does not give the true dilatation because the wave length of the

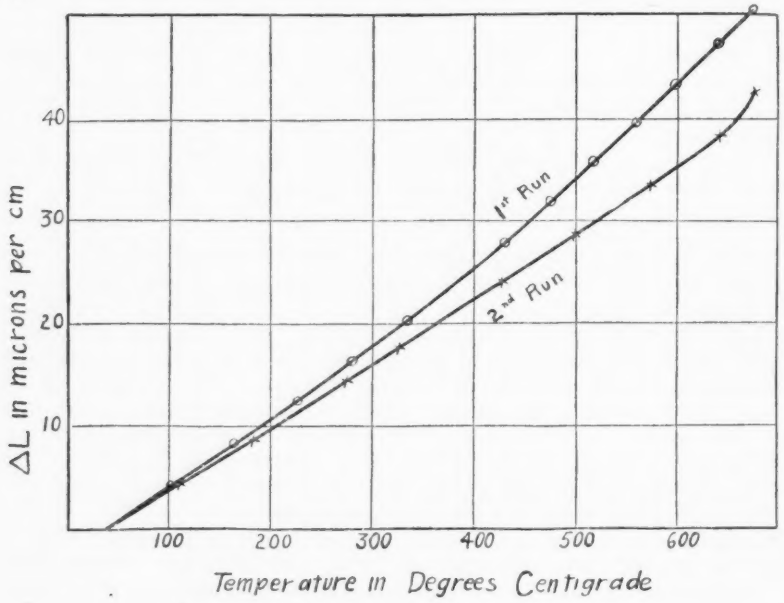

FIGURE 5.—*Sample thermal expansion curve*

light is affected by the temperature and pressure [8] of the air between the two plates. To correct for changes in temperature, Table 2 (see Appendix), has been calculated from the data of Scientific Paper No. 327. If the first temperature recorded is above 20° C. the entry in the table opposite that number should be subtracted from each of the succeeding corrections. These corrections should be entered in the fourth column. The fifth column is the sum of the third and fourth.

In plotting, the temperatures are laid off along the horizontal axis and the dilatation along the vertical axis. The fifth columr is then plotted against the eighth and the resulting graph is the expansion curve of the substance. An example is shown in Figure 5. The average coefficient of expansion for any temperature range is usually, for reasons of convenience, expressed in parts per million. To obtain

[7] This is equivalent to "parts per ten thousand" or "hundredths of a per cent."
[8] The effect of changes in pressure usually encountered during a run is negligible.

the average coefficient of expansion for a certain temperature range, it is necessary to divide the change in length expressed in parts per million by the number of degrees in this particular temperature range. For example, the average coefficient of expansion of iron between 20° and 100° C. is 12 parts per 1,000,000 per °C. This may also be expressed as 12×10^{-6} or 0.000012 per °C.

VIII. APPENDIX

TABLE I.—*Reference table for Pt. to Pt.–10 per cent Rh thermocouple*

Emf-temperature relation for platinum to platinum–10 per cent rhodium thermocouples as calculated by Adams [1] from gas thermometer determinations made at the Geophysical Laboratory by Day and Sosman.

[Emfs are expressed in microvolts and temperatures in °C. Cold junctions at 0° C.]

E Microvolts	0	1,000	2,000	3,000	4,000	5,000	6,000	7,000	8,000
0	0	147.1	265.4	374.3	478.1	578.3	675.3	769.5	861.1
	17.8	*12.6*	*11.2*	*10.6*	*10.2*	*9.8*	*9.5*	*9.3*	*9.0*
100	17.8	159.7	276.6	384.9	488.3	588.1	684.8	778.8	870.1
	16.7	*12.4*	*11.1*	*10.5*	*10.1*	*9.8*	*9.5*	*9.2*	*9.0*
200	34.5	172.1	287.7	395.4	498.4	597.9	694.3	788.0	879.1
	15.8	*12.2*	*11.0*	*10.5*	*10.1*	*9.8*	*9.5*	*9.2*	*9.0*
300	50.3	184.3	298.7	405.9	508.5	607.7	703.8	797.2	888.1
	15.1	*12.0*	*11.0*	*10.4*	*10.1*	*9.7*	*9.5*	*9.2*	*9.0*
400	65.4	196.3	309.7	416.3	518.6	617.4	713.3	806.4	897.1
	14.6	*11.8*	*10.9*	*10.4*	*10.0*	*9.7*	*9.4*	*9.2*	*9.0*
500	80.0	208.1	320.6	426.7	528.6	627.1	722.7	815.6	906.1
	14.1	*11.6*	*10.9*	*10.4*	*10.0*	*9.7*	*9.4*	*9.1*	*8.9*
600	94.1	219.7	331.5	437.1	538.6	636.8	732.1	824.7	915.0
	13.7	*11.5*	*10.8*	*10.3*	*10.0*	*9.7*	*9.4*	*9.1*	*8.9*
700	107.8	231.2	342.3	447.4	548.6	646.5	741.5	833.8	923.9
	13.4	*11.5*	*10.7*	*10.3*	*9.9*	*9.6*	*9.4*	*9.1*	*8.9*
800	121.2	242.7	353.0	457.7	558.5	656.1	750.9	942.9	932.8
	13.1	*11.4*	*10.7*	*10.2*	*9.9*	*9.6*	*9.3*	*9.1*	*8.8*
900	134.3	254.1	363.7	467.9	568.4	665.7	760.2	852.0	941.6
	12.8	*11.3*	*10.6*	*10.2*	*9.9*	*9.6*	*9.3*	*9.1*	*8.8*
1,000	147.1	265.4	374.3	478.1	578.3	675.3	769.5	861.1	950.4

E Microvolts	9,000	10,000	11,000	12,000	13,000	14,000	15,000	16,000	17,000
0	950.4	1,037.3	1,122.2	1,205.9	1,289.3	1,372.4	1,454.8	1,537.5	1,620.9
	8.8	*8.6*	*8.4*	*8.3*	*8.4*	*8.3*	*8.2*	*8.3*	*8.3*
100	959.2	1,045.9	1,130.6	1,214.2	1,297.7	1,380.7	1,463.0	1,545.8	1,629.2
	8.8	*8.5*	*8.4*	*8.4*	*8.3*	*8.3*	*8.2*	*8.3*	*8.4*
200	968.0	1,054.4	1,139.0	1,222.6	1,306.0	1,389.0	1,471.2	1,554.1	1,637.6
	8.7	*8.5*	*8.4*	*8.3*	*8.3*	*8.3*	*8.2*	*8.3*	*8.3*
300	976.7	1,062.9	1,147.4	1,230.9	1,314.3	1,397.3	1,479.4	1,562.4	1,645.9
	8.7	*8.5*	*8.4*	*8.4*	*8.3*	*8.3*	*8.3*	*8.4*	*8.4*
400	985.4	1,071.4	1,155.8	1,239.3	1,322.6	1,405.6	1,487.7	1,570.8	1,654.3
	8.7	*8.5*	*8.4*	*8.3*	*8.3*	*8.2*	*8.3*	*8.3*	*8.3*
500	994.1	1,079.9	1,164.2	1,247.6	1,330.9	1,413.8	1,496.0	1,579.1	1,662.6
	8.7	*8.5*	*8.3*	*8.3*	*8.3*	*8.2*	*8.3*	*8.4*	*8.3*
600	1,002.8	1,088.4	1,172.5	1,255.9	1,339.2	1,422.0	1,504.3	1,587.5	1,670.9
	8.7	*8.5*	*8.4*	*8.4*	*8.3*	*8.2*	*8.3*	*8.3*	*8.4*
700	1,011.5	1,096.9	1,180.9	1,264.3	1,347.5	1,430.2	1,512.6	1,595.8	1,679.3
	8.6	*8.5*	*8.3*	*8.3*	*8.3*	*8.2*	*8.3*	*8.4*	*8.3*
800	1,020.1	1,105.4	1,189.2	1,272.6	1,355.8	1,438.4	1,520.9	1,604.2	1,687.6
	8.6	*8.4*	*8.4*	*8.4*	*8.3*	*8.2*	*8.3*	*8.3*	*8.4*
900	1,028.7	1,113.8	1,197.6	1,281.0	1,364.1	1,446.6	1,529.2	1,612.5	1,696.0
	8.6	*8.4*	*8.3*	*8.3*	*8.3*	*8.2*	*8.3*	*8.4*	*8.3*
1,000	1,037.3	1,122.2	1,205.9	1,289.3	1,372.4	1,454.8	1,537.5	1,620.9	1,704.3

[1] J. Am. Chem. Soc., vol. 36, p. 65; 1914; Int. Crit. Tables, vol. 1, p. 57; 1926.

TABLE 2.—*Air corrections from 20° C. to λ temperatures indicated (microns per centimeter)*

[Atmospheric pressure, 760 mm]

Temperature	Corrections	Temperature	Corrections	Temperature	Corrections	Temperature	Corrections	Temperature	Corrections	Temperature	Corrections
20	0.00	70	0.40	142	0.80	252	1.20	439	1.60	840	2.00
1	.01	2	.41	4	.81	5	1.21	446	1.61	850	2.01
2	.02	4	.42	6	.82	8	1.22	453	1.62	870	2.02
3	.03	5	.43	8	.83	263	1.23	9	1.63	880	2.03
4	.04	6	.44	150	.84	6	1.24	466	1.64	900	2.04
5	.05	8	.45	4	.85	9	1.25	470	1.65	920	2.05
6	.06	80	.46	6	.86	273	1.26	480	1.66	940	2.06
7	.07	2	.47	8	.87	7	1.27	7	1.67	960	2.07
8	.08	3	.48	160	.88	280	1.28	493	1.68	980	2.08
9	.09	4	.49	3	.89	5	1.29	502	1.69	1,000	2.09
30	.10	6	.50	5	.90	9	1.30	510	1.70	1,020	2.10
2	.11	8	.51	8	.91	292	1.31	7	1.71	1,040	2.11
3	.12	9	.52	170	.92	6	1.32	521	1.72	1,060	2.12
5	.13	90	.53	3	.93	300	1.33	534	1.73	1,080	2.13
6	.14	2	.54	5	.94	5	1.34	542	1.74	1,100	2.14
7	.15	4	.55	8	.95	9	1.35	551	1.75		
8	.16	6	.56	180	.96	313	1.36	9	1.76		
40	.17	7	.57	3	.97	7	1.37	568	1.77		
1	.18	8	.58	5	.98	320	1.38	578	1.78		
2	.19	102	.59	8	.99	6	1.39	587	1.79		
3	.20	3	.60	190	1.00	331	1.40	596	1.80		
5	.21	4	.61	4	1.01	5	1.41	606	1.81		
6	.22	6	.62	7	1.02	340	1.42	615	1.82		
7	.23	8	.63	200	1.03	3	1.43	620	1.83		
8	.24	110	.64	2	1.04	350	1.44	635	1.84		
50	.25	2	.65	5	1.05	4	1.45	646	1.85		
1	.26	4	.66	8	1.06	9	1.46	657	1.86		
2	.27	6	.67	210	1.07	364	1.47	668	1.87		
4	.28	8	.68	4	1.08	9	1.48	679	1.88		
5	.29	9	.69	7	1.09	374	1.49	690	1.89		
6	.30	122	.70	220	1.10	8	1.50	700	1.90		
7	.31	4	.71	3	1.11	386	1.51	712	1.91		
9	.32	6	.72	6	1.12	392	1.52	726	1.92		
61	.33	8	.73	9	1.13	7	1.53	740	1.93		
3	.34	130	.74	232	1.14	403	1.54	752	1.94		
4	.35	2	.75	5	1.15	9	1.55	766	1.95		
65	.36	4	.76	8	1.16	415	1.56	780	1.96		
6	.37	6	.77	241	1.17	421	1.57	790	1.97		
8	.38	8	.78	5	1.18	7	1.58	810	1.98		
9	.39	140	.79	9	1.19	433	1.59	820	1.99		

TABLE 3.—*Air corrections from 20° C. to low temperatures indicated (microns per centimeter)*

Atmospheric pressure, 760 mm.

Temperature	Correction	Temperature	Correction	Temperature	Correction	Temperature	Correction	Temperature	Correction	Temperature	Correction
+20	0.00	−20	−0.43	−60	−1.02	−100	−1.89	−140	−3.27	−180	−5.85
19	−.01	21	.44	61	1.04	101	1.91	141	3.32	181	5.94
18	.02	22	.45	62	1.06	102	1.94	142	3.36	182	6.04
17	.03	23	.47	63	1.07	103	1.97	143	3.41	183	6.13
16	.04	24	.48	64	1.09	104	1.99	144	3.46	184	6.23
15	.05	25	.49	65	1.11	105	2.02	145	3.50	185	6.33
14	.06	26	.51	66	1.13	106	2.05	146	3.55	186	6.44
13	.07	27	.52	67	1.15	107	2.08	147	3.60	187	6.54
12	.08	28	.53	68	1.17	108	2.11	148	3.65	188	6.65
11	.09	29	.55	69	1.19	109	2.14	149	3.71	189	6.76
10	.10	30	.56	70	1.21	110	2.17	150	3.76	190	6.88
9	.11	31	.57	71	1.22	111	2.20	151	3.81	191	7.00
8	.12	32	.59	72	1.24	112	2.23	152	3.86	192	7.12
7	.13	33	.60	73	1.26	113	2.26	153	3.92	193	7.24
6	.14	34	.61	74	1.28	114	2.29	154	3.98	194	7.36
5	.15	35	.63	75	1.30	115	2.32	155	4.03		
4	.16	36	.64	76	1.32	116	2.36	156	4.09		
3	.17	37	.66	77	1.35	117	2.39	157	4.15		
2	.18	38	.67	78	1.37	118	2.42	158	4.21		
1	.19	39	.69	79	1.39	119	2.45	159	4.27		
0	.20	40	.70	80	1.41	120	2.49	160	4.33		
−1	.21	41	.71	81	1.43	121	2.52	161	4.39		
2	.22	42	.73	82	1.45	122	2.56	162	4.46		
3	.23	43	.74	83	1.47	123	2.59	163	4.52		
4	.24	44	.76	84	1.50	124	2.63	164	4.59		
5	.25	45	.78	85	1.52	125	2.66	165	4.66		
6	.26	46	.79	86	1.54	126	2.70	166	4.73		
7	.28	47	.81	87	1.56	127	2.74	167	4.80		
8	.29	48	.82	88	1.59	128	2.78	168	4.87		
9	.30	49	.84	89	1.61	129	2.81	169	4.94		
10	.31	50	.85	90	1.63	130	2.85	170	5.02		
11	.32	51	.87	91	1.66	131	2.89	171	5.09		
12	.33	52	.89	92	1.68	132	2.93	172	5.17		
13	.35	53	.90	93	1.71	133	2.97	173	5.25		
14	.36	54	.92	94	1.73	134	3.01	174	5.33		
15	.37	55	.94	95	1.76	135	3.05	175	5.41		
16	.38	56	.95	96	1.78	136	3.10	176	5.49		
17	.39	57	.97	97	1.81	137	3.14	177	5.58		
18	.41	58	.99	98	1.83	138	3.18	178	5.67		
19	.42	59	1.00	99	1.86	139	3.23	179	5.76		

1. COMPUTATIONS RELATING TO OXIDIZABLE SPECIMENS

In some cases, where the expansion of an oxidizable specimen is desired and the formation of an oxide film during the run causes a spurious expansion to be introduced, the true expansion may often be obtained by running two sets of specimens of different lengths of the same material. The true expansion may then be calculated by the following method, assuming that the oxide film is the same in both cases.

Two samples are made up, S_1 and S_2. In this case $S_1 = 0.22$ cm and $S_2 = 0.37$ cm at 20° C.

Over a temperature range (for example, 20° to 500°), S_1 shows an apparent increase of 73.5 μ/cm and S_2 shows an apparent increase of 70.0 μ/cm.

Apparent increase of S_1 $\quad S_1 = 73.5 \times 0.22 = 16.17$.
Apparent increase of S_2 $\quad S_2 = 70.0 \times 0.37 = 25.90$.

$$S_1 = S_1 \times C \times (t_2 - t_1) + R \tag{1}$$

where C = average coefficient expansion between t_1 and t_2 and R = oxide film.

$$S_2 = S_2 \times C \times (t_2 - t_1) + R \tag{2}$$

Subtract equation (1) from equation (2) after substituting numerical values.

$$\begin{aligned} 16.17 &= 0.22 \times C \times 480 + R \\ 25.90 &= 0.37 \times C \times 480 + R \\ \hline 9.73 &= (0.37 - 0.22) \times C \times 480 \end{aligned}$$

$$C = \frac{9.73}{0.15 \times 480} = 13.5 \ \mu\text{/cm or } 13.5 \times 10^{-6}.$$

WASHINGTON, October, 1932.

EFFECT OF LATHE CUTTING CONDITIONS ON THE HARDNESS OF CARBON AND ALLOY STEELS

By T. G. Digges

Previous work at the Bureau of Standards on machinability has been primarily concerned with the relation of the composition and heat treatment of both the tools and the steels cut to lathe-tool life. An investigation recently completed had a quite different object, namely, a quantitative study of the work hardening near the machined surface of steel forgings resulting from cutting with lathe tools.

Comparisons were made of the work hardening resulting from changes in size, form, and composition of tools; speed, feed, and depth of cut; and composition and heat treatment of the steels cut. Observations were also made of the influence of cutting conditions on aging, corrosion resistance, chip hardness, structure near the machined surface of some of the steels cut, and of the effect of annealing temperatures (100° to 720° C.) on the surface hardness of some of the steels work hardened in the lathe tests. All the lathe tests were made without cutting liquids and with sharp high-speed steel or cemented tantalum carbide tools. A detailed report of this work was contributed to the American Society of Mechanical Engineers and presented at the annual meeting of the society, New York, N. Y., December 5 to 9, 1932.

The amount and extent of work hardening of the forgings caused by the lathe tools was determined by making hardness surveys with a Vickers machine using a 10 kg load on the diamond pyramid having an included angle of 136°.

The hardness as close to the machined surface as it was possible to measure it was greater than the original hardness of the forging. The hardness decreased at increasing depths below the machined surface until it was the same as the original forging.

The amount of work hardening—that is, both the magnitude of the surface hardness and the depth of hardening—was not influenced by changes in the cutting speeds of the lathe tools.

With a given area of cut, the amount of work hardening was affected equally by changes in the feed or depth of cut. The work hardening depended not only upon the cutting conditions, such as the area of cut, but also upon the composition and heat treatment of the steels cut. Furthermore, two steels similar in chemical composition and heat treatment had different work-hardening properties.

Data on the work hardening of 10 annealed plain carbon steel forgings, with carbon contents varying from 0.12 to 1.10 per cent, with three different areas of cut are summarized in Figure 1. The increase in surface hardness is plotted against the carbon contents. The hardness of the annealed steels before machining is also represented graphically. For the cutting conditions under consideration, the steel of lowest carbon content, namely, 0.12 per cent, showed the greatest increase in hardness at the machined surface. The work

hardness at the surface decreased rapidly as the carbon content increased to about 0.4 per cent and then less rapidly with further increase in the carbon content of the annealed steels.

The depth to which the annealed carbon steels were hardened with the different areas of cut appeared to decrease uniformly with increase in carbon contents.

With small areas of cut, approximately 0.003 square inch, the surface hardness of an annealed 0.12 per cent carbon steel and an annealed carbon steel screw stock forging increased by about the same amount, but with the heavy cuts the screw stock had the highest increase in surface hardness. The depth of work hardening for all similar areas of cut was greater with the plain carbon steel than with the screw stock.

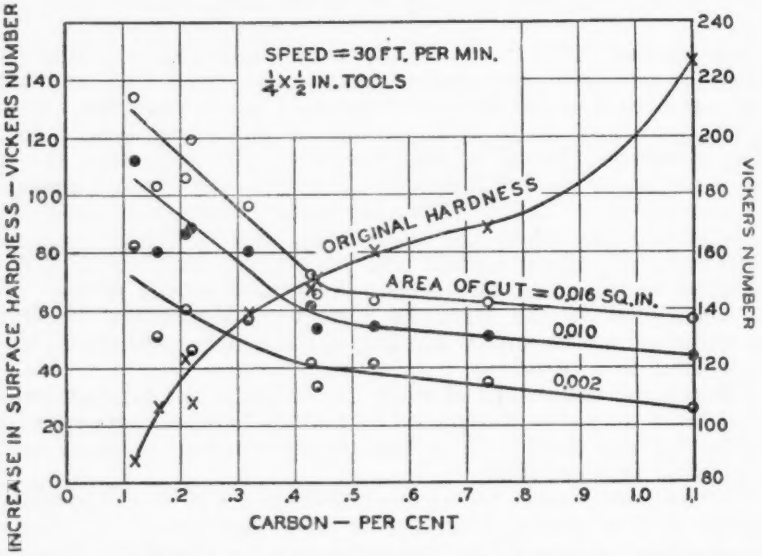

FIGURE 1.—*Influence of the carbon contents of the steel cut upon the surface work hardening with different areas of cut*

Stainless steel of the ordinary "18–8" (18 Cr, 8 Ni) composition (not free machining) had a very high capacity to work harden near the machined surface even with small areas of cut, but with increase in area of cut the change in work hardening values was not so marked. The "free-machining" "18–8" stainless steel with small areas of cut had no marked increase in surface hardness, but with increase in area of cut there was a continuous increase in the hardness.

Work-hardening the ordinary "18–8" stainless steel in the lathe tests to the extent of increasing the surface hardness about 40 to 100 per cent had no marked influence on the resistance of the steel to hot nitric acid attack.

The hardness of the cold-worked plain carbon and 3½ per cent nickel steel was, in general, increased by annealing within the range of 100° to 400° C., but with further increase in annealing temperature the hardness decreased. The hardness from cold working with lathe tools was removed by heating to 720° C.

WASHINGTON, October 8, 1932.

MEASUREMENTS OF ULTRA-VIOLET SOLAR RADIATION IN VARIOUS LOCALITIES

By W. W. Coblentz, R. Stair, and J. M. Hogue

ABSTRACT

In the present paper a description is given of the calibration of a selective photochemical, ultra-violet dosage intensity meter against a balanced thermocouple and filter radiometer, used as a standard. Data are given of the ultra-violet intensities of solar radiation in various localities at various elevations at various stations in Europe and upon the ocean.

The measurements show a high ultra-violet reflection from clean fresh snow. The ultra-violet intensities over the ocean are not conspicuously higher than at a sea level, dust-free station on land at the same latitude and the same season of the year.

CONTENTS

	Page
I. Introduction	79
II. Experimental procedure	80
1. Standardization of dosimeter	81
III. Observational data	82
IV. Bibliography	88

I. INTRODUCTION

During the past summer one of the writers (W. W. C.) was delegated to visit various European heliotherapy stations. The occasion presented an excellent opportunity for measuring the ultra-violet solar intensity at various stations, thus obtaining some idea of the amount available under various atmospheric conditions. Unfortunately, and contrary to the usual experience, there was an excessive amount of cloudy weather in Switzerland which greatly interfered with the attempted survey.

Nevertheless, in spite of the fragmentary data collected, a study of the tabulated measurements discloses highly interesting information on the amount of ultra-viloet radiation transmitted through fog and clouds and reflected from ocean waves, clouds, snow, and the north sky. Incidently, it is relevant to comment on the excessive erythema experienced by travelers on the ocean during cloudy weather. This physiological reaction appears to be far greater than would be experienced under similar conditions on land when the sky is completely overcast. Evidently the "sunburn" is not caused solely by ultra-violet radiation, but is accelerated by the wind and the fine, almost imperceptible, ocean spray.

148938—33——6

II. EXPERIMENTAL PROCEDURE

The primary instrument for measuring ultra-violet radiation is a balanced thermocouple and filter radiometer (1)[1] calibrated against a standard of radiation which equates the measurement in absolute value (microwatts per $cm^2 = \mu w/cm^2$).

The reliability of this device is indicated by the accuracy with which the ultra-vioelt radiation of a source (having a discontinuous spectrum of strong emission lines distributed fairly uniformly throughout the ultra-violet spectrum) can be evaluated (*a*) by summation of the intensities of the individual lines, each one measured separately in absolute value and (*b*) by means of the filter method which measures the ultra-violet component in the undispersed source.

In this comparison good agreement was found not only in the ultra-violet radiation emitted by lamps, as measured by both methods in our own laboratory, but also by comparing the summation of the spectral radiation intensities (in absolute value) as observed in other laboratories with measurements on the same lamps by the balanced thermocouple and filter method as used in our laboratory.

Fortified with this agreement in measurements on a discontinuous spectrum which does not involve subsidiary calculations to reduce the data to a normal spectrum, it is assumed that the filter method is equally reliable for making measurements of short wave length ultra-violet in sources emitting a continuous spectrum. The fact that there is good agreement in the correlation of the physiological (erythemal) and the radiometric determinations on the various sources (2) seems to indicate that this agreement can not be fortuitous.

In this connection, it is relevant to cite an earlier research (3) in which the process was reversed, and a close agreement was found between the observed and the calculated transmission of the filters, for wide bands of the ultra-violet spectrum.

As a secondary instrument, convenient for field use it was decided to use an ultra-violet dosimeter, made by the I. G. Farbenindustrie (4). This is a photochemical device, consisting of a solution of a leuco-cyanide of triphenylamine dye which is colorless in the dark and turns pink in color temporarily when exposed to short wave length ultra-violet radiation. The pink color is reduced to a neutral gray by insertion of green filters of different densities. As issued by the factory the various filters (called "fields" which are numbered 0 to 9) are calibrated arbitrarily (against a quartz mercury arc lamp, used as a standard) to indicate intensities and corresponding times of exposure to produce a minimum perceptible erythema.

Two instruments were used: No. 1 obtained in March, 1932, and calibrated as will be described on a subsequent page, and No. 2, which was shipped from the factory to Davos, Switzerland in July, 1932. The latter was found less sensitive (for the same intensity, filter 2 = filter 3 of No. 1) owing to the fact that in the later model a less sensitive solution having a smaller temperature coefficient is used.

[1] Figures in parentheses here and throughout the text indicate references given in the bibliography at the end of this paper.

1. STANDARDIZATION OF DOSIMETER

The question of standardization of selective (photo-electric and photochemical) dosage intensity meters was discussed in previous communications (1) and (5) where an actual example of such a calibration is given.

For the present investigation, the ultra-violet dosimeter (No. 1) was calibrated against the standard balanced thermocouple and filter radiometer (1) by simultaneous measurements of the ultra-violet solar intensity on the clearest days in Washington in June before going to Europe, and again soon after the return in September. Good agreement was observed in the two calibrations indicating that the portable instrument had not changed appreciably in the mean time.

The procedure in obtaining a calibration of the dosimeter for measuring solar radiation is relatively simple. The measurements were begun in the forenoon when the ultra-violet solar intensity was relatively low, and continued through midday when the intensities were a maximum ($85\mu w/cm^2$ in June, $55\mu w/cm^2$ in September for ultra-violet radiation of wave lengths less than 313 $m\mu$ as observed with the balanced thermocouple and filter radiometer).

A uniform time of exposure was adopted—1 minute, 2 minutes, etc., and the "field number" was determined for neutralizing the pink color. This, of course, varies with the intensity. Manifestly for zero intensity there is no chemical reaction. Hence, for intensities less than 10 to 20 $\mu w/cm^2$ (as observed with the balanced thermopile) requiring neutralizing fields No. 1 to No. 2, there is no need of making observations with the dosimeter. In order to avoid heating of the dosimeter the exposures were not continued longer than three minutes, except when the intensities were low.

In Figure 1 is shown a series of calibration curves of dosimeter No. 1 for different exposures of 1, 2, 3, 5, and 10 minutes, obtained by comparison against the standard thermopile and filter radiometer.

In this illustration the abscissas represent the observed field numbers of the filters in the eyepiece of the dosimeter required to neutralize the pink color of the solution after an exposure (of say two minutes) to the intensities in microwatts per cm^2 as observed by the balanced thermopile and filter radiometer.

As used in practice, the dosimeter was exposed for, say, two minutes, and the filter necessary to neutralize the pink color was noted. The corresponding intensity was then read from Figure 1. After a little experience, it was found possible to estimate fractional numbers. For example, if, after a certain exposure, field No. 3 appeared slightly pink and No. 4 appeared deep green, the neutralizing field was estimated 3.2 (see Table 1); if, say, field No. 3 was appreciably pink it was estimated at 3.5; and if field No. 3 appeared decidedly pink and field No. 4 appeared only faintly green, the estimate was No. 3.8 (see Table 1).

In order to shield the end of the tube containing the solution from reflected skylight, it was covered while making measurements, although exposure of only the end of the glass tube for one to two minutes showed no appreciable reddening of the solution.

While making observations in bright sunlight, the eyes were shielded to keep them adapted to color discrimination at low intensities, such as encountered in looking into the eyepiece of the dosimeter. This method of observing was adopted after making some erratic field

settings which seemed to be caused by a change in the color estimation while the eye adapted itself to lower intensities.

Since all the measurements (except in the ice fields of Jungfraujoch, temperature 1.5° C.) as well as the calibration against the standard instrument, were obtained at average summer temperatures, no attempt was made to apply a temperature coefficient, which is reported to be small in the newer model.

When this instrument had not been used for several days the first reading seemed to be appreciably lower than those made subsequently, just as though the end point in decolorizing was a slower process than estimated by the eye. Furthermore, field "No. 0"

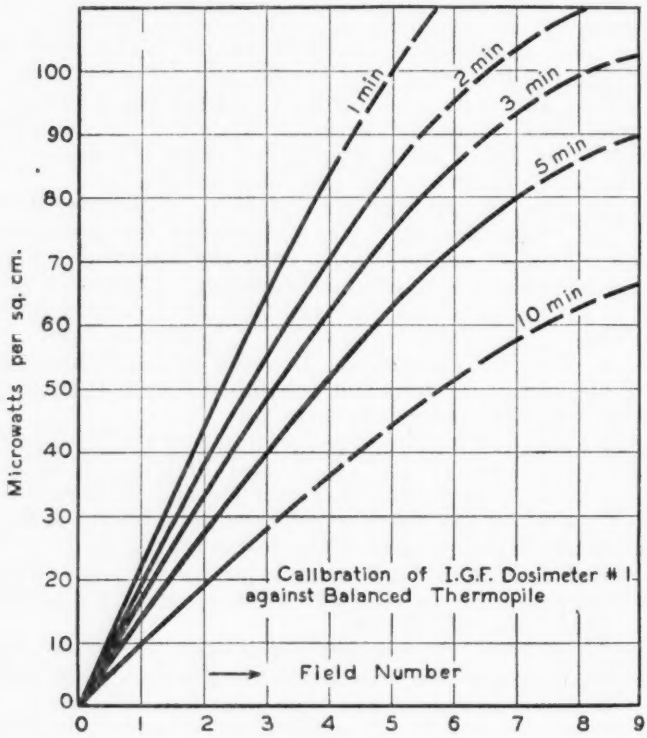

FIGURE 1

always appeared greenish, rather than neutral after extended rest periods. Hence, just sufficient time for field "No. 0" to become neutral was allowed to elapse between successive measurements.

III. OBSERVATIONAL DATA

The tabulated measurements, though meager, contain useful information that can be only briefly summarized in the text.

The observations made in different localities are recorded in Table 1. The time of the day is eastern standard time (E. S. T.) for Washington and the Atlantic Ocean, and western Europe standard time for stations in Europe.

The "angle" given in column 7 of Table 1 is the estimated solid angle (circular area) of the sky, as viewed by the radiometer, that was free from clouds.

Since the dosimeter intercepts radiation from practically the whole hemisphere, it is inclined to register uniform values for a longer period during the noon hour than the thermopile which subtends an angle of 45°.

The ocean measurements were made at a great distance from the shore, hence, should not be affected by smoke and dust. An impressive physiological observation was the severe "sunburn" experienced by ocean travelers when there was cloudiness and mist throughout the day.

TABLE 1.—*Ultra-violet solar radiation intensity, U.-v. Q. in microwatts per cm² (μw/cm²) as observed in different localities (Switzerland, Denmark, etc.) by means of a photochemical dosage intensity meter (an I. G. Farbenindustrie dosimeter) calibrated against a balanced thermocouple and filter radiometer which is standardized to indicate the ultra-violet intensity of wave lengths less than and including 313 mμ*

[The time is the beginning of the observation. The asterisk (*) indicates measurements of ultra-violet reflected from clouds, snow, water, etc.]

Date	Exposure	Neutralizing filter No.	U.-v. Q. in μw/cm²	Location	Elevation	Remarks
1	2	3	4	5	6	7
1932						
June 3:	*Min.*				*Feet*	
11.17 a. m.	2	5	84	Washington (latitude, 38° 55′ N.).	350	Sky very clear, blue.
11.52 a. m.	2	5.1	86			
12.20 p. m.	3	3	*48			North sky, clear blue.*
1.49 p. m.	2	5	83			
June 8:						
9.46 a. m.	2	3.8	67			Sky cloudless.
10.39 a. m.	2	4	71			
11.10 a. m.	2	4.5	79			
11.38 a. m.	2	5	84			
12.11 p. m.	3	2.5	*40			North sky, very clear.*
12.22 p. m.	2	5	84			
1.23 p. m.	2	4.5	79			
2.12 p. m.	2	4	71			
3.11 p. m.	2	3	54			
4.12 p. m.	2	2	37			
June 29:						
10.25 a. m.	5	2.3	30	Atlantic Ocean (latitude 41° 21′ N.).	100	Faint sunlight through mist 400 miles from New York.
July 3:						
9.43 a. m.	5	2	27	(Latitude 49° 20′ N.)		Broken clouds, no direct sunlight; 650 miles from Plymouth.
10.00 a. m.	5	4.5	58			Sun through broken clouds.
10.12 a. m.	1	2.5	55			Direct sunlight.
12.15 p. m.	3	3.5	54			Fracto-cumulus clouds.
12.55 p. m.	3	5.5	80			Sun through fine cirrus.
1.15 p. m.	1	4.5	90			Sky clear; cumulus to west.
1.39 p. m.	2	5	85			Sky clear.
2.00 p. m.	2	5	85			Fine cirrus haze, otherwise clear over hemisphere.
2.19 p. m.	2	4.5	80			Sky clear; fine cirrus for last 20 seconds exposure.
2.48 p. m.	1	3.3	70			Observations terminated by thin fleeting clouds.
3.15 p. m.	3	1	*17			Reflection from waves in line with sun.*
3.58 p. m.	1	2	43			Observations stopped by fracto-cumulus near sun.
6.20 p. m.	5	1	10			Sky hazy, clouds west of sun.

TABLE 1.—*Ultra-violet solar radiation intensity, U.-v. Q. in microwatts per cm² (μw/cm²) as observed in different localities (Switzerland, Denmark, etc.) by means of a photochemical dosage intensity meter (an I. G. Farbenindustrie dosimeter) calibrated against a balanced thermocouple and filter radiometer which is standardized to indicate the ultra-violet intensity of wave lengths less than and including 313 mμ*—Continued.

Date	Exposure	Neutralizing filter No.	U.-v. Q. in μw/cm²	Location	Elevation	Remarks
1	2	3	4	5	6	7
1932						
July 4:	*Min.*				*Feet*	
1.08 p. m.	5	4.5	58			Coast of England, broken clouds no direct sunlight.
1.40 p. m.	2	4	71			Sun through thin clouds.
July 14:						
1.15 p. m.	2	4	71	Chamounix (latitude 45° 55′ N.).	3,200	Sun through fine cirrus.
1.49 p. m.	2	3.8	70			Sun through rift in dense cloud banks.
July 17:						
9.35 a. m.	2	2	37	Lausanne (Ouchy)	1,250	Thick cirrus haze.
10.06 a. m.	2	3.5	63	Lake Geneva	1,240	Sky clear, but hazy.
10.18 a. m.	2	4.0	71	(Latitude 46° 30′ N.).		Sky clear, cirrus coming from south. Sky overcast at 10.33 a. m.
5.38 p. m.	2	0	0	Ouchy		Sky clear.
July 18:						
9.10 a. m.	2	2	37	Aigle	1,368	Sky clear; cirrus S.E. of sun.
10.14 a. m.	1	3	65	Leysin Village (latitude 46° 20′ N.).	4,420	Exposure terminated by cumulus clouds.
12.36 p. m.	1	2	43			Sun through fine clouds.
12.56 p. m.	1.5	3.3	65			Sun through thin clouds; observations terminated by thick cumulus.
1.47 p. m.	2	4	70			Sun through thick cirrus.
2.19 p. m.	2	5	84			Sun through thick cirrus; clearer for 20 seconds.
2.59 p. m.	2	2.1	*40			Sky radiation reflected from clouds on mountain (east) opposite the sun which shines through thin cirrus.*
July 19:						
10.34 a. m.	1	2	45	Brigue	2,260	Sky clear, angle 30°, clouds to side.
1.23 p. m.	2	4.3	75	Gletch	5,780	Sky clear; smoke from engine interfered.
1.44 p. m.	1	3	65	Furka Pass	7,990	Sky clear blue; thin cirrus interfered for 20 seconds.
2.24 p. m.	1	3	65	Andermatt	4,740	Sky perfectly clear blue; best set.
July 20:						
10.11 a. m.	2	4	70	Peist	3,000	Sky clear; thin cirrus for 15 seconds.
11.12 a. m.	2	5	85	Arosa	5,795	Sky clear blue between rift in thick clouds.
2.00 p. m.	5	1	*8			Reflection from thick cloud on mountain S.E. of sun which is clouded.*
July 22:						
12.44 p. m.	1	2.5	55	Davos Platz (latitude 46° 47′ N.).	5,120	Sky clear, angle 45°, clouds to side.
12.50 p. m.	3	5	75			Sky clear, angle 45°.
1.52 p. m.	1	2.5	55			Sky hazy.
2.17 p. m.	1	2.3	50			Fine cirrus.
July 27:						
11.08 a. m.	2	1	*18	Jungfrau-joch (latitude 46° 32′ N.).	11,350	Sunlight through fog; bright glare. Roof of Forschungsinstitut.*
11.49 a. m.	5	2.5	*34			Sunlight reflected from glacier through thin fog.*
1.29 p. m.	5	2	*28			Reflection from fresh snow from glacier below Berghaus. Sky overcast. Glare uncomfortable to the eye.*
2.15 p. m.	5	3	*40			Reflection from snow across valley from roof of Forschungsinstitut. Temperature, 1.4° C.*
2.28 p. m.	5	2.5	*34			Sky radiation; sun obscured by mist. Light snow falling.*

TABLE 1.—*Ultra-violet solar radiation intensity, U.-v. Q. in microwatts per cm² (μw/cm²) as observed in different localities (Switzerland, Denmark, etc.) by means of a photochemical dosage intensity meter (an I. G. Farbenindustrie dosimeter) calibrated against a balanced thermocouple and filter radiometer which is standardized to indicate the ultra-violet intensity of wave lengths less than and including 313 mμ*—Continued

Date	Exposure	Neutralizing filter No.	U.-v. Q. in μw/cm²	Location	Elevation	Remarks
1	2	3	4	5	6	7
1932						
July 27—Con.	*Min.*				*Feet*	
2.40 p. m.	5	3.5	*46			Reflection from fresh glacier snow. Sun obscured by mist and fine ice spicules.*
2.55 p. m.	5	2.5	*34			Sky radiation; light snow falling.*
3.10 p. m.	5	3.5	*46			Reflection from glacier snow; sun obscured. Temperature, 1.3° C. Humidity, 74 per cent.*
July 28:						
10.05 a. m.	1	3	65	Jungfraujoch	11,350	Fine snow falling part of time.
10.19 a. m.	1	3	65			Blowing cloud wisps.
10.27 a. m.	3	3.5	*56			Reflection from snow banks 3 to 4 feet distant.*
10.45 a. m.	1	1	*23			Reflection from snow, cloud wisps over sun.*
10.59 a. m.	1	2.5	55			High wind, cloud wisps for last 10 seconds.
11.12 a. m.	1	1.5	*34			Reflection from snow in valley.*
11.25 a. m.	1	3.2	70			Sky cloudless most of time, no wind.
11.42 a. m.	1	3.5	75			Sky cloudless.
11.50 a. m.	1	3.5	*75			Reflection from snow bank distant 3 feet. Sky clear; bright sun.*
11.59 a. m.	2	2.5	*45			Sky radiation to west; perhaps a little from snow peaks.*
12.07 p. m.	2	4.5	78			Sky perfectly clear. Temperature, 2.8° C.
1.04 p. m.	1	3.5	76			
1.11 p. m.	1	3	*65			Reflection from snow bank.*
1.21 p. m.	1	3.5	76			Temperature, 1.7° C. Humidity, 61 per cent.*
1.32 p. m.	2	5	84			Sky perfectly clear; light wind.
1.43 p. m.	1	3.8	80			
1.54 p. m.	1	3.5	*76			Reflection from snow bank Sun's rays normal to surface.*
July 29:						
10.32 a. m.	1	2.5	54	Harder Kulm near Interlaken (latitude, 46° 41′ N.).	4,350	Sky perfectly clear.
10.40 a. m.	2	4.5	78			
10.52 a. m.	3	6	85			
11.08 a. m.	1	4	85			
11.26 a. m.	1	3.5	75			
11.39 a. m.	1	3.8	82			
11.50 a. m.	1	3.8	82			
12.21 p. m.	1	3	65	Interlaken (latitude, 46° 41′ N.).	1,870	Funiculare station at foot of Kulm; street dust reduces intensity.
1.26 p. m.	1	3	65	do	1,866	In open field near Ost Bahnhof.
1.39 p. m.	1	3	65			Sky perfectly clear to horizon.
1.53 p. m.	1	3	65			
2.13 p. m.	1	3.5	75			
2.28 p. m.	3	5	75			
2.46 p. m.	3	5	75			Sky cloudless.
3.07 p. m.	3	5	75			
3.46 p. m.	3	3.8	60			
4.08 p. m.	3	3.5	55			
4.23 p. m.	3	3	48			
4.41 p. m.	3	3	48			Sky clear. Small cloud north of sun.
4.58 p. m.	3	2.5	40			
5.18 p. m.	3	2.2	36			Small cirrus north and west of sun.
5.42 p. m.	5	1.5	20			Small cloud north of sun.
August 11:						
1.24 p. m.	2	3.5	63	Copenhagen (latitude 55° 30′ N.)	150	Raadhusplads. Sky clear to horizon; sun has wide corona.
1.37 p. m.	2	3.8	66			Christianberg Palace Canal.

TABLE 1.—*Ultra-violet solar radiation intensity, U.-v. Q. in microwatts per cm² (μw/cm²) as observed in different localities (Switzerland, Denmark, etc.) by means of a photochemical dosage intensity meter (an I. G. Farbenindustrie dosimeter) calibrated against a balanced thermocouple and filter radiometer which is standardized to indicate the ultra-violet intensity of wave lengths less than and including 313 mμ*—Continued

Date	Exposure	Neutralizing filter No.	U.-v. Q. in μw/cm²	Location	Elevation	Remarks
1	2	3	4	5	6	7
1932						
Aug. 11—Con.	*Min.*				*Feet*	
1.53 p. m.	2	3.5	63			Faint cirrus southwest of sun; in front of palace.
2.20 p. m.	2	3.2	58			Fine cirrus southwest of sun; court of Royal Library.
3.16 p. m.	2	2.8	51			Fine cirrus on horizon; observatory on top of Runde Taarn.
4.12 p. m.	3	1.2	20			Sky clear. Street corner; Turist Hotel.
August 14:						
11.41 a. m.	2	2.8	51	Copenhagen		Sky hazy. City square.
12.01 p. m.	2	3.8	66			Near railroad station.
August 23:						
8.01 a. m.	5	.5	7	North sea (latitude 54° N.)	50	Thin cirrus. Enroute Esbjerg to Harwich.
8.16 a. m.	5	1.2	16			Clear sky.
9.40 a. m.	2	2.5	45			Forward deck, no smoke; sky clear.
9.55 a. m.	3	2.5	45			Sky clear through angle 60°.
10.26 a. m.	3	3	48			Cirrus on horizon.
11.21 a. m.	3	4	62			Small cloud south of sun.
11.42 a. m.	2	3.8	67			Clouds on horizon.
12.05 p. m.	2	4	70			Sky clear through angle 90°.
12.54 p. m.	2	4	70			Sky clear through angle 90°. Large clouds to north.
1.46 p. m.	2	3.8	67			Cirrus clouds around sun. Clear through angle 45°.
2.01 p. m.	2	3.5	63			Fine cirrus. Clear through angle 30°.
2.41 p. m.	2	3	54	(Latitude 52° N.)		Approaching Harwich. Sky clear except horizon.
3.06 p. m.	2	3.5	63			Sky clear. Clouds on north horizon.
3.27 p. m.	2	3.2	57			Less hazy and smaller corona.
September 12:						
1.16 p. m.	2	3	54	Atlantic Ocean (latitude 48° N.).	100	Thick cirrus.
2.05 p. m.	2	3	54			Cirrus; high wind.
2.31 p. m.	2	3.5	63			Fairly clear.
2.49 p. m.	2	2.8	51			Clear sky.
September 13:						
8.49 a. m.	2	2	37	Atlantic Ocean (latitude 46° 40′ N.) (longitude 38° 30′ W.).		Sky clear between fleeting clouds.
8.57 a. m.	2	2.5	45			Wide corona.
9.09 a. m.	2	3	54			Sky clear except on horizon; no smoke.
9.21 a. m.	2	3.5	62			Sky clear except horizon southeast of sun.
9.36 a. m.	2	3.8	67			Same as preceding; small corona.
9.49 a. m.	2	3.5	65			Fine cirrus in west; covers sun at 9.58.
11.49 a. m.	2	3.3	58			Fire haze and cirrus; wisps of smoke.
September 14:						
9.41 a. m.	2	2	37	Atlantic Ocean (latitude 42° 50′ N.) (longitude 50° 58′ W.).	100	Thin fracto cumulus.
10.21 a. m.	2	2.5	45			Fleeting clouds.
September 15:						
1.09 p. m.	2	3	55			Thick cirrus moved over the sun.
1.30 p. m.	2	2.8	51	(Latitude 41° 20′ N.) (longitude 63° 50′ W.).		Thin cirrus over the sun.

TABLE 1.—*Ultra-violet solar radiation intensity, U.-v. Q. in microwatts per cm² (μw/cm²) as observed in different locations (Switzerland, Denmark, etc.) by means of a photochemical dosage intensity meter (an I. G. Farbenindustric dosimeter) calibrated against a balanced thermocouple and filter radiometer which is standardized to indicate the ultra-violet intensity of wave lengths less than and including 313mμ*—Continued

Date	Exposure	Neutralizing filter No.	U.-v. Q. in μw/cm²	Location	Elevation	Remarks
1	2	3	4	5	6	7
1932						
September 29:	*Min.*				*Feet*	
9.24 a. m.	2	1.5	30	Washington (latitude 38° 55′ N.).	350	Sky clear of dust after rain.
9.37 a. m.	2	2	36			
10.00 a. m.	2	2.2	38			
10.21 a. m.	2	2.2	38			Fracto-cumulus over sun at 10.35 a. m.
September 30:						
8.06 a. m.	5	.5	8	Washington	350	Sky clear.
9.06 a. m.	5	1.1	15			Sky cloudless. Small corona.
9.38 a. m.	2	1.5	28			
10.01 a. m.	2	2	38			Observed with balance thermocouple=47μw/cm².
10.24 a. m.	2	2.5	46			Observed with balance thermocouple=50μw/cm².
10.45 a. m.	2	2.8	50			
11.07 a. m.	2	3	54			
11.28 a. m.	2	3.3	57			Fracto-cumulus southeast of sun.
11.49 a. m.	2	3.3	57			Fracto-cumulus to north and east of sun. Sky clear through angle 60°.
12.07 p. m.	2	3.3	57			

The observed high ultra-violet reflecting power of fresh clean snow is in agreement with physiological observations, and is to be expected from our knowledge of the high transparency of water for ultra-violet radiation. Some of these measurements were made on ultra-violet solar radiation reflected from freshly fallen snow on a glacier, situated several miles across a mountain valley from the observing station (the hotel and the Forschungs Institut on Jungfraujoch).

The observation on Jungfraujoch showing that the ultra-violet component in sunlight is not much greater than at lower altitudes is in agreement with previous measurements in Arizona, showing that while the spectral quality is changed the loss in ultra-violet intensity in the direct solar rays is compensated to some extent by scattering, in the lower altitudes.

The reflection from numerous "breakers" on a rough sea and the churned white surface near the boat, all viewed in line with the sun, seems low. However, the frequent reports of sunburn by reflection from water probably means the combined effect of direct and reflected sunlight, that is incident upon a skin that is sensitized by moisture.

The observed ultra-violet solar radiation intensities over the ocean do not appear to be conspicuously higher than at a sea level, dust-free station on land, at the same latitude and season of the year. This is to be expected in view of the fact that after traversing the extensive atmospheric envelope of the earth (21 miles in thickness if it were homogeneous) the lower layer over the ocean can not increase the intensity and the similar layer over the solid earth, when dust free,

does not deplete the ultra-violet intensity to the extent that might be inferred from the observed, relatively greater, physiological (erythemal) reaction experienced on the ocean.

In conclusion, especial acknowledgment is due Dr. W. R. Hess (Zurich), President of the International Foundation of the Jungfraujoch Scientific Station; Dr. W. Mörikofer, Director of the Physical-Meteorological Observatory at Davos; and Dr. F. W. Paul Götz, Director of the Climatological Observatory at Arosa, for numerous courtesies extended in connection with this investigation.

IV. BIBLIOGRAPHY

1. W. W. Coblentz, R. Stair, and J. M. Hogue, A Balanced Thermocouple and Filter Method of Ultra-violet Radiometry with Practical Applications, B. S. Jour. Research, vol. 7 (RP370), p. 723, 1931.
2. W. W. Coblentz, R. Stair, and J. M. Hogue, Tests of a Balanced Thermocouple and Filter Radiometer as a Standard Ultra-violet Dosage Intensity Meter, B. S. Jour. Research, vol. 8 (RP450), p. 759, 1932.
3. W. W. Coblentz and H. R. Fulton, A Radiometric Investigation of the Germicidal Action of Ultra-violet Radiation, B. S. Sci. Papers (S495), vol. 19, p. 461 (Table 1), 1924.
4. Über die Grundlagen Eines Neuen U. V. Messinstrumentes, E. Weyde, Strahlentherapie, vol. 38, p. 378, 1930. Ultra-violet Dosimeter, I. G. Farbenindustrie Aktiengesellschaft, Oppau, Ludwigshafen am Rhein. This instrument in a cylindrical metal case was less than 2 inches (5 cm) in diameter, and 7 inches (18 cm) in length.
5. W. W. Coblentz, Erythemal and Radiometric Comparisons of the Ultra-violet Emitted by Various Sources as a Basis for a Specification of the Unit of Dosage Intensity, II° Congres International de la Lumière, Copenhagen, August 15–18, 1932.

WASHINGTON, October 10, 1932.

EFFECT OF SERVICE TEMPERATURE CONDITIONS ON THE ELECTROMOTIVE FORCE OF UNSATURATED PORTABLE STANDARD CELLS

By J. H. Park

ABSTRACT

The effect of external temperature disturbances such as might occur in practice on the electromotive force (emf) of unsaturated portable standard cells of the models in general use as secondary standards, was investigated. The experiments included unequal heating of different parts of the cell and sudden changes of temperature. Temporary changes in cell emf, caused by these disturbances, in some cases as large as 1.8 mv (nearly 0.2 of 1 per cent), were measured and the results are shown by curves. During all tests the cell elements were left in the cases furnished with them. Methods of protecting the cells from external temperature disturbances were tried and their effectiveness is shown.

CONTENTS

	Page
I. Introduction and purpose	89
II. Effect of temperature inequality of the limbs	90
III. Hysteresis effects	96
IV. Summary	98

I. INTRODUCTION AND PURPOSE

Nearly all persons who regularly use the unsaturated portable cadmium cell (also called the Weston cell) as a standard of emf have been cautioned (1) to keep all parts of their cells at the same temperature, (2) to avoid sudden changes in the temperature of the cell, (3) not to submit the cells to temperatures below 4° C. or above 40° C., and (4) not to draw more than 0.0001 ampere from a cell. Changes in the emf of a cell due to deviations from these rules have been investigated and briefly summarized in a very comprehensive discussion of standard cells by Eppley.[1] However, results were not given for the cell elements in their cases, as they are generally used, and temperature effects depend upon the thermal insulation which envelops the cell element as well as the external temperature conditions.

The purpose of this investigation was to determine the effect on the emf of an unsaturated cell (1) when the limbs of the cell are at unequal temperatures as a result of conditions simulating those which might exist in practice, and (2) when the cell is subjected to a sudden change in temperature. All experiments were performed on the models of cells in general use and the glass elements of these cells

[1] Eppley, Trans. of the A. I. E. E., vol. 50, No. 4, p. 1293, December, 1931.

were thermally insulated by the cases furnished with them. In some experiments additional thermal shielding was used to determine its effectiveness in protecting the cells from temperature disturbances.

The general nature of the effects here described has been known for a long time, but it is believed their magnitude has often been underestimated. The present paper is intended therefore to show these magnitudes and to direct attention to the importance of taking suitable precautions in order to obtain the precision of which standard cells are capable. Further studies are being made of the causes underlying these effects.

II. EFFECT OF TEMPERATURE INEQUALITY OF THE LIMBS

The temperature coefficients of unsaturated portable cells are negligible [2] for practical purposes. However, the over-all temperature coefficient is the algebraic sum of the coefficients of the two limbs of the cell. The temperature coefficient of each limb taken separately [3] is quite large, but the two are opposite in sign. Thus, when the temperatures of the two limbs of a cell are changed by an equal amount the resulting change in the final steady value of the emf of the cell will usually be very small, but when the temperatures of the two limbs are changed by unequal amounts the resulting change in the emf of the cell will be relatively large, its magnitude depending upon the amount of temperature inequality. Inequalities of temperature are liable to occur in practice (1) if the cell is placed near a hot radiator, a resistor carrying current, a lighted lamp, or a cold wall; (2) if the cell is placed where the sun's rays will strike it; (3) if the cell is held in the bare hand; or (4) if the cell is placed where hot or cold air will strike it (such as in the draft from a register or cold-air duct or near an open window in the winter time). The above are the more obvious causes of irregular heating of cells, but must not be considered to be every possibility.

Several models of cells were subjected to most of the temperature conditions just mentioned, the procedure being as follows: The emf of the cell under test was first noted for a sufficient time to make sure it was steady. Then the cell was subjected to the temperature condition and its emf was measured every 10 minutes until it had reached a steady value. Next, the source of heat was removed and the emf was again measured every 10 minutes until it was steady and very close to its original value. In one experiment the temperature difference between limbs was also measured by placing a thermocouple inside the cell case with each junction in contact with one of the limbs.

The emf of the cell under test was found by comparing it with the emf of a reference cell, the small difference being measured by means of a simple potentiometer of the Lindeck-Rothe type. An unsaturated cell in good condition, placed in an additional container (shown in fig. 1) for protection against temperature inequality, was used as the reference cell.

Three models (designated here as A, B, and C) of unsaturated portable standard cells which are in general use as secondary standards of emf, were tested. Cells of models A and C were in bakelite cases,

[3] Weston, The Electrician, vol. 30, p. 741, 1892. Vosburgh and Eppley, J. Opt. Soc. of Am., vol. 9, p. 72, 1924.
[4] F. E. Smith, Phil. Mag., vol. 19, p. 272, 1910.

and cells of model B were in metal cases. Several cells of each model were tested, but since all cells of the same model gave practically the same performance, data are given here for only one cell of each model.

The results of the experiments to determine the effect of temperature inequalities are shown by the curves in Figures 2 to 6. Curves in Figure 2 show the results on a standard cell of model A, when it was placed near a 16-inch slide rheostat dissipating 288 watts. The inserted diagram shows the position of the cell with respect to the rheostat. Curves *A* and *B* show the effect on emf when the cell was placed 10 inches from the heated rheostat. When the positive limb is nearer to the rheostat (curve *A*), its temperature is higher

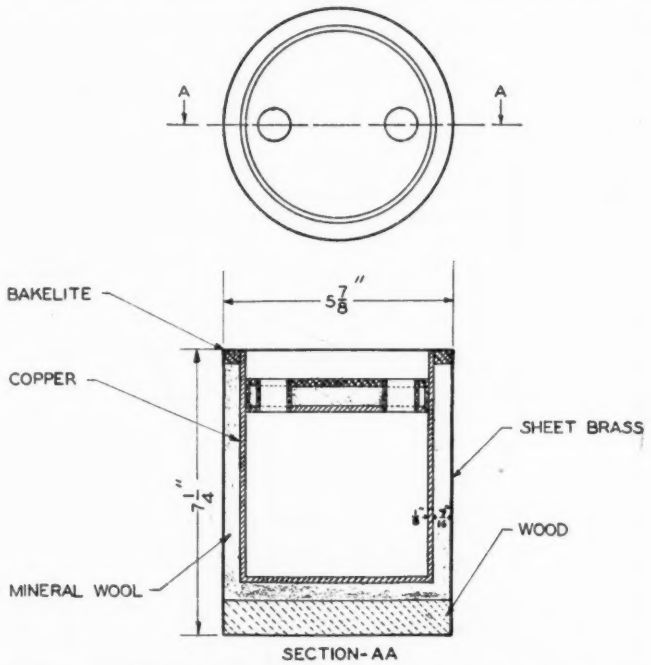

FIGURE 1.—*Standard cell container for protection against temperature inequality*

Designed at the Bureau of Standards in 1927.

than that of the negative limb, and the cell emf increases. When the negative limb is nearer to the rheostat (curve *B*), its temperature is higher than that of the positive limb, and the cell emf decreases. These curves illustrate the fact that the temperature coefficients of the two limbs of the cell taken separately have the opposite effect on the cell emf, also that the effects are about the same per degree difference in temperature. In curve *A* the emf of the cell does not return to its normal value until about 36 hours after removing the source of heat; this and other slight irregularities which may occur in the cooling part of the curves are due to the hysteresis effect which will be taken up later. Curve *E* shows the temperature difference between the limbs of the cell under the same heating conditions as for curves *A* and *B*. As seen from curves *A*, *B*, and *E*, a temperature difference

of 2.7° C. between the limbs of the cell causes a change in emf of about 1 mv.

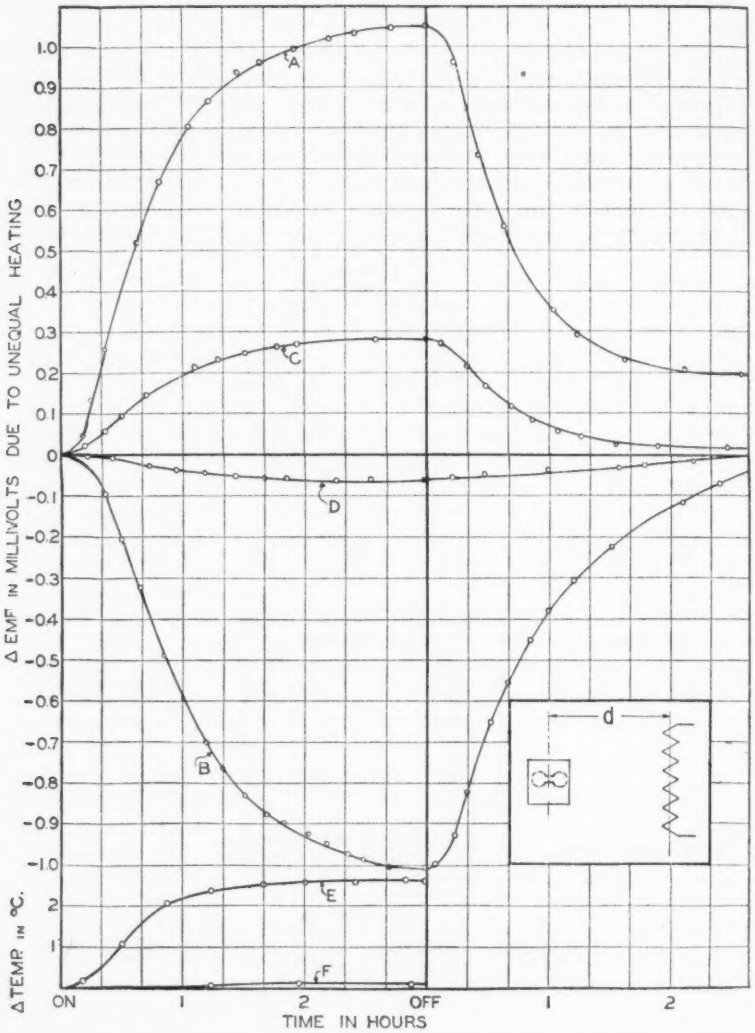

FIGURE 2.—*Temperature inequality effects on standard cell model A, caused by heat from a 16-inch slide rheostat dissipating 288 watts*

Curve *A*, effect on emf when $d=10$ inches, positive limb nearer to rheostat. Curve *B*, effect on emf when $d=10$ inches, negative limb nearer to rheostat. Curve *C*, effect on emf when $d=20$ inches, positive limb nearer to rheostat. Curve *D*, same as curve *B* with cell in special container. Curve *E*, temperature difference between limbs when $d=10$ inches. Curve *F*, same as curve *E* with cell in special container

Curve *C* (fig. 2) shows the effect on the emf when the cell was placed 20 inches from the heated rheostat. By comparing this curve with curve *A*, it is seen that the change in emf due to unequal heating happens to vary approximately inversely as the square of the distance from the rheostat.

Curves *D* and *F* (fig. 2) show the results when the cell was placed in a protecting container (shown in fig. 1) and submitted to the same heating conditions as for curves *A*, *B*, and *E*. As seen from curve *F*, a container of this sort practically eliminates temperature inequality in the cells. The change in the emf of the cell, shown by curve *D*, is partially due to the fact that the temperatures of both limbs of the cell were increased about 5° C. due to the radiation of heat from the rheostat.

The curves in Figure 3 show the results obtained when the experiments just described were repeated, using a standard cell of model B.

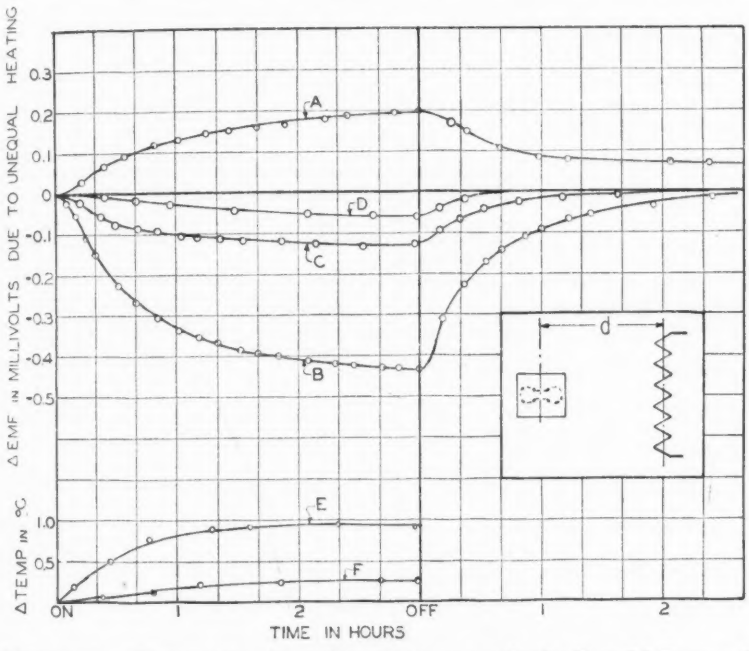

FIGURE 3.—*Temperature inequality effects on standard cell model B, caused by heat from a 16-inch slide rheostat dissipating 288 watts*

Curve *A*, effect on emf when $d=10$ inches, positive limb nearer to rheostat. Curve *B*, effect on emf when $d=10$ inches, negative limb nearer to rheostat. Curve *C*, effect on emf when $d=20$ inches, negative limb nearer to rheostat. Curve *D*, same as curve *B*, with cell in special container. Curve *E*, temperature difference between limbs when $d=10$ inches. Curve *F*, same as curve *E*, with cell in special container

The metal case of this model tends to equalize the temperatures of the two limbs, and the curves show that the same heating condition causes a much smaller temperature difference and therefore a much smaller change in emf than for a cell in a bakelite case. The difference in maximum values between curves *A* and *B* may have been due to a difference in the cotton and wood thermal insulation between the metal case and the limbs of the cell.

The curves in Figure 4 are the results of similar experiments performed on a standard cell of model C. The case of this cell was too large to fit into the container used for the previous cells in obtaining data for curves *D* and *F*. However, there was sufficient space inside the bakelite case to allow the insertion of a copper lining one-sixteenth-inch thick. The results indicate this method of equalizing cell tem-

perature to be as effective for a cell of this model as the use of a special container was for cells of models *A* and *B*.

The curves in Figure 5 show the change in the emf of the cell due to the heat of the hand, held continuously on one side of the cell case for over two hours. The curves in Figure 6 show the change in emf

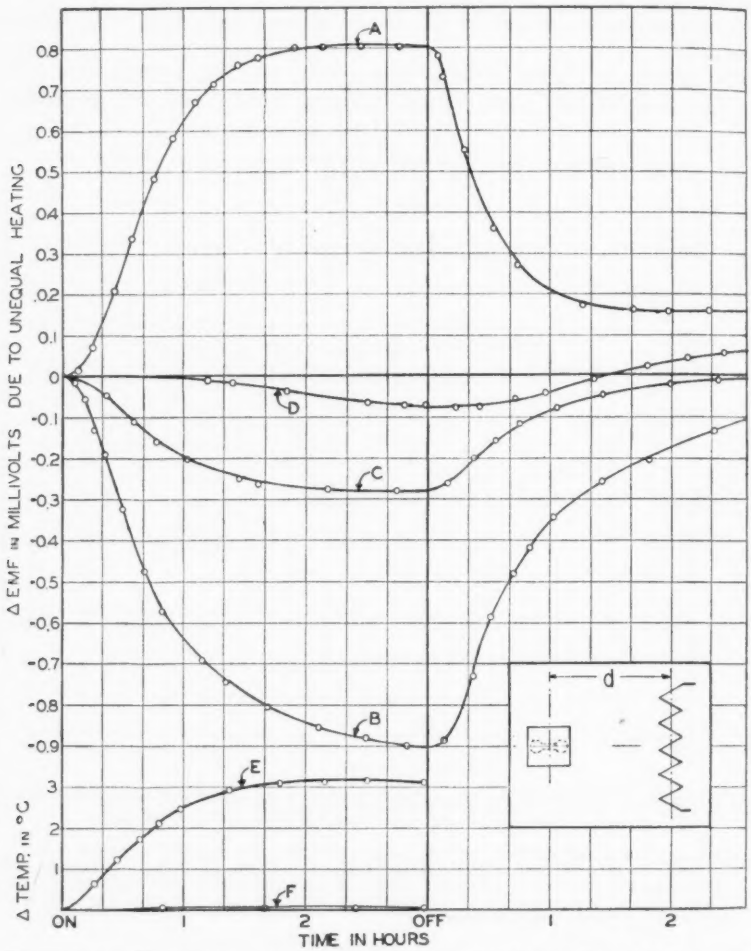

FIGURE 4.—*Temperature inequality effects on standard cell model C, caused by heat from a 16-inch slide rheostat dissipating 288 watts*

Curve *A*, effect on emf when $d=10$ inches, positive limb nearer to rheostat. Curve *B*, effect on emf when $d=10$ inches, negative limb nearer to rheostat. Curve *C*, effect on emf when $d=20$ inches, negative limb nearer to rheostat. Curve *D*, same as curve *A*, with cell case copper lined. Curve *E*, temperature difference between limbs when $d=10$ inches. Curve *F*, same as curve *E*, with cell case copper lined

due to the heat of the sun's rays, shining continuously on one side of the cell case for over two hours. For both of the above conditions the cell and the source of heat were arranged to give the maximum opportunity for temperature inequality of the two limbs of the cell. Curves are shown for the three models of cells in their usual cases and the differences between the behavior of these cells under the same conditions are largely due to the differences of their cases.

Change in the emf of a cell due to unequal heating caused by radiation from a 40-watt lamp placed 1 foot from the cell was found to be under 50μv.

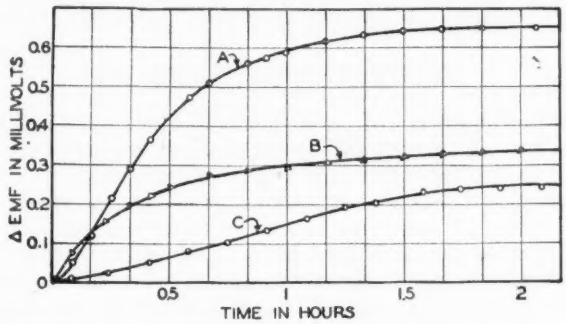

FIGURE 5.—*Change in standard cell emf due to the heat of the hand, held continuously on one side of the cell case*

Curve *A*, standard cell model A. Curve *B*, standard cell model B. Curve *C*, standard cell model C

The results of the above experiments should not be applied quantitatively as a correction to other cells of the same model under like temperature disburbances, because variables such as room tempera-

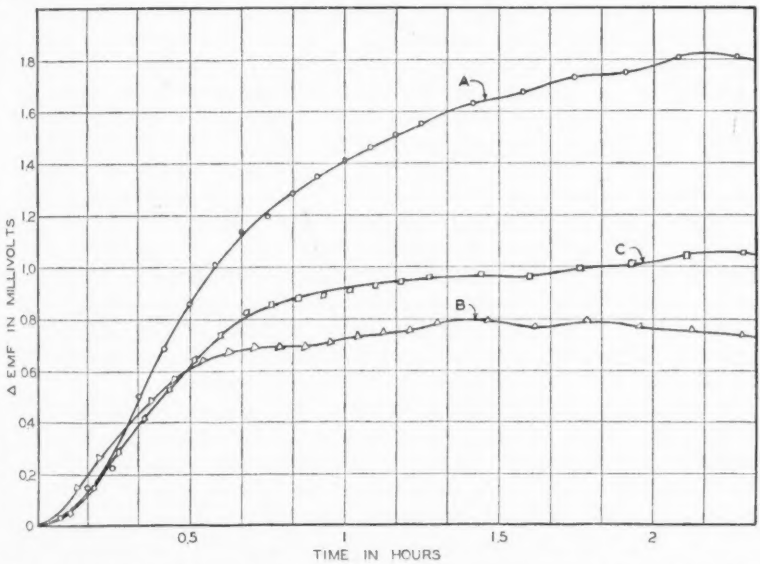

FIGURE 6.—*Change in standard cell emf due to exposure of one side of cell case to sunlight*

Curve *A*, standard cell model A. Curve *B*, standard cell model B. Curve *C*, standard cell model C

ture or condition of the cell may cause cells of the same model to have different changes in emf for the same external temperature disturbance. However, the results shown may be used as a guide for the user to determine whether protection against temperature inequality is

needed for the accuracy required. The methods mentioned here for protection against temperature inequality are probably sufficient for all practical work. However, where high precision (0.01 of 1 per cent or better) is required, more effective methods of protection against temperature disturbances should be used.

III. HYSTERESIS EFFECTS

When the temperature of an unsaturated standard cell is changed, all parts of the cell being held at equal temperatures throughout the change, the emf of the cell will change rapidly until a steady temperature is reached. Then the emf will slowly return to approximately its original value. This effect is known as hysteresis.

Several different theories have been advanced to explain the causes of this hysteresis effect. However, it was not the purpose of this investigation to explain any of these theories or to obtain data in support of them. It is well known that hysteresis is present in most cells to a greater or less extent, and that the effect is more pronounced with a declining temperature than with a rising temperature. The purpose of the experiments to be described was to find within what limits the hysteresis error lies for the unsaturated portable cells which are in general use, also to determine what means might be employed to reduce these errors.

Six cells, of various models and ages, taken from a group in regular laboratory use, were tested for hysteresis. In order to duplicate as nearly as possible the conditions in practice, the cells in their usual cases were placed in a temperature-controlled air bath.[4] The air was circulated by a blower and its temperature was held constant to within $\pm 0.1°$ C. by a thermostat which operated a heater in the air stream. The bath temperature was first held at 23° C. until the cell emf's became constant. Then it was changed to 27° C. (time required being about two hours) and held there, measurements of the emf of all cells being made at frequent intervals until the equilibrium values for 27° C. were reached. Next the air temperature was changed back to 23° C. (in about two hours) and held there, measurements again being made until equilibrium was reached. These measurements were made in the same way as in the temperature-inequality experiments except that a saturated cell [5] in a temperature-controlled oil bath was used as a reference standard.

The results of the hysteresis experiments are shown by the curves in Figure 7. Time after starting to change the ambient temperature was plotted as abscissas and change in the emf of the cell as ordinates. Curve *A* shows the effect on the emf of Cell II (cell with the least hysteresis) when the temperature was raised from 23° to 27° C. Curve *B* shows the effect on the emf of the same cell when the temperature was lowered from 27° to 23° C. Curves *C* and *D* show the effect on the emf of Cell IV (cell with the most hysteresis) under the same temperature changes as for Cell II. Hysteresis curves of Cells I, III, V, and VI lie between those of Cells II and IV, but are not shown. The results of measurements on these six cells did not show any correlation between cell emf, model of cell, or age of cell and hysteresis effect. One of the newest cells with a high emf showed

[4] This temperature-controlled cabinet was designed by A. E. Peterson.

[5] The emf of this cell was checked by Miss M. L. Howard at least once a week against the average of the 20 cells which constitute the bureau's reference standard of emf.

much greater hysteresis than one of the oldest cells with a low emf. Therefore, it is very difficult, if not impossible, at the present time to predict just what the hysteresis error of any given cell will be. However, from the curves in Figure 7, an approximation may be had as to within what limits the hysteresis error of any unsaturated portable cell in good condition [6] might fall. Eppley [7] found that when an unsaturated cell was suddenly cooled from 30° to 25° C. the average hysteresis error was from 0.02 to 0.027 per cent. This average error lies within the limit shown here.

A method of protecting cells from hysteresis errors was applied to Cell IV, which was chosen because of its large hysteresis. It was placed inside a container (such as shown in fig. 1) and this container

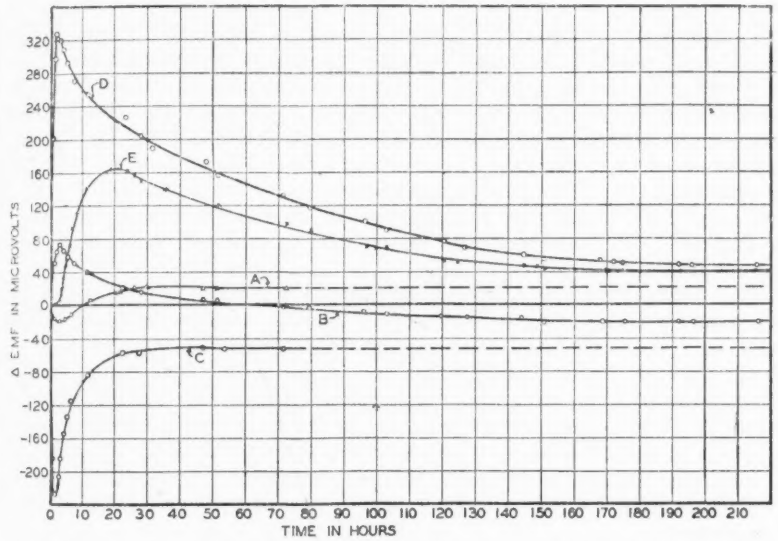

FIGURE 7.—*Hysteresis effect on portable unsaturated standard cells*

Curve *A*, effect on emf of Cell II, when temperature was changed from 23° to 27° C. Curve *B*, effect on emf. of Cell II, when temperature was changed from 27° to 23° C. Curve *C*, effect on emf of Cell IV, when temperature was changed from 23° to 27° C. Curve *D*, effect on emf of Cell IV, when temperature was changed from 27° to 23° C. Curve *E*, same as curve *D* with cell in insulated box

was placed in a wooden box which was sufficiently large to leave about 3 inches of space between the container and the box on all sides, mineral wool being loosely packed in this space. The cell, thus thermally insulated, was placed in the constant-temperature cabinet, set for 27° C. and maintained at this temperature until the emf of the cell became steady. Then the air temperature was lowered to 23° C. and held there, readings of the emf being taken regularly until it again became constant. The results of this experiment are shown by curve *E* in Figure 7. By comparing this curve with curve *D* it may be seen that thermally insulating the cell decreases the hysteresis effect by about 50 per cent in the case of a sustained temperature change. However, under ordinary laboratory conditions, where the average temperature over a period of 24 hours does not change much from day

[6] Cells which are not in good condition may show much greater hysteresis errors.
[7] See reference 1, p. 1299.

to day, thermally insulating a cell would be of great benefit in smoothing out the hour-to-hour temperature changes, thus greatly reducing the hysteresis error.

In instances where large sustained temperature changes occur, the only means of eliminating hysteresis errors is to keep the cell in a container whose temperature can be thermostatically controlled. However, as noted from curves *A* and *B* (fig. 7) some cells have very low hysteresis errors. In cases where high accuracy is required and the necessary means for eliminating hysteresis are not feasible, it would be advisable to use a particular cell whose hysteresis has been observed and found to be small.

IV. SUMMARY

Temperature inequality between the two limbs of a standard cell, which may occur (1) when the cell is placed near a heat source, such as a hot radiator or a rheostat carrying current; (2) when the cell is placed where the sun's rays will strike it; (3) when the cell is placed where cold air will strike it; or (4) when the cell is held in the hand, caused an error in the emf of the cell of about 300 μv per °C. difference in temperature. The temperature inequality between limbs can be practically eliminated by placing the cell in a container such as shown in Figure 1, or, where possible, by lining the cell case with sheet copper one-sixteenth inch thick.

The hysteresis error, which occurs in portable unsaturated cells when their temperature is changed, varies widely among different cells, and the only way to determine this error for a given cell is to check its emf immediately after its temperature has been changed. Errors due to hysteresis may be reduced by sufficiently insulating the cell against changes in temperature; but the only way to eliminate these errors is to keep the cell in a box whose temperature is thermostatically controlled. Under normal laboratory conditions precautions against hysteresis need be taken only if accuracies of 0.03 per cent or better are required.

WASHINGTON, October 12, 1932.

THE THOMAS RECORDING GAS CALORIMETER

By R. S. Jessup

ABSTRACT

The Thomas recording gas calorimeter is described. Calculations are made showing the effects on the reading of the calorimeter of change in temperature and barometric pressure. Results of comparisons of the Thomas calorimeter with the Junkers calorimeter on Washington City gas and on commercial propane are given. The agreement of the results obtained with the two calorimeters is well within the accuracy claimed for the Thomas calorimeter. Measurements of the lag of the Thomas calorimeter are described.

CONTENTS

		Page
I.	Introduction	99
II.	Description of Thomas calorimeter	100
III.	Standardization of calorimeter with hydrogen	104
IV.	Effect of changes in temperature, barometric pressure, and atmospheric humidity	108
V.	Comparisons with the Junkers calorimeter	114
VI.	Heating values outside the usual working range	117
VII.	Lag of the Thomas calorimeter	118
VIII.	Previous work	120
IX.	Acknowledgments	120
X.	Conclusion	121

I. INTRODUCTION

The subject of gas calorimetry has been investigated in considerable detail at this bureau by Waidner and Mueller.[1] These authors discuss the principles underlying the determinationof heating values of gases, and describe exhaustive tests of a number of commercial gas calorimeters. It was shown that several of the calorimeters tested could be used for measuring total heating values of gases to an accuracy of about 0.3 per cent. This accuracy can be attained, however, only at the expense of considerable time in making the necessary adjustments and observations, and in computing the results.

Since the above-mentioned work was done various types of recording gas calorimeters have come into use, and numerous inquiries have been received by this bureau regarding the reliability of such instruments. One of these types, which is widely used at the present time, is known as the Thomas recording gas calorimeter, and the present paper describes the results of a critical study of this instrument and its behavior. A Thomas calorimeter, having a range of 0 to 700 Btu per cubic foot, was loaned by the manufacturers for this investigation.

[1] B. S Tech. Paper No. 36, 1914.

II. DESCRIPTION OF THE THOMAS CALORIMETER

The Thomas calorimeter or any other recording calorimeter may be used as a secondary instrument, designed to be adjusted to indicate the heating value of the gas as determined with a standard instrument; for example, a water flow calorimeter of the ordinary type. If used in this way, the questions of interest concern the length of time the indications will remain correct, and whether the correctness will be affected by ordinary changes in temperature, barometric pressure, and atmospheric humidity.

The Thomas calorimeter was designed, however, not as a secondary instrument, but as a self-contained one, which could be standardized by the use of pure hydrogen. This self-contained feature necessarily leads to complications in design, and requires the operator to be familiar with the process of standardization, but provides some of the advantages inherent in a primary instrument. If a calorimeter has the characteristics demanded of a self-contained instrument, it will necessarily be equally or more satisfactory if used merely as a secondary instrument. In this investigation, therefore, the suitability of the Thomas calorimeter as a self-contained instrument was of major interest.

The principle upon which the Thomas calorimeter operates is as follows: Gas is burned at a constant rate and the heat developed is absorbed by a stream of air. The rates of flow of the gas, air for combustion, and the heat-absorbing air are regulated by metering devices, similar in construction to the ordinary wet gas meters. These metering devices are geared together and driven by an electric motor, so that the ratio of the rates of flow of gas and heat-absorbing air is constant. The products of combustion are kept separate from the heat-absorbing air, and are cooled very nearly to the initial temperature of the air. The water formed in the combustion is condensed to the liquid state. The rise in temperature of the heat-absorbing air is therefore proportional to the total heating value of the gas. This rise in temperature is measured by means of resistance thermometers of nickel, translated into Btu per cubic foot of gas under standard conditions, and recorded graphically.

The meters are mounted in a tank of water, within which is a smaller tank containing a reserve supply of water. A chain pump draws water from the reserve tank and delivers it into the main tank; the excess flows over a weir and returns to the reserve tank. Thus the water level in the main tank is automatically kept constant.

A schematic diagram of the calorimeter is shown in Figure 1, which was taken from the book of instructions for the care and operation of the calorimeter. Gas flows from the gas supply line through a pressure reducing orifice into a chamber from which part of it escapes through a bleeder burner. The area of the bleeder burner openings is sufficiently large so that the gas pressure in the chamber does not differ appreciably from that of the atmosphere. The remainder of the gas flows through the gas meter and connecting tubing to a mixing chamber where it is mixed with air from the combustion air meter. The mixture flows from the mixing chamber to the calorimeter burner. Figure 2 is an enlarged view of the burner unit.

The air from the combustion air meter is divided into two streams, one of which flows to the mixing chamber, while the other flows up

around the outside of the burner tube and constitutes a supply of secondary air for combustion.

The burner is located in a chamber which is closed at the top and open at the bottom, so that the products of combustion rising from

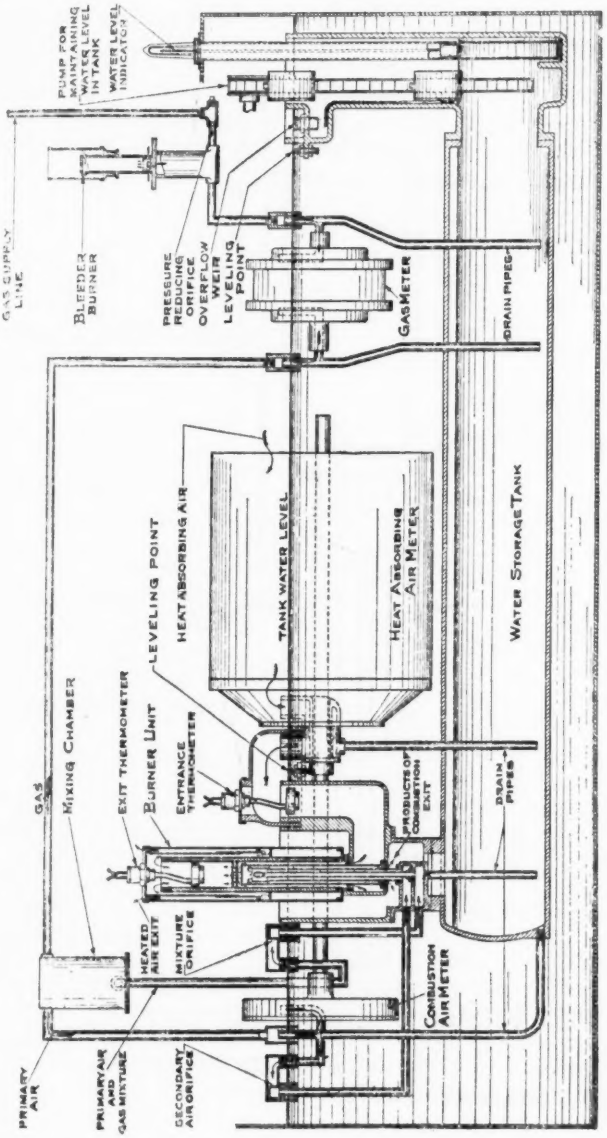

FIGURE 1.—*Schematic diagram of the Thomas calorimeter*

the burner are deflected and caused to flow downward. The heat-absorbing air flows upward past a system of fins which are attached to the outside of the burner chamber to promote heat transfer. The heat liberated in the combustion is nearly all absorbed by the heat-

absorbing air, so that the products of combustion are cooled very nearly to the initial temperature of the air. The water formed in

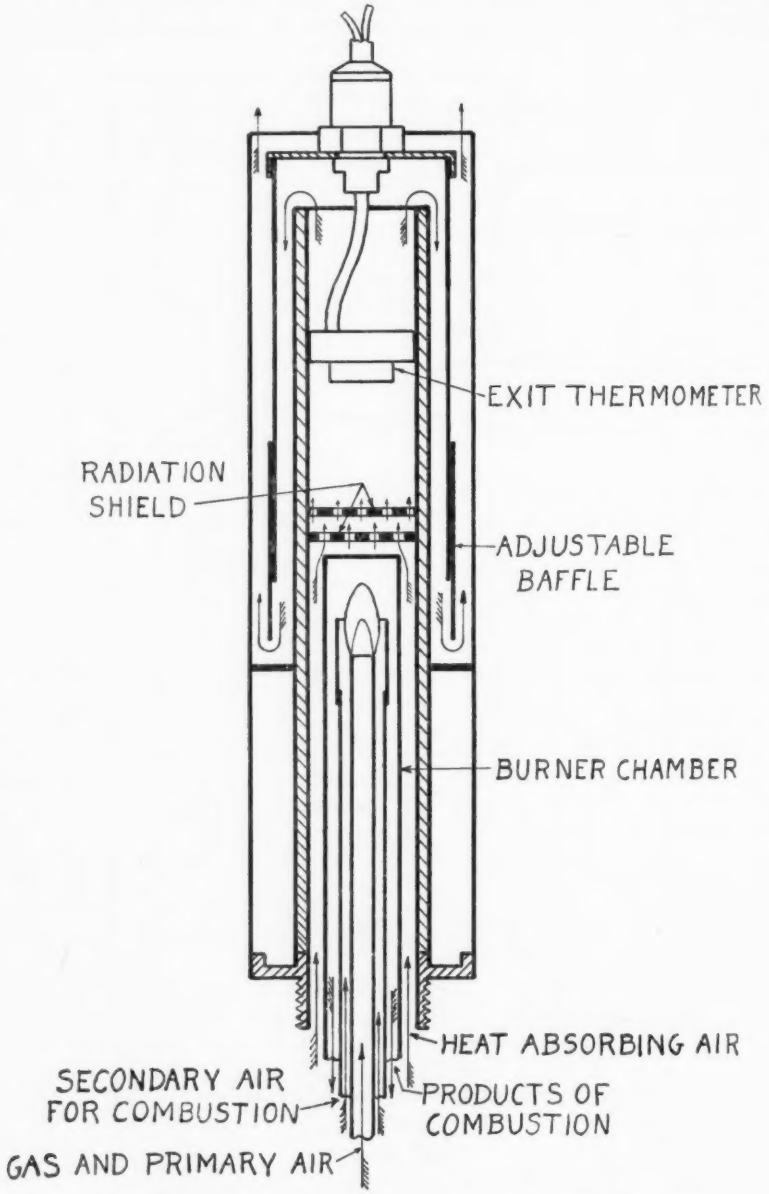

FIGURE 2.—*Diagram of burner unit and jacket*

the combustion is condensed to the liquid state and drops into the water storage tank.

The volume of the heat absorbing air is nearly a thousand times the volume of gas burned,[2] so that the heat capacity of the heat absorbing air in relation to the amount of gas burned is comparable with the heat capacity of the water used to absorb heat in the ordinary water flow calorimeter. The temperature rise of the heat-absorbing air is measured by means of the entrance and exit thermometers shown in Figure 1. These are resistance thermometers made of nickel wire.

Figure 3, which was taken from the Thomas calorimeter instruction book, is a schematic diagram of the Leeds & Northrup recording system, used with the calorimeter. The inlet thermometer, T_1, and

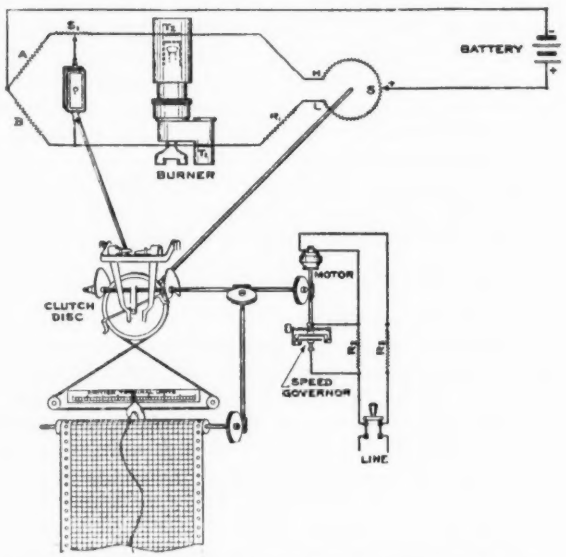

FIGURE 3.—*Schematic diagram of recording system*

outlet thermometer, T_2, are connected in adjacent arms of a Wheatstone bridge. Any lack of balance in the bridge causes the galvanometer needle to deflect and actuate the recording mechanism, which moves the sliding contact, S, so as to bring the bridge back into balance. The recording pen is simultaneously moved into a position corresponding to the new position of the contact, S.

The sliding contact, S_1, (fig. 3), is used to balance the bridge when heat-absorbing air is flowing through the system with the burner out and the recording pen set on the zero of the scale. This is called cold balancing the calorimeter, and its effect is to compensate for any small changes which may have occurred in the resistances or connecting wires of the thermometers. Current for the bridge is furnished by dry cells, or by a "trickle charger" connected to the A. C. power line.

[2] The ratio of the volumes of heat absorbing air and gas is approximately $126.7 \times \frac{S}{100}$ to 1, where S is the full-scale reading. For the 0 to 700 range calorimeter the ratio is 126.7×7, or 887 to 1.

The ratio of the rates of flow of gas and heat-absorbing air may change with time due to unequal wear of the bearings, and to corrosion or deposits in the meters. To avoid errors due to this cause the gas meter is installed in such a way that it can be raised or lowered so as to vary the volume delivered by it per revolution. Gears are provided, by means of which the relative speeds of the gas meter and heat-absorbing air meter can be changed, so that when the gas meter is at the proper height, the two meters deliver at the same rate. The two meters can then be connected so that one delivers into, and the other pumps from a "prover bell" partially immersed in the water of the tank and suspended from one arm of a balance. The other arm of the balance is loaded with a counterweight so adjusted that the gas pressure in the bell does not differ appreciably from that of the atmosphere. The balance is provided with a pointer and scale to indicate the height of the prover bell. Any difference in the delivery rates of the two meters will cause the prover bell to rise or fall, and the height of the gas meter can be adjusted accordingly. This test is called the air-gas ratio test.

The adjustment made in this test is such that if the air and gas meters delivered the same volumes per revolution during operation as they do during the test, the volume of heat-absorbing air would be $126.73 \times \frac{S}{100}$ times the volume of gas, where S is the full-scale reading. In the test, however, the speed of the air meter is of the order of one two-hundredth of its usual operating speed, while the speed of the gas meter in the 0 to 700 range calorimeter is of the order of five times its usual operating speed. It is not to be expected that over this range of speeds the ratio of the volumes delivered by the two meters will remain constant to 0.01 per cent, so that the ratio of heat absorbing air to gas for practical purposes may be given as $126.7 \times \frac{S}{100}$ to 1.

To reduce heat loss the burner chamber is surrounded by a double-walled, nickel-plated jacket, between the walls of which the heat-absorbing air flows after passing the outlet thermometer. The flow of air between the walls of the jacket is regulated by a baffle (shown in fig. 2) which can be adjusted. This baffle is adjusted by the manufacturers so that the calorimeter records the value 320.6 Btu per cubic foot under standard conditions [3] for the heating value of pure hydrogen.

III. STANDARDIZATION OF CALORIMETER WITH HYDROGEN

When hydrogen is being burned in the 0 to 700 range calorimeter, the speed of the gas meter relative to that of the heat-absorbing air meter is increased in the ratio 21/11, by appropriate changes in the gears in the gear train between the driving motor and the gas meter. The purpose of this is to bring the reading of the calorimeter when burning hydrogen into the usual operating range; that is, in the

[3] The standard conditions are: A temperature of 60° F., the gas saturated with water vapor at that temperature, and a total pressure equivalent to that of a 30-inch column of mercury at 32° F., and under standard gravity.

neighborhood of 600 on the scale. Under these conditions the calorimeter should read

$$320.6 \times \frac{21}{11} = 612$$

The value 320.6 Btu per cubic foot for the heating value of hydrogen is based on 68,635 calories $_{15}$ per mole for the heat of formation of water, which is the mean of values obtained by Berthelot and Matignon,[4] Mixter,[5] Thomsen,[6] and Rumelin.[7] Roth [8] has critically reviewed the data of the observers mentioned above, and of Schuller and Wartha,[9] and has selected 68,380 calories $_{15}$ per mole at 18° C. as the most probable value for the heat of formation of water. More recently Rossini [10] has made a careful determination of the heat of formation of water, obtaining the value $68{,}313 \pm 10$ calories $_{15}$ per mole at 25° C. These last two values, when reduced to the same temperature on the assumption that the heat of formation changes by −8 calories per mole per ° C., differ by less than 0.02 per cent. The value used in adjusting the Thomas calorimeter is thus about 0.4 per cent higher than that deduced from the best available data. If uncompensated, this would cause the Thomas calorimeter to read high by 0.4 per cent when operating on illuminating gas. However, the calorimeter will indicate relatively too high a value for hydrogen and too low a value for ordinary illuminating gas, because of the fact that when burning hydrogen more water vapor will be condensed than is formed by combustion and less when burning illuminating gas. The amounts of water condensed relative to the amount formed depend upon two factors: (*a*) The difference in volume of the products of combustion and of the initial gas and air, and (*b*) the difference in temperature of the products and of the initial gas and air.

The decrease in volume when combustion takes place tends to cause more water to be condensed than is formed in the combustion. This tendency is opposed by the excess in the temperature of the products over that of the initial gas and air. In order to calculate the effect of these two factors it was necessary to know the ratio of combustion air to gas, the contraction due to combustion, and the temperature of the products.

The delivery rates of the gas meter and combustion air meter were measured by connecting each of them in series with a calibrated 0.1 cubic foot wet meter and observing the time required for any convenient integral number of revolutions of the 0.1 cubic foot meter drum. The results obtained were as follows:

Meter	Delivery rate in cubic feet per hour
Gas	0.2729
Combustion air	2.264

[4] Ann. Chim. Phys. (6) vol. 30, p. 550, 1893.
[5] Am. Jour. of Science, vol. 16, p. 214, 1903.
[6] Thermochemische Untersuchungen II, p. 45; Leipzig, 1885.
[7] Zeits. für physik-Chem., vol. 58, p. 449, 1907.
[8] Zeits. für Electrochemie, vol. 26, p. 288, 1920.
[9] Ann. d. Phys. und Chemie, vol. 2, p. 359, 1877.
[10] B. S. Jour. Research, vol. 6, p. 1, 1931.

The ratio of combustion air to gas is therefore $\frac{2.264}{0.2729}=8.3$.

The contraction due to combustion of the illuminating gas used in this investigation was calculated from analyses of Washington city gas made by Branham.[11] The calculated contraction was on the average 1.24 cubic feet per cubic foot of gas.

The temperature of the products of combustion was measured by means of a thermocouple, one junction of which was placed in the stream of products at the point where it leaves the burner chamber, and the other junction in the water of the tank. The temperature of the products of combustion was found to be 7° F. higher than the temperature of the tank, both when illuminating gas was being burned in the calorimeter at the normal rate and when hydrogen was being burned at 21/11 times the normal rate.

TABLE 1.—*Difference between amounts of water formed and condensed when burning illuminating gas and effect on indicated heating value*

Temperature of tank t	Contraction per cubic foot of gas at t° F. and 30 inches	Density of water vapor at t° d	Water condensed per cubic foot of gas due to contraction w	Density of water vapor at $(t+7)$° d'	$d'-d$	$8.2\ (d'-d)$ w'	$w-w'$	$L(w-w')$	Percent of 600 Btu
° F.	*Ft.³*	*Lbs./ft.³*	*Pound*	*Lbs./ft.³*	*Lb./ft.³*	*Pound*	*Pound*	*Btu*	
60	1.24	0.000828	0.00103	0.001044	0.000216	0.00177	−0.00074	−0.78	−0.13
70	1.24	.001151	.00143	.001437	.000286	.00235	−.00092	−.97	−.16
80	1.24	.001578	.00196	.001953	.000375	.00308	−.00112	−1.17	−.21
90	1.24	.002134	.00265	.002616	.000482	.00395	−.00130	−1.35	−.24

Using these data the combined effect of the two factors (*a*) and (*b*) was calculated. The results for illuminating gas are shown in Table 1. The first column gives the temperature of the tank and therefore the initial temperature of gas and combustion air. Column 2 gives the contraction per cubic foot of gas saturated with water vapor at the temperature of the tank. Column 3 gives the density of water vapor at the temperature of the tank. The values of density of water vapor were taken from Keenan's steam tables. Column 4 is the product of the corresponding figures in columns 2 and 3, and represents the amount of water in excess of that formed in the combustion which would be condensed per cubic foot of gas burned if the products of combustion were cooled to the temperature of the tank. Column 5 gives the density of water vapor at the final temperature of the products of combustion. Column 6 gives the difference in the densities of water vapor at the temperature of the tank and at the temperature of the products of combustion; that is, the excess of the density of water vapor in the products of combustion over what it would be if the products were cooled to the temperature of the tank. Column 7 gives the increase in the quantity of water carried off by the products of combustion due to the fact that they were not cooled to the temperature of the tank. The factor 8.2 represents the volume of the products of combustion of 1 cubic foot of gas, and is the volume of gas (1.0) plus the volume of the combustion air (8.3), minus the contrac-

[11] Am. Gas. J., vol. 135, No. 2, p. 42, August, 1931.

tion (1.2), plus the increase in volume due to the higher temperature of the products (0.1). Column 8 gives the excess in the quantity of water condensed over that formed in the combustion, and column 9 gives the increased heat evolved due to this excess. Column 10 gives the percentage of increase in the heat evolved due to this excess condensation. It is seen that for this illuminating gas less water is condensed than is formed in the combustion, and that this results in from 0.13 to 0.24 per cent less heat being evolved than would be if all the water formed in the combustion were condensed.

The special test gears used when hydrogen is burnedin the 0 to 700 range calorimeter reduce the ratio of combustion-air to gas in the ratio 11/21, so that with these gears this ratio becomes

$$8.3 \times \frac{11}{21} = 4.3$$

Since the contraction when one cubic foot of hydrogen is burned is 1.5 the ratio of the volume of the products to volume of gas is $(1.0+4.3-1.5)=3.8$.

Table 2 shows the calculations for hydrogen similar to those for illuminating gas in Table 1. It is seen that in this case more water is condensed than is formed in the combustion, resulting in an increase in the heat evolved amounting to from 0.14 to 0.47 per cent.

TABLE 2.—*Difference between amounts of water vapor formed and condensed when burning hydrogen and effect on indicated heating value*

Temperature of tank t	Contraction per cubic foot of gas at $t°$ F. and 30 inches	Density of water vapor at $t°$ d	Water condensed per cubic foot of gas due to contraction w	Density of water vapor at $(t+7)°$ d'	$d'-d$	$3.8\ (d'-d)$ w'	$w-w'$	$L\ (w-w')$	Per cent of 319 Btu
°F.	*Ft.*³	*Lbs./ft.*³	*Pounds*	*Lbs./ft.*³	*Lbs./ft.*³	*Pounds*	*Pounds*	*Btu*	
60	1.50	0.000828	0.00124	0.001044	0.000216	0.00082	0.00042	0.44	+0.14
70	1.50	.001151	.00173	.001437	.000286	.00109	.00064	.67	.22
80	1.50	.001578	.00237	.001953	.000375	.00143	.00094	.94	.31
90	1.50	.002134	.00320	.002616	.000482	.00183	.00137	1.43	.47

These calculations indicate that if the Thomas calorimeter were adjusted to give the correct total heating value for hydrogen (319.4 Btu per cubic foot) then when burning illuminating gas at any given temperature it would read low by an amount depending on the temperature of the tank during the hydrogen test. For example, if the hydrogen test were made with the tank temperature 65° F., then when burning illuminating gas the calorimeter would read low by 0.3 per cent with the tank temperature at 60° F., and by 0.4 per cent with the tank temperature at 90° F. On the other hand, if the Thomas calorimeter is adjusted so as to read 0.4 per cent high when burning hydrogen with the tank temperature at 65° F., then it would not be in error by more than 0.1 per cent due to condensation or evaporation of water at any temperature between 60° and 90° F.

It would appear from the foregoing considerations that, in standardizing the Thomas calorimeter with hydrogen, it would be better to use 320.6 Btu per cubic foot for the heating value of hydrogen rather

than Rossini's value (319.4), which is almost certainly more nearly correct. This conclusion, however, is not supported by the experimental data obtained in comparing the Thomas and Junkers calorimeters. These data will be discussed more in detail later.

IV. THE EFFECTS OF CHANGES OF TEMPERATURE, BAROMETRIC PRESSURE, AND ATMOSPHERIC HUMIDITY

The calorimeter is designed to give the total heating value of gas in Btu per cubic foot, the gas being saturated with water vapor at 60° F. and under a total pressure equivalent to that of a 30-inch column of mercury at 32° F. and under standard gravity. In the actual operation of the calorimeter the gas is metered at the temperature of the tank and is saturated with water vapor at that temperature. If the temperature of the tank is higher than 60° F. the density of the gas will be less than if the temperature were 60° F., due partly to its thermal expansion and partly to the increase in vapor pressure of water which results in lower partial pressure of gas. The thermal expansion alone would not cause any appreciable error in the indications of the calorimeter, since the expansion of the heat absorbing air is practically the same as that of the gas. The effect of the higher vapor pressure of water at the higher temperature, however, is to decrease the amount of combustible material per unit volume of gas, and to increase the heat capacity per unit volume of the heat absorbing air. Both of these factors cause a decrease in the temperature rise of the heat absorbing air. This effect is approximately compensated for over the tank temperature range 60° to 90° F. by the change with temperature of the slope of the resistance-temperature curve of the thermometers. This may be seen from the following considerations.

When gas of a constant composition is being burned in the calorimeter the temperature rise of the heat-absorbing air is given by the relation

$$\Delta t = k\left[\frac{D_g\left(1-\frac{p}{B}\right)}{C_a D_a\left(1-\frac{p}{B}\right)+C_w D_w}+e\right]$$

where the symbols are defined as follows:

Δt = temperature rise of the heat absorbing air.
D_g = density of the dry gas at the temperature of the tank and under the existing barometric pressure. (Since the composition of the gas is constant D_g depends only on temperature and pressure.)
D_a = density of dry air under the same conditions.
D_w = density of water vapor under saturation conditions at the temperature of the tank.
C_a = heat capacity of unit mass of air.
C_w = heat capacity of unit mass of water vapor.
B = barometric pressure.
p = vapor pressure of water at the temperature of the tank.
e = a term arising from the excess of water condensed over that formed by combustion.
k = a constant whose magnitude depends on the units used for the other quantities, and on the air-gas ratio.

The difference in resistance of the two thermometers will be given by

$$\Delta R = \frac{\Delta t \Delta R}{\Delta t} = k\left[\frac{D_g\left(1-\frac{p}{B}\right)}{C_a D_a\left(1-\frac{p}{B}\right)+C_w D_w}+e\right]\frac{\Delta R}{\Delta t}$$

where $\frac{\Delta R}{\Delta t}$ is the average change in resistance of the thermometers per degree between the initial and final temperatures of the heat-absorbing air. Since the total resistance of the slide wire (S, fig. 3) remains constant, the term

$$\left[\frac{D_g\left(1-\frac{p}{B}\right)}{C_a D_a\left(1-\frac{p}{B}\right)+C_w D_w}+e\right]\frac{\Delta R}{\Delta t}$$

must be a constant independent of the tank temperature if the calorimeter reading is to be independent of tank temperature.

The resistance-temperature relation of the outlet thermometer was determined by measuring its resistance when immersed in a stirred kerosene bath whose temperature was measured by a platinum-resistance thermometer. It was found that over the temperature range 60° to 135° F. the resistance of the thermometer could be expressed as a function of temperature by means of the quadratic equation.

$$R_t - R_{60} = 0.12520\ (t-60) + 0.00008562\ (t-60)^2$$

Observed values of resistance obtained in two series of measurements are compared in Table 3 with values computed from this equation.

TABLE 3.—*Resistance of outlet thermometer at various temperatures*

Temperature	$R_t - R_{60}$			
	Observed			Calculated
	First series	*Second series*	*Mean*	
°F.	*ohms*	*ohms*	*ohms*	*Ohms*
60	0.000	0.000	0.000	0.000
75	1.899	1.896 5	1.898	1.897
90	3.835	3.833	3.834	3.833
105	5.807	5.805	5.806	5.807
120	7.821	7.820	7.820 5	7.820
135	9.873	9.871 5	9.872	9.872

Calculated values of the difference in resistance of the inlet and outlet thermometers when the calorimeter is burning a gas having a heating value equal to 700 Btu per cubic foot under standard conditions are given in Table 4. The values used for the specific heat of

water vapor and air in calculating this table are 0.460 and 0.2401 Btu per pound per °F., respectively. Data on the density of air were taken from Bureau of Standards Circular No. 19, entitled "Standard Density and Volumetric Tables." Data on the properties of water vapor were taken from Keenan's steam tables. The relative densities of the gas were calculated on the assumption that the thermal expansion of gas is the same as that of air. The values of e given in Table 4 are the products of the values of

$$\frac{D_g\left(1-\frac{p}{30}\right)}{C_aD_a\left(1-\frac{p}{30}\right)+C_wD_w}$$

in the preceding column and the figures given in the last column of Table 1. The values of the temperature rise of the heat-absorbing air given in the next to the last column of Table 4 were calculated from the corresponding values of

$$\left[\frac{D_g\left(1-\frac{p}{30}\right)}{C_aD_a\left(1-\frac{p}{30}\right)+C_wD_w}+e\right]$$

on the assumption that the temperature rise of the heat-absorbing air is 42.45° when the tank temperature is 60° F. The values of ΔR in the last column were calculated from the corresponding values of Δt with the aid of the resistance-temperature relation given above. The maximum difference between any two values of ΔR in Table 4 is seen to be 0.4 per cent.

TABLE 4.—*Calculated difference in resistance of inlet and outlet thermometers for gas having a heating value of 700 B. t. u. per cubic foot*

Temperature of tank t	Vapor pressure of water p	Density of water vapor	Density of dry air	$C_aD_a\times\left(1-\frac{p}{30}\right)$	C_wD_w	$C_aD_a\times\left(1-\frac{p}{30}\right)+C_wD_w$
°F.	*in. Hg*	*Lbs./ft.*³	*Lbs./ft.*³	*Btu/ft.*³ °F.	*Btu/ft.*³ °F.	*Btu/ft.*³ °F.
60	0.522	0.000828	0.07656	0.018062	0.000381	0.018443
70	.739	.001151	.07511	.017590	.000529	.018119
80	1.032	.001578	.07372	.017091	.000726	.017816
90	1.421	.002134	.07238	.016555	.000982	.017537

Temperature of tank t	Density of dry gas D_g	$D_g\left(1-\frac{p}{30}\right)$	$\frac{D_g\left(1-\frac{p}{30}\right)}{C_aD_a\left(1-\frac{p}{30}\right)+C_wD_w}$	e	$\Delta t'_1$	ΔR
°F.	(*Relative*)				°F.	*Ohms*
60	1.0000	0.9826	53.27	−0.07	42.45	5.469
70	.9811	.9569	52.81	−.08	42.07	5.491
80	.9629	.9298	52.19	−.11	41.56	5.494
90	.9454	.9006	51.35	−.12	40.88	5.471

If the calorimeter reads correctly at full scale with the tank at any given temperature, and if the reading were proportional to the difference in resistance of the two thermometers then the calorimeter would read too low at points between zero and full scale due to the fact that the resistance temperature relation of the thermometers is not linear. The smooth curve in Figure 4 illustrates the relation which should exist between resistance and reading if the reading is to be proportional to temperature rise of the heat absorbing air rather than to difference in resistance of the two thermometers. The actual

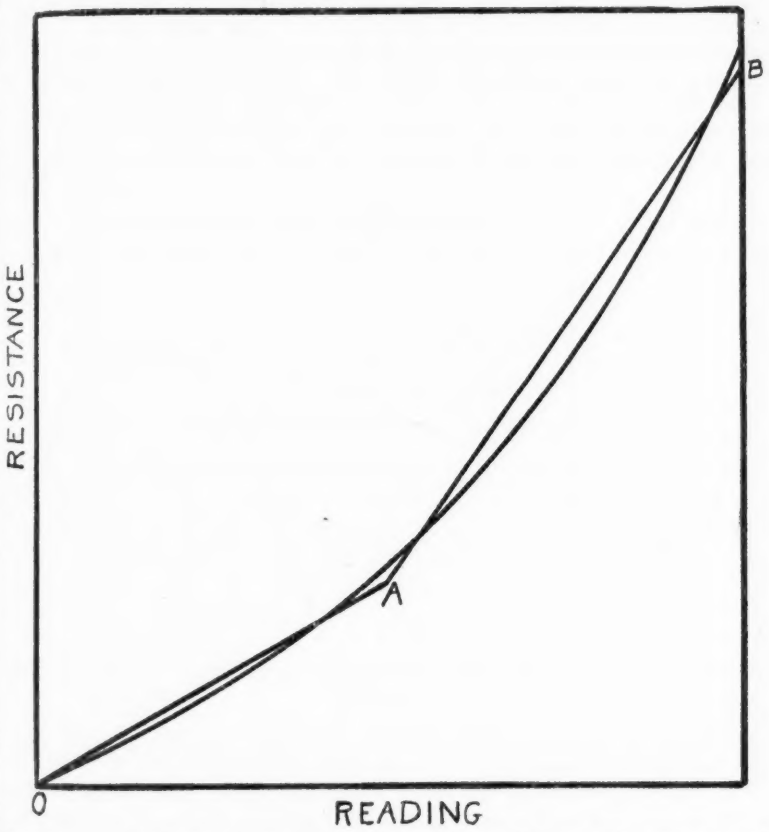

FIGURE 4.—*Illustrating theoretical relation between difference in resistance of thermometers and reading of calorimeter (smooth curve), and actual relation (straight lines OA and AB)*

resistance-reading curve is made to approximate the ideal relation illustrated by the smooth curve, by spacing the scale divisions closer together in the range from zero to half scale than in the range half to full scale. This gives a resistance-reading relation illustrated by the two straight lines, *OA* and *AB* (fig. 4).

To obtain the actual resistance-reading curve (*OA*, *AB*, fig. 4) the two thermometers (T_1 and T_2, fig. 3) were disconnected, and the resistance R_1 and slide wire were connected to a Wheatstone bridge with the battery lead connected to the sliding contact, *S*, as shown

in Figure 5. The recording pen was then set at various points on the recorder scale and the corresponding readings of the bridge were observed. These measurements were checked by a second method, suggested by representatives of the manufacturers. The inlet and outlet thermometers were disconnected, the inlet thermometer was replaced by a fixed resistance of about 50 ohms while the outlet thermometer was replaced by a resistance which could be varied by steps of 0.1 ohm from 50 to 60 ohms. The connecting leads were so adjusted that the recorder bridge was balanced at the zero of the scale for some particular value of the variable resistance. The variable resistance was then increased by any convenient amount, and the recording pen was moved along the scale until the recorder bridge was again balanced, when the reading of the recorder was observed. This procedure could be repeated for as many values of the variable resistance as desired. By both methods it was found that the change in the resistance of the outlet thermometer cor-

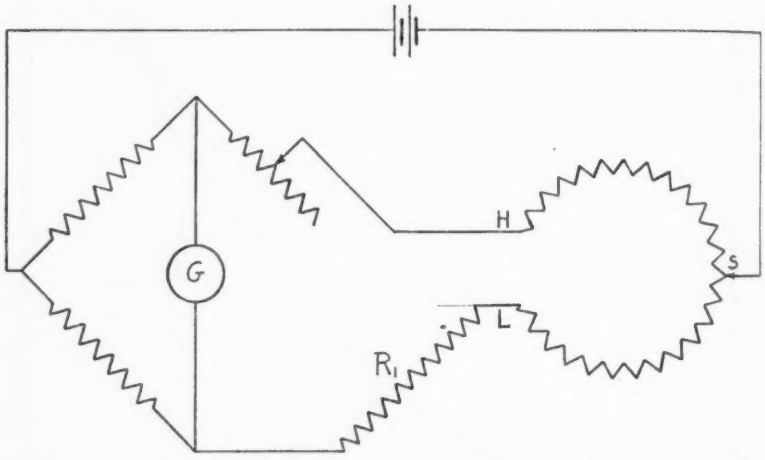

FIGURE 5.—*Bridge connections used in measuring actual resistance-reading relation*

responding to a movement of the recording pen from zero to full scale was 5.476 ohms.

The results obtained by both methods are shown graphically in Figure 6, in which are plotted the deviations of the observed resistances from a straight line through the points *O* and *B* of Figure 4. The circles and crosses in Figure 6 represent observations by the first and second methods, respectively. It is seen that there is no appreciable systematic difference between the two sets of observations. There is a slight systematic deviation of the observed points from the straight line *OA* in the range from zero to half scale.

Figure 7 shows the deviations from a straight line through the points *O* and *B* (fig. 4) of the actual resistance-reading curve *OAB* and of calculated resistance-reading curves for tank temperatures of 60°, 70°, 80°, and 90° F. Data for the calculated curves were deduced from the resistance-temperature equation for the thermometers on the assumption that the temperature rise of the heat-absorbing air for a gas having a heating value of 700 Btu per cubic foot is that

given in the next to the last column of Table 4, and that temperature rise for a given tank temperature is proportional to heating value of the gas. The temperature rise given in Table 4 for a tank tempera-

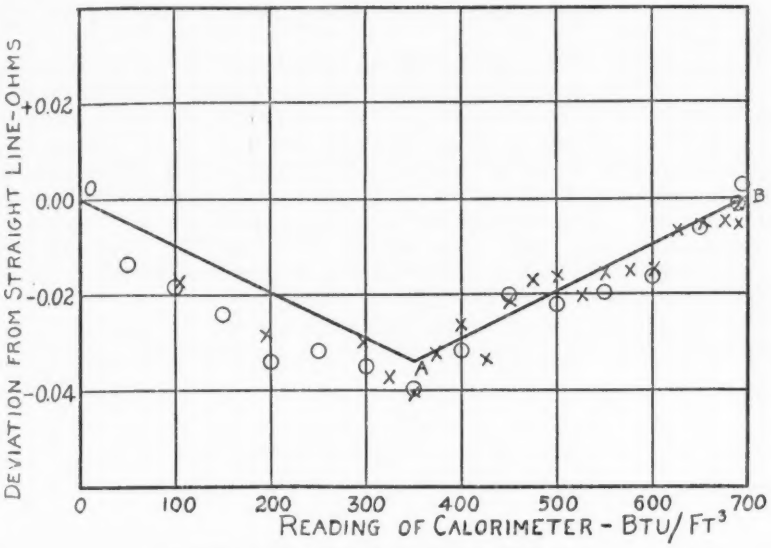

FIGURE 6.—*Calibration curve of slide wire*

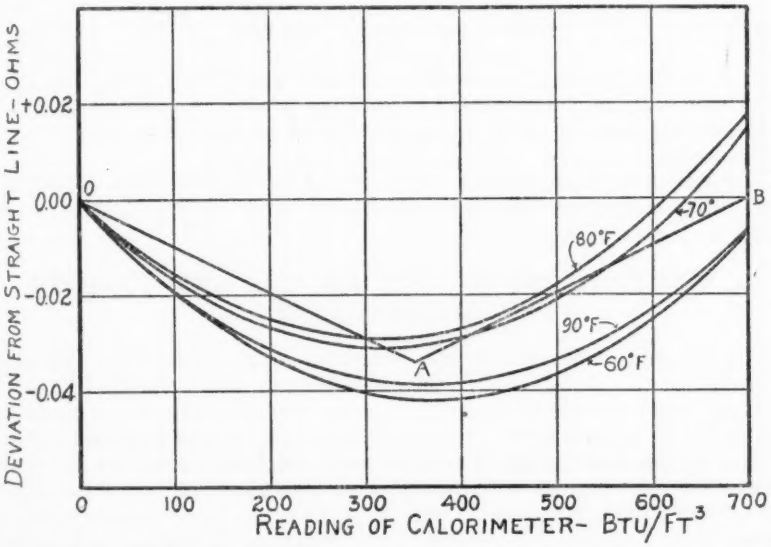

FIGURE 7.—*Deviation from straight line of actual resistance-reading curve (straight lines OA and AB), and calculated curves for 60°, 70°, 80°, and 90° F.*

ture of 60° F. was so chosen that the calculated curve for 66° crosses the straight line *AB* at 610 Btu. The calculated curves of Figure 7 therefore correspond to a calorimeter adjusted to read correctly at 610 Btu. when the tank temperature is 66° F. A calorimeter so

adjusted would read somewhat too high at tank temperatures between 66° and about 85° F. and somewhat too low at tank temperatures below 66° and above 85° F. The maximum difference between the straight line *AB* and the calculated curves in the range from half to full scale is 0.018 ohms, which corresponds to about 2 Btu per cubic foot.

The positions of the calculated curves relative to the actual curve, *OA* and *AB*, will depend on the tank temperature at which the calorimeter is adjusted to read correctly. For example, if the calorimeter is adjusted to read correctly at 610 with the tank at 80° F., then the calculated curve for 80° F. will cross the straight line *AB* at 610, and the other calculated curves will be lowered at this point by about the same amount. The calorimeter would then read low at all temperatures except in the range from about 75° to 80° F. The condition represented by the curves of Figure 7 is approximately the condition which the manufacturers attempt to realize.

The effect of varying barometric pressure on the reading of the calorimeter may be obtained by differentiating the expression.

$$\frac{D_g\left(1-\frac{p}{B}\right)}{C_a D_a\left(1-\frac{p}{B}\right)+C_w D_w}$$

with respect to B. When this is done, and the proper numerical values substituted in the expression for the derivative, it is found that the change in reading for 1 inch change in barometric pressure is less than 0.01 per cent for any tank temperature between 60° and 90° F.

Representatives of the manufacturers have stated that it is their practice to adjust calorimeters to read as nearly as possible correctly at the prevailing barometric pressure of the locality in which they are to be used.

The effect of atmospheric humidity is eliminated because all gas and air passing through the calorimeter are saturated with water vapor in the meters.

V. COMPARISONS OF THE THOMAS AND JUNKERS CALORIMETERS

The Thomas calorimeter was installed in the chemistry building of this bureau late in 1926. The installation was inspected by U. O. Hutton, representing the manufacturers, who also ran an air-gas ratio test and a hydrogen test. The hydrogen used in this test and in most of the subsequent hydrogen tests was obtained from the low-temperature laboratory of this bureau and was 99.98 per cent pure. In one of the hydrogen tests hydrogen from this source was used alternately with hydrogen produced by the action of water on hydrone, an alloy of sodium and lead. No difference was observed in the reading of the calorimeter depending on which sample of hydrogen was being burned.

Numerous comparisons of the Thomas calorimeter with Junkers calorimeters were made in 1928, 1929, and 1931. The gas used in these comparisons was drawn from the Washington city gas mains,

and was stored in a holder in order to obtain gas of constant composition for the tests. Before January, 1931, this gas was a carbureted water gas; after that time it was a carbureted water gas enriched with natural gas. The heating value of the gas varied from about 510 to 620 Btu per cubic foot.

Two Junkers type calorimeters were used at different times. One of these was an original type Junkers (No. 1209) which had been investigated by Waidner and Mueller,[12] and the other a Hinman-Junkers (No. 724) which had been tested by comparison with No. 1209.

The Junkers calorimeters were operated in accordance with directions given in Bureau of Standards Circular No. 48, entitled "Standard Methods of Gas Testing." The 0.1 cubic foot meter used with the Junkers calorimeters was calibrated frequently by means of a 0.1 cubic foot bottle, following the procedure described in Circular 48. Several sets of mercurial thermometers were used, all of which had been calibrated by the thermometry section of this bureau. The differential corrections for these thermometers were determined at frequent intervals during the investigation.

The Thomas calorimeter was operated in accordance with directions given in the instruction book furnished by the manufacturers. The periodic care recommended in this instruction book was given regularly.

The results of the comparisons with the Junkers calorimeter are summarized in Table 5. It is seen from this table that the two instruments nearly always agreed within 1 per cent,[13] which is the accuracy guaranteed for the Thomas calorimeter by the manufacturers. In only 1 of the 43 comparisons listed in Table 5 did the difference exceed 1 per cent. On the average, the results obtained with the Thomas calorimeter were higher than those obtained with the Junkers calorimeter by 0.35 Btu. per cubic foot, or less than 0.1 per cent.

Hydrogen tests were made at various times during the investigation. It was found that the reading of the calorimeter depended somewhat on the current used in the bridge circuit of the recorder. Thus with the trickle charger (2.2 volts) the reading during the hydrogen tests was always 612, while with dry cells (1.5 volts) the reading was always 610. The reading was also 2 Btu. higher with the trickle charger than with dry cells when illuminating gas was being burned in the calorimeter.[14]

The results on illuminating gas given in Table 5 were obtained with dry cells furnishing the bridge current. They therefore correspond to a reading of 610 in the hydrogen test instead of the design value

[12] See footnote 1, p. 99.

[13] In some of the preliminary measurements the Thomas calorimeter readings were systematically higher than the Junkers results by about 1.5 per cent. This difference was apparently due to not allowing sufficient time for the water in the 0.1 cubic foot meter used with the Junkers calorimeter to become thoroughly saturated with gas. The results obtained in investigating this point indicate that about 15 or 20 cubic feet of carbureted water gas must be passed through the meter at the rate of 5 cubic feet per hour to thoroughly saturate the water. With the present Washington city gas, which is carbureted water gas enriched with natural gas, the lowering in heating value due to fresh water in the meter was about 1 per cent. About 10 cubic feet of gas must be passed through the meter to saturate the water. This is not in accord with the results obtained by Waidner and Mueller (footnote 1, p. 99), who report that the effect, due to fresh water in the meter, on the observed heating value of a gas was of the order of 0.5 per cent and that the water was practically saturated, so far as calorimetric measurements were concerned, after the passage of 2 or 3 cubic feet of gas. Some results obtained recently by members of the gas chemistry section of the bureau indicate that part of the difference originally observed between the Junkers and Thomas calorimeters may have been due to selective absorption of constituents of the gas by rubber tubing.

[14] A different type of rectifier is now furnished with the Thomas calorimeter. One of these new rectifiers has been installed recently in the calorimeter at this bureau, and it is found that the reading of the calorimeter is practically the same with the rectifier as with the dry cells.

612. If the trickle charger had been used, or if the calorimeter had been adjusted so as to read 612 on the hydrogen test with dry cells, it seems probable that the readings on illuminating gas would have been higher by 2 Btu, or, on the average, 2.35 Btu higher than the results obtained with the Junkers calorimeter.

TABLE 5.—*Comparisons of the Thomas and Junkers calorimeters on illuminating gas*

Date	Heating value of gas		Difference, Thomas minus Junkers	Date	Heating value of gas		Difference, Thomas minus Junkers
	Thomas	Junkers			Thomas	Junkers	
1928	*Btu/ft.*³	*Btu/ft.*³	*Btu/ft.*³	1929	*Btu/ft.*³	*Btu/ft.*³	*Btu/ft.*³
May 18	540	539	+1	Feb. 21	561	561	0
Do	542	539	+3	Feb. 23	555	555	0
May 19	537	537	0	Feb. 25	572	575	−3
June 19	583	579	+4	Feb. 26	568	564	+4
June 21	573	571	+2				
June 27	566	562	+4	Feb. 27	570	570	0
				Feb. 28	567	564	+3
1929				Mar. 1	565	564	+1
Feb. 5	520	528	−8	Mar. 2	560	562	−2
Feb. 7	513	513	0	Mar. 20	510	509	+1
Do	513	513	0				
Feb. 8	509	506	+3	Mar. 21	613	619	−6
Do	510	507	+3	Mar. 22	559	560	−1
				June 3	558	557	+1
Feb. 11	593	591	+2	June 6	556	555	+1
Feb. 13	593	593	0				
Do	592	592	0	1931			
Feb. 14	583	583	0	July 27	611	608	+3
Feb. 19	568	570	−2	July 28	607	607	0
				July 31	610	608	+2
Do	568	568	0	Aug. 4	605	607	−2
Do	569	571	−2				
Feb. 20	565	563	+2	Aug. 7	606	606	0
Do	565	565	0	Aug. 12	550	550	0
Do	564	564	0	Aug. 13	550	552	−2
Feb. 21	561	558	+3	Aug. 17	569	569	0

Thus the results of the calculations given in Section III of this paper, which indicate that it is better to use 320.6 Btu per cubic foot for the heating value of hydrogen in standardizing the Thomas calorimeter, are not confirmed by the experimental results. The experimental results indicate that it is better to use 319.3 Btu per cubic foot, which is practically identical with the value obtained by Rossini. The difference is about 0.4 per cent, which is well within the accuracy guaranteed for the Thomas calorimeter and not much greater than the uncertainty of the results obtained with the Junkers calorimeter.

Although the manufacturers guarantee an accuracy of only 1 per cent for the Thomas calorimeter they believe that if properly adjusted and given the periodic attention which they recommend, it will give results which are accurate within 0.4 per cent. The results obtained in comparisons with the Junkers calorimeter indicate that the Thomas calorimeter may be expected to give results which are at least precise within 0.4 per cent, since in only 12 of the 43 comparisons did the difference between the results obtained with the two calorimeters exceed that amount. These comparisons, however, indicate that if the Thomas calorimeter had been adjusted to read 612 instead of 610 in the hydrogen test, there would have been a systematic difference of 0.4 per cent between the Thomas and Junkers calorimeters. It is obviously impossible to decide from these comparisons whether the Thomas calorimeter, when adjusted to read 612 in the hydrogen test,

gives results which are too high by 0.4 per cent on the average, or whether the Junkers calorimeter results are too low by the same amount, or whether part of the difference should be charged to each calorimeter. All that can be said is that the two instruments agreed within the combined experimental errors.

VI. HEATING VALUES OUTSIDE THE USUAL WORKING RANGE

The data given in Table 5 were obtained on samples of gas having heating values ranging from about 510 to 620 Btu per cubic foot. This is probably the usual working range of the Thomas calorimeter having the range 0 to 700 Btu per cubic foot. It is of interest, however, to have data on the performance of the instrument over other parts of the range. Such data might have been obtained by comparisons with the Junkers calorimeter, using gases of various heating values. It was simpler, however, to use a gas of constant heating value and vary the speed of the gas meter. This could be done by changing some of the gears in the gear train between the driving motor and the gas meter. Table 6 shows data obtained in this way with hydrogen and illuminating gas.

TABLE 6.—*Effect of changing speed of gas meter in the Thomas calorimeter*

Gas	Relative speed of gas meter	Reading of Thomas calorimeter	Calculated reading
Hydrogen	1	612	----------
	$3\frac{3}{64}$	374	374
	$1\frac{1}{21}$	321	321
Illuminating gas	1	550	----------
	$2\frac{1}{36}$	321	322
	$2\frac{1}{18}$	643	643
	$2\frac{1}{45}$	256	257
	1	553	----------

The figures in the column headed "calculated reading" were obtained from the average reading when the speed of the gas meter was 1 on the assumption that the reading should be proportional to speed. The agreement between the actual and calculated readings indicates that the calorimeter should give satisfactory results in the range covered, although the manufacturer's guaranty of 1 per cent accuracy holds only from half to full scale.

Thomas calorimeters having different ranges are practically identical with the one investigated here except that the delivery rates of the gas meters are different. The necessary changes were made in the 0 to 700 range instrument at this bureau to change the range to 0 to 3,000, and two comparisons with the Junkers calorimeter were made on commercial propane. The net heating value of the gas was determined by means of the Junkers calorimeter, and the total heating value calculated from the net on the assumption that the gas was pure propane. The results obtained are shown in Table 7. The agreement is seen to be within about 0.3 per cent.

TABLE 7.—*Comparison of Thomas and Junkers calorimeters on propane*

Date	Test No.	Thomas	Junkers	Difference Thomas-Junkers
Aug. 21, 1931	1	2,481	2,479	
	2	2,481	2,473	

VII. LAG OF THE THOMAS CALORIMETER

The comparisons of the Thomas and Junkers calorimeters described in the preceding section were made on gas drawn from holders, and therefore having approximately constant heating value. The comparisons were made after the calorimeters had been operating on this gas for a sufficiently long time so that the results were not affected by lag. When operating on gas whose heating value changes with time the reading of the calorimeters will lag behind the heating value of the gas. The lag of the Thomas calorimeter depends on four factors, namely, (*a*) the time required for gas to flow from the point at which it enters the calorimeter to the burner; (*b*) the thermal lag; that is, the lag of the heated metal parts of burner and jacket and of the outlet thermometer; (*c*) mechanical lag, that is, the lag of the recording mechanism; (*d*) lag due to change in the amounts of the various constituents of the gas which are dissolved in the water in the gas meter.

The magnitudes of (*b*) and (*c*) may be inferred from Figure 7 which is the record obtained during a hydrogen test. At *A* and *B* the recording pen was moved from its equilibrium position and then allowed to return. The time required is a measure of the mechanical lag, which is seen to be negligibly small, although in some cases the pen stops at about 1 Btu from its equilibrium position and remains there for some time.

The combined effect of thermal and mechanical lag is illustrated in that part of the curve from *C* to *D* (fig. 7). When the burner was extinguished at *C* the recording pen moved to the zero of the scale along the curve *CD*. Ninety per cent of the change had taken place in 4.2 minutes.

The combined effect of all of the lags was determined as follows: The calorimeter was connected through a 3-way stop-cock to the gas mains and to a holder containing gas which had been diluted with nitrogen. Gas could then be drawn either from the mains or from the holder. Figure 8 shows the record obtained when the calorimeter was switched from gas from the mains to gas from the holder. It was 4.5 minutes after switching to the holder gas before the first indication of a change in heating value was observed, and 6.5 minutes more before 90 per cent of the change had taken place. Practically the same results were obtained when the calorimeter was switched from the gas of lower heating value to that of higher heating value.

It is not possible from these observations to determine each of the factors (*a*) and (*d*) separately. For example, when the first change in heating value is observed after switching from one gas to another, it is probable that all of the original gas has not been swept out of the mixing chamber, and therefore the time required for all this original gas to be swept out is greater than 4.5 minutes.

While the lag would cause an error in the values recorded by the calorimeter if the heating value of the test gas was changing, the effects of lag would tend to balance out in the average heating value calculated from records over considerable periods of time.

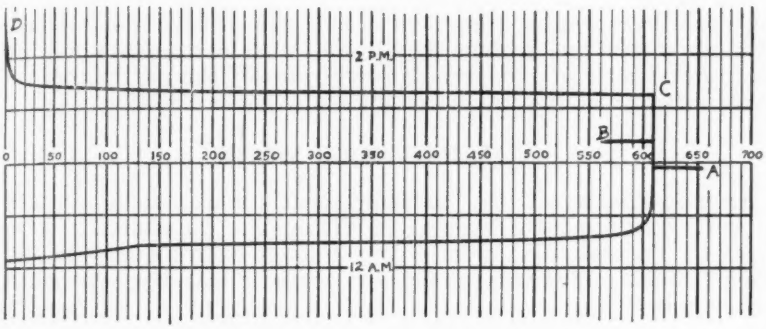

FIGURE 8.—*Record made during a hydrogen test*

The time required for gas to flow from the point at which it enters the calorimeter to the burner will be different for different range calorimeters on account of the different speeds of the gas meters. According to measurements made by the manufacturers the time interval

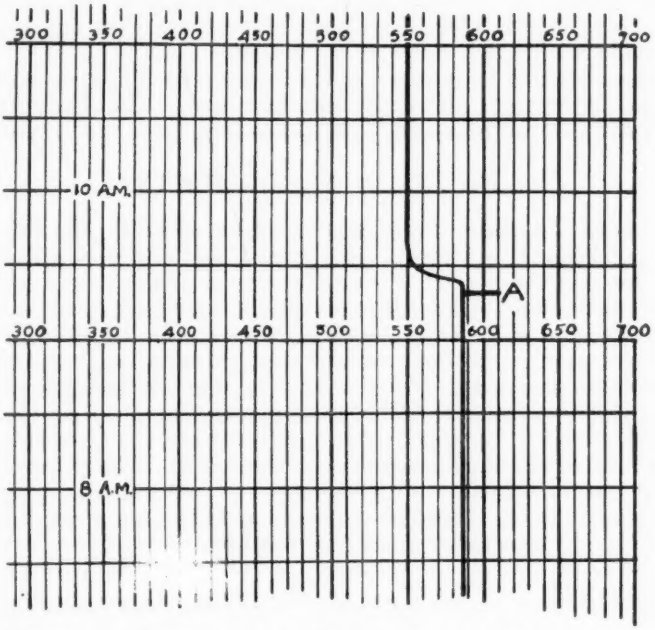

FIGURE 9.—*Record made in determining the lag of the Thomas calorimeter*

between turning off the gas and the first indication of a change in heating value of the gas varies from 1.5 minutes for the 0 to 150 range calorimeter to 8.5 minutes for the 0 to 2,100 range calorimeter.

The thermal lag of the 0 to 150 range instrument is greater than that of any of the higher range instruments. This is due to the fact that it is necessary to preheat the gas in order to get it to burn satisfactorily, and the preheating device greatly increases the heat capacity of the burner.

Calorimeters having ranges of 0 to 1,800 or higher are provided with larger mixing chambers than lower range instruments in order to damp out fluctuations in the delivery rates of the gas meters. The larger mixing chamber increases the lag to some extent.

VIII. PREVIOUS WORK

An investigation of the Thomas calorimeter was made in 1923 by R. A. Ragatz [15] at the University of Wisconsin. He made 24 comparisons of a Thomas calorimeter with a Junkers calorimeter. In all but three of these comparisons the results obtained with the two calorimeters agreed within 1 per cent. His measurements of the lag of the Thomas calorimeter were in good agreement with those described here. He found, when the Thomas calorimeter was operating on gas of a constant heating value, that a sudden decrease in room temperature of 34° F. caused a lowering of 4 Btu per cubic foot in the reading.

A Thomas calorimeter, manufactured in England, and differing in some details from the one studied at this bureau, has been investigated by Blackie, Ockelford, Baker, and Hales.[16]

The accuracy of the instrument was investigated by comparing it with a Boys calorimeter, and the authors state that the agreement was usually within ±1 Btu per cubic foot.

Results obtained in measuring the lag of the Thomas calorimeter are in good agreement with those obtained here. The effect of changes in gas pressure, motor speed, and water level were also investigated.

IX. ACKNOWLEDGMENTS

This work was done under the direction of E. F. Mueller, of the heat measurements section of this bureau, and the author is indebted to him for valuable advice during the course of the work. Acknowledgment is due to Cutler-Hammer (Inc.), for the loan of a Thomas calorimeter, and to U. O. Hutton, E. X. Schmidt, and T. M. Gilbert, of that company, who have contributed valuable suggestions during the course of the work. The work was done in the gas chemistry section of this bureau and the author is indebted to E. R. Weaver and J. H. Eiseman of that section for the use of the laboratory facilities and for advice and assistance in the work. The comparisons of the Thomas calorimeter with the Junkers calorimeter during 1929 were made by S. A. Guerrieri who was at that time a member of the staff of the gas chemistry section of the bureau.

---

[15] Thesis, unpublished.

[16] Department of Scientific and Industrial Research of Great Britain. Fuel Research Technical Paper No. 20, 1927.

X. CONCLUSION

It may be concluded from the results obtained in this investigation that the Thomas calorimeter can be used to measure total heating values of gases with an accuracy well within 1 per cent, provided the calorimeter is given the necessary care, and provided the heating value of the gas does not vary rapidly. If the heating value of the gas varies with time the recorded readings of the calorimeter will be in error due to lag by an amount depending on the rapidity of the variation. The average reading over considerable periods of time will be unaffected by lag.

WASHINGTON, November 16, 1932.

COMPRESSIVE STRENGTH OF STEEL COLUMNS INCASED IN BRICK WALLS

By Albert L. Harris, A. H. Stang, and J. W. McBurney

ABSTRACT

Three H–shaped steel columns, 23 feet long, 6 inches in depth, weighing 20 pounds per foot, and having flat ends, were tested in compression. Six similar columns, incased in brick walls 14 inches thick, 6 feet long, and carried up to about 8 inches from the top of the columns, were also tested in compression. The six incased columns were divided into two groups of three each depending on the orientation of the steel column in the brick wall.

Compressometer and deflection measurements were made on all columns.

The incased columns were much stronger than the bare specimens. The increase in strength may arise from two different causes. The load may be partially transferred from the steel to the incasement by the bond between them. Added strength from this cause might be expected in columns of any length. Long columns when laterally unrestrained fail by bending at loads much smaller than the yield strength of the steel. Incasement of long columns would act as a continuous lateral restraint which might be sufficient to prevent the lateral bending and cause the columns to fail in the same manner as short columns at much higher loads.

The compressometer readings over a 150-inch gage length centered at mid-height showed that the steel in the incased columns was stressed, on the average, less than 20 per cent as much as was the steel in the bare columns for the same load. The lateral deflection of the incased columns was very small and the brick-work was not appreciably affected by the tests.

CONTENTS

	Page
I. Introduction	123
1. Purpose	123
2. Acknowledgments	124
II. The specimens	126
III. Testing procedure	127
1. The bare and the incased columns	127
2. Auxiliary tests	128
(*a*) The steel coupons	128
(*b*) The short lengths of steel columns	128
(*c*) The bricks	128
(*d*) The mortar	128
IV. Results and discussion of the tests	129
1. Auxiliary tests	129
2. The bare and the incased columns	131
V. Conclusions	138

I. INTRODUCTION

1. PURPOSE

The engineer department, Government of the District of Columbia, Washington, D. C., requested the Bureau of Standards to test 9 steel columns, 3 bare and 6 incased in brick walls, to determine the relative

strengths of the bare and the incased columns. The purpose of the tests was to determine whether for design purposes, the strength of steel columns incased in brick walls should be calculated by considering them as long, bare columns which would fail by bending at low loads or whether the brick walls could be relied upon to restrain the lateral bending and enable them to carry the higher loads which short columns of the same material would carry.

2. ACKNOWLEDGMENTS

The incasement for the steel columns was designed by Albert L. Harris, municipal architect, and H. H. Marsh, chief of the structural division, engineer department, Government of the District of Columbia. The steel columns were donated by the Bethlehem Steel Co. The cost of incasing the columns in brick walls was borne by the Washington division, Common Brick Manufacturers' Association of America, Jordan A. Pugh, district manager.

The tests of the columns were made in the engineering mechanics section, of the Bureau of Standards, under the direction of H. L. Whittemore.

II. THE SPECIMENS

The nine steel columns were 6-inch, 20-pound Bethlehem H-sections. The nominal dimensions and section properties of the steel columns are given in Table 1. The ends of each column were machined with a face mill to give a nominal column length of 23 feet. After the columns were tested, a short length of each steel column was weighed and the length measured. The cross-sectional area of this short length was computed on the assumption that 1 cubic inch of steel weighs 0.283 pound. This value was taken as the cross-sectional area of the steel column.

TABLE 1.—*Nominal dimensions and sectional properties of the steel columns*

Weight per foot	pounds	20
Depth	inches	6.00
Flange width	do	6.00
Web thickness	inch	.25
Area	square inches	5.89
Least moment of inertia, centroidal axis parallel to web	in.^{4}	13.5
Least radius of gyration, centroidal axis parallel to web	inch	1.51
Greatest moment of inertia, centroidal axis perpendicular to web	in.^{4}	32.2
Greatest radius of gyration, centroidal axis perpendicular to web	inch	2.58
Length	feet	23
Slenderness ratio		183

The steel columns which were tested without the brick incasement were designated as columns 1, 2, and 3.

Six of the steel columns were incased in brick walls as shown in Figures 1 and 2. The nominal dimensions of the walls were as follows: Thickness 14 inches, length 6 feet, and height 22 feet 4 inches.

Previous tests on sturdy columns of this length indicated that these incased columns might be compressed 6 inches before the maximum compressive strength was obtained. The distance between the top of the wall and the upper end of the steel column was about 8 inches to allow the maximum load on the steel column to be determined before the upper platen of the testing machine came into contact with the top of the wall. This unincased length of the steel columns above

the walls was greater than would be likely to occur in an actual structure. The actual unincased lengths and the heights of the walls are given in Table 5. The unincased lengths varied from 7½ to 11 inches. For the three incased columns, designated A1, A2, and A3, the web of the steel column was perpendicular to the face (length) of the wall; and for the three designated as B1, B2, and B3, it was parallel to the face. (Fig. 2.)

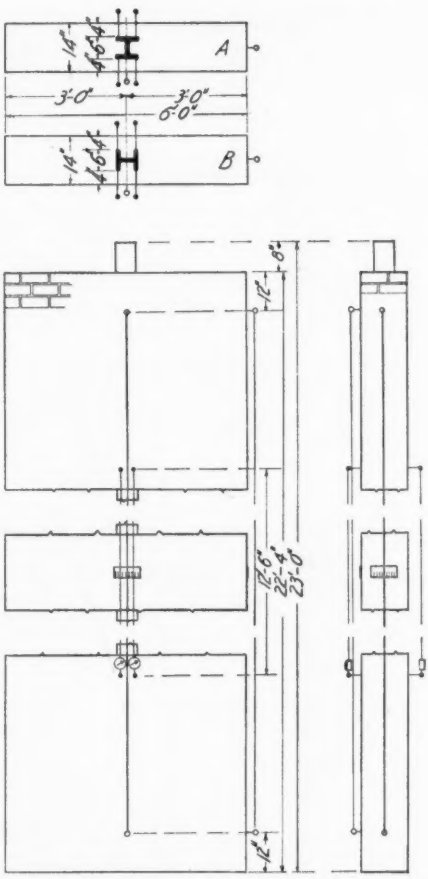

FIGURE 1.—*Incased columns showing nominal dimensions and the apparatus for measuring the compression and lateral deflection*

The bricks were made in Virginia from surface clay by the semidry press process. The mortar was composed of 1 part of Portland cement to 3 parts of damp sand, by volume. Hydrated lime was added equal to 10 per cent of the cement, by weight. The proportions by weight were 1 part cement, 0.1 part lime to 2.34 parts dry sand.

The steel columns were secured in a vertical position on the floor of the laboratory and plumbed before the brick walls were built. The bricks were laid on smooth, horizontal mortar beds and with full-shoved vertical joints. Every fifth course was a header course. The

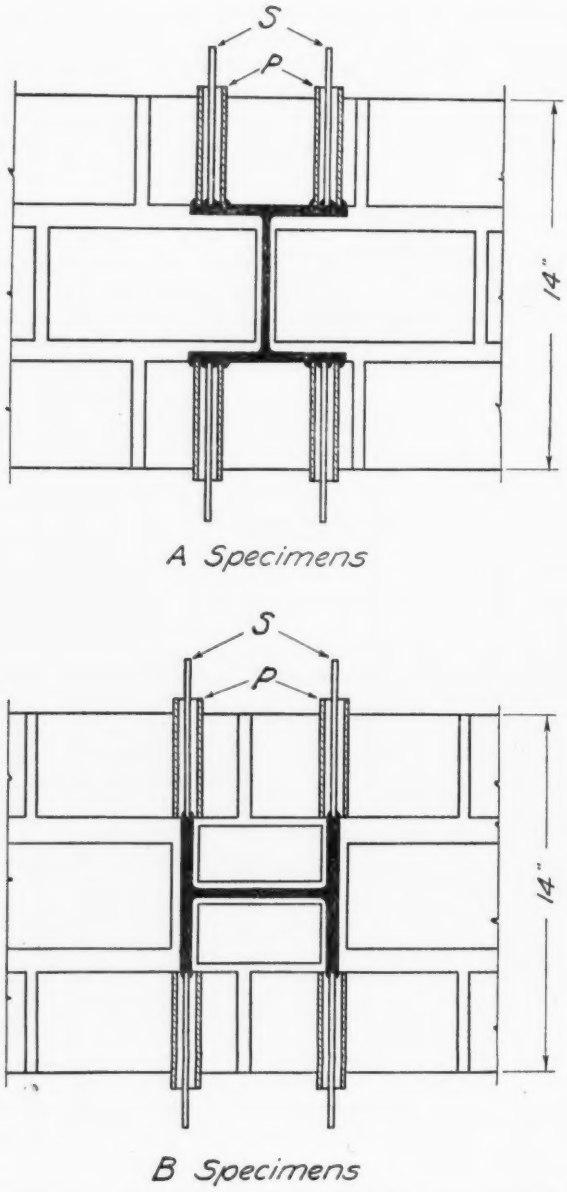

FIGURE 2.—*Cross sections of the incased columns showing the orientation of the steel columns and the bonding of the brick*

The section is taken through the supports for the compressometers to show the method of attaching them to the columns

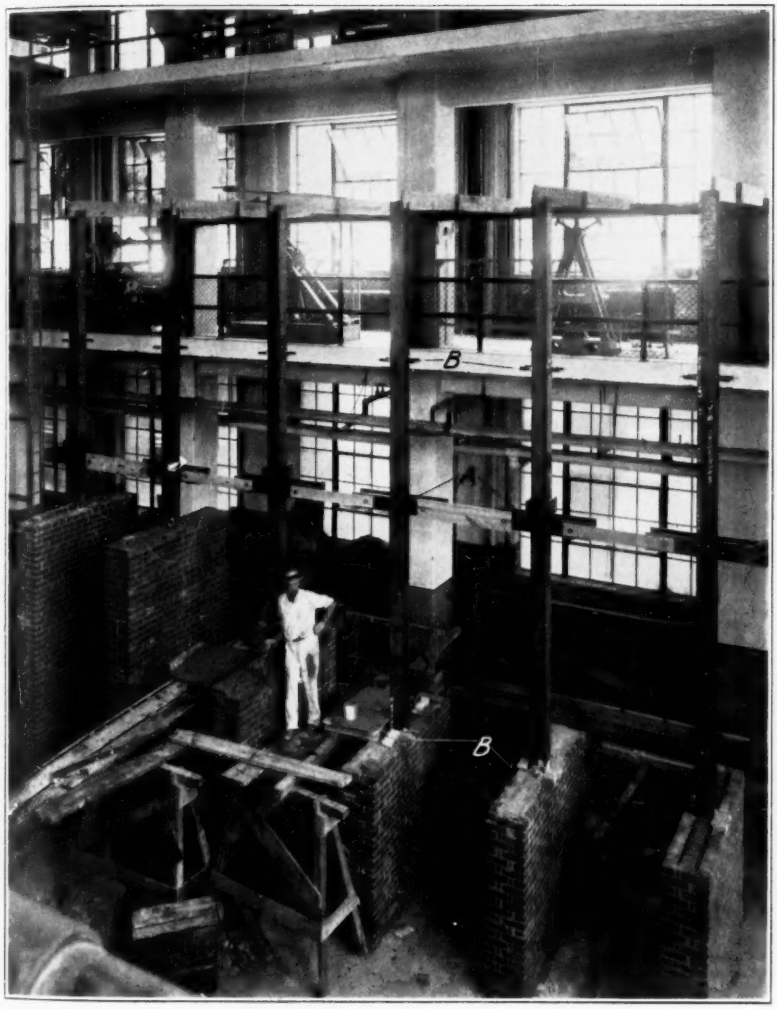

FIGURE 3.—*Incased specimens during construction*

A, The lifting plates; *B*, the compressometer supports.

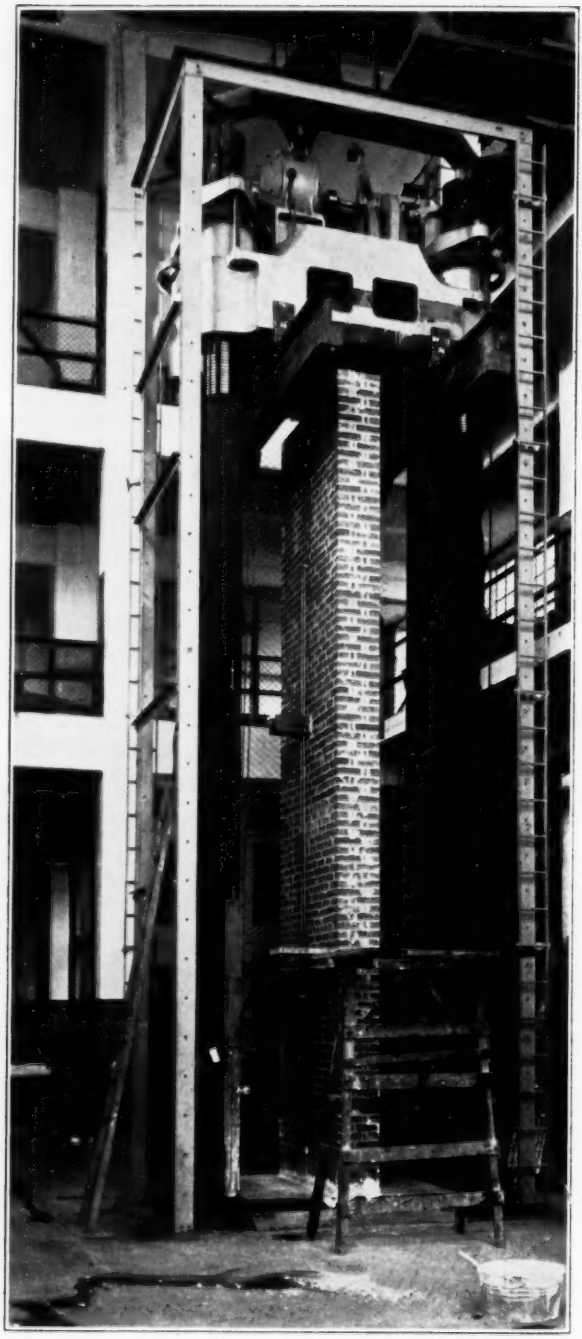

FIGURE 4.—*Incased column B3 in the testing machine before test*

bricks were carefully fitted between the flanges of the steel columns, and the spaces between the bricks and the column were grouted with the mortar mixed with additional water.

The incased columns during construction are shown in Figure 3. The steel plates, shown at *A*, were bolted to the steel column about 10 feet from the top. They projected from the face of the wall as shown in Figure 4 and were used to lift the incased columns from the floor and place them in the testing machine. The incased columns were tested about 30 days after the completion of the walls.

III. TESTING PROCEDURE

1. THE BARE AND THE INCASED COLUMNS

All the columns were tested as flat-end columns in a vertical, hydraulic testing machine having a capacity of 10,000,000 pounds. Steel plates, 8 inches square and one-half inch thick, were placed between each end of the columns and the platens of the testing machine. For the incased columns, therefore, there was a ½-inch space between the bottom of the brick wall and the lower platen. This space was filled with a mixture of plaster of Paris and water, the plaster being allowed to harden before the loads were applied.

The shortening of the columns under load was measured with four compressometers having a gage length of 12 feet 6 inches. The rods of the compressometers actuated dial micrometers graduated to 0.001 inch. Readings were estimated to one-tenth of a division. On the bare columns the middle of the gage length was at the middle of the column. The compressometers were attached by studs screwed into the outside surfaces of the flanges, one near each edge. On the incased columns (fig. 1) they were attached to rod supports welded to the flanges, as shown at *S*, Figure 2, and *B*, Figure 3. Pieces of pipe surrounded the rods and were welded to the flanges, as shown at *P*, Figure 2, so that the compressometer supports were not in contact with the brickwork. After the column had been set in place and the compressometers attached, the lower platen of the testing machine was adjusted in its spherical seat until, at low loads, the compressometer differences for the bare columns were all within 10 per cent of the average compression. For the incased column A1, these differences were 32 per cent. For the other incased columns, they did not exceed 16 per cent.

The lateral deflections of the columns at midheight were measured by the taut-wire mirror-scale method. The scales were graduated to 0.1 inch and readings were estimated to one-tenth division.

On the bare columns three wires were used. They were attached 6 inches from each end of the column by studs screwed into the middle of each flange and the middle of one side of the web. On the incased columns (fig. 1), two wires were used, attached 12 inches from the top and bottom of the wall to steel supports built into the wall.

2. AUXILIARY TESTS

(a) THE STEEL COUPONS

As large differences were to be expected between the strength of the bare and the incased columns, it was not felt necessary to test as many coupons as would be required in the case of column tests planned to determine small differences in column strength caused by differences in construction.[1] Only two coupons were, therefore, taken from each steel column. Since no extra lengths of the columns were furnished, one coupon was cut from the flange and the other from the web of the column, after test, the portion being used which was considered to have been subjected to the lowest stress during the column tests. The coupons from the bare column were cut from the region of the contraflexure and those from the incased columns from the lower end. They were A.S.T.M. type specimens having a gage length of 8 inches and a reduced width of 1½ inches. They were tested in a screw-power, beam-and-poise testing machine having a capacity of 100,000 pounds. The yield point was obtained from the "drop of the beam" of the testing machine.

(b) THE SHORT LENGTHS OF STEEL COLUMNS

Lengths equal to the unincased length of the columns were cut from each of the incased columns after test. These short lengths were cut from the lower end next to the lengths from which the coupons were taken. The ends were milled perpendicular to the axis of the sections and the maximum compressive strength determined by loading them between hardened steel plates in a screw-power, beam-and-poise testing machine having a capacity of 600,000 pounds. The compressive strengths were computed by dividing the maximum load by the computed cross-sectional area of the steel column from which the length was cut.

(c) THE BRICKS

Twenty-five bricks were selected at random and tested in accordance with Federal specification No.504 for brick, clay, common.

(d) THE MORTAR

Each working day a sample of the mortar was taken and the flow value determined in accordance with paragraphs F–3g(3) *a* and *b* of Federal specification No. SS–C–181 for cement, masonry. Six cylindrical specimens (diameter 2 inches, length 4 inches) were made from each sample. Three of these cylinders were stored in water and the compressive strength determined after 28 days. The other three cylinders were stored in air in the laboratory and the compressive strength determined on the day the incased column which they represented was tested.

---

[1] L. B. Tuckerman and A. H. Stang, Tests of Large Columns with H-Shaped Sections, B. S. Tech. Paper No. 328, Oct. 20, 1926.

IV. RESULTS AND DISCUSSION OF THE TESTS

1. AUXILIARY TESTS

The results of the tensile tests of the steel coupons are given in Table 2. The average values for each group of columns do not show any important differences in the properties of the steel in the steel columns. The tensile strength of some of the steel coupons was less than the minimum value specified in A. S. T. M. standard specification for structural steel for buildings, designation A9–29.

TABLE 2.—*Properties of steel coupons*

Specimen		Thickness	Yield point	Tensile strength	Elongation in 8 inches
From column—	Cut from—				
		Inch	*Lbs./in.²*	*Lbs./in.²*	*Per cent*
1	Flange	0.340	38,300	54,600	31.2
1	Web	.278	47,200	56,700	29.4
Average			42,800	55,600	30.3
2	Flange	.350	45,300	54,200	34.5
2	Web	.278	49,700	58,900	30.9
Average			47,500	56,600	32.7
3	Flange	.350	37,000	53,900	30.5
3	Web	.277	47,100	54,400	34.2
Average			42,000	54,200	32.4
A1	Flange	.332	40,200	54,800	33.9
A1	Web	.275	42,000	55,500	30.8
Average			41,100	55,200	32.4
A2	Flange	.348	38,600	55,200	33.1
A2	Web	.280	39,400	55,100	32.0
Average			39,000	55,200	32.6
A3	Flange	.345	39,100	54,900	31.7
A3	Web	.283	41,100	55,000	32.5
Average			40,100	55,000	32.1
B1	Flange	.375	39,600	55,000	29.2
B1	Web	.285	38,500	54,500	30.7
Average			39,000	54,800	30.0
B2	Flange	.393	39,700	54,500	33.0
B2	Web	.286	43,200	57,400	23.0
Average			41,400	56,000	28.0
B3	Flange	.351	39,400	55,600	29.7
B3	Web	.280	41,600	56,600	35.8
Average			40,500	56,100	32.8
Average values:					
1, 2, 3			44,100	55,400	31.8
A1, A2, A3			40,100	55,100	32.3
B1, B2, B3			40,300	55,600	30.2

The results of the compressive tests of the short lengths of the steel columns are given in Table 5.

The results of the tests of the bricks are given in Table 3. Each average value is the mean from tests on 25 bricks. As a measure of the dispersion of the results of individual tests about their corresponding averages, values for the standard deviations are given which were calculated by means of the following formula:

$$\sigma = \sqrt{\frac{\Sigma V^2}{n-2}},$$

where

σ = standard deviation,
n = number of individual values,
ΣV^2 = sum of the squares of the deviations of the individual values from their mean.

The bricks complied with the requirements for the hard grade in Federal specification No. 504, brick, clay, common.

The results of the tests on the mortar are given in Table 4.

TABLE 3.—*Properties of bricks*

	Length	Breadth	Depth	Weight	Transverse breaking load (7-inch span)	Modulus of rupture	Compressive strength, flat	Water absorption		
								5-hour cold	48-hour cold	5-hour boil
	Inches	*Inches*	*Inches*	*Pounds*	*Pounds*	*Lbs./in.²*	*Lbs./in.²*	*Per cent*	*Per cent*	*Per cent*
Minimum	8.25	3.80	2.20	5.15	970	476	2,960	6.70	7.8	10.4
Average	8.38	3.97	2.27	5.63	1,555	800	5,253	8.94	9.95	11.8
Maximum	8.55	4.10	2.30	5.81	2,540	1,335	7,750	12.0	12.6	14.2
Standard deviation	.091	.074	.037	.215	358	201	1,230	1.21	1.12	1.04

TABLE 4.—*Properties of mortar*

	Mortar flow values	Compressive strength of mortar cylinders (average of 18 specimens) conditioned in—	
		Air, age about 30 days [1]	Water, age 28 days
	Per cent	*Lbs./in.²*	*Lbs./in.²*
Average	136	2,090	2,510
Maximum	142	2,310	2,770
Minimum	128	1,820	2,090

[1] See Table 5, time between completion of wall and test.

The workmanship of the walls of the incased columns was the same as the workmanship of walls 43, 44, and 45 (Mississippi brick) reported by Stang, Parsons, and McBurney.[2]

These three walls were solid brick walls having no steel columns or other reinforcement. They were 12½ inches thick, 6 feet long, and 9feet high. The average compressive strength was 1,640 pounds per square inch. Differences other than workmanship make it difficult

[2] Compressive Strength of Clay Brick Walls, B. S. Jour. Research, vol. 3 (RP108), October, 1929.

to estimate the strength of the brick masonry of the incased columns. These differences are: First, although the modulus of rupture of the Virginia brick used for the incased columns was almost the same as that of the Mississippi brick, the compressive strength (flat) of the Mississippi brick (3,410 pounds per square inch) was much lower than that of the Virginia brick (5,253 pounds per square inch); second, the absorption of the Mississippi brick was about twice that of the Virginia brick; and third, the shape and surfaces of the Mississippi brick were much more uniform than those of the Virginia brick.

2. THE BARE AND THE INCASED COLUMNS

The results of the tests of the bare and of the incased columns are given in Table 5. Stress-strain diagrams were drawn for each column using the average strain computed from the compressometer readings. The stress for both the bare and the incased columns was obtained by dividing the load by the computed cross-sectional area of the steel columns. Due to the fact that a portion of the load was carried by the brick walls of the incased columns, the actual stress in the steel within the compressometer gage length was much lower than the values used in plotting the diagrams. The average stress-strain diagrams for the three bare columns, for the three A incased columns, and for the three B incased columns were also drawn. The diagrams for the columns are shown in Figures 5, 6, and 7. The average stress-strain diagrams are shown in Figure 8.

TABLE 5.—*Results of compressive tests of the columns and of auxiliary short lengths*

Column	Condition	Computed area of steel column	Uncased length of steel column and of the short length	Height of wall	Time between completion of walls and test	Yield point of coupon	Compressive strength		Load carried by	
							Column	Short length	Steel column	Brick wall
		Square inches	*Inches*	*Ft. In.*	*Days*	*Lbs./In.²*	*Lbs./in.²*	*Lbs./in.²*	*Per cent*	*Per cent*
1	Bare	5.90				42,800	23,900		100	0
2	do	5.90				47,500	23,000		100	0
3	do	5.85				42,000	23,100		100	0
Average						44,100	23,300		100	0
A1	Incased	5.85	7½	22 4½	28	41,100	40,000	41,200	18	82
A2	do	6.02	7½	22 4½	31	39,000	41,500	43,200	17	83
A3	do	5.98	11	22 1	30	40,100	40,700	38,300	19	81
Average					30	40,100	40,700	40,900	18	82
B1	Incased	6.03	10	22 2	29	39,000	38,800	40,600	16	84
B2	do	6.14	8	22 4	31	41,400	42,100	41,500	19	81
B3	do	6.10	8½	22 3½	31	40,500	41,100	42,200	16	84
Average					30	40,300	40,700	41,400	17	83

All the stress-strain curves are nearly straight. The slope of the straight lines shown on each diagram is the average ratio of stress to strain for that series of observed values. These average ratios are given in Table 6.

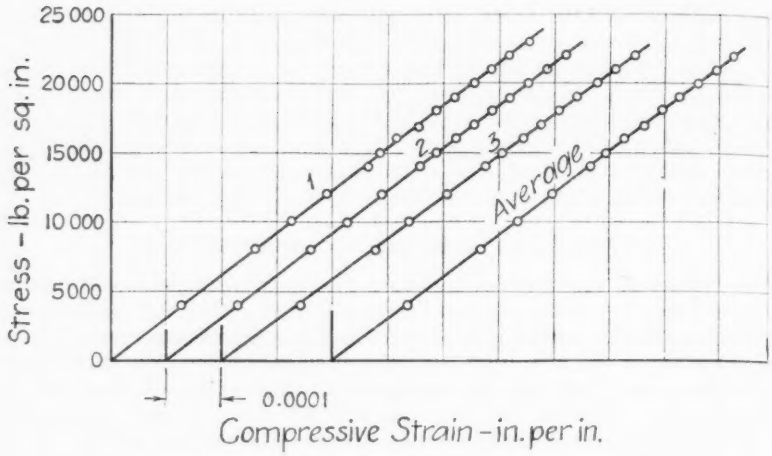

FIGURE 5.—*Stress-strain diagrams of the bare columns*

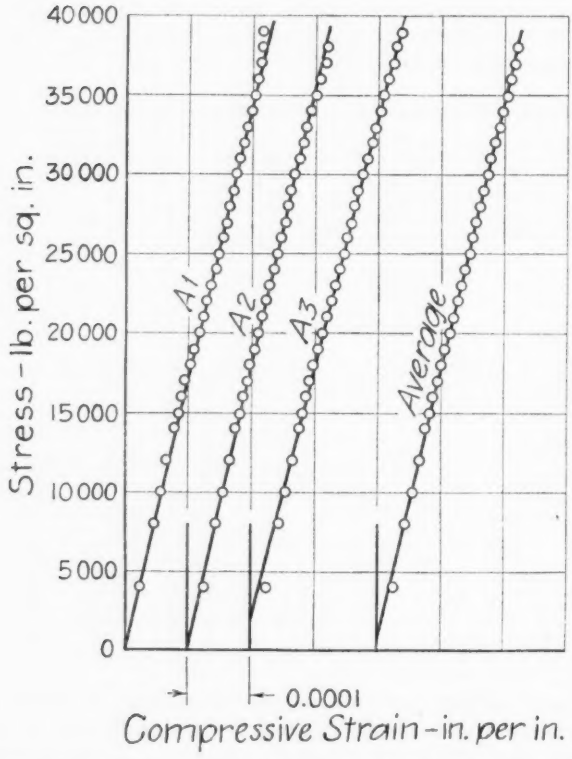

FIGURE 6.—*Stress-strain diagrams of the incased columns, group A, in which the web of the column was perpendicular to the length of the wall*

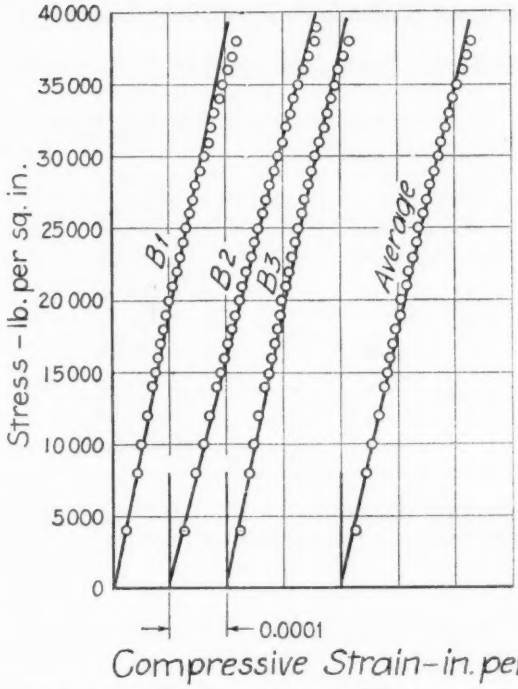

FIGURE 7.—*Stress-strain diagrams of the incased columns, group B, in which the web of the column was parallel to the length of the wall*

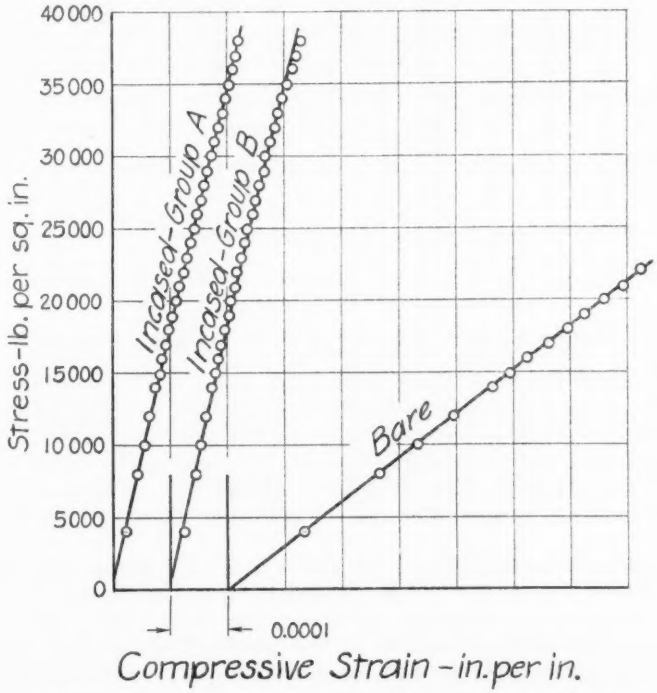

FIGURE 8.—*Average stress-strain diagrams for the columns*

TABLE 6.—*The ratios of stress to strain for the columns*

Column	Average ratio stress to strain
	*Lbs./in.*²
1	30, 800, 000
2	30, 700, 000
3	29, 600, 000
Average	30, 400, 000
A1	170, 800, 000
A2	179, 200, 000
A3	154, 200, 000
Average	168, 100, 000
B1	191, 500, 000
B2	154, 200, 000
B3	182, 400, 000
Average	176, 000, 000

The stress-deflection diagrams for the bare columns are shown in Figure 9. There was no measurable deflection up to a stress of

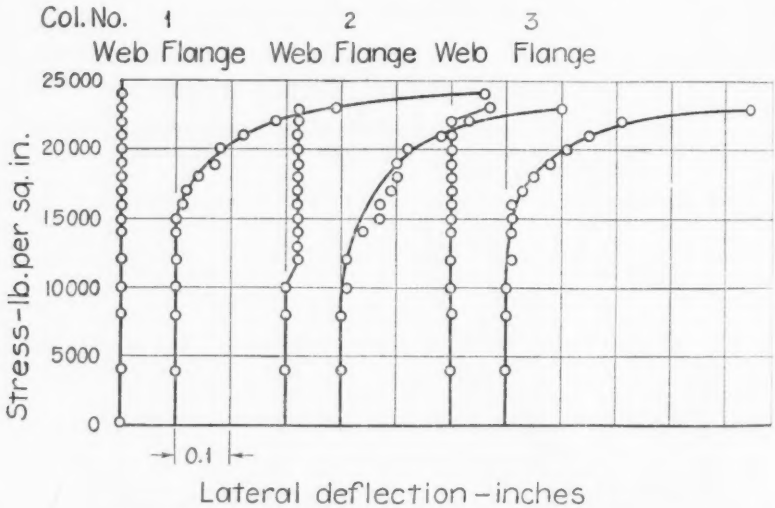

FIGURE 9.—*Stress-deflection diagrams of the bare columns*

about 10,000 lbs./in.². For higher stresses the deflection in the plane of the web of the H section was negligible, but the deflection at midlength in a plane perpendicular to the web increased more and more rapidly until the maximum load was reached. There were no signs of secondary failure such as buckling of the flanges or webs. These curves are typical of those for columns which fail by deflecting laterally.

The stress-deflection curves for the A incased columns are shown in Figure 10 and those for the B incased columns in Figure 11. There was no measurable deflection in the plane of the side (face) of the walls and very little deflection in the plane of the end of the walls. These curves are typical of stress-deflection curves for short, sturdy

columns which deflect little before the maximum compressive strength of the material is reached.

When discussing the strength of steel columns it is convenient to use the column "efficiency." This term is defined by W. C. M. Pettingill [3] as the ratio of the column strength (average maximum compressive stress) to the compressive yield point of the material. When comparing the efficiencies of columns it has been found satisfactory to use the tensile yield point of the material which is obtained

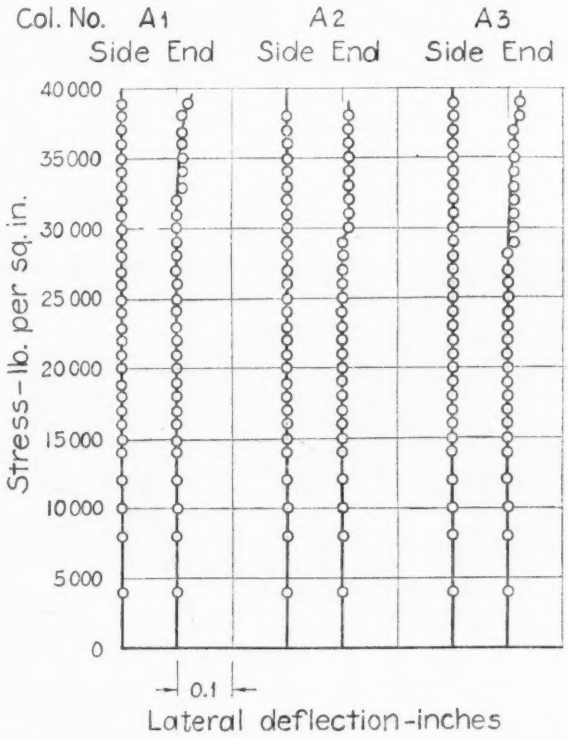

FIGURE 10.—*Stress-deflection diagrams of the incased columns, Group A*

in routine tests instead of the compressive yield point. The same method of determining the yield point should, of course, be used when comparisons of this sort are made.

The efficiencies of the columns and of the short lengths reported in this paper are given in Table 7. The yield point was taken as the average of the yield points of the flange and web coupons without considering the weighting; that is, the proportion of the total cross section represented by each coupon.

[3] R. V. Southwell, The Strength of Struts, Aircraft Engineering, vol. 1, pp. 136–138, 1920. Also see footnote 1, p. 128, and refer to pages 36 and 37 of that reference.

TABLE 7.—*Efficiencies of the columns and of the short lengths*

Column	Column efficiency of bare and incased columns	Column efficiency of short lengths
1	0.559	
2	.484	
3	.550	
Average	.531	
A1	.973	1.002
A2	1.064	1.108
A3	1.015	.955
Average	1.017	1.022
B1	.995	1.041
B2	1.017	1.002
B3	1.015	1.042
Average	1.009	1.028

For the short lengths, in which lateral buckling did not appreciably affect the strength, the efficiencies are very nearly 1.00. As the

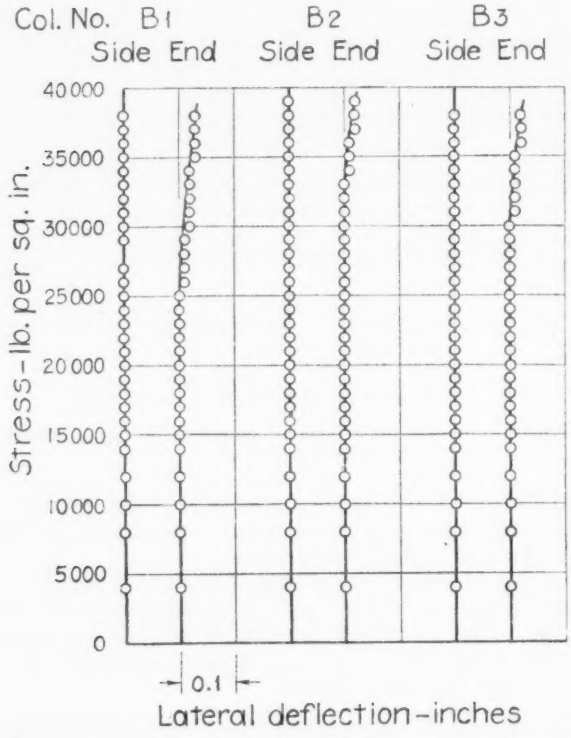

FIGURE 11.—*Stress-deflection diagrams of the incased columns, Group B*

slenderness ratio increases, the effect of lateral buckling gradually lowers the efficiency. For low-carbon structural steel columns having slenderness ratios greater than about 95 for "round end"

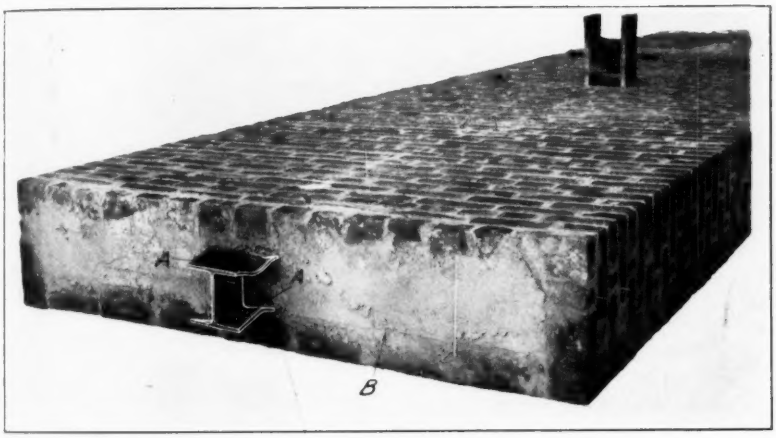

FIGURE 12.—*The top of column A1 after test*

Note the buckling of the unincased length of the column at *A* and the crack between the brick wythes at *B*.

UNIV OF MICH.

FIGURE 13.—*An incased column being removed from the testing machine after test*

No bricks fell from the wall when it was laid horizontally on the floor.

columns or greater than about 190 for "fixed end" columns, the failure is almost entirely flexural (Euler failure) and the strength depends almost entirely upon Young's modulus of elasticity of the material, the end conditions, and the slenderness ratio. All the efficiencies of the incased columns and of the short lengths cut from the steel columns are of the order of magnitude (approximately 1.00) to be expected for "round end" steel columns having slenderness ratios less than 30 or for "fixed end" steel columns having slenderness ratios less than 60. All the efficiencies of the bare columns are of the order of magnitude (approximately 0.50) to be expected for "round end" steel columns having slenderness ratios of about 110 or for "fixed end" steel columns having slenderness ratios of about 220.[4]

The many tests which have been made on columns indicate that a "flat end" column and a "round end" column having about 0.6 the length may be expected to support the same maximum load.[5] This fraction of the length (0.6) may vary somewhat, depending upon the distribution of the load over the end of the columns and other conditions which affect the degree of end restraint.

The bare columns having a slenderness ratio of 183 and "flat ends" probably would have about the same efficiency as a "round end" column having a slenderness ratio of about 110.

All of the incased columns failed by yielding, followed by local buckling of the unincased portion of the steel columns. The lateral deflection of the brick walls under the maximum load did not exceed 0.03 inch for any of the incased columns. The brick walls, therefore, restrained the steel columns and prevented failure by lateral buckling. The only failure in the brick walls was at the top where small cracks appeared between the brick wythes, apparently caused by the local buckling of the unincased portion of the steel column. The buckling of the unincased portion of the steel columns is shown in Figure 12 at *A*, and the cracks in the vertical mortar joints at *B*. One of the incased columns after test (weight 19,000 pounds) is shown in Figure 13. The fact that all the incased columns could be handled in this way by the overhead crane without any indication of failure in the brick walls is evidence that the brick walls were not appreciably affected by the loads applied during the tests.

For the bare columns the entire load was carried by the steel. The average ratio of stress to strain for these columns, Table 6, is therefore, the average compressive modulus of elasticity of the steel in the bare columns. The values are as close to the usual value (30,000,000 lbs./in.^{2}) for mild steel as was to be expected from tests made with these specimens and apparatus.

For the incased columns in the 150-inch gage length a portion of the load was transferred to the brick walls by the bond between the walls and the steel. On the assumption that the average compressive modulus of the steel in the incased columns was 30,000,000 lbs./in.^{2}, 30,000,000 divided by the computed ratio of stress to strain gives the portion of the applied load which was carried by the steel column. The remainder of the load was carried by the brick wall. These values are given in Table 5. The average load in the steel over the

[4] See footnote 1, p. 128, and refer to Fig. 13, p. 43, of that reference.
[5] Columns, Salmon, pp. 171–174.

150-inch gage length in no case exceeded 20 per cent of the applied load.

The values given in Table 5 show, also, that the orientation of the steel column in the brick wall had no appreciable effect upon the strength of the incased columns.

From the fact that the steel in the incased columns carried only a small proportion of the load, it is evident that a more comprehensive investigation should be made in an attempt to develop a load-carrying structure which would also serve to inclose the building. There is apparently no reason why the load cannot be economically applied directly to the top of a brick wall of suitable material and workmanship. The steel in the incased columns undoubtedly served to reinforce the brick masonry, but the question arises whether a number of vertical steel bars of small diameter placed near both faces of the wall would not have provided much greater restraint against lateral buckling of the brick wall and at the same time reduced the cost. The results of further investigations are needed to give a definite answer to this question. Attention should also be given to developing methods for tying the structure supported by the brick wall into the top of the wall so that they will act as a unit under any forces which are likely to come upon them.

These results show that the compressive strength of long steel columns, incased as these were in brick walls, is much greater than if the columns are not incased, but they do not indicate the final solution of the problem of using brick masonry and steel to build more safely and more economically.

V. CONCLUSIONS

Three H-shaped steel columns, 23 feet long, 6 inches in depth, weighing 20 pounds per foot, and having flat ends, were tested in compression. Six similar steel columns incased in brick walls, 14 inches thick, 6 feet long, and extending up to about 8 inches from the top of the steel columns were also tested in compression.

With steel columns of this size, incased in brick walls of the quality used:

1. The brick walls effectively prevented lateral buckling of the steel column so that the maximum compressive load for the structure was, for all practical purposes, the maximum compressive load for the portion of the steel column above the wall, which in turn was, for all practical purposes, the tensile yield point of the steel multiplied by the cross-sectional area of the steel column.

2. The maximum compressive load carried by the short unincased portion of the steel columns was much greater than the maximum compressive load carried by the long unincased columns (slenderness ratio of 183) which failed by lateral buckling.

3. The lateral deflection of the incased columns was negligible because in no case did it exceed 0.03 inch under the maximum load. The brick masonry showed only small cracks at the top near the steel columns.

4. Over the gage length of 150 inches at midheight of the incased columns, the steel carried, on the average, less than 20 per cent of the applied load.

5. The orientation of the steel column with respect to the face of the brick wall had no effect upon the strength of the incased columns.

WASHINGTON, November 23, 1932.

RP521

FURTHER DESCRIPTION AND ANALYSIS OF THE FIRST SPECTRUM OF XENON

By C. J. Humphreys and W. F. Meggers

ABSTRACT

An entirely new description of the first spectrum of Xenon has been completed. Geissler tubes with a small bore capillary, exposed end on, were used as sources and afforded sufficient intensity to permit the use of spectrographs of high resolving power to a greater extent than in the preliminary investigation previously reported. The new description covers the region between 3,340 and 11,140 A. The spectrum has been photographed by aid of a Rowland 20,000-line per inch grating over the range included between 3,440 and 9,800 A. Interferometer measurements have been made on 130 lines, including 45 reported in a previous paper. Several new lines have been found in the ultra-violet between 3,340 and 3,440 where the use of a source of higher intensity has led to the detection of several higher members of the $1s_5$–mp_4 series. Most of the new data have been obtained in the infra-red region. Each of the new types of Eastman red and infra-red sensitive plates, F, N, P, and Q have been exposed to the radiation in the spectral region for which their respective sensitivity is greatest. It is believed that the spectrum has been completely recorded throughout the region investigated.

Of the 538 lines included in the description all but 13 have been classified. Almost all terms predicted by the Hund theory have been obtained. The new term table embodies a small change in the absolute term values indicated by new measurements of greater precision, several newly discovered terms, and extensions to practically all the series. Some rearrangement of the d-terms has been made necessary, due to the elimination of uncertainties in the assignment of j-values. A new f-type sequence, lying very close to mZ, and designated by mT, has been found.

CONTENTS

	Page
I. Introduction	139
II. Experimental details	140
III. Wave-length measurements	141
IV. Discussion of Xe I terms	146

I. INTRODUCTION

A preliminary description and analysis of the first spectrum of xenon was published in 1929.[1] As in the case of the investigation of Kr I which was undertaken simultaneously, it was expected to give in later publications extensions of the series to higher members permitted by the detection of fainter lines, interferometer comparisons of wave lengths, and measurements of hyperfine structures. Interferometer measurements of 45 xenon lines,[2] and measurements of the hyperfine structures of 6 xenon lines,[3] are presented in two papers by

[1] W. F. Meggers, T. L. deBruin, and C. J. Humphreys, B. S. Jour. Research, vol. 3 (RP115), p. 731, 1929.
[2] C. J. Humphreys, B. S. Jour. Research, vol. 5 (RP245), p. 1041, 1930.
[3] C. J. Humphreys, B. S. Jour. Research, vol. 7 (RP351), p. 453, 1931.

one of us in which the results of a similar investigation of Kr I are given. In the case of the first spectrum of krypton it was found that a large number of new lines could be recorded by using as a source a Geissler tube exposed end on. A much more intense illumination of the slit could be obtained in this manner than with the usual type of tube, the construction of which permits only side-on exposures. Extended and improved measurements of Kr I are contained in a paper published about a year ago.[4] The present paper represents a more complete description of Xe I than could then be made in the case of krypton because in the meantime new photosenstitizing dyes have been discovered which have greatly extended both the speed of recording and the upper limit of the range of investigation in the infra-red region. All the rare gas spectra have been reinvestigated, using these specially sensitized plates, and "end on" Geissler tubes (from Robert Goetze in Leipzig). The results for those other than xenon are being published in separate papers. The use of more intense sources and more sensitive plates has made possible additional interferometer comparisons, the results of which for Xe I lines are incorporated in the present description. The application of these superior infra-red sensitive photographic plates to spectrographic investigations has created a demand for accurate standards of wave length in the extended range now accessible and it appears that the emission spectra of the noble gases will be useful for this purpose. The results for Xe I lines presented here may be regarded as a contribution to standard wave lengths, since many of the lines have been measured interferometrically either in terms of neon standards or of sharp xenon lines so determined and enough of the spectral terms have thus been accurately fixed in relative value to guarantee the calculated values of the remaining classified lines to within 0.01 A.

Since the publication of our first paper, the spectrum of Xe I has been investigated by Gremmer[5] and by Rasmussen.[6] Gremmer's classification is essentially the same as ours. He succeeded in obtaining 16 classified lines not recorded in our first description in the ultra-violet region. These are in all cases higher members of known series. Rasmussen found a considerable number of lines in the infra-red, gave classifications for 80 additional lines, and introduced a number of changes in term designations which are confirmed by the present investigation.

II. EXPERIMENTAL DETAILS

New spectograms have been made over the entire region of the Xe I spectrum accessible to photography in air. The Hilger E1 spectograph was used to describe the ultra-violet region. The last recorded line appears at 3,340 A. There is no Xe I radiation to be expected between the $1s_5$ series limit at 3,250 A and the Schumann region. Between 3,440 and 9,800 A the Rowland grating with 20,000 lines per inch was used, which gives a scale of 3.7 A/mm in the first order spectrum. The description previously published (RP115) was made for the most part with a grating of 7,500 lines per inch, giving a scale of 10.4 A/mm. The region between 6,600 and 8,600 A was also photographed with a scale of 2.7 A/mm, given by a plane grating with 20,000 lines per inch and lenses of 16 feet focal length. The published obser-

[4] W. F. Meggers, T. L. deBruin, C. J. Humphreys, B. S. Jour. Research, vol. 7 (RP 364), p. 643, 1931.
[5] W. Gremmer, Zeit. f. Physik, vol. 59, p. 154, 1930.
[6] E. Rasmussen, Zeit. f. Physik, vol. 73, p. 779, 1932.

vations beyond 9,800 A have been made with the 7,500-line-per-inch grating, although the infra-red region was also photographed by aid of a Hilger E2 prism spectograph with glass optics. Interferometer measurements have been made of the wave lengths of 130 Xe lines including those reported in RP245. For lines shown by the interference observations to have hyperfine structure, the wave length of the strongest component only is here reported. A pair of crystal quartz interferometer plates of 60 mm aperture, silvered by the evaporation method, have been used in the more recent work. The fixed étalon method has been employed, using invar separators of 3, 6, 10, 15, and 25 mm length.

In the red and infra-red regions, plates prepared with the new types of sensitizers developed by the Eastman laboratories and designated F, N, P, and Q have been used. The characteristics of these special plates are discussed in a recent paper by Mees.[7] We have used the F plate to cover the region from 5,000 to 6,600 A, the N plate from 6,500 to 8,500, the P plate between 8,000 and 9,000, and the Q plate above 9,000. There is considerable overlapping of the regions of sensitivity of these emulsions except that the F type falls off rather abruptly above 6,800 A. The N plate shows two maxima near 7,000 and 8,200 A. The respective maxima of the P and Q types lie at 8,600 and 9,700 A, respectively. Exposures of from 2 to 24 hours have been made. One exposure was prolonged to 40 hours in order to observe the resolution of the pair of lines at 9,374A with the Rowland grating, which was necessary to establish experimentally the existence of the mT series as discussed below. The stronger lines are considerably overexposed in the case of the longer exposures and, in the work with the Rowland grating, show from 1 to 8 orders of Rowland ghosts. It is believed that the spectrum has been completely recorded in the region studied. Radiometric investigation of still longer waves is highly desirable.

III. WAVE-LENGTH MEASUREMENTS

The wave-length measurements have been made relative to the international standards in the iron arc spectrum. The results from each spectrogram were brought to the scale of the interference measurements by applying a correction where a systematic difference was noted. While such corrections were usually of the order of from 0.01 to 0.02 A, it was found necessary to apply a correction as great as 0.1 A in the region above 9,000 A. The cause of this displacement between the xenon, and second order comparison spectrum of iron, too great to be accounted for by atmospheric dispersion, appears to lie in some unexplained temperature displacement of the plate or mounting during prolonged exposure. Wave lengths which have been determined by interference methods are given to thousandths or ten-thousandths of an angstrom unit and can thus be distinguished from those lines for which only prism or grating measurements are available. The vacuum wave numbers corresponding to the wave lengths determined by interference methods have been computed directly from the atmospheric dispersion formula of Meggers and Peters.[8] The use of spectrographs of higher dispersion and resolving power, together with

[7] C. E. K. Mees, J. Opt. Soc. Am., vol. 22, p. 204, 1932.
[8] W. F. Meggers and C. G. Peters, B. S. Sci. papers, vol. 14 (S. P. 327), p. 722; 1918.

the application of interference methods to one-fourth of the lines, has not only greatly increased the accuracy of the wave-length determinations, but has made possible the resolution of nearly all close pairs of lines. Such pairs occur at 6,111, 6,163, 6,206, 6,840, 7,584, 7,642, 7,664, 8,348, 8,952, and 9,374 A. In a few cases, notably 7,119 A, lines formerly regarded as double for purposes of classification are now shown to be single.

The list of Xe I wave lengths as finally adopted is presented in Table 1. After eliminating known lines due to Xe II, faint unclassified lines of doubtful origin, and identifiable Rowland ghosts, we have retained 538 lines. The real lines were in practically all cases distinguished from false lines or ghosts by repeated observations with different gratings. With but 13 exceptions, all of the lines are accounted for by combinations of identified spectral terms. The calculated values of the wave numbers of all classified lines, computed from the experimental terms, are also given in Table 1, and indicate the degree of accuracy of the wave-length determinations.

TABLE 1.—*List of Xe I lines*

Intensity	Wave length	Wave number observed	Combination	Wave number calculated	Intensity	Wave length	Wave number observed	Combination	Wave number calculated
1—	3,340.04	29,931.18	$1s_3$–$11p_8$	1.2	1	3,742.22	26,714.54	$1s_4$– 6V	.732
1—	3,348.63	29,854.41	$1s_5$–11U	3.97	10	3,745.38	26,692.00	$1s_4$– 6Y	1.95
1*h*—	3,358.17	29,769.60	$1s_3$–$10p_8$	.60	4	3,745.69	26,689.79	$1s_4$– 6X	.750
1*h*—	3,358.96	29,762.60	$1s_3$–$10p_9$	.60	3	3,795.95	26,336.42	$1s_5$– 5V	.437
1*h*	3,370.34	29,662.11	$1s_3$–10U	1.95	40	3,796.30	26,333.99	$1s_5$– 5U	.95
1	3,383.20	29,549.36	$1s_5$– $9p_8$	.36	30	3,801.39	26,298.73	$1s_5$– 5Y	.717
1	3,384.36	29,539.23	$1s_3$– $9p_8$	.23	3	3,801.90	26,295.20	$1s_5$– 5X	.152
2	3,400.07	29,402.75	$1s_5$– 9U	.19	30	3,809.84	26,240.40	$1s_4$– $5p_8$	.35
1—	3,400.79	29,396.53	$1s_5$– 9Y	5.73	10	3,823.74	26,145.02	$1s_4$– $5p_6$	.09
2	3,418.37	29,245.35	$1s_5$– $8p_8$	.35	15	3,826.86	26,123.70	$1s_4$– $5p_7$	.70
2	3,420.00	29,231.41	$1s_3$– $8p_8$	.41	2	3,835.6	26,064.2	$1s_4$– $5p_9$	5.00
3	3,442.66	29,039.01	$1s_3$– 8U	8.77	2	3,942.29	25,358.81	$1s_4$– 5V	.821
1	3,443.83	29,029.15	$1s_3$– 8Y	8.77	60	3,948.163	25,321.095	$1s_4$– 5Y	.101
4	3,469.81	28,811.80	$1s_3$– $7p_8$	.86	10	3,948.72	25,317.52	$1s_4$– 5X	.536
4	3,472.36	28,790.64	$1s_3$– $7p_8$	.64	120	3,950.925	25,303.393	$1s_5$– $4p_6$	.395
1	3,496.86	28,588.93	$1s_4$– $9p_5$	.93	6	3,956.85	25,265.50	$1s_5$– $4p_7$	.541
5	3,506.74	28,508.39	$1s_5$– 7U	.43	200	3,967.541	25,197.423	$1s_5$– $4p_8$	.423
2	3,508.42	28,494.74	$1s_5$– 7Y	5.032	40	3,974.417	25,153.835	$1s_5$– $4p_9$	.837
2	3,517.90	28,417.95	$1s_4$– 9Y	8.12	30	3,985.202	25,085.762	$1s_5$– $4p_{10}$	.762
2	3,533.48	28,292.66	$1s_4$– $8p_5$	.66	100	4,078.8207	24,509.996	$1s_4$– $4p_5$	.996
1—	3,536.61	28,267.62	$1s_4$– $8p_6$	.74	60	4,109.7093	24,325.782	$1s_4$– $4p_6$	.779
1	3,537.35	28,261.70	$1s_4$– $8p_7$	.70	80	4,116.1151	24,287.925	$1s_4$– $4p_7$	.925
10	3,549.86	28,162.11	$1s_5$– $6p_6$	.05	20	4,135.1337	24,176.222	$1s_4$– $4p_9$	.221
10	3,554.04	28,128.99	$1s_5$– $6p_8$	.99	2	4,146.78	24,108.32	$1s_4$– $4p_{10}$	.146
1	3,555.92	28,114.12	$1s_5$– $6p_9$	.12	20	4,193.01	23,842.52	$1s_5$– 4V	.536
3	3,563.80	28,051.95	$1s_4$– 8Y	2.16	150	4,193.5296	23,839.567	$1s_5$– 4U	.567
4	3,587.02	27,870.37	$1s_4$– $7p_5$	.37	50	4,203.6945	23,781.922	$1s_5$– 4Y	.921
1	3,591.67	27,834.29	$1s_4$– $7p_6$	.25	10	4,205.404	23,772.254	$1s_5$– 4X	.253
2	3,592.80	27,825.53	$1s_4$– $7p_7$	.53	20	4,372.287	22,864.925	$1s_4$– 4V	.920
15	3,610.32	27,690.51	$1s_5$– 6U	.53	100	4,383.9092	22,804.306	$1s_4$– 4Y	.305
8	3,613.06	27,669.50	$1s_5$– 6Y	.56	70	4,385.7693	22,794.635	$1s_4$– 4X	.637
6	3,633.06	27,517.19	$1s_4$– 7Y	.416	500	4,500.9772	22,211.188	$1s_5$– $2p_2$	.186
10	3,669.91	27,240.90	$1s_4$– $6p_5$	.90	400	4,524.6805	22,094.833	$1s_5$– $2p_3$	.833
2	3,677.54	27,184.38	$1s_4$– $6p_6$	.44	2	4,576.60	21,844.18		
4	3,679.31	27,171.30	$1s_4$– $6p_7$	.30	300	4,582.7474	21,814.878	$1s_4$– $2p_1$	.877
40	3,685.90	27,122.72	$1s_5$– $5p_6$	.70	100	4,611.8896	21,677.034	$1s_5$– $3p_7$	.034
1	3,688.80	27,101.40	$1s_5$– $5p_7$	.32	1,000	4,624.2757	21,618.973	$1s_5$– $3p_8$	.973
40	3,693.49	27,066.99	$1s_5$– $5p_8$	.99	2,000	4,671.226	21,401.685	$1s_5$– $3p_8$	.685
4	3,696.82	27,042.61	$1s_5$– $5p_9$	.61	100	4,690.9711	21,311.603	$1s_5$– $2p_4$	.600
2	3,702.74	26,999.37	$1s_5$– $5p_{10}$	.41	300	4,697.020	21,284.155	$1s_5$– $3p_9$	.154

TABLE 1.—*List of Xe I lines*—Continued

Intensity	Wave length	Wave number observed	Combination	Wave number calculated
5	4,708.21	21,233.57	$1s_4-2p_2$	.570
600	4,734.1524	21,117.217	$1s_4-2p_3$	.217
150	4,792.6192	20,859.605	$1s_5-3p_{10}$	.605
500	4,807.019	20,797.118	$1s_4-3p_8$	.118
400	4,829.709	20,699.415	$1s_4-3p_7$	.418
300	4,843.294	20,641.357	$1s_4-3p_6$	.357
500	4,916.508	20,333.981	$1s_4-2p_4$	.984
300	4,923.1522	20,306.538	$1s_4-3p_9$	.538
3h	5,023.88	19,899.40	$1s_3-8X$	.47
200	5,028.2796	19,881.989	$1s_4-3p_{10}$	.989
10	5,162.711	19,364.290	$1s_2-7X$	.290
1h	5,164.39	19,357.99	$2p_{10}-10d_3$	.94
1h	5,167.30	19,347.09	$2p_{10}-10d_5$	.08
2h	5,185.85	19,277.89	$1s_2-9Y$	8.22
1	5,206.07	19,203.01	$2p_{10}-8s_5$	2.99
4h	5,245.27	19,059.51	$2p_{10}-9d_3$	.48
4h	5,248.98	19,046.03	$2p_{10}-9d_5$	.02
2h	5,251.89	19,035.48		
1h	5,273.48	18,957.55	$1s_3-6p_{10}$	.59
2h	5,283.30	18,922.31	$1s_2-8V$	.31
4h	5,286.11	18,912.25	$1s_2-8Y$	.26
3h	5,286.38	18,911.29	$1s_2-8X$	.20
3	5,306.37	18,840.05	$2p_{10}-7s_5$	.08
1h–	5,335.91	18,735.75	$2p_8-11d_1''$	.78
2h	5,337.89	18,728.80	$2p_8-11d_4$ $2p_8-13d_4'$	.80
1	5,356.80	18,662.68	$2p_{10}-8d_1''$	.66
15	5,362.244	18,643.739	$2p_{10}-8d_5$	.739
30	5,364.626	18,635.459	$2p_{10}-8d_3$	.459
6	5,367.03	18,627.11		
1h–	5,373.74	18,603.85	$2p_8-12d_4'$	.85
100	5,392.795	18,538.119	$1s_2-6X$	.119
20	5,394.738	18,531.443	$2p_{10}-8d_6$	.443
1h	5,397.63	18,521.51	$2p_8-10d_1''$ $2p_8-10s_5$	.55 .54
4h	5,400.45	18,511.84	$2p_9-10d_4$	.84
5	5,418.02	18,451.81		
2h	5,421.76	18,439.08	$2p_8-11d_4'$	.08
5h	5,435.60	18,392.13	$1s_2-7V$	.13
30	5,439.923	18,377.519	$1s_2-7Y$	.519
15	5,440.39	18,375.94	$1s_2-7X$	6.022
1h	5,444.87	18,360.82	$2p_9-8s_4$	.82
1h	5,454.54	18,328.27	$2p_8-9s_5$	.27
2	5,456.45	18,321.85	$2p_{10}-6s_4$	.83
15	5,460.037	18,309.820	$2p_{10}-6s_5$	.820
1h	5,479.12	18,246.05	$2p_8-10d_1'$	.01
1h	5,481.33	18,238.69	$2p_9-9d_1'$	.77
1h	5,484.16	18,229.28	$2p_8-10d_4$	8.60
4h	5,484.46	18,228.28	$2p_9-9d_1''$	.24
6h	5,487.03	18,219.75	$2p_8-10d_4'$	.75
20h	5,488.555	18,214.684	$2p_9-9d_4$	.684
2h	5,532.78	18,069.10	$2p_8-8s_5$	.08
3h	5,540.38	18,044.30	$1s_2-6p_8$ $2p_{10}-7d_1''$	.54 .270
80	5,552.385	18,005.291	$2p_{10}-7d_3$	.291
3h	5,553.10	18,002.97	$2p_9-7s_4$	.97
1–	5,555.06	17,996.62	$1s_2-6p_9$	.61
2	5,557.28	17,989.43	$2p_9-7s_5$	.43
2	5,563.50	17,969.32	$1s_2-6p_{10}$	.32
5h	5,566.22	17,960.54		
100	5,566.615	17,959.264	$2p_{10}-7d_5$	.264
2h	5,567.77	17,955.54	$2p_8-9d_1'$	.51
2h	5,575.27	17,931.38	$2p_8-9d_4$	.425
40	5,579.28	17,918.50	$2p_8-9d_4'$	.50
30	5,581.784	17,910.458	$2p_{10}-7d_6$	.458
1–	5,585.18	17,899.57	$2p_7-11d_1''$	.54
6	5,594.37	17,870.16	$1s_2-5p_{10}$	.17
3	5,607.99	17,826.76	$2p_8-8d_1'$	.820
15	5,612.65	17,811.96	$2p_9-8d_1''$	2.01
80	5,618.878	17,792.220	$2p_9-8d_4$	.220
1	5,621.24	17,784.74	$2p_9-8d_3$	.805
5	5,646.19	17,706.16	$2p_8-7s_5$	.17
2h	5,652.84	17,685.33	$2p_7-10d_1''$	.31
1h–	5,654.31	17,680.73	$2p_9-8d_6$	.77
1h	5,664.46	17,649.05	$2p_6-11d_1'$	.05
40	5,688.373	17,574.855	$1s_2-6V$	.855
100	5,695.750	17,552.094	$1s_2-6Y$	.094
80	5,696.479	17,549.845	$1s_2-6X$	.851
8	5,698.54	17,543.50	$2p_8-8d_1'$	.561
1	5,703.34	17,528.73	$2p_8-8d_1''$	.75
3	5,706.87	17,517.89	$2p_{10}-5s_4$	.954
10h	5,709.80	17,508.90	$2p_8-8d_4$	.961
2	5,712.21	17,501.52	$2p_8-8d_3$	.546
70	5,715.716	17,490.780	$2p_{10}-5s_5$	.783
80	5,716.252	17,489.140	$2p_8-8d_4'$	.140
15h	5,722.14	17,471.15	$2p_9-6s_4$	.18
1h	5,723.26	17,467.72	$2p_7-9d_2$	.74
4	5,726.10	17,459.06	$2p_9-6s_5$	.131
4h	5,733.48	17,436.59	$2p_6-10d_1'$	.60
6	5,740.17	17,416.27	$2p_{10}-6d_2$	.29
1h	5,740.73	17,414.57	$2p_6-10d_3$	.62
8h	5,748.20	17,391.94	$2p_7-9d_1''$	2.00
1h	5,754.60	17,372.59	$2p_7-9d_3$	.59
1h	5,792.26	17,259.64	$2p_6-8s_5$	.67
15	5,807.311	17,214.912	$2p_8-7d_1'$	.922
60	5,814.505	17,193.614	$2p_8-7d_1''$	.616
25	5,820.52	17,175.84	$2p_8-6s_5$	.907
300	5,823.890	17,165.906	$1s_2-5X$	.907
150	5,824.800	17,163.225	$2p_9-7d_4$	.225
1	5,827.72	17,154.63	$2p_9-7d_3$	.636
20h	5,830.63	17,146.06	$2p_9-9d_1'$	.10
4h	5,840.83	17,116.12	$2p_9-9d_3$	.16
5	5,843.43	17,108.51	$2p_9-7d_5$	.610
1	5,845.46	17,102.56	$2p_9-9d_5$	.70
2	5,846.21	17,100.37	$1s_2-5p_8$	.45
3h	5,849.85	17,089.73	$2p_7-8d_2$	.74
15	5,856.509	17,070.300	$2p_{10}-6d_1''$	.300
100	5,875.018	17,016.519	$2p_{10}-6d_3$	.519
6	5,878.92	17,005.23	$1s_2-5p_6$	.19
20	5,889.12	16,975.77	$2p_7-8d_1''$	.77
100	5,894.988	16,958.874	$2p_{10}-6d_5$	.874
2h	5,895.62	16,957.05	$2p_7-8d_5$	6.850
8	5,898.56	16,948.60	$2p_7-8d_3$	.570
20	5,904.462	16,931.663	$2p_8-7d_1'$	.663
3	5,906.76	16,925.07	$1s_2-5p_9$	.10
5	5,911.90	16,910.36	$2p_8-7d_1''$	.357
4	5,916.65	16,896.78	$2p_8-7s_5$	.76
10	5,921.85	16,881.95	$1s_2-5p_{10}$	.90
20	5,922.550	16,879.953	$2p_8-7d_4$	.966
6	5,925.56	16,871.38	$2p_8-7d_5$	.377
80	5,931.241	16,855.219	$2p_{10}-6d_6$	.220
100	5,934.172	16,846.894	$2p_8-7d_4'$	.894
1–	5,970.41	16,744.64	$3d_5-10V$	.64
1h	5,972.82	16,737.88	$3d_5-10X$, Y	
40	5,974.152	16,734.153	$2p_9-8d_1'$	.153
2	5,978.29	16,722.57	$3d_4'-11T$, Z	.57
1	5,979.42	16,719.41	$2p_8-8d_1''$	.34
4	5,986.23	16,700.39	$2p_8-8d_5$	.418
20	5,989.18	16,692.16	$2p_8-8d_3$	.138
30	5,998.115	16,667.300	$2p_9-5s_4$	.300
15	6,007.909	16,640.128	$2p_8-5s_5$	.128
8	6,009.78	16,634.94	$2p_7-6s_4$	.94

TABLE 1.—*List of Xe I lines*—Continued

Intensity	Wave length	Wave number observed	Combination	Wave number calculated	Intensity	Wave length	Wave number observed	Combination	Wave number calculated
1*h*	6,014.10	16,623.00	$2p_7$– $6s_3$	2.931	20	6,430.155	15,547.436	$2p_8$– $5s_5$	.461
1*h*–	6,022.89	16,598.74	$3d_3$–11U	.74	2*h*	6,448.70	15,502.72	$3d_4$– 9W	.71
4	6,026.76	16,588.08	$2p_8$– $8d_5$	.10	7	6,450.48	15,498.45	$2p_9$– $2s_2$	.45
1*h*–	6,031.36	16,575.43	$2p_5$–$10d_3$	.46	10*hl*	6,451.79	15,495.30	$3d_4$– 9Z	.30
2	6,034.92	16,565.65	$2p_9$– $6d_3$	.64	3	6,461.50	15,472.02	$2p_8$– $6s_4$	.01
10	6,043.38	16,542.46	$2p_7$– $7d_2$	.45	300	6,469.705	15,452.394	$2p_{10}$– $5d_2$	.394
6*h*	6,048.00	16,529.82	$3d_4'$–10T, Z	.82	150	6,472.841	15,444.906	$2p_{10}$– $5d_3$	.906
1*h*	6,064.91	16,483.74	$3d_5$– 9V	.74	120	6,487.765	15,409.378	$2p_{10}$– $5d_1''$	.382
2*h*	6,067.52	16,476.65	$3d_3$– 9Y	.62	30*hl*	6,497.43	15,386.46	$3d_4'$– 7W	.48
1*h*	6,067.77	16,475.97	$3d_5$– 9X	.98	100	6,498.718	15,383.407	$2p_7$– $6d_1''$	.411
3	6,093.38	16,406.72	$3d_3$–10U	.72	15	6,500.37	15,379.50	$2p_8$– $7d_2$	.52
1–	6,095.15	16,401.96	$3d_3$–10X, Y		200*h*	6,504.18	15,370.49	$3d_4'$– 7T, Z	.49
3	6,103.88	16,378.50	$2p_8$– $6s_4$	.51				$1s_2$– $4p_5$	.10
8	6,108.37	16,366.46	$2p_9$– $6s_5$	.519	3	6,507.50	15,362.65		
30	6,111.759	16,357.384	$2p_7$– $7d_1''$	.381	40	6,521.508	15,329.648	$2p_7$– $6d_3$	.630
40	6,111.951	16,356.870	$2p_8$– $5s_5$	.869	100	6,533.159	15,302.312	$2p_9$– $4s_4$	.312
10	6,114.86	16,349.09	$2p_{10}$– $2s_2$	.10	40	6,543.360	15,278.456	$2p_9$– $4s_5$	.455
5	6,123.91	16,324.93	$3d_5$– 8X	.96	20	6,546.12	15,272.01	$2p_7$– $6d_5$	1.985
15	6,126.36	16,318.40	$2p_7$– $7d_3$	.401	4	6,553.66	15,254.45	$3d_3$– 7V	.43
1	6,131.47	16,304.80	$2p_8$– $9d_2$	.80	50*hl*	6,554.196	15,253.196	$3d_3$– 7U	.20
1*h*	6,142.13	16,276.50	$3d_4'$– 9W	.53	25	6,559.97	15,239.77	$3d_2$– 7Y	.80
4	6,143.70	16,272.34	$2p_7$– $7d_5$	.375	4*h*	6,560.65	15,238.19	$3d_2$– 7X	.30
20*hw*	6,144.97	16,268.98	$3d_4'$– 9T, Z	.98	20	6,583.27	15,185.83	$1s_2$– $4p_5$	.882
20	6,152.069	16,250.206	$2p_9$– $6d_1'$	.201	8	6,590.86	15,168.35	$2p_7$– $6d_5$	.331
3	6,162.16	16,223.60	$2p_7$– $7d_5$	.569	100	6,595.561	15,157.534	$2p_6$– $6d_1'$	.534
90	6,163.660	16,219.648	$2p_9$– $6d_1''$	.646	4*h*	6,602.87	15,140.75	$3d_4$– 8W	.73
80	6,163.935	16,218.924	$1s_2$– 5V	.924	30*h*	6,607.41	15,130.35	$3d_4$– 8Z	.30
150	6,178.302	16,181.209	$1s_2$– 5Y	.204	10	6,608.87	15,127.01	$2p_6$– $6d_1''$	6.979
120	6,179.665	16,177.640	$1s_2$– 5X	.639	2	6,630.44	15,077.80	$2p_8$– $6d_4$	.765
300	6,182.420	16,170.431	$2p_9$– $6d_4$	.432	50	6,632.464	15,073.198	$2p_6$– $6d_3$	.198
3	6,184.16	16,165.88	$2p_8$– $6d_3$	.865	3	6,648.75	15,036.28	$1s_2$– $4p_9$	.324
20	6,189.10	16,152.98	$2p_{10}$– $4s_4$	.966	20	6,657.92	15,015.57	$2p_6$– $6d_5$	.553
4*h*	6,191.40	16,146.98	$3d_2$– 9U	.96	4	6,664.85	14,999.95		
1*h*	6,193.89	16,140.49	$3d_2$– 9Y	.50	60	6,666.965	14,995.196	$2p_8$– $4s_5$	.196
1	6,195.49	16,136.32	$1s_2$– $4p_7$	.296	150	6,668.920	14,990.800	$2p_{10}$– $5d_6$	.800
100	6,198.260	16,129.108	$2p_{10}$– $4s_5$	.109	25	6,678.972	14,968.239	$1s_2$– $4p_{10}$	.249
60	6,200.890	16,122.266	$2p_9$– $7d_1'$	.255	20	6,681.036	14,963.615	$3d_5$– 6X	.613
3*h*	6,201.49	16,120.71	$3d_5$–8V	.71	1	6,706.46	14,906.89	$3d_5$– $6p_5$	.82
6*h*	6,205.35	16,110.68	$3d_5$– 8Y	.66	200	6,728.008	14,859.146	$2p_{10}$– $5d_5$	.148
4	6,205.75	16,109.64	$3d_5$– 8X	.60				$3d_3$– $6p_9$	8.89
20	6,206.297	16,108.220	$2p_9$– $6d_5$	.220	10	6,767.12	14,773.27	$3d_5$– 6V	.26
3	6,209.11	16,100.92	$2p_9$– $7d_1''$	.949	50	6,777.57	14,750.48	$3d_5$– 6Y	.49
1	6,220.84	16,070.56	$2p_9$– $7d_4$	.558	40	6,778.60	14,748.25	$3d_5$– 6X	.251
40	6,224.169	16,061.968	$2p_9$– $7d_3$	.969	12	6,815.64	14,668.09	$2p_8$– $5s_4$	.129
8	6,242.09	16,015.85	$2p_8$– $7d_5$	.943	15	6,818.38	14,662.20	$2p_7$– $2s_2$	.21
50	6,261.212	15,966.942	$2p_8$– $6d_1'$	.942	200	6,827.315	14,643.014	$1s_2$– 4X	.008
40	6,265.301	15,956.522	$1s_2$– $4p_{10}$	.517	8	6,840.96	14,613.80	$2p_9$– $5d_1'$	.804
1*h*	6,268.34	15,948.78	$3d_4$–11Z	.78	20	6,841.50	14,612.65	$3d_4$– 7W	.66
10	6,273.23	15,936.35	$2p_8$– $6d_1''$	.387	1	6,844.27	14,606.74	$3d_4$– 7V	.73
4	6,276.99	15,926.81	$2p_8$– $8d_2$	.81	2*h*	6,844.84	14,605.52	$3d_4$– 7U	.50
5*h*	6,281.81	15,914.58	$3d_4'$– 8W	.57	60	6,846.613	14,601.740	$2p_9$– $5d_2$	.740
100	6,286.011	15,903.950	$3d_4'$– 8T	.95	50	6,848.82	14,597.04	$3d_4$– 7Z	.05
50	6,292.649	15,887.173	$2p_9$– $6d_4$	.173	30	6,850.13	14,594.24	$2p_9$– $5d_3$	.252
15	6,294.45	15,882.63	$2p_8$– $6d_2$	.608	40	6,860.19	14,572.84	$3d_4'$– 6W	.82
15	6,314.97	15,831.02	$2p_7$– $5s_4$	.065	20	6,863.20	14,566.45	$2p_5$– $6d_2$	.47
500	6,318.062	15,823.273	$2p_8$– $6d_1'$	.273	5	6,865.58	14,561.40	$3d_4'$– 6U	.42
2	6,325.81	15,803.89	$2p_7$– $5s_5$	.893	50	6,866.838	14,558.734	$2p_9$– $5d_1''$	.729
20	6,331.50	15,789.69	$3d_5$– 7X	.784	100	6,872.107	14,547.571	$3d_4'$– 6T	.57
40*hl*	6,333.97	15,783.53	$3d_2$– 8U	.54	300	6,882.155	14,526.332	$2p_9$– $5d_4$	.333
8*hl*	6,337.58	15,774.54	$3d_2$– 8Y	.54	30	6,910.82	14,466.08	$2p_7$– $4s_4$	.077
2*h*	6,344.98	15,756.14	$3d_4$–10Z	.15					
20	6,355.77	15,729.40	$2p_7$– $6d_2$	.40	8	6,922.22	14,442.25	$2p_7$– $4s_5$	.220
10	6,412.38	15,590.53	$3d_5$– 7V	.55	15	6,924.67	14,437.15	$3d_3$– 6V	.14
30	6,418.41	15,575.89	$3d_5$– 7Y	.92	100	6,925.53	14,435.35	$3d_2$– 6U	.30
30*h*	6,418.98	15,574.50	$2p_8$– $5s_4$	.633	50	6,935.62	14,414.35	$3d_2$– 6Y	.37
			$3d_5$– 7X	.42	8	6,936.69	14,412.13	$3d_2$– 6X	.13

TABLE 1.—*List of Xe I lines*—Continued

Intensity	Wave length	Wave number observed	Combination	Wave number calculated	Intensity	Wave length	Wave number observed	Combination	Wave number calculated
1	6,949.76	14,385.02			10	7,666.61	13,039.99	$3d_3$– 5X	.92
100	6,976.182	14,330.542	$2p_8$– $5d_1'$	.545	1	7,670.81	13,032.85	$2p_6$– $3s_1''$	.86
30	6,982.05	14,318.50	$2p_8$– $5d_2$	.481	40	7,740.31	12,915.83	$2p_6$– $5d_3$	.825
1	6,991.65	14,298.84	$3d_3$– $5p_3$	.85	50	7,783.66	12,843.90	$3d_1''$– 6W	.86
4	7,003.10	14,275.46	$2p_8$– $5d_1''$	.470	15	7,789.42	12,834.40	$3d_1''$– 6V	.30
30	7,019.02	14,243.08	$2p_8$– $5d_4$	.073	1	7,790.53	12,832.57	$3d_1''$– 6U	.46
3	7,034.80	14,211.13			100	7,802.651	12,812.636	$2p_9$– $3s_4$	.636
20	7,035.53	14,209.66	$2p_6$– $4s_4$	.645	10	7,832.98	12,763.02	$2p_{10}$– $4d_2$	.00
30	7,047.37	14,185.79	$2p_6$– $4s_5$	.788	15	7,841.23	12,749.60	$2p_6$– $3s_1''$	.60
1h	7,049.07	14,182.36	$3d_3$– $5p_7$	.21	100	7,881.320	12,684.745	$2p_9$– $3s_5$	.742
1h	7,049.36	14,181.78	$3d_1''$– 8V	.75	300	7,887.395	12,674.975	$1s_3$– $2p_1$	.978
3	7,051.06	14,178.36	$2p_{10}$– $3s_1''''$	.34	40	7,937.41	12,595.11	$2p_8$– $5d_2$	.081
1	7,078.46	14,123.48	$3d_3$– $5p_9$	.50	4	7,954.22	12,568.49	$3d_3$– $4p_5$	.50
300	7,119.598	14,041.872	$2p_8$– $5d_4'$	.872	500	7,967.341	12,547.792	$1s_3$– $3p_7$	.789
15	7,136.57	14,008.48	$2p_9$– $5d_5$	.491	8	7,976.03	12,534.12	$2p_6$– $3s_1'''$	.100
10	7,172.70	13,937.92	$3d_4'$– $5p_8$	.88					
					10	8,003.26	12,491.48	$2p_7$– $3s_1''''$	.45
15	7,200.79	13,883.54	$2p_{10}$– $3s_1''$	.51	100	8,029.67	12,450.39	$3d_4$– 5W	.41
5	7,209.14	13,867.46	$3d_2$– $5p_6$	.47	10	8,040.56	12,433.53	$3d_4$– 5V	.51
1	7,220.24	13,846.14	$3d_3$– $5p_7$	.09	15	8,042.18	12,431.02	$3d_4$– 5U	.02
3	7,238.20	13,811.79	$3d_2$– $5p_8$	.76	200	8,057.258	12,407.762	$3d_4$– 5Z	.75
20	7,244.94	13,798.94	$3d_4$– 6W	9.00					
					150	8,061.340	12,401.480	$2p_8$– $3s_3$	.483
2	7,249.92	13,789.46	$3d_4$– 6V	.44	2	8,064.94	12,395.94	$3d_4$– 5Y	.79
5h	7,250.87	13,787.66	$3d_2$– $5p_9$	.38	1	8,073.99	12,382.05	$3d_6$– $4p_{10}$	.011
			$3d_4$– 6U	.60	3	8,097.24	12,346.50	$3d_3$– $4p_7$	.43
60	7,257.94	13,774.22	$3d_4$– 6Z	.23	100	8,101.98	12,339.27	$3d_1'$– 6W	.26
20	7,262.54	13,765.50	$2p_7$– $5d_2$	.505					
					6	8,107.91	12,330.25	$3d_1'$– 6V	9.71
25	7,266.49	13,758.02	$2p_7$– $5d_3$	.017	15	8,109.46	12,327.89	$3d_1'$– 6U	.86
40	7,283.961	13,725.018	$1s_2$– 4V	.023	15	8,118.29	12,314.48	$3d_1'$– 6Z	.49
60	7,285.301	13,722.494	$2p_7$– $5d_1''$	.494	2	8,123.29	12,306.90	$3d_1'$– 6Y	.93
5h	7,307.37	13,681.05	$3d_1'$– 8W	.01	2	8,165.37	12,243.48		
1h	7,313.01	13,670.50	$3d_1'$– 8Z	.56					
					100	8,171.02	12,235.01	$3d_5$–4 p_9	4.74
70	7,316.272	13,664.405	$1s_2$– 4Y	.408				$2p_6$– $3s_1''''$	.02
20	7,316.87	13,663.28	$2p_{10}$– $3s_4$	.290	1–	8,182.93	12,217.21	$3d_2$– 8V	.40
15	7,319.94	13,657.56	$3d_1''$– 7W	.52	2	8,196.73	12,196.63	$2p_7$– $3s_1''$	.62
80	7,312.452	13,654.737	$1s_3$– 4X	.740	700	8,206.341	12,182.354	$1s_3$– $2p_4$	.355
2	7,323.05	13,651.76	$3d_1''$– 7V	.59	10,000	8,231.6348	12,144.921	$1s_5$– $2p_6$	.923
50	7,336.480	13,626.767	$2p_9$– $3s_1'''$	.767	500	8,266.519	12,093.671	$1s_2$– $2p_2$	.673
40	7,355.58	13,591.38	$3d_6$– 5X	.401	7,000	8,280.1163	12,073.811	$1s_5$– $2p_3$	.811
100	7,386.002	13,535.397	$2p_{10}$– $3s_5$	.396	15	8,297.71	12,048.21	$3d_2$– $4p_6$	.16
150	7,393.793	13,521.140	$2p_6$– $5d_1'$	.137	2	8,323.90	12,010.31	$3d_3$– $4p_7$	.31
30	7,400.41	13,509.04	$2p_6$– $5d_3$	.077	20	8,324.58	12,009.32	$2p_3$– $5d_5$	.301
12	7,404.51	13,501.57	$2p_6$– $5d_2$	.585	2,000	8,346.823	11,977.318	$1s_2$– $2p_3$	.320
3	7,405.77	13,499.26	$2p_8$– $2s_2$	.28	60	8,347.45	11,976.42	$2p_7$– $3s_4$	.401
20	7,424.05	13,466.03	$2p_6$– $5d_1''$	.062	40	8,349.05	11,974.12	$2p_{10}$– $4d_1''$	.10
20	7,441.94	13,433.66	$2p_6$– $5d_4$	.665	3	8,371.38	11,942.18	$3d_3$– $4p_8$	.19
25	7,451.00	13,417.33	$3d_3$– 5V	.33	5	8,372.79	11,940.17	$2p_6$– $3s_1''$	.19
40	7,472.01	13,379.60	$3d_3$– 5Y	.61	20	8,392.37	11,912.32	$2p_6$– $4d_2$	.35
25	7,474.01	13,376.02	$3d_3$– 5X	.04	5	8,402.03	11,898.62	$3d_2$– $4p_9$	.60
20	7,492.23	13,343.49	$2p_8$– $3s_1'''$	.508	2,000	8,409.190	11,888.489	$1s_5$– $2p_7$	.491
20	7,501.13	13,327.66	$2p_9$– $3s_1''''$	.69	10	8,437.55	11,848.53	$2p_7$– $3s_5$	.507
8	7,514.54	13,303.88	$2p_7$– $5d_6$	.911	1h	8,450.37	11,830.55	$3d_2$– $4p_{10}$	.53
3	7,514.96	13,303.13	$2p_5$– $4s_4$	.141	1	8,501.02	11,760.07		
40	7,559.79	13,224.25	$3d_4'$– 5W	.23	30	8,522.55	11,730.35	$1s_3$– $3p_{10}$	.360
6	7,570.93	13,204.79	$3d_4'$– 5U	.84	30	8,530.10	11,719.98	$2p_6$– $3s_4$	.969
10	7,584.29	13,181.53	$3d_4'$– 5Z	.57	2	8,553.97	11,687.27	$3d_2$– 7V	.24
200	7,584.680	13,180.849	$3d_4'$– 5T	.85	1–	8,564.7	11,672.63	$3d_2$– 7Y	.60
6	7,589.61	13,172.28	$2p_7$– $5d_5$	.257	200	8,576.01	11,657.24	$1s_2$– $3p_5$	.221
1	7,594.36	13,164.04	$3d_4$– $5p_8$	.06	80	8,624.24	11,592.04	$2p_6$– $3s_5$	.075
10	7,600.77	13,152.95	$3d_1'$– 7W	.92	250	8,648.54	11,559.47	$1s_2$– $3p_7$	.521
2h	7,604.97	13,145.68	$3d_1'$– 7U	.80	100	8,692.20	11,501.41	$1s_2$– $3p_8$	.460
5	7,608.46	13,139.65	$3d_4$– $5p_9$	.68	200	8,696.86	11,495.25	$3d_1''$– 5W	.27
3	7,609.82	13,137.30	$3d_1'$– 7Z	.31	40	8,709.64	11,478.38	$3d_1''$– 5V	.37
500	7,642.025	13,081.940	$1s_3$– $2p_2$	.941	2	8,711.54	11,475.88	$3d_1''$– 5U	.88
	7,642.30	13,081.47	$3d_2$– 5V	.21	300	8,739.39	11,439.31	$2p_{10}$– $4d_3$	.31
100	7,643.91	13,078.71	$3d_2$– 5U	.72	100	8,758.20	11,414.74	$2p_9$– $4d_1'$	.75
10	7,664.02	13,044.40	$2p_8$– $3s_1''''$	.43	5,000	8,819.412	11,335.515	$1s_5$– $2p_8$	.515
30	7,664.56	13,043.48	$3d_2$– 5Y	.49					

TABLE 1.—*List of Xe I lines*—Continued

Intensity	Wave length	Wave number observed	Combination	Wave number calculated	Intensity	Wave length	Wave number observed	Combination	Wave number calculated
1	8,851.44	11,294.50	$3d_4 - 4p_3$	.49	3	9,605.80	10,407.53	$3d_1'' - 4p_7$	.47
300	8,862.32	11,280.63	$2p_{10} - 4d_5$	.63	1	9,614.43	10,398.18		
10	8,885.71	11,250.94	$3d_4 - 4p_2$	.90	1	9,616.95	10,395.46		
200	8,908.73	11,221.87	$2p_{10} - 4d_4$	.87	1	9,668.94	10,339.56		
200	8,930.83	11,194.10	$1s_2 - 2p_4$	4.087	150	9,685.32	10,322.08	$2p_6 - 4d_1'$	.08
1,000	8,952.254	11,167.309	$1s_4 - 2p_8$	.307	20	9,700.99	10,305.40	$2p_8 - 4d_2$	.40
50	8,952.78	11,166.65	$1s_2 - 3p_9$	.641	2	9,710.03	10,295.81	$3d_1'' - 4p_9$	.76
100	8,981.05	11,131.50	$2p_8 - 4d_1'$	.49	100	9,718.16	10,287.20	$2p_7 - 4d_1''$	.21
200	8,987.57	11,123.43	$2p_9 - 4d_1''$	.45	2,000	9,799.699	10,201.600	$1s_5 - 2p_{10}$	.602
30	9,025.98	11,076.09	$2p_7 - 4d_2$	.11	3,000	9,923.192	10,074.643	$1s_4 - 2p_9$	.640
50	9,032.18	11,068.49	$3d_3 - 4X$	.502	10	9,966.58	10,030.78	$2p_6 - 4d_1''$	.78
400	9,045.446	11,052.256	$1s_5 - 2p_6$	.256	50	10,023.72	9,973.60	$3d_4 - 4W$	.58
50	9,096.13	10,990.67	$3d_1' - 5W$	.67	1	10,056.84	9,940.76		
4	9,112.24	10,971.24	$3d_1' - 5U$	.28	5	10,057.96	9,939.66	$3d_4 - 4V$	.60
3	9,131.59	10,947.99	$3d_1' - 5Z$	.01	10	10,060.96	9,936.69	$3d_4 - 4U$	.62
2	9,141.8	10,935.8	$3d_1' - 5Y$	6.05	20	10,084.79	9,913.21	$2p_5 - 4d_2$	.18
20	9,152.12	10,923.44	$3d_3 - 4V$	.42	80	10,107.34	9,891.10	$3d_4 - 4Z$	.08
2	9,158.38	10,915.97			1	10,119.8	9,878.88	$3d_4 - 4Y$	.99
500	9,162.654	10,910.877	$1s_4 - 2p_7$	.875	20	10,125.47	9,873.38	$3d_5 - 2p_1$	.35
100	9,167.52	10,905.09	$2p_9 - 4d_4$	.09	10	10,188.36	9,812.44	$2p_6 - 4d_4$	.42
2	9,197.18	10,869.92	$3d_2 - 6V$	.96	20	10,251.07	9,752.41	$2p_7 - 4d_3$	.42
30	9,203.20	10,862.81	$3d_5 - 4Y$	.81	1	10,420.52	9,593.83	$2p_7 - 4d_5$	.74
25	9,211.38	10,853.16	$3d_5 - 4X$	.14	8	10,484.83	9,534.98	$2p_7 - 4d_6$	.98
1	9,216.51	10,847.12	$3d_2 - 6Y$	.18	6	10,507.91	9,514.03	$3d_2 - 5V$	.02
5	9,222.39	10,840.20	$2p_8 - 4d_1''$	.19	10	10,515.15	9,507.48	$3d_6 - 2p_2$	.44
3	9,245.18	10,813.48	$2p_5 - 3s_4$	.465	40	10,527.84	9,496.03	$2p_6 - 4d_3$	5.99
30	9,301.95	10,747.49	$3d_4' - 4W$	.40	4	10,549.75	9,476.30	$3d_2 - 5Y$	.30
40	9,306.64	10,742.07	$1s_2 - 3p_{10}$	.092	25	10,706.77	9,337.33	$2p_6 - 4d_5$	.31
3	9,334.08	10,710.49	$3d_4' - 4U$	.45	15	10,788.85	9,292.13	$3d_5 - 2p_2$	.07
10	9,374.02	10,664.86	$3d_4' - 4Z$	.90	100	10,838.37	9,223.95	$1s_4 - 2p_{10}$	.998
100	9,374.76	10,664.02	$3d_4' - 4T$	.02	10	10,895.39	9,175.68	$3d_5 - 2p_3$	.72
60	9,412.01	10,621.81	$2p_9 - 4d_4$	.83	10	11,085.39	9,018.42	$3d_1'' - 4W$	.44
20	9,441.46	10,588.68	$2p_9 - 4d_2$	.66	2	11,127.29	8,984.46	$3d_1'' - 4V$	.46
20	9,442.68	10,587.31	$3d_3 - 4V$	.30	1	11,140.90	8,973.48		
80	9,445.34	10,584.33	$3d_3 - 4U$	.33					
4	9,487.76	10,537.01							
40	9,497.07	10,526.68	$3d_3 - 4Y$	.69					
10	9,505.73	10,517.03	$3d_3 - 4X$	.02					
200	9,513.379	10,508.633	$2p_8 - 4d_4'$	.633					
20	9,585.14	10,429.96	$2p_9 - 4d_5$	.98					

IV. DISCUSSION OF Xe I TERMS

The numerical values of previously known terms have been subject to only slight revisions. The new term table incorporates the changes due to more precise data, the extensions of series, new low terms and changes in the assignment of quantum numbers. The values of the $1s$, $2p$, and $3p$ terms as determined from interference measurements (RP245) form the basis of the present table. The numerical values of a considerable number of terms can now be completely determined from interference measurements. These are given to three places of decimals. Table 2 gives the final set of terms and effective quantum numbers. In calculating the effective quantum numbers for non-Ritzian terms, the value of the displacement constant A was taken as 10,540, representing the level separation of the ground doublet ($^2P^o_{1½, ½}$) identified[9] in the Xe II spectrum.

[9] C. J. Humphreys, T. L. deBruin, and W. F. Meggers, B. S. Jour. Research, vol. 6 (RP275), p. 287, 1931.

TABLE 2.—*Terms and effective quantum numbers of XI*

Electron	j	Paschen notation		1		2		3		4		5		6		7		8		9
p	0	p_0	97, 834. 8																	
s	2	s_5		30, 766. 353	1. 8886			7, 029. 355	3. 9511	4, 435. 642	4. 9739	3, 073. 969	5. 9748	2, 254. 931	6. 9760	1, 724. 67	7. 9767	1, 361. 76	8. 9769	1, 102. 57
	1	s_4		29, 788. 737	1. 9193			6, 901. 461	3. 9876	4, 411. 785	4. 9873	3, 046. 797	6. 0014	2, 242. 92	6. 9947	1, 711. 12	8. 0082	1, 353. 27	9. 0030	
	0	s_3		21, 637. 108	1. 8467															
	1	s_2		20, 648. 840	1. 8758	4, 215. 65	2. 7271													
p	1	p_{10}				20, 564. 751	2. 3100	9, 906. 748	3. 3282	5, 680. 591	4. 3952	3, 766. 94	5. 3974	2, 679. 52	6. 3994					
	2	p_9				19, 714. 097	2. 3593	9, 482. 199	3. 4019	5, 612. 516	4. 4218	3, 723. 74	5. 4286	2, 652. 23	6. 4324					
	3	p_8				19, 430. 838	2. 3764	9, 364. 668	3. 4232	5, 568. 930	4. 4391	3, 699. 36	5. 4464	2, 637. 36	6. 4505	1, 975. 71	7. 4528	1, 534. 94	8. 4553	1, 227. 12
	1	p_7				18, 877. 862	2. 4110	9, 089. 319	3. 4746	5, 500. 812	4. 4665	3, 665. 03	5. 4719	2, 617. 43	6. 4750	1, 963. 20	7. 4764	1, 527. 03	8. 4773	
	2	p_6				18, 621. 430	2. 4276	9, 147. 380	3. 4636	5, 462. 958	4. 4819	3, 643. 65	5. 4879	2, 604. 30	6. 4913	1, 954. 49	7. 4931	1, 521. 00	8. 4940	1, 216. 99
	0	p_5				17, 714. 926	2. 4889	8, 991. 619	3. 4935	5, 278. 741	4. 5595	3, 548. 39	5. 5611	2, 547. 83	6. 5628	1, 918. 36	7. 5633	1, 496. 07	8. 5645	1, 199. 80
	1	p_4				9, 454. 753	2. 3427													
	2	p_3				8, 671. 520	2. 3900													
	1	p_2				8, 555. 167	2. 3972													
	0	p_1				7, 973. 862	2. 4682													
d	0	d_6						18, 062. 602	2. 4648	9, 342. 88	3. 4272	5, 573. 951	4. 4370	3, 709. 531	5. 4390	2, 654. 293	6. 4298	2, 033. 308	7. 3464	
	4	d_5'						17, 637. 24	2. 4944	8, 922. 205	3. 5070	5, 388. 966	4. 5126	3, 607. 565	5. 5153	2, 583. 944	6. 5168	1, 941. 698	7. 5177	1, 512. 34
	3	d_4						16, 863. 42	2. 5510	8, 809. 01	3. 5295	5, 187. 765	4. 5992	3, 543. 665	5. 5648	2, 550. 872	6, 5589	1, 921. 877	7. 5564	1, 499. 413
	2	d_3						17, 511. 12	2. 5035	9, 125. 44	3. 4678	5, 112. 357	4. 6330	3, 548. 232	5. 5612	2, 559. 461	6. 5479	1, 929. 292	7. 5418	1, 505. 27
	1	d_5						17, 847. 24	2. 4797	9, 284. 12	3. 4380	5, 705. 605	4. 3856	3, 605. 877	5. 5166	2, 605. 487	6. 4897	1, 921. 012	7. 5581	1, 518. 73
	1	d_2						13, 943. 93	2. 8053	7, 801. 75	3. 7504	5, 119. 845	4. 6297	3, 148. 46	5. 9037	2, 335. 41	6. 8548	1, 788. 12	7. 8339	1, 410. 12
	2	d_1''						15, 908. 28	2. 6264	8, 590. 65	3. 5741	5, 155. 368	4. 6137	3, 494. 451	5. 6039	2, 520. 481	6. 5984	1, 902. 09	7. 5954	1, 485. 86
	3	d_1'						15, 403. 68	2. 6691	8, 299. 35	3. 6363	5, 100. 293	4. 6385	3, 463. 896	5. 6285	2, 499. 175	6. 6264	1, 887. 277	7. 6252	1, 475. 33
	2	s_1''						6, 681. 24	2. 5243											
	2	s_1''''						6, 386. 41	2. 5462											
	3	s_1'''						6, 087. 330	2. 5690											
	1	s_1'																		
f	1	X								6, 994. 100	3. 9610	4, 471. 201	4. 9541	3, 098. 989	5. 9507	2, 272. 818	6. 9484	1, 737. 64	7. 9469	1, 371. 26
	2	Y								6, 984. 432	3. 9638	4, 467. 636	4. 9561	3, 096. 746	5. 9528	2, 271. 321	6. 9508	1, 736. 58	7. 9493	1, 370. 62
	4	Z								6, 972. 34	3. 9672	4, 455. 67	4. 9627	3, 089. 19	5. 9601	2, 266. 37	6. 9584	1, 733. 12	7. 9572	1, 368. 12
	5	T								6. 973. 22	3. 9670	4, 456. 39	4. 9623	3, 089. 67	5. 9596	2, 266. 75	6. 9578	1, 733. 29	7. 9569	1, 368. 26
	3	U								6, 926. 786	3. 9802	4, 432. 40	4. 9757	3, 075. 82	5. 9731	2, 257. 92	6. 9715	1, 727. 58	7. 9700	1, 364. 16
	2	V								6, 923. 817	3. 9811	4, 429. 916	4. 9771	3, 073. 985	5. 9748	2, 256. 69	6. 9733	1, 726. 53	7. 9724	1, 363. 50
	3	W								6, 889. 84	3. 9909	4, 413. 01	4. 9866	3, 064. 42	5. 9841	2, 250. 76	6. 9825	1, 722. 67	7. 9813	1, 360. 71

ntum numbers of XI

		7		8		9		10		11		12	
931	6.9760	1,724.67	7.9767	1,361.76	8.9769	1,102.57	9.9764	909.3	10.98				
92	6.9947	1,711.12	8.0082	1,353.27	9.0050								
32	6.3994												
23	6.4324												
36	6.4505	1,975.71	7.4528	1,534.94	8.4553	1,227.12	9.4565	1,003.75	10.4559	835.2	11.46		
43	6.4750	1,963.20	7.4764	1,527.03	8.4773								
30	6.4913	1,954.49	7.4931	1,521.00	8.4940	1,216.99	9.4958	996.75	10.4926				
83	6.5628	1,918.36	7.5633	1,496.07	8.5645	1,199.80	9.5112						
531	5.4390	2,654.293	6.4298	2,033.308	7.3464								
565	5.5153	2,583.944	6.5168	1,941.698	7.5177	1,512.34	8.5183	1,211.09	9.5190	991.76	10.5191	826.99	11.5193
665	5.5648	2,550.872	6,5589	1,921.877	7.5564	1,499.413	8.5549	1,202.24	9.5539	985.30	10.5534		
232	5.5612	2,559.461	6.5479	1,929.292	7.5418	1,505.27	8.5383	1,206.81	9.5319				
877	5.5166	2,605.487	6.4897	1,921.012	7.5581	1,518.73	8.5003	1,217.67	9.4932				
46	5.9037	2,335.41	6.8548	1,788.12	7.8339	1,410.12	8.8216	1,139.47	9.8135				
451	5.6039	2,520.481	6.5984	1,902.09	7.5954	1,485.86	8.5939	1,192.55	9.5926	978.32	10.5909		
896	5.6285	2,499.175	6.6264	1,887.277	7.6252	1,475.33	8.6245	1,184.83	9.6238	972.39	10.6232		
989	5.9507	2,272.818	6.9484	1,737.64	7.9469	1,371.26	8.9457						
746	5.9528	2,271.321	6.9508	1,736.58	7.9493	1,370.62	8.9478						
19	5.9601	2,266.37	6.9584	1,733.12	7.9572	1,368.12	8.9560	1,107.27	9.9552	914.64	10.9535		
67	5.9596	2,266.75	6.9578	1,733.29	7.9569	1,368.26	8.9556	1,107.42	9.9545	914.67	10.9533		
82	5.9731	2,257.92	6.9715	1,727.58	7.9700	1,364.16	8.9690	1,104.40	9.9681	912.38	10.9671		
985	5.9748	2,256.69	6.9733	1,726.53	7.9724	1,363.50	8.9712	1,102.60	9.9762				
42	5.9841	2,250.76	6.9825	1,722.67	7.9813	1,360.71	8.9804						

TABLE 3.—*Determination of absolute term values of XeI*

$2p_3 - md_4'$ $\quad (5_p{}^3D_3 - 5d^3F_4)$

$$\nu = A - \frac{R}{[m+\mu+\alpha(A-\nu)]^2}$$

$R_{Xe} = 109{,}736.965$

$A = 19{,}430.838$

$\mu = +0.5208392314$

$\alpha = -0.000001534768614$

m	Int.	$\lambda_{obs.}$	$\nu_{obs.}$	$\nu_{calc.}$	$\nu_{calc.} - \nu_{obs.}$
2	----------	----------	[1, 793. 60]	1, 784. 900	+8. 70
3	200	9, 513. 32	10, 508. 70	10, 509. 189	−. 49
4	500	7, 119. 598	14, 041. 872	14, 041. 873	−. 001
5	300	6, 318. 062	15, 823. 272	15, 823. 272	−. 000
6	100	5, 934. 170	16, 846. 900	16, 846. 946	−. 046
7	70	5, 716. 255	17, 489. 131	17, 489. 217	−. 086
8	40	5, 579. 276	17, 918. 51	17, 918. 584	−. 07
9	6h	5, 487. 026	18, 219. 76	18, 219. 760	−. 000
10	2h	5, 421. 756	18, 439. 10	18, 439. 144	−. 04
11	1h−	5, 373. 74	18, 603. 85	18, 603. 886	−. 04

$2p_3 = 19{,}430.838$

$1s_3 - 2p_3 = 11{,}335.515$

$\therefore 1s_5 = 30{,}766.353$

The absolute value of the term $1s_5$ has been redetermined using the more accurate wave length data now available and a new value of the Rydberg constant for xenon calculated from the value of $R\infty$ given by Birge.[10] The new value of $1s_5$ differs very slightly from the old, 30,766.353 as compared with 30,766.98 previously calculated. This revised term value represents the precision attainable with the data selected for the determination. It is still subject to a variation of from 1 to 2 wave number units, depending on the series chosen for computation. As in the work previously reported, we have estimated $1s_5$ from the limit of the series $2p_8$–md'_4 and the combination $1s_5$–$2p_8$. All other terms are fixed relative to $1s_5$, so that the error in absolute value is the same for all terms.

The sequence ms_5 remains unchanged except that it has been extended to the tenth member. Attempts to find $2s_5$ from combinations in the infra-red region have not been successful, and it seems probable that the required combinations are beyond our range of photographic observations. The sequence ms_4 has also been extended. The term 13,943.93 previously given as $2s_4$ is now interpreted as $3d_2$. The reason for the new assignment will be discussed in connection with the *d*-series. The old terms, $2s_3$ and $2s_2$, originally obtained from the interpretation of the ultra-violet data of Abbink and Dorgelo [11] are not confirmed by expected combinations in the range of the present observations and are not retained. The term, 4,215.65, is a new term, interpreted as $2s_2$ by Rasmussen, and is confirmed by observed combinations.

No changes have been made in the interpretation of the *p*-series. Higher members have been found in the case of all sequences which form Ritz series. The sequence mp_8 is the longest; it has been extended to $11p_8$

A considerable number of changes have been introduced in the interpretation of the *d*-series. Several new terms have been found

[10] R. T. Birge, Reviews of Modern Physics, vol. 1, p. 1, 1929.
[11] J. H. Abbink and H. B. Dorgelo, Zeit. f. Phys., vol. 47, p. 221, 1928.

and all Ritzian series except md_6 have been extended. In the work previously reported, the failure to find all expected combinations, due to the faintness of the sources used and the lack of the superior sensitizers now available for the infra-red region, left the assignment of inner quantum numbers uncertain in many cases. With the more extended and accurate data now available these ambiguities have been eliminated and it is believed that the j-values are now determined correctly for all the d-terms. In the work of Rasmussen referred to above, new interpretations have been placed on many of the old terms and several additional d-terms have been found. The present work entirely confirms Rasmussen's assignment of j-values, and we agree also on interpretation of the terms in most cases.

The md_6-sequence has been altered only by the substitution of the new term 9,342.88 for $4d_6$ in place of 9,125.44, which by virtue of its j-value 2 is assigned to $4d_3$.

The md_4' sequence is left unchanged. It is the longest as well as the most regular of the d-series, and has been extended in the present work to $12d_4'$. Attention is again called to Table 3 in which a Ritz formula is applied to the series $2p_8$–md_4'. The only large departure from the calculated position of a line is in the case of the photographically inaccessible infra-red line $2p_8$–$3d_4'$, at 1,793.60 cm^{-1}. The position of this line is predicted accurately from the known values of both terms, and differs from the position given by the series formula by 8.70 cm^{-1}.

The first term only of the md_4 sequence has been changed. The term 16,863.42, previously assigned to $3d''$, is now designated $3d_4$; 17,511.12, formerly called $3d_4$, becomes the first term of the new sequence md_3 with inner quantum number 2. Subsequent terms of md_3 are assembled from members of other d-series incorrectly interpreted. The second number $4d_3$ is 9,125.44, formerly $4d_6$, the third $5d_3$ is 5,112.357, formerly $5d''$, whereas the remaining terms of md_3 are taken from the old md_5 sequence.

The md_5 sequence begins as before with 17,847.24, as $3d_5$. The term 9,284.12, formerly $4d_2$, is now assigned to $4d_5$. The term 5,705.605 was formerly designated as $3s_1'''$. It is now certain that its j-value is 1. Rasmussen designated it as $5d_5$. We give it the same classification with reservations, since its interpretation as the missing non-Ritzian term $3s_1'$ seems equally probable. The present classification introduces a sharp downward inflection in the graph of the effective quantum numbers, which is not paralleled for Kr I. In any case either $5d_5$ or $3s_1'$ has not been found.

With the exception of the first and third members, the md_2 sequence is made up of newly found terms. The term 13,943.93 is now designated as $3d_2$ instead of $2s_4$. This assignment is supported by the effective quantum number which fits better into this d-series than into the s_4-series where an unexpected deviation from an otherwise fairly regular series would occur. Furthermore, if $2s_4$ is found, $2s_5$ should also be observed, since the combinations would be displaced to shorter wave lengths than those of $2s_4$. The combination of 13,944 with the ground term giving the line, 83,891.2 cm^{-1}, found in Abbink and Dorgelo's data is permitted with either interpretation. The term 5,119.845, designated $5d_2$, was formerly $5d_5$. Three new terms, 7,801.75, 3,148.46, 2,335.41, have been interpreted by Rasmussen as

$4d_2$, $6d_2$, and $7d_2$, respectively. We have how extended the series to $10d_2$.

The first three members of the d_1'' sequence have been replaced. The first member 15,908.28, now $3d_1''$, was formerly $3d_1'$. The term 8,289.42, appearing in the original table, is not supported by observed combinations and is obviously spurious. It is replaced by 8,590.65, designated $4d_1''$ instead of $4d_5$ as before. The third term, 5,155.368, has been changed to $5d_1''$ from $5d_2$. The original interpretation has been retained for subsequent members of the series.

A new term 15,403.68 has been interpreted by Rasmussen as $3d_1'$. The md_1' sequence is otherwise unchanged.

Of the original group of d-type non-Ritzian terms, two are retained; 6,087 is designated $3s_1'''$ instead of $3s_1''''$, and 6,386, now $3s_1''''$, was formerly $3s_1''$. These changes were suggested by Rasmussen to make the notation uniform among the rare gas spectra. A new term 6,681 becomes $3s_1''$. Our old $3s_1'$ term is not confirmed. The only remaining possibility for $3s_1'$ is 5,705 as explained above.

Changes in the f-type or hydrogenlike terms have been limited to small corrections and extensions of series, except that one entirely new sequence mT has been found. A discrepancy between observed and calculated wave numbers, too great to be accounted for by errors of observation, was found in the case of the series of lines formerly designated $3d_4'$–mZ. Examination of the first and second members of the series at 9,374 and 7,584 A with the Rowland grating revealed a companion line in each case in the calculated position of the corresponding member of the mZ series. The stronger series was, therefore, given a separate designation mT and the weaker retained as mZ. The separation is 0.9 cm^{-1} for the first member 0.7 cm^{-1} for the second, the two series merging in the higher members. Members beyond the second can not be resolved not only because the wave number separation is smaller, but also since the wave length difference diminishes much more rapidly as one goes to shorter wave lengths.

The data here presented, because of greater completeness, accuracy, and the elimination of errors, should be regarded as superseding those given in RP115.

WASHINGTON, November 3, 1932.